

Investigation of the Fire Behaviour of PEEK-based Polymers and Compounds

by

Parina Patel

A thesis submitted in partial fulfilment for the requirements of the degree of
Doctor of Philosophy
at the
University of Central Lancashire
in collaboration with
Victrex plc

February 2011

ABSTRACT

Polyetheretherketone (PEEK) is a polymer with outstanding performance, particularly concerning temperature resistance, chemical resistance and mechanical characteristics. Literature shows a gap in the knowledge with regards to PEEK flammability and decomposition products.

The aim of this thesis is to describe the decomposition and flammability behaviour of PEEK, in order to develop new fire safe PEEK-based materials. By relating the measured thermal decomposition behaviour and changes in physical properties of PEEK materials to their performance in standard flammability tests, the dependence of these tests has been investigated with regards to orientation, thickness, presence of fillers, moisture absorption and absorption of infrared radiation. This understanding can inform the development of modified PEEK materials with enhanced fire safety.

Various industry standard tests have been utilised to examine PEEK such as the Cone Calorimeter (ISO 5660), UL-94 (EN 60695-10-11), Limiting Oxygen Index (LOI), Thermogravimetric Analysis (TGA) in both air and inert atmospheres and the Small Flame Ignitability Test (ISO 11925). PEEK decomposition has been investigated using Thermogravimetric Analysis (TGA), Simultaneous Thermal Analysis coupled with Fourier Transform Infrared (STA-FTIR) and Pyrolysis Gas Chromatography coupled with Mass Spectrometry (pyGC/MS). Residue analysis has been carried out using Diamond Attenuated Total Reflectance coupled with Fourier Transform Infrared (dATR-FTIR), Solid State Nuclear Magnetic Resonance (MAS-NMR) and Scanning Electron Microscopy coupled with Electron Dispersive X-ray Analysis (SEM-EDX).

Thermal analysis shows a rapid mass loss around 580°C followed by a slower mass loss of the resultant char. The stages of decomposition have been investigated by using FTIR and NMR on the condensed phase residues. Samples subjected to various temperature regimes have been observed in the dATR-FTIR and MAS-NMR and the results shows differences in the structures of the residue during decomposition.

Generally, filled PEEK materials (with glass fibre, carbon fibre and talc) tend to have lower flammability in the Cone Calorimeter with a longer time to ignition and a lower peak heat release rate compared to the unfilled materials. The same is true in the LOI, where filled materials give a higher oxygen index, and in the UL-94 test where shorter burn times are recorded. PEEK shows inconsistent behaviour in some flammability tests, possibly due to the critical heat flux for ignition of PEEK being so close to the heat fluxes employed in many industry standard tests. The presence of moisture within the samples also reduces the time to ignition of PEEK in the Cone Calorimeter and increases the burning time in the UL-94, possibly due to the formation of a foamed sample close to the melting temperature of the polymer.

TABLE OF CONTENTS

ABSTRACT	I
TABLE OF CONTENTS	II
INDEX OF FIGURES	VII
INDEX OF TABLES	XI
ACKNOWLEDGEMENTS	XIII
CHAPTER 1. INTRODUCTION	1
1.1 POLYMER STRUCTURE	3
1.2 POLYMER DECOMPOSITION	5
1.2.1 METHODS FOR STUDYING POLYMER DECOMPOSITION	8
1.3 POLYMER COMBUSTION	10
1.3.1 POLYMER BURNING	10
1.3.2 COMMON BURNING PRODUCTS	11
1.3.3 TECHNIQUES FOR MEASURING POLYMER BURNING PROCESSES	12
1.3.3.1 Limiting Oxygen Index (LOI)	13
1.3.3.2 UL-94	14
1.3.3.3 Cone Calorimeter	15
1.3.3.4 Pyrolysis Combustion Flow Calorimeter	17
1.3.3.5 Small Flame Ignitability Test (ISO 11925)	18
1.3.3.6 Ohio State University Calorimeter (OSU)	18
1.3.3.7 Lateral Spread of Flame Test LIFT Apparatus (or IMO LIFT ISO 5658)	18
1.3.3.8 Chemical Analysis	19
1.4 POLYETHERETHERKETONE STRUCTURE, PROPERTIES AND BURNING BEHAVIOUR	19
1.4.1 POLYETHERETHERKETONE STRUCTURE	19
1.4.2 PEEK DECOMPOSITION AND FLAMMABILITY	21
1.4.3 PEEK DECOMPOSITION – PRODUCTS AND MECHANISMS	25
1.4.4 COMPARISON OF RESULTS OF FLAMMABILITY TESTS FOR PEEK	29
1.4.4.1 Polyimide (PI)	30
1.4.4.2 Polyetherimide (PEI)	30
1.4.4.3 Polyphenylene Sulphide (PPS)	31
1.5 STUDIES AIMED AT FIRE RETARDING PEEK	33
1.5.1 BLENDING	33
1.5.2 FILLERS	34
1.5.3 STRUCTURAL MODIFICATIONS	35
1.5.4 NANOCOMPOSITES	35
1.6 STUDIES AIMED AT FIRE RETARDING OTHER HIGH TEMPERATURE POLYMERS	36

1.6.1	POLYIMIDE (PI)	37
1.6.2	POLYETHERIMIDE (PEI)	38
CHAPTER 2. EXPERIMENTAL PROCEDURES		40
2.1	THERMAL DECOMPOSITION	40
2.1.1	THERMOGRAVIMETRIC ANALYSIS (TGA)	41
2.1.1.1	INSTRUMENTATION	41
2.1.1.2	CALIBRATION	42
2.1.1.3	SAMPLE PREPARATION	42
2.1.1.4	MATERIALS	42
2.1.1.5	PROCEDURE	42
2.1.2	SIMULTANEOUS THERMAL ANALYSIS - FOURIER TRANSFORM INFRARED (STA-FTIR)	42
2.1.2.1	INSTRUMENTATION	43
2.1.2.2	SAMPLE PREPARATION	43
2.1.2.3	MATERIALS	43
2.1.2.4	PROCEDURE	43
2.1.2.5	DATA INTERPRETATION	44
2.1.3	PYROLYSIS GAS CHROMATOGRAPHY - MASS SPECTROMETRY (PYGC/MS)	44
2.1.3.1	INSTRUMENTATION	44
2.1.3.2	SPECIFICATIONS	45
2.1.3.3	SAMPLE PREPARATION	46
2.1.3.4	MATERIALS	46
2.1.3.5	PROCEDURE	46
2.1.3.6	DATA INTERPRETATION	46
2.2	IGNITABILITY	47
2.2.1	BUNSEN BURNER TEST (UL-94)	47
2.2.1.1	INSTRUMENTATION	47
2.2.1.2	CALIBRATION	48
2.2.1.3	SAMPLE PREPARATION	49
2.2.1.4	MATERIALS	49
2.2.1.5	PROCEDURE	49
2.2.1.6	ANALYSIS	50
2.2.2	SINGLE-FLAME SOURCE TEST (ISO 11925)	50
2.2.2.1	INSTRUMENTATION	50
2.2.2.2	CALIBRATION	52
2.2.2.3	SAMPLE PREPARATION	52
2.2.2.4	MATERIALS	52
2.2.2.5	PROCEDURE	53
2.2.2.6	SURFACE EXPOSURE METHOD (FACE IGNITION)	53
2.2.2.7	EDGE EXPOSURE METHOD (EDGE IGNITION)	53
2.3	EASE OF EXTINCTION	54
2.3.1	LIMITING OXYGEN INDEX (LOI)	54
2.3.1.1	INSTRUMENTATION	55

2.3.1.2	CALIBRATION	55
2.3.1.3	SAMPLE PREPARATION	56
2.3.1.4	MATERIALS.....	56
2.3.1.5	PROCEDURE.....	56
2.4	HEAT RELEASE.....	56
2.4.1	CONE CALORIMETER	57
2.4.1.1	INSTRUMENTATION.....	57
2.4.1.2	CALIBRATION	58
2.4.1.3	SAMPLE PREPARATION	60
2.4.1.4	MATERIALS.....	60
2.4.1.5	PROCEDURE.....	61
2.4.1.6	DATA INTERPRETATION.....	61
2.4.2	PYROLYSIS COMBUSTION FLOW CALORIMETER.....	62
2.4.2.1	INSTRUMENTATION.....	62
2.4.2.2	SAMPLE PREPARATION	62
2.4.2.3	MATERIALS.....	62
2.4.2.4	PROCEDURE.....	63
2.5	CHAR ANALYSIS	63
2.5.1	SCANNING ELECTRON MICROSCOPE/ENERGY DISPERSIVE X-RAY (SEM/EDAX) ANALYSIS	63
2.5.1.1	INSTRUMENTATION.....	64
2.5.1.2	SAMPLE PREPARATION	65
2.5.1.3	PROCEDURE.....	65
2.5.1.4	DATA INTERPRETATION.....	65
2.5.2	DIAMOND ATTENUATED TOTAL REFLECTANCE/FOURIER-TRANSFORM INFRARED (DATR-FTIR)	65
2.5.2.1	INSTRUMENTATION.....	66
2.5.2.2	SAMPLE PREPARATION	66
2.5.2.3	PROCEDURE.....	66
2.5.2.4	DATA INTERPRETATION.....	67
<u>RESULTS AND DISCUSSION</u>		<u>68</u>
<u>CHAPTER 3. THERMAL DECOMPOSITION.....</u>		<u>68</u>
3.1	THERMOGRAVIMETRIC ANALYSIS	68
3.1.1	THERMOGRAVIMETRIC ANALYSIS IN AIR	68
3.1.1.1	Experiments on Viscosity	Error! Bookmark not defined.
3.1.1.2	Experiments on Fillers.....	72
3.1.1.3	Conditioned Samples	76
3.1.1.4	Calculated Thermogravimetric Curves.....	79
3.1.2	THERMOGRAVIMETRIC ANALYSIS IN NITROGEN	80
3.1.2.1	Effect of Variation of PEEK Viscosity on Thermal Decomposition	81
3.1.2.2	Effect of Various Additives on Thermal Decomposition.....	82
3.1.3	COMPARISONS BETWEEN 450G IN AIR AND NITROGEN	84
3.1.4	ACTIVATION ENERGY AND ARRHENIUS FACTOR DETERMINATION.....	86

3.2	SIMULTANEOUS THERMAL ANALYSIS – FOURIER TRANSFORM INFRARED (STA-FTIR)	88
3.2.1	STA-FTIR IN AIR.....	88
3.2.2	STA-FTIR IN NITROGEN	90
3.3	PYROLYSIS GAS CHROMATOGRAPHY – MASS SPECTROMETRY (PYGC/MS)	90
3.3.1	PEEK 450G	91
3.3.2	FILLED MATERIALS.....	94
3.4	SUMMARY	95
CHAPTER 4. FLAMMABILITY		97
4.1	UL-94	97
4.1.1	HORIZONTAL AND VERTICAL BURN	97
4.1.2	WET, DRY AND HUMID CONDITIONS	99
4.1.3	HIGHER FLAME TEMPERATURE	101
4.2	LIMITING OXYGEN INDEX (LOI)	103
4.2.1	WET AND DRY CONDITIONS	104
4.3	PYROLYSIS COMBUSTION FLOW CALORIMETER (PCFC)	105
4.3.1	EFFECT OF VISCOSITY	105
4.3.2	EFFECT OF FILLERS	107
4.4	CONE CALORIMETER	109
4.4.1	EFFECT OF THICKNESS ON BURNING BEHAVIOUR	109
4.4.2	EFFECT OF VISCOSITY ON BURNING BEHAVIOUR	115
4.4.3	EFFECT OF FILLERS ON BURNING BEHAVIOUR	118
4.4.4	SCATTER IN THE CONE CALORIMETER.....	121
4.4.4.1	Effect of PEEK Viscosity on t_{ig} and PHRR.....	122
4.4.4.2	Effect of Additives on Scatter	128
4.4.4.3	Char Heights Experiments.....	134
4.4.5	VARIED HEAT FLUX EXPERIMENTS	136
4.4.6	CONDITIONED EXPERIMENTS	140
4.4.7	0.5% CARBON BLACK (CB) PIGMENT EXPERIMENTS	141
4.4.8	PRESENCE OF 0.1, 0.5 AND 1 % CB EXPERIMENTS	147
4.4.9	PRESENCE OF 0.5% FILLER EXPERIMENTS	151
4.4.10	SURFACE MOISTURE EXPERIMENTS	154
4.4.11	WET, DRY AND HUMID CONDITIONING EXPERIMENTS	160
4.4.12	CRYSTALLINE AND AMORPHOUS SURFACE EXPERIMENTS.....	162
4.4.13	PROBLEMS WITH PEEK IN THE CONE CALORIMETER	167
4.5	SINGLE-FLAME SOURCE TEST (ISO 11925)	170
4.6	SUMMARY	172
CHAPTER 5. CHAR ANALYSIS		174
5.1	DIAMOND ATTENUATED TOTAL REFLECTANCE/FOURIER-TRANSFORM INFRARED (DATR-FTIR)	174
5.2	SCANNING ELECTRON MICROSCOPE/ENERGY DISPERSIVE X-RAY (SEM/EDAX)	177
5.3	¹³C NUCLEAR MAGNETIC RESONANCE	178

5.4 SUMMARY	181
<u>CHAPTER 6. THERMAL PROPERTY CALCULATIONS</u>	<u>183</u>
6.1 MOLAR GROUP CONTRIBUTIONS	183
6.1.1 THERMAL ANALYSIS	183
6.1.2 FLAMMABILITY	187
6.1.3 CHAR FORMATION.....	189
6.2 CONE CALORIMETER TIME TO IGNITION	192
6.3 THERMAKIN	195
<u>CHAPTER 7. CONCLUSIONS AND FURTHER WORK.....</u>	<u>197</u>
<u>REFERENCES.....</u>	<u>204</u>

INDEX OF FIGURES

FIGURE 1. REPEAT UNIT OF POLY(OXY-1,4-PHENYLENEOXY-1,4-PHENYLENECARBONYL-1,4-PHENYLENE) (PEEK)	1
FIGURE 2. DIAGRAMMATIC REPRESENTATION OF THERMOPLASTIC POLYMERS	4
FIGURE 3. DIAGRAMMATIC REPRESENTATION OF THERMOSET POLYMERS	4
FIGURE 4. AMORPHOUS AND SEMI-CRYSTALLINE POLYMER STRUCTURE	5
FIGURE 5. ACTIVATION ENERGY.....	6
FIGURE 6. SCHEMATIC DIAGRAM OF POLYMER BURNING [10]	11
FIGURE 7. SCHEMATIC VIEW OF SAMPLE ORIENTATION WITHIN LOI INSTRUMENT [31]	14
FIGURE 8. FRONT VIEW OF HB EXPERIMENTAL SET-UP [35].....	15
FIGURE 9. SCHEMATIC VIEW OF A CONE CALORIMETER [37]	16
FIGURE 10. TYPICAL HEAT RELEASE CURVES FOR DIFFERENT BURNING BEHAVIOURS [38]	17
FIGURE 11. HEAT RELEASE CURVES FOR SAMPLES WITH VARIED THICKNESSES (PMMA) [38]	17
FIGURE 12. REPEAT UNIT OF POLY ETHER ETHER KETONE	20
FIGURE 13. SPECIFIC HEAT RELEASE RATE FOR SEVERAL POLYMERS [32]	21
FIGURE 14. THERMAL DECOMPOSITION OF PEEK AND COMPOSITES IN N ₂ [10].....	22
FIGURE 15. THERMAL DECOMPOSITION OF PEEK AND COMPOSITES IN AIR [10]	23
FIGURE 16. CONE CALORIMETER HEAT RELEASE CURVES OF PEEK AND COMPOSITES [10]	24
FIGURE 17. PEEK DEGRADATION PRODUCTS AT 450°C.....	26
FIGURE 18. RECOMBINATION OF ADJACENT RADICALS TO FORM DIBENZOFURAN [52]	26
FIGURE 19. RECOMBINATION OF ADJACENT RADICALS TO FORM BIPHENYL [52]	28
FIGURE 20. PYROLYSIS OF SOLID RESIDUES TO FORM PHENYL PHENOL [52]	28
FIGURE 21. PEEK WITH INVOLVED CARBONS [56]	28
FIGURE 22. PEEK WITH CROSSLINKING AT C-5 [56]	29
FIGURE 23. PEEK WITH CROSSLINKING AT C-4 [56]	29
FIGURE 24. SCHEMATIC VIEW OF TGA APPARATUS.....	41
FIGURE 25. SCHEMATIC VIEW OF A PYGC/MS	45
FIGURE 26. FRONT VIEW OF VB EXPERIMENTAL SET-UP [35].....	48
FIGURE 27. SCHEMATIC VIEW OF A CONTROLLED VENTILATION CHAMBER [88]	51
FIGURE 28. SCHEMATIC VIEW OF TYPICAL SUPPORT AND BURNER POSITIONING [88]	52
FIGURE 29. POINT OF FLAME IMPINGEMENT FOR TEST SPECIMENS LESS THAN OR EQUAL TO 3 MM THICK [88].....	54
FIGURE 30. VIEW OF THE OXYGEN INDEX FRONT PANEL [31]	55
FIGURE 31. SCHEMATIC VIEW OF A PYROLYSIS COMBUSTION FLOW CALORIMETER	62
FIGURE 32. SCHEMATIC VIEW OF A SEM	65
FIGURE 33. SCHEMATIC DIAGRAM OF THE INTERACTION OF THE ATR CRYSTAL WITH INFRARED RADIATION	66
FIGURE 34. TGA OF 450G IN AIR	69
FIGURE 35. TGA WITH DIFFERENT HEATING RATES IN AIR	70
FIGURE 36. TGA AND DTG OF 90G, 150G AND 450G IN AIR	71
FIGURE 37. TGA AND DTG OF 450G, 450CA30 AND 450GL30 IN AIR.....	72
FIGURE 38. TGA AND DTG OF 450G AND 381TL30 IN AIR.....	73
FIGURE 39. TGA AND DTG OF 150G AND 150TI30 IN AIR	75
FIGURE 40. TGA OF 450G CONDITIONED IN AIR	76
FIGURE 41. TGA OF 450G CONDITIONED IN AIR – FIRST DECOMPOSITION STEP	77
FIGURE 42. TGA OF 450G CONDITIONED IN AIR – SECOND DECOMPOSITION STEP	78
FIGURE 43. TGA CALCULATED CURVES 450CA30 FROM CONSTITUENTS IN AIR.....	79
FIGURE 44. TGA CALCULATED CURVES 450GL30 FROM CONSTITUENTS IN AIR.....	80
FIGURE 45. 450G TGA IN NITROGEN	81

FIGURE 46. TGA OF 90G, 150G AND 450G IN NITROGEN.....	82
FIGURE 47. TGA OF 450G, 450CA30 AND 450GL30 IN NITROGEN	83
FIGURE 48. TGA OF 381TL30 AND 150TI30 IN NITROGEN	84
FIGURE 49. 450G TGA IN AIR AND NITROGEN COMPARISON	85
FIGURE 50. DIFFERENT VISCOSITY TGA IN AIR AND NITROGEN COMPARISON	85
FIGURE 51. ASTM KINETICS METHOD 450G	86
FIGURE 52. ASTM KINETICS METHOD 450CA30 AND 450GL30.....	87
FIGURE 53. 450G, 450CA30 AND 450GL30 ISO-CONVERSION COMPARISON.....	88
FIGURE 54. CARBON DIOXIDE FROM 450G PEEK IN AIR TO 900°C.....	89
FIGURE 55. BENZENE FROM 450G PEEK IN AIR TO 900°C.....	89
FIGURE 56. CARBON MONOXIDE FROM 450G PEEK IN N ₂ TO 900°C.....	90
FIGURE 57. PYGC/MS FLASH PYROLYSIS OF 450G AT 750°C	91
FIGURE 58. DIPHENYLETHER AND PHENOL PRODUCTION	92
FIGURE 59. PYGC/MS FLASH PYROLYSIS OF 450G AT 900°C	92
FIGURE 60. BIPHENYL PRODUCTION	93
FIGURE 61. PYGC/MS FLASH PYROLYSIS OF 450CA30 AT 900°C	94
FIGURE 62. PYGC/MS FLASH PYROLYSIS OF 450GL30 AT 900°C.....	94
FIGURE 63. PYGC/MS FLASH PYROLYSIS OF 381TL30 AT 900°C	94
FIGURE 64. PYGC/MS FLASH PYROLYSIS OF PEEK AND ADDITIVES AT 900°C.....	95
FIGURE 65. WET AND DRY SAMPLES POST UL-94	101
FIGURE 66. 450CA30 POST LOI.....	103
FIGURE 67. 450GL30 POST LOI	104
FIGURE 68. PCFC VISCOSITY EXPERIMENTS HEAT RELEASE RATES	106
FIGURE 69. PCFC ADDITIVES EXPERIMENTS HEAT RELEASE RATES.....	107
FIGURE 70. 150G 2.5 MM HEAT RELEASE RATE	109
FIGURE 71. 150G 3.2 MM HEAT RELEASE RATE	110
FIGURE 72. 150G 3.5 MM HEAT RELEASE RATE	111
FIGURE 73. 150G 6 MM HEAT RELEASE RATE	112
FIGURE 74. 150G 10 MM HEAT RELEASE RATE	113
FIGURE 75. 150G AVERAGE HEAT RELEASE RATE OF VARIED THICKNESSES.....	114
FIGURE 76. 90G 3.2 MM HEAT RELEASE RATE	115
FIGURE 77. 150G 3.2 MM HEAT RELEASE RATE	116
FIGURE 78. 450G 3.2 MM HEAT RELEASE RATE	117
FIGURE 79. VISCOSITY 3.2 MM AVERAGE HEAT RELEASE RATES	118
FIGURE 80. 450CA30 3.2 MM HEAT RELEASE RATE	119
FIGURE 81. 450GL30 3.2 MM HEAT RELEASE RATE	120
FIGURE 82. ADDITIVES EXPERIMENTS 3.2 MM AVERAGE HEAT RELEASE RATES.....	121
FIGURE 83. 90G 2.5 MM HEAT RELEASE RATE	123
FIGURE 84. RELATIONSHIP BETWEEN 90G T _{IG} AND PHRR.....	124
FIGURE 85. 150G 2.5 MM HEAT RELEASE RATE	125
FIGURE 86. 450G 2.5 MM HEAT RELEASE RATE	126
FIGURE 87. 600G 2.5 MM HEAT RELEASE RATE	127
FIGURE 88. T _{IG} AND PHRR CORRELATION BETWEEN ALL VISCOSITIES	128
FIGURE 89. 450CA30 2.5 MM HEAT RELEASE RATE	129
FIGURE 90. 450GL30 2.5 MM HEAT RELEASE RATE	130
FIGURE 91. 381TL30 2.5 MM HEAT RELEASE RATE	131
FIGURE 92. 450903 2.5 MM HEAT RELEASE RATE.....	132
FIGURE 93. VISCOSITY AND ADDITIVES 2.5 MM AVERAGE HEAT RELEASE RATES	133
FIGURE 94. CHAR HEIGHT VS. PHRR CORRELATION	135

FIGURE 95. CORRELATION BETWEEN PHRR AND CHAR HEIGHT	136
FIGURE 96. PEEK 450G CRITICAL HEAT FLUX FOR IGNITION 30-40 KW M ⁻²	137
FIGURE 97. PEEK 450G CRITICAL HEAT FLUX FOR IGNITION 35-37 KW M ⁻²	138
FIGURE 98. 450G 2.5 MM VARIED HEAT FLUX HEAT RELEASE RATES (GROUPED DATA)	139
FIGURE 99. 450G 2.5 MM CONDITIONED PLAQUES – AVERAGE HEAT RELEASE RATES	140
FIGURE 100. 150G 2.5 MM HEAT RELEASE RATE	142
FIGURE 101. 150903 2.5 MM HEAT RELEASE RATE.....	143
FIGURE 102. 450G 2.5 MM HEAT RELEASE RATE	144
FIGURE 103. 450903 2.5 MM HEAT RELEASE RATE.....	145
FIGURE 104. 150G, 150903 450G AND 450903 2.5 MM HEAT RELEASE RATE AVERAGES.....	146
FIGURE 105. 450G 2.5 MM WITH 0.1 % CB HEAT RELEASE RATE	147
FIGURE 106. 450G 2.5 MM WITH 0.5% CB HEAT RELEASE RATE	148
FIGURE 107. 450G 2.5 MM WITH 1% CB HEAT RELEASE RATE	149
FIGURE 108. 450G 2.5 MM VARIED CB EXPERIMENTS AVERAGE HEAT RELEASE RATES	150
FIGURE 109. 450G 2.5 MM WITH 0.5% KETJAN BLACK.....	151
FIGURE 110. 450G 2.5 MM WITH 0.5% ZEEOSPHERES.....	152
FIGURE 111. 450G 2.5 MM 0.5% FILLER EXPERIMENTS AVERAGE HEAT RELEASE RATES	153
FIGURE 112. 450G 2.5 MM ‘WET’ AND ‘DRY’ CONDITION HEAT RELEASE RATES COMPARISON AT 60 KW M ⁻²	155
FIGURE 113. 450G 2.5 MM ‘WET’ CONDITION 60 KW M ⁻² REMOVED AFTER 60 SECONDS.....	157
FIGURE 114. 450G 2.5 MM ‘DRY’ CONDITION 60 KW M ⁻² REMOVED AFTER 60 SECONDS.....	157
FIGURE 115. CROSS SECTION OF BUBBLED CONE CALORIMETER SAMPLES.....	158
FIGURE 116. 450GL30 2.5 MM ‘WET’ AND ‘DRY’ CONDITION HEAT RELEASE RATES COMPARISON AT 60 KW M ⁻²	159
FIGURE 117. 150G 2.5 MM ALL CONDITIONS COMPARISON HEAT RELEASE RATE AT 60 KW M ⁻²	161
FIGURE 118. 150G 2.5 MM AMORPHOUS SAMPLES WITH VARIED CONDITIONS HEAT RELEASE RATE AT 60 KW M ⁻²	163
FIGURE 119. 450G 2.5 MM AMORPHOUS SAMPLES WITH VARIED CONDITIONS HEAT RELEASE RATE AT 60 KW M ⁻²	163
FIGURE 120. 150G 2.5 MM CRYSTALLINE SAMPLES WITH VARIED CONDITIONS HEAT RELEASE RATE AT 60 KW M ⁻²	166
FIGURE 121. 450G 2.5 MM CRYSTALLINE SURFACE WITH VARIED CONDITIONS HEAT RELEASE RATE AT 60 KW M ⁻²	166
FIGURE 122. 90G 3.2 MM CONE CALORIMETER SAMPLE AFTER 50 KW M ⁻²	167
FIGURE 123. 450G 3.2 MM CONE CALORIMETER SAMPLE AFTER 50 KW M ⁻²	167
FIGURE 124. 450CA30 3.2 MM CONE CALORIMETER SAMPLE AFTER 50 KW/M ⁻²	168
FIGURE 125. 450GL30 3.2 MM CONE CALORIMETER SAMPLE AFTER 50 KW/M ⁻²	168
FIGURE 126. 450G WITH GRID CONE CALORIMETER SAMPLE AFTER 35 KW M ⁻²	169
FIGURE 127. 450G 3.2 MM WITH GRID HEAT RELEASE RATE	169
FIGURE 128. 450G 3.2 MM WITH AND WITHOUT GRID HEAT RELEASE RATE (GROUPED DATA).....	170
FIGURE 129. DATR-FTIR OF NATURAL PEEK FILM	174
FIGURE 130. DATR-FTIR OF NATURAL PEEK FILM AGED AT 400°C FOR 30 MINUTES	175
FIGURE 131. DATR-FTIR OF NATURAL PEEK FILM AGED AT 500°C FOR 20 MINUTES	176
FIGURE 132. CARBONYL SCISSION FOR 1-PHENOXY-4(4-PHENOXYL ALDEHYDE)	176
FIGURE 133. SEM IMAGE OF 450GL30 RESIDUE	177
FIGURE 134. ELEMENTAL ANALYSIS OF 450GL30 CONE CALORIMETER CHAR	178
FIGURE 135. PEEK REPEAT UNIT WITH ASSIGNED ¹³ C NMR PEAKS.....	178
FIGURE 136. ¹³ C NMR 400°C FOR 30 MINUTES 12K.....	179
FIGURE 137. ¹³ C NMR 600°C FOR 10 MINUTES 11.3K.....	180

FIGURE 138. ¹³ C NMR 650°C FOR 10 MINUTES 11.3K.....	181
FIGURE 139. PEEK ASSIGNED WITH STRUCTURAL GROUP CONTRIBUTIONS FOR DECOMPOSITION	184
FIGURE 140. PEEK ASSIGNED WITH MOLAR GROUP CONTRIBUTIONS.....	187
FIGURE 141. AVERAGE FLAMING HEAT RELEASE RATE (HRR) VS HEAT RELEASE CAPACITY (H _c) FOR NAMED POLYMERS [32]	189
FIGURE 142. PEEK ASSIGNED WITH STRUCTURAL GROUP CONTRIBUTIONS FOR CHAR	190
FIGURE 143. SCHEMATIC OF THE PROCESSES OCCURING IN THE CONE CALORIMETER, AS MODELLED BY THERMAKIN	196

INDEX OF TABLES

TABLE 1. CHAR YIELD (%) OF PEEK AND ITS COMPOSITES IN NITROGEN [10]	24
TABLE 2. DECOMPOSITION PRODUCTS OF PEEK BY TEMPERATURE – PYGC/MS [52]	25
TABLE 3. ONSET DECOMPOSITION (TD), PEAK MASS LOSS TEMPERATURE (TP), AND IGNITION (TIG) TEMPERATURES OF PEEK, PEI AND PPS [59]	32
TABLE 4. LOI AND UL-94 RATING FOR PEEK, PI, PEI AND PPS [59]	32
TABLE 5. MASS LOSS RATE (MLR) AND HEAT RELEASE RATE (HRR) AT IGNITION AND HEAT RELEASE CAPACITY AND CHAR YIELD OF PEEK, PI AND PEI [59]	32
TABLE 6. DECOMPOSITION TEMPERATURES OF GENERAL POLYMERS [60]	33
TABLE 7. UL-94 VB TEST CRITERIA	50
TABLE 8. TEMPERATURE CORRESPONDING TO 40% RESIDUE	75
TABLE 9. 450G, 450CA30 AND 450GL30 ASTM KINETICS	87
TABLE 10. UL-94 HORIZONTAL BURNING	98
TABLE 11. UL-94 DATA 90G, 150G AND 450G	98
TABLE 12. UL-94 DATA FOR 450G, 450CA30 AND 450GL30	99
TABLE 13. WET, DRY AND HUMID CONDITIONS SAMPLE MASS LOSSES AND GAINS	99
TABLE 14. WET, DRY AND HUMID CONDITIONS RESULTS	100
TABLE 15. UL-94 450G 50 W FLAME RESULTS	102
TABLE 16. UL-94 450G 60 W FLAME RESULTS	102
TABLE 17. LOI OF FILLED AND UNFILLED PEEK	103
TABLE 18. SAMPLE MASS LOSSES AND GAINS	104
TABLE 19. 450G WET AND DRY LOI RESULTS	105
TABLE 20. PCFC VISCOSITIES EXPERIMENTS SUMMARY OF DATA	106
TABLE 21. PCFC ADDITIVES EXPERIMENTS SUMMARY OF DATA	108
TABLE 22. 90 G 2.5 MM CONE CALORIMETER PROPERTIES	123
TABLE 23. 150G 2.5 MM CONE CALORIMETER PROPERTIES	125
TABLE 24. 450G 2.5 MM CONE CALORIMETER PROPERTIES	126
TABLE 25. 600G 2.5 MM CONE CALORIMETER PROPERTIES	127
TABLE 26. 450CA30 2.5 MM CONE CALORIMETER PROPERTIES	129
TABLE 27. 450GL30 2.5 MM CONE CALORIMETER PROPERTIES	130
TABLE 28. 381TL30 2.5 MM CONE CALORIMETER PROPERTIES	132
TABLE 29. 450903 2.5 MM CONE CALORIMETER PROPERTIES	133
TABLE 30. CHAR HEIGHTS	135
TABLE 31. 450G 2.5 MM VARIED HEAT FLUXES CONE CALORIMETER PROPERTIES	139
TABLE 32. AVERAGE PROPERTIES FOR 2.5 MM CONDITIONED SAMPLES	141
TABLE 33. 150G AND 450G CB PIGMENT CONE CALORIMETER PROPERTIES	146
TABLE 34. 450G VARIED CB PIGMENT CONE CALORIMETER PROPERTIES	150
TABLE 35. 450G 0.5% FILLER CONE CALORIMETER PROPERTIES	153
TABLE 36. EFFECT OF BLACK SAMPLES ON T_{IG} SCATTER	154
TABLE 37. 450G 2.5 MM ‘WET’ AND ‘DRY’ SAMPLE GAINS AND LOSSES	155
TABLE 38. 450G 2.5 MM ‘WET’ AND ‘DRY’ CONE CALORIMETER PROPERTIES	156
TABLE 39. 450GL30 2.5 MM ‘WET’ AND ‘DRY’ SAMPLE GAINS AND LOSSES	158
TABLE 40. 450GL30 2.5 MM ‘WET’ AND ‘DRY’ CONE CALORIMETER PROPERTIES	160
TABLE 41. WET, DRY AND HUMID CONDITIONS AND DETAILS	160
TABLE 42. 150G ALL CONDITIONS CONE CALORIMETER PROPERTIES	161
TABLE 43. 150G AND 450G AMORPHOUS SAMPLES WITH VARIED CONDITIONS CONE CALORIMETER PROPERTIES AT 60 KW M^{-2}	164
TABLE 44. 150G AND 450G CRYSTALLINE SAMPLES WITH VARIED CONDITIONS CONE CALORIMETER PROPERTIES AT 60 KW M^{-2}	164

TABLE 45. ISO 11925 FOR 'NATURAL' PEEK AT VARIED THICKNESSES	171
TABLE 46. ISO 11925 FOR 'BLACK' PEEK AT VARIED THICKNESSES	171
TABLE 47. SUMMARY OF STRUCTURAL GROUP CONTRIBUTIONS FOR DETERMINATION OF $T_{D,1/2}$	185
TABLE 48. SUMMARY OF DECOMPOSITION MOLAR GROUP CONTRIBUTION CALCULATIONS	186
TABLE 49. SUMMARY OF MOLAR GROUP CONTRIBUTIONS AND THEIR MOLE FRACTIONS	188
TABLE 50. SUMMARY OF STRUCTURAL GROUP CONTRIBUTIONS AND THEIR CHAR-FORMING TENDENCIES	190
TABLE 51. SUMMARY OF FLAMMABILITY MOLAR GROUP CONTRIBUTION CALCULATIONS	191
TABLE 52. TIME TO IGNITION PARAMETERS, PREDICTION AND COMPARISON WITH ACTUAL DATA AT 50 KW M ⁻²	193
TABLE 53. T_{IG} CALCULATED AND EXPERIMENTAL FOR VARIED HEAT FLUXES	194
TABLE 54. T_{IG} CALCULATED AND EXPERIMENTAL FOR VARIED THICKNESSES	195

ACKNOWLEDGEMENTS

I would like to thank the following for the assistance given, without which this would not have been possible:

Professor T. Richard Hull at the University Of Central Lancashire's Centre of Fire and Hazard's Science, PhD Director of Studies for his inspiration, dedication and guidance throughout this project and more importantly for having faith in me on the many occasions when I'd doubted myself.

Mike Percy, John Grasmeyer and Dianne Flath at Victrex plc for their technical advice, time and extensive knowledge of PEEK.

Dr. Richard W. McCabe at the University Of Central Lancashire's Centre for Material's Science, second supervisor for his broad familiarity with organic chemistry and assistance with decomposition mechanisms and studies.

Dr. Richard E. Lyon at the Federal Aviation Administration (FAA) Fire Research Program, second supervisor for the opportunity to visit and make use of his laboratory (and colleagues!) and to experience the hidden gem on the east coast: Atlantic City.

The Engineering and Physical Science Research Council (EPSRC) and Victrex plc for granting the Industrial CASE PhD Studentship award (Number 07001444).

All the members of the Centre of Fire and Hazard's Science past and present, namely Jen and Cameron for the lunchtime 'meetings', attempts at sport and general laboratory debauchery, Artur for when the conversations turned from fire to politics and history and David and Luke for always putting the whole thing into perspective. Eternal gratitude is expressed to Steve Harris and John Milnes for taking on maintenance challenges and to those in the Material's Laboratory for granting 'cream cake' favours.

Finally, my family and friends, whose combined support has been invaluable, I would like to thank my mother and father for instilling ambition but never expecting too much, my brothers for the years of constant ridiculing which they still insist was 'character building', my best friends Lisa and Rachel for their calming influence and for generally keeping me sane and James for being so patient.

CHAPTER 1. INTRODUCTION

Polymers are fast replacing traditional materials such as metals and ceramics in many industrial sectors. In many cases, polymers and their composites are now being used where the fire risk scenario is dissimilar to any encountered previously. As well as ignition resistance and a low rate of heat release, engineering polymers are now required to resist burn-through and maintain structural integrity whilst continuing to provide protection when exposed to fire or heat.

Poly(oxy-1,4-phenyleneoxy-1,4-phenylenecarbonyl-1,4-phenylene) (PEEK), an aryl poly ether ether ketone, is one such engineering polymer, discovered by Imperial Chemical Industries (ICI) in 1978 [1].

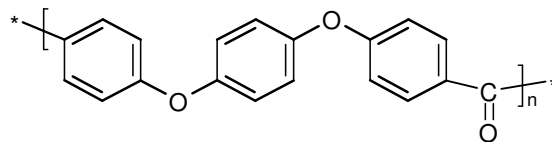


FIGURE 1. REPEAT UNIT OF POLY(OXY-1,4-PHENYLENEOXY-1,4-PHENYLENECARBONYL-1,4-PHENYLENE) (PEEK)

Its excellent thermal, chemical and mechanical properties have allowed for its use in a variety of high performance applications: the polymer has recently been adopted in the aviation and automotive industries where conventional thermally durable materials, such as metals, are being replaced by lighter weight, high thermal stability polymers [2] [3] [4]. As an example, PEEK has around half the density of aluminium whilst retaining the same tensile strength. To date, little research has been completed on the flammability of poly(aryletheretherketones) with more attention assigned to the material's thermal [5] [6] and thermo-kinetic properties [7] [8] [9]. As a result of the increased interest in engineered polymers such as PEEK and its composites, robust flammability data is necessary for applications requiring lightweight fire-safe performance. The normal semi-crystalline PEEK has a glass transition temperature (T_g) of 143°C, a continuous use temperature of 260°C, a melting point (T_m) of 343°C and an onset of decomposition temperature between 575 and 580°C [10] [11], and thus, is one of the most thermally stable thermoplastic polymers available.

The aim of the project is to acquire an understanding of the decomposition, flammability and burning behaviour of PEEK, in order to develop fire safe applications for PEEK or PEEK-based materials, and thus open up new markets. An insight into polymer flammability is provided in Chapter 1 which includes the polymer decomposition, ignition and burning processes and a review of the literature with regards to fire retarding PEEK. Chapter 2 presents the details on the experimental procedures utilised as standards for industry and within this thesis. The results are shown in Chapters 3-6. Chapter 3 deals with the thermal decomposition of PEEK and its compounds, employing techniques such as thermogravimetric analysis (TGA) and Pyrolysis Gas Chromatography coupled with Mass Spectrometry (pyGC/MS). Chapter 4 presents a study on the flammability of PEEK and the effects of thickness, viscosity, pre-conditioning and moisture on this parameter. Analysis of the 50% residue which remains after decomposition and flammability studies is completed in Chapter 5 utilising Nuclear Magnetic Resonance Spectroscopy (NMR) and Scanning Electron Microscopy (SEM). Thermal property calculations comprise an important part of the screening process when developing materials and Chapter 6 determines the contributions to decomposition and flammability made by the molar groups which make up PEEK.

1.1 Polymer Structure

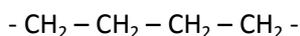
A polymer is a large molecule constructed from many smaller repeating units. These smaller molecules are referred to as monomers. When the molecular weight of the structure surpasses 1500 g mol^{-1} (the upper limit for molecular distillation) [12] the material is classed as a polymer. When the polymer is constructed from the same monomer unit, it is termed a homopolymer;



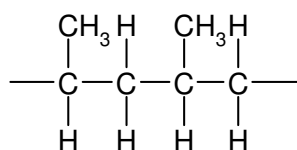
When the polymer is composed of differing monomer units, it is termed a copolymer;



Polyethylene (PE) is the simplest carbon-carbon chain polymer:



Other polymers are obtained when one or more of the hydrogen atoms are replaced by other atoms or groups of atoms. The simplest example of this, using the polyethylene structure, is a methyl group substituting alternate hydrogen atoms, as in polypropylene (PP):



PP

Such polymers (in the form of plastics, rubbers, adhesives, and fibres) are all in common use. Polymeric materials are popular due to the range of properties they exhibit which can easily be tailored for a specific application. They are also popular due to the ease with which they can be processed [13]. In certain industries, light-weight, high performance polymeric materials are often favoured over their metal and ceramic equivalents [10].

Polymers can be divided into two classes; thermosetting and thermoplastic. The key difference in their classification is how the molecules behave when heated. Polymers of a thermosetting nature do not soften where as thermoplastics tend to soften, although regain their rigidity upon cooling. Both are constructed from a large number of molecules and the differences in their thermal behaviour can be attributed to differences in internal structure.

The macromolecules which make up thermoplastic polymers form a long-chain structure with relatively little branching, as seen in Figure 2. These molecules are not linked to each other chemically but do intertwine and interact physically. When heated, the molecules within the chain are able to move freely in relation to each other thus enabling the material to soften and flow. On cooling, rigidity is regained.

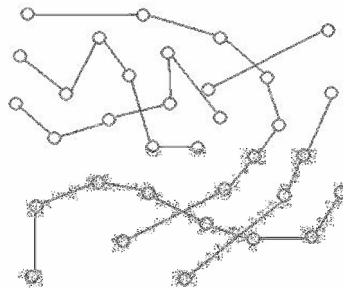


FIGURE 2. DIAGRAMMATIC REPRESENTATION OF THERMOPLASTIC POLYMERS

The macromolecules which make up thermosetting polymers are often highly branched and joined chemically through crosslinking, forming a complex network as shown in Figure 3. Upon heating, as a result of the restraints of the chemical crosslinks, there is a lesser possibility of free movement; and therefore, the material remains rigid.

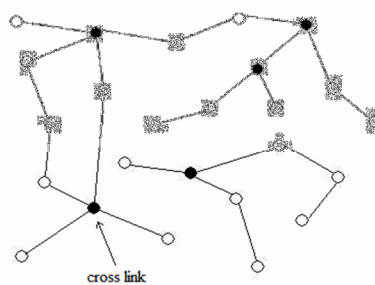


FIGURE 3. DIAGRAMMATIC REPRESENTATION OF THERMOSET POLYMERS

Non-crystalline polymers are those which consist of high levels of irregularity within their structure. Irregularity may arise from extensive chain branching, co-polymerisation with significant amount of two or more monomers and the presence of bulky side groups [14]. These aspects are referred to as amorphous. For polymers to be crystalline, some stereo-regularity is essential, either along the polymer backbone or among side chains. Polymers exist in both the amorphous and crystalline form. Some partially crystalline (semi-crystalline) polymers consist of crystalline regions dispersed within an amorphous material, as shown in Figure 4. A polymer with increased crystallinity has improved abrasion resistance, greater hardness and higher density [15].

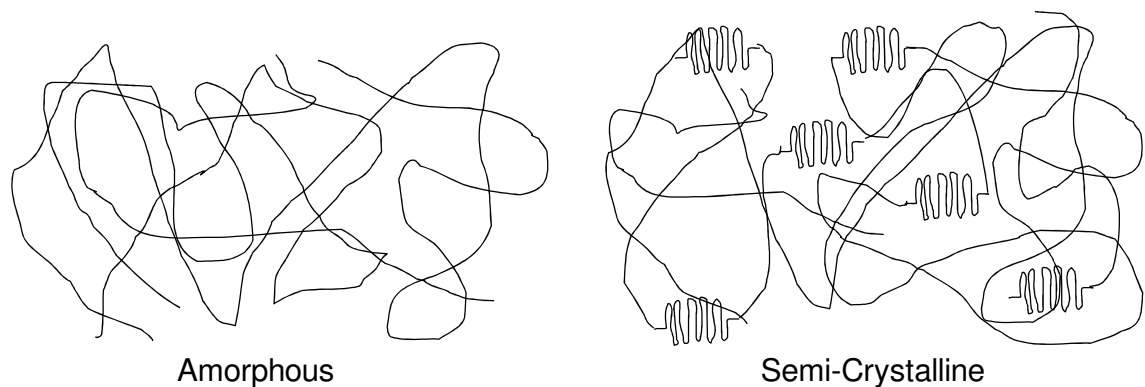


FIGURE 4. AMORPHOUS AND SEMI-CRYSTALLINE POLYMER STRUCTURE

1.2 Polymer Decomposition

When a polymeric material is exposed to excessive heating, both chemical and physical changes occur. Firstly, the polymer is heated to a temperature at which it starts to decompose and begins yielding volatile products that are usually combustible. The formation of these products is a much more complex occurrence than the process of volatilisation in flammable liquids. Additionally, whether or not the polymer melts before decomposition is dependent upon the degree of crosslinking and its stability.

The initial stage of decomposition involves degradation of the polymer chain which can occur through a variety of mechanisms – shear action, chemical attack, and nuclear, thermal, ultraviolet and ultrasonic radiation [16]. The energy required for degradation to occur, or for any chemical reaction to occur is referred to as the activation energy. For a

reaction to proceed there should be a significant number of molecules with energy equal to, or greater than the activation energy. The concept is shown graphically in Figure 5. The energy required for the reaction to proceed from X to Y is greater than that required to return to X. The difference in energy is referred to as the enthalpy of formation (ΔH) which is defined as the change in enthalpy that required for the formation of one mole of a substance in its standard state from its constituent elements (also in their standard states).

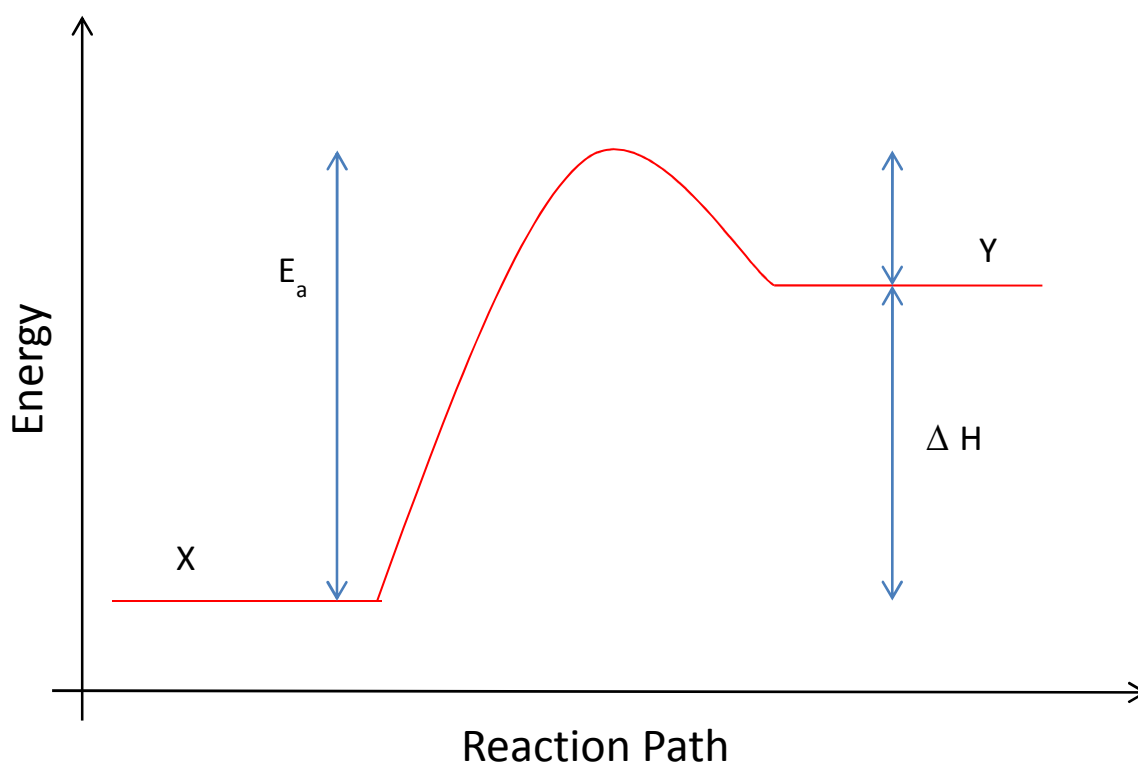


FIGURE 5. ACTIVATION ENERGY

Classical chemical kinetics also describes the Arrhenius factor (A) or the frequency factor, relating to the number of molecular collisions and their orientations. The Arrhenius equation shows the relationship between the reaction rate and these factors. The activation energy is expressed as:

$$k = Ae^{-E_a/RT}$$

(1)

Where

R is the universal gas constant ($8.314 \text{ J K}^{-1} \text{ mol}^{-1}$)

T is the temperature (in K)

k is the reaction rate coefficient

The combination of an exponential function and a pre-exponential is a very versatile way of expressing a wide range of numerical relationships. However, apart from very simple chemical reactions involving a single step, it is probably better to consider it a tool for understanding the temperature dependence of reaction rates than a quantitative description of the chemical processes occurring.

Upon further heating, the material begins to decompose. There are four common mechanisms through which polymer decomposition occurs. Some polymers involve combinations of mechanisms, while others follow a single one.

In thermoplastic materials, the most common of the mechanisms involves the breaking of chemical bonds in the main polymer chain. Chain scission can occur in random parts of the polymer chain (random chain scission) which is more common, or at the end of the polymer chain (end chain scission) which is less common. End chain scission (often known as 'unzipping') will result in the production of monomer units, whereas random chain scission can produce monomers, oligomers (polymer units with fewer than ten monomer units) and a range of reactive chemical species. The process often involves free radicals and features all the steps of a radical chain reaction: initiation, propagation, branching and termination.

Chain stripping occurs through reactions which remove side-chain substituents and result in the loss of small molecules. Elimination reactions are often followed by cross-linking cyclisation reactions involving side chains and groups. In elimination reactions, the side groups of the polymer chain are broken; these side groups then tend to react with other side groups which have been lost through the same process, the products of which are small enough to be volatile. In cyclisation reactions, two adjacent side groups form bonds between each other resulting in a cyclic structure. This process is important in char formation as the product is much richer in carbon than the original polymer. These char structures, at very high temperatures, will tend to continue breaking down by chain scission.

Cross-linking is a reaction mechanism that partially involves the main chain. The process generally occurs after chain stripping and involves the creation of bonds between two

adjacent polymer chains. This process, along with chain stripping, is also important in char formation due to the generation of structures which are more compact, and therefore, less easily volatilisable. Melting temperature can also be increased through this process. The presence of char on the surface of the solid phase reduces the rate of flammable gas production. In addition, the char also forms a barrier between the source of the heat and the virgin polymeric material present below that layer. Char formation, generally reduces flammability; however, solid-phase char combustion (which generally occurs at extremely high temperatures) can cause sustained smouldering combustion.

Although the decomposition products vary depending upon the composition of the polymer, rate of volatile development and the rate of temperature increase [17], generally, the decomposition process produces two types of material; the polymer chain residue and the resulting polymer fragments. The polymer chain residue will continue to provide structural integrity; the resulting polymer fragments on the other hand, at a high enough temperature and in the presence of a significant amount of oxygen are highly prone to oxidation, producing heat and flaming in the gas phase [17].

1.2.1 Methods for Studying Polymer Decomposition

The processes involved in the decomposition of polymers can be measured in various ways to obtain such information as rate of decomposition and identification of decomposition products. Thermogravimetric Analysis (TGA) is a technique that provides quantitative decomposition information with regards to polymeric materials. The sample is subjected to a temperature regime (which usually consists of a constant heating rate) and is weighed continuously to give a measurement of mass loss or gain as a function of temperature. As the material is heated, it can lose mass through drying or liberation of gases or volatiles as well as gain mass by reacting with the atmosphere in which the sample is being tested. The mass loss in an inert atmosphere, such as nitrogen, is more representative of the production of fuel after ignition has occurred. This is because the concentration of oxygen under a flame is close to 0% [18]. Even in sample decomposition before ignition, the existence of vapour bubbles in the polymer matrix shows that fuel formation is a predominantly anaerobic process, with the exception of polymers which are very susceptible to surface oxidation, such as polypropylene. Thermal stability of the polymer can be evaluated from the data produced. TGA can be used to

study degradation kinetics and factors affecting thermal stability including crystallinity, molecular mass, effects of orientation, and copolymerisation [19].

In TGA sample sizes are kept small to prevent bulk effects and to avoid thermal gradients being set up within the sample at elevated temperatures [19]. The method is utilised to determine the activation energy (E_a) and Arrhenius factor (A) for various reactions. These parameters can be determined using several methods. The ASTM method [20] employs Kissinger's equation where the pre-exponential factor (A) is evaluated on assumption of a first order reaction. The iso-conversion method assumes that the degree of conversion (α) can be assigned to each point of the curve and for each conversion, E_a and A determined [21]. Determining the activation energy and Arrhenius factor are important when using computer models to investigate the processes occurring during thermal decomposition and pyrolysis. This is further discussed in Chapter 6.

Differential Thermogravimetry (DTG) is identical to the TGA excluding that the results are presented as the differential of mass loss over time giving mass loss rate versus temperature. DTG curves also provide a good indication as to when the various stages of polymer decomposition occur and the order in which they occur. This can be used to determine the effectiveness of additives in the mixture.

In Differential Thermal Analysis (DTA), a sample and inert reference sample with approximately the same heat capacity are subjected to the same temperature programme. If the decomposition process of the sample is endothermic, the temperature of the sample will trail behind the reference material. If the process is exothermic, then the temperature of the sample will exceed that of the reference. The differential temperature is then plotted either against time or temperature. Differential temperatures can also be seen in two inert samples which respond differently when heated. As a result, DTA curves can be used to study thermal properties which do not lead to a change in enthalpy, for example, when no heat is absorbed or released by the process.

Differential Scanning Calorimetry (DSC) is a microscale technique for quantifying the energy absorbed or released during controlled heating. The heat flow is measured by maintaining a thermal balance between the reference and sample, in two separate pans, by varying the current which passes through the heaters under each pan. The heating of a sample

and reference pan proceeds at the same (predetermined) heating rate until heat is either emitted or consumed by the sample. The system maintains a constant temperature between the sample and reference by, for example, feeding excess current into the sample if an endothermic event takes place and as a result, the temperature of the sample is less than that of the reference. The current required to maintain the temperature between these two pans is recorded [15].

The products of decomposition can be qualified and quantified through Pyrolysis Gas Chromatography coupled with Mass Spectrometry (pyGC/MS). The pyrolyser can be temperature programmed in the same way as a TGA, but as the sample size is smaller, faster heating rates are possible, thus products of thermal decomposition in air or nitrogen may be analysed by GC-MS. This technique can provide information with regards to the combustibility and toxicity of the products of decomposition. The sample can be heated to temperatures of interest for the material's decomposition by the pyrolyser and then transferred into the Gas Chromatograph to determine the products of combustion at a specific stage of pyrolysis. Provided these products remain volatile, analysis can be readily undertaken and coupling with the Mass Spectrometer allows for structural identification and even semi-quantitative concentrations to be determined.

1.3 Polymer Combustion

Polymer combustion can be broken into a series of events: (a) heating of the polymer; (b) decomposition; (c) ignition and (d) combustion [10]. The thermal decomposition of the solid material brings about the formation of flammable volatiles (mainly in the form of gaseous fuel vapours) which then react with the oxidant in the air above the condensed phase, slowly at first, then as a critical concentration of free radicals is reached, ignition occurs resulting in flaming combustion above the solid material. Part of the heat produced during this process is transferred back to the solid so the gaseous fuel vapours and volatiles will be replaced. The consequence of this is a continuous feedback loop where the material can maintain or increase the amount of burning.

1.3.1 Polymer Burning

In the presence of a significant amount of oxygen, the combustible gases and low molecular mass products of decomposition can ignite. This phenomenon either requires an external source of ignition such as a 'pilot' (an electrical source or independent flame) or can occur through 'auto-ignition' where flames spontaneously develop above the polymer, occurring typically 200°C above the piloted ignition temperature [22]. The products of decomposition diffuse to the flame front. Ignition occurs when the heat transferred from the flame to the polymer is sufficient to regenerate a corresponding amount of fuel. This is shown below:

$$\chi \times \Delta H_{\text{combustion}} > \Delta H_{\text{gasification}}$$

Where χ = the fraction of heat released to be transferred back to the polymer.

After the material has ignited, the polymer acts to propagate the fire and self sustaining combustion can occur in either oxygen or air [10]. The heat produced by the combustion of polymer fragments is fed back to the polymer surface and so a greater volume of volatile products are available and the combustion cycle is sustained.

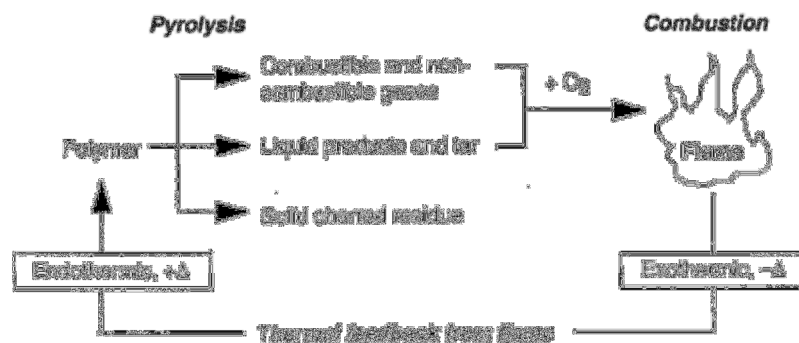


FIGURE 6. SCHEMATIC DIAGRAM OF POLYMER BURNING [10]

This is shown pictorially in Figure 6. The heat produced by combustion increases the temperature of the volatile polymer fragments and non combustible gases surrounding the flame, which increases heat transfer through conduction. These gases then expand, increasing heat transfer by convection and heating the solid particles entrained in the flame which results in increased heat transfer by radiation [22].

1.3.2 Common Burning Products

The nature of the products of combustion for a given polymer depends on the following:

- The combustion model (smouldering, flaming, or thermal degradation);
- The availability of air; and
- The addition of chemical agents for retardation purposes [23].

Commonly, the products associated with the combustion of hydrocarbon materials such as polymers are carbon monoxide, carbon dioxide, oxygen, water and carbon in the form of soot [23].

1.3.3 Techniques for Measuring Polymer Burning Processes

Polymer flammability has no intrinsic meaning; the flammability of a polymer is defined by the method used to measure it [24]. Flammability has been described as the ease at which a substance will ignite [25]. Such methods are fundamental in the screening and evaluation of fire retardant materials. A variety of small scale methods are available for this purpose such as the Limiting Oxygen Index (LOI) and Underwriter's Laboratory 94 Test (UL-94). Small-scale tests require small sample sizes and are relatively inexpensive to perform, however can seldom be related to the performance of the end-use product. Another option would be large-scale fire testing and, although this method provides information on how a material would behave in a real fire scenario, it is both expensive and time consuming.

Currently, the cone calorimeter is considered to be the best bench-scale test in use due to the variety of flammability parameters it produces, and is employed as a means of predicting how a material will behave in a real fire scenario. The method does have its limitations: the test conditions are only specific to a well ventilated fire scenario and so results cannot be attributed to under-ventilated fires or post flashover fires [26].

Techniques employed for measuring the conditions created by the ignition and burning processes of a polymer are numerous and varied. The majority of fire tests in common use aim to determine the following fire properties of materials:

- Ease of ignition – how readily the material ignites;
- Rate of flame spread – how rapidly fire spreads across a surface;

- Rate of heat release – how much heat is released and how quickly;
- Ease of extinction – how easily the flame chemistry leads to extinction;
- Smoke/Toxic gas evolution – evolution rate, amount, and the composition of smoke released during the various stages of a fire [27].

Many authors ascertain that the single most important parameter for determining a material's fire hazard is its heat release rate (HRR) [28] [29].

When selecting a test method, one needs to determine what the end purpose of the test will be. In fire testing, there are generally two end purposes:

- To meet a regulatory requirement; and
- To demonstrate that the material being tested will perform adequately in a specific fire scenario [30].

It has been stated that flammability is both a function of gas and solid phase chemistry [10]. For this reason, a variety of techniques have been employed to study the numerous parameters used to determine this concept.

1.3.3.1 Limiting Oxygen Index (LOI)

The BS EN ISO 4589-2 [31] is shown in Figure 7. This standard measures the ease of ignition of a sample. In the Limiting Oxygen Index (LOI), a candle-like sample is supported in a vertical glass chimney and a slow stream of oxygen/nitrogen mix is fed in. There are two procedures for this test; 'top surface ignition' and 'propagating ignition'. The sample is then ignited according to the procedure and the duration of burning after ignition and extent of burning are recorded. The oxygen concentration is then adjusted accordingly to give an oxygen index value [32]. The results are expressed as oxygen index values by volume percentage which provides a value that can be used in comparison with other polymeric materials. Since the method was developed for utilisation with polymers in 1966 [33], the LOI has found use as a means of screening and ranking polymeric materials, in particular, those of a flame retardant nature. The higher the material's oxygen index, the better it will be able to retard a flame. Polymers which have a LOI of less than 21% are referred to as flammable whereas polymers with a LOI greater than 21% are said to be inherently flame retardant and those with a LOI of over 30% are said to be self-extinguishing [34]. This notion is somewhat misleading and it

should be noted that materials with a LOI greater than 21% are still capable of burning in air should the material become involved in a fire situation.

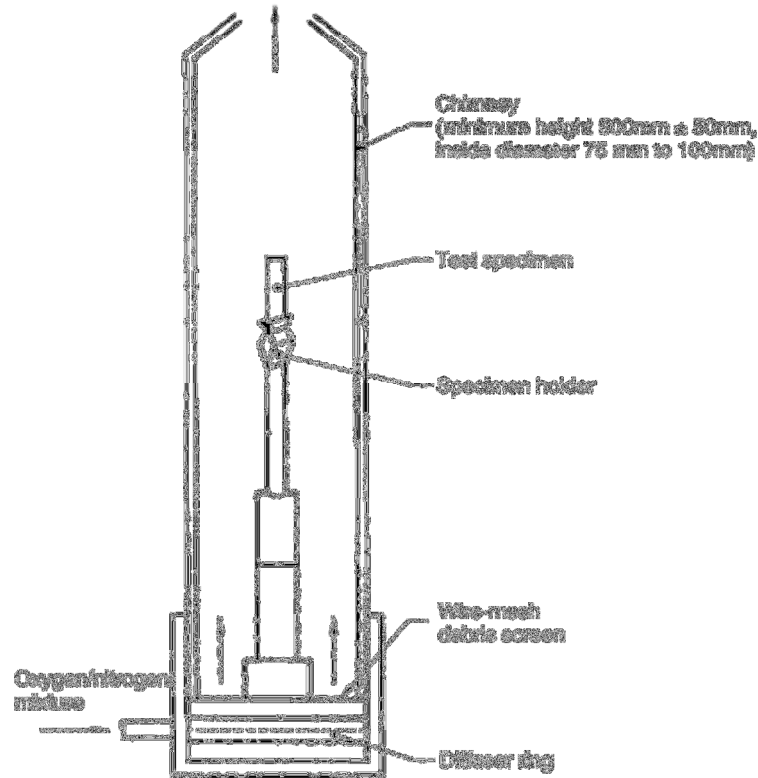


FIGURE 7. SCHEMATIC VIEW OF SAMPLE ORIENTATION WITHIN LOI INSTRUMENT [31]

1.3.3.2 UL-94

To measure the ease of ignition, ease of extinction and rate of flame spread, the most common small flame test for plastics is the Underwriter's Laboratory (UL) 94 standard. The UL-94 standard is arranged and operated as stated in BS EN 60695-11-10 [35], a diagram of one sample orientation for this standard is shown in Figure 8. The standard contains two test methods: the horizontal burning test and the vertical burning test, the latter being more stringent due to vertical upward propagation. These methods determine linear burning rate, after flame/afterglow times and damaged length of the specimens.

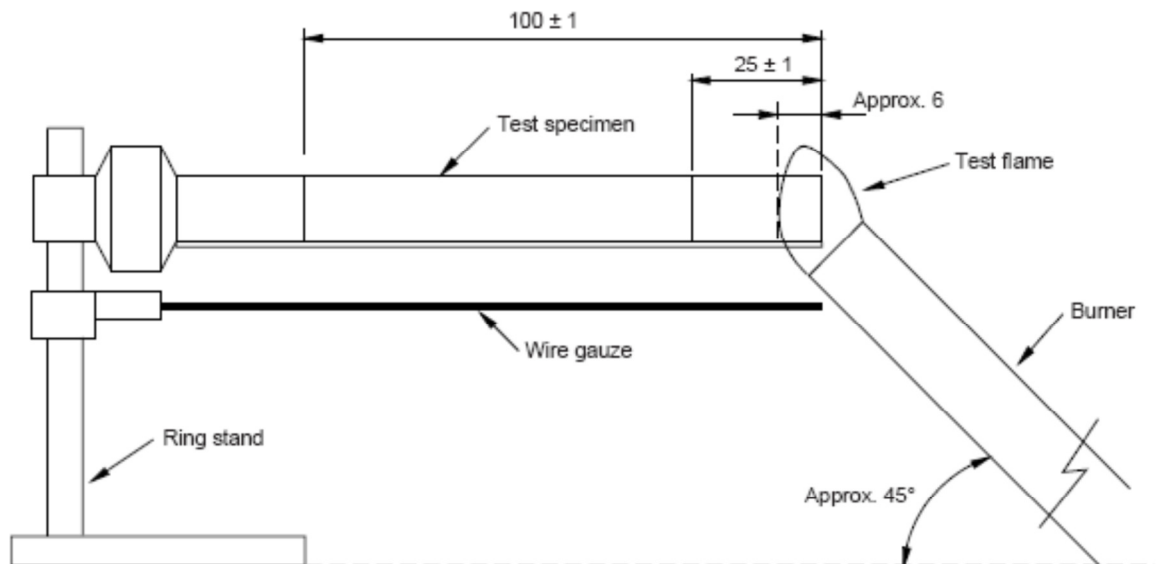


FIGURE 8. FRONT VIEW OF HB EXPERIMENTAL SET-UP [35]

Specimens for the horizontal burning test should equal 125 mm in length, 13 mm in width and should not have a thickness greater than 13 mm. The test flame is applied for 30 seconds or before the flame front reaches the 25 mm mark. Following the removal of the burning source, the duration of the after flame is measured as is the damaged length if the flame travels across the specimen. The material is then given a classification of HB, HB40 or HB75 depending on specified criteria [35].

For the UL-94 vertical burning test, the conditions and measures are slightly varied. The burner is applied to the specimen for two ten-second periods and the after flame and afterglow times are measured. Again there are three criteria, V-0, V-1 and V-2. The V-0 criterion is the most stringent and emphasises that the total after flame time for the first or second burner application must not exceed 10 seconds, the material must not drip and consequently ignite the cotton wool that is placed under the specimen. Additionally, specimens must not burn fully to the top of the clamp.

1.3.3.3 Cone Calorimeter

A method for measuring several of the parameters related to flammability is by use of the cone calorimeter [36] [37] as shown in Figure 9.

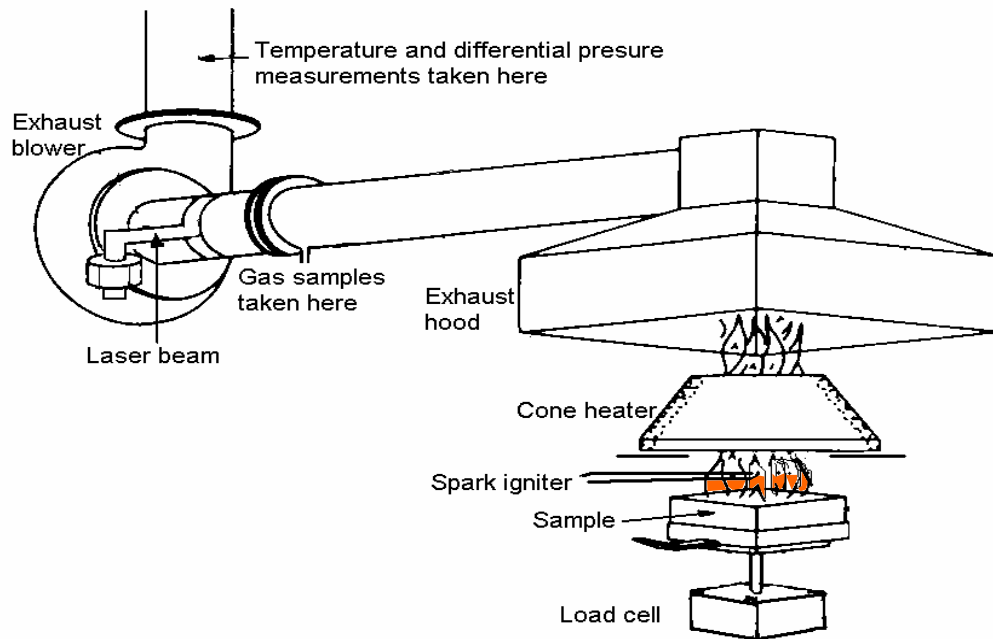


FIGURE 9. SCHEMATIC VIEW OF A CONE CALORIMETER [37]

The method is based on the principle that the net heat of combustion is proportional to the amount of oxygen required for combustion. It has been established that approximately 13.1×10^3 kJ of heat are released per kilogram of oxygen that is consumed. The specimens are subjected to a radiant heat source and measurements are made of oxygen concentration and exhaust gas flow rates. Specimens are 100 mm by 100 mm and may be up to 50 mm thick. The standard is particularly useful for fire retardant polymer formations which may not be ignited initially by a direct source by thermal radiation from nearby flames [23] such as wall or ceiling materials. The thermal radiation can be set for any heat flux between 0 and 100 kW m^{-2} .

The cone calorimeter is used to measure the heat release rate, mass loss rate, smoke production, flame spread and ignition properties [10]. The material is heated uniformly by a radiant heating source and then ignited. The ignition source within the cone calorimeter is a spark igniter. The material is weighed constantly to determine mass loss as a parameter in its own right, and as a function of time. Smoke obscuration can also be measured using a laser photometer system. The cone calorimeter is arranged and operated as stated in ISO 5660-1 [36].

There is little in the literature regarding the interpretation of cone calorimeter heat release rate curves. Some work has been completed [38] to determine the typical shapes of

curves created by different materials as shown in Figure 10 and different thicknesses as shown in Figure 11.

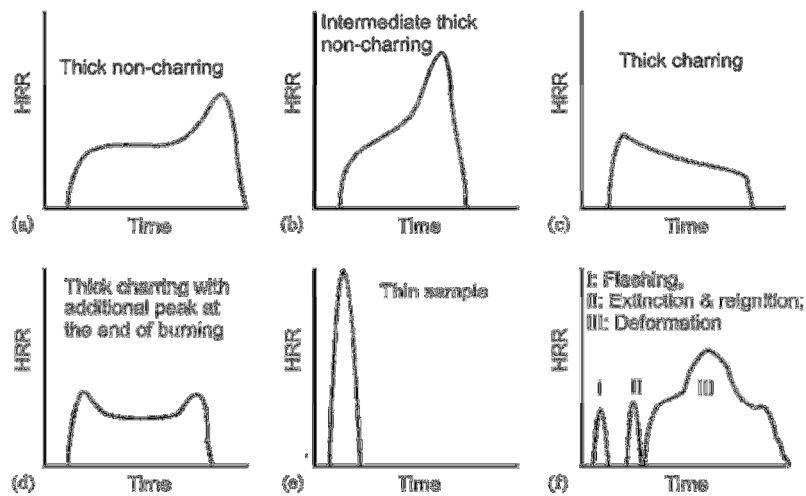


FIGURE 10. TYPICAL HEAT RELEASE CURVES FOR DIFFERENT BURNING BEHAVIOURS [38]

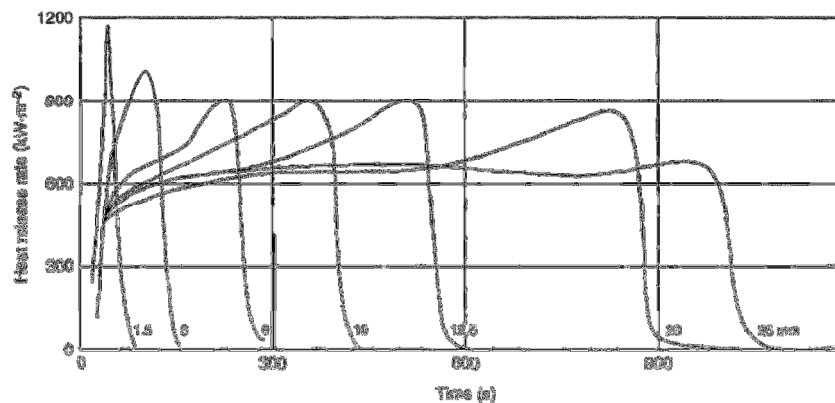


FIGURE 11. HEAT RELEASE CURVES FOR SAMPLES WITH VARIED THICKNESSES (PMMA) [38]

1.3.3.4 Pyrolysis Combustion Flow Calorimeter

The Pyrolysis Combustion Flow Calorimeter (PCFC) apparatus is utilised to determine the flammability characteristics of polymeric materials by use of combustion calorimetry on a micro-scale. The apparatus is used according to ASTM D 7309 [39]. The method was developed by the FAA [28] [106], and uses the principle of oxygen consumption as its basis. Similar to the cone calorimeter, the method can determine several of the parameters related to flammability

including the heat release rate, the heat of combustion, char yield and ignition temperature, however unlike the cone calorimeter, the apparatus requires only milligram quantities of sample. As the technique utilises oxygen consumption calorimetry for determining heat release rate (similar to the cone calorimeter) using these techniques together can provide valuable heat release data at both the micro and bench scale.

1.3.3.5 Small Flame Ignitability Test (ISO 11925)

The apparatus for the single-flame source test is based on the German Kleinbrenner method for determining the ignitability of building products – as part of the reaction to fire tests developed to investigate the contribution a material makes to fire growth. Samples are orientated vertically and directly impinged with a small flame under zero impressed radiance. Flame impingement can occur at the edge and/or at the surface of the test specimen. This method essentially measures the ignitability of the specimen to be tested but can also provide information on the extent and rate of flame spread, the presence of flaming drips and other physical behaviour of the specimen during the test such as shrinking.

1.3.3.6 Ohio State University Calorimeter (OSU)

The Ohio State University Calorimeter (OSU) [40] is used to determine the heat release of aircraft cabin interior materials. The ASTM E 906 standard complies with the Federal Aviation Administration (FAA) FAR Part 25 requirements for aircraft [41]. In the OSU test, a 15 cm x 15 cm vertically mounted sample is subjected to a 35 kW m⁻² external heat flux. For the FAR regulation, samples should not reach a peak of heat release above 65 kW m⁻² or a total heat release of 65 kW m⁻² in the first two minutes of exposure. Additional requirements for smoke are also detailed as FAR criteria.

1.3.3.7 Lateral Spread of Flame Test LIFT Apparatus (or IMO LIFT ISO 5658)

The IMO LIFT apparatus [42] uses a radiative heat source, in the presence of a pilot flame to measure the time to ignition and lateral spread of flame along the surface of a vertically orientated material. The test is utilised for flat samples which are primarily used as the exposed surfaces of walls. Subsequent to ignition, the horizontal progression of any flame

along the sample is noted. The results are expressed in terms of flame spread distance/time, the flame front velocity versus heat flux, the critical heat flux at extinguishment and the average heat for sustained burning.

1.3.3.8 Chemical Analysis

Instrumental chemical analysis in the form of Nuclear Magnetic Resonance (NMR), Mass Spectrometry (MS) and Fourier-Transform Infrared Spectroscopy (FTIR) can provide information on the type and quantity of the products of pyrolysis from analysis of the effluents and residue.

Many materials produce carbonaceous char upon thermal decomposition, the physical structure of which can influence the decomposition process. A Scanning Electron Microscope (SEM) has been used as a means of studying char residues present on the polymer samples [43]. The same technique has been employed to observe the distribution of nanoparticles and fillers within a polymer [44]. This measure tends to be qualitative in nature but may help towards the understanding of the burning process of a specific material which the EDAX accessory allows for elemental analysis of the char or residue. The most important characteristics of char have been identified as density, continuity, thermal insulation properties and permeability [12].

1.4 Polyetheretherketone Structure, Properties and Burning Behaviour

1.4.1 Polyetheretherketone Structure

Poly(oxy-1,4-phenyleneoxy-1,4-phenylenecarbonyl-1,4-phenylene), (PEEK), is a semi-crystalline polymer with excellent mechanical, chemical and thermal properties which permits for its use in a variety of industries and particularly as an ideal metal replacement with exceptionally high thermal stability [45]. PEEK is an example of an aromatic polyketone which are commonly-used engineering thermoplastics combining the ketone and aromatic moieties. The material was invented and patented in 1978 by Imperial Chemical Industries (ICI). Since then little work has been carried out on the thermal decomposition and decomposition mechanism of the polymer.

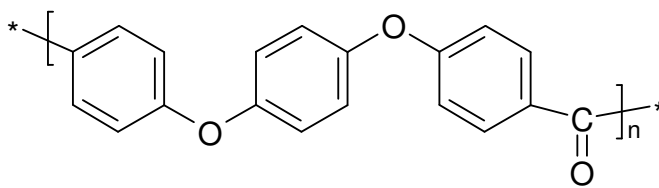


FIGURE 12. REPEAT UNIT OF POLY ETHER ETHER KETONE

The structure of PEEK is depicted in Figure 12. The stable aromatic backbone, which makes up the bulk of the monomer unit, is attributed to giving the polymer its excellent thermal properties [46] [47].

Polymers containing aromatic carbon and/or heterocyclic links in the polymer main chain, such as PEEK, have certain features which relate to their pyrolysis and char yield. These features are as follows:

- Thermal stability and char yield both increase with the relative number of aromatic groups in the main chain per repeat unit of the polymer chain.
- Pyrolysis tends to begin with scission of the weakest bonds in the bridging groups between aromatic rings [48].

PEEK, as produced by Victrex plc is available as three polymers of different chain length or molecular weight. From lowest to highest molecular weight, PEEK is named 90G, 150G and 450G. 450G, is also obtained filled with 30% carbon fibre (450CA30) and 30% glass fibre (450GL30).

Using a Pyrolysis Combustion Flow Calorimeter (PCFC), the heat release rate has been measured for some commonly used polymers [32] (see Figure 13). Polyethylene (PE) is one such polymer which is used in abundance. However, in terms of heat release rate per gram of polymer, polyethylene has a heat release rate which is eight times greater than that of PEEK. Due to the material's highly regarded properties, its applications are varied and, unlike commodity polymers, also task specific.

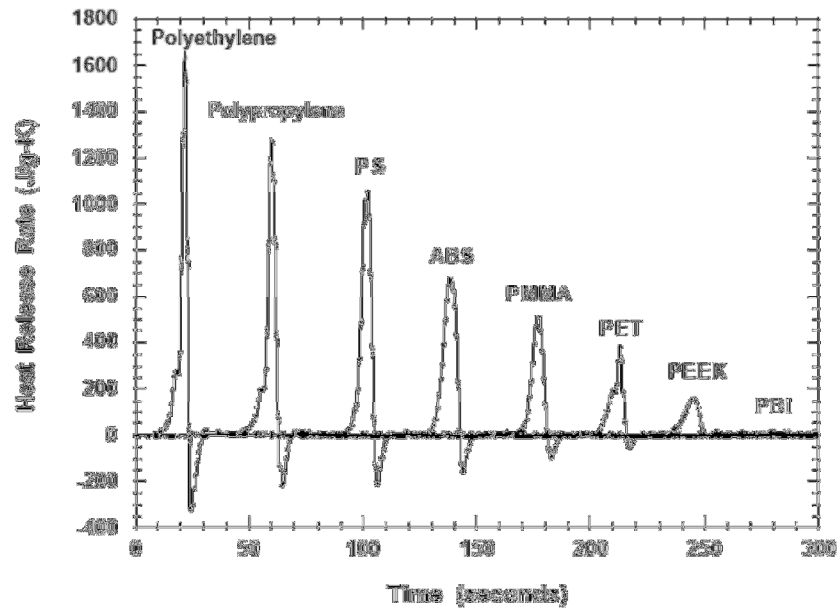


FIGURE 13. SPECIFIC HEAT RELEASE RATE FOR SEVERAL POLYMERS [32]

1.4.2 PEEK Decomposition and Flammability

PEEK has superior high temperature resistance with a continuous use temperature of 260°C and a melting point of 343°C [49]. The onset of thermal decomposition occurs between 575-580°C [10] [11]. The thermal decomposition of PEEK is different in both oxygen and nitrogen environments, however, both show a two step decomposition process. In the first reaction region, random chain scission of the ether and ketone bonds is believed to be the main mechanism [50]. Figure 14 shows the thermal decomposition process of PEEK and its composites in a nitrogen environment.

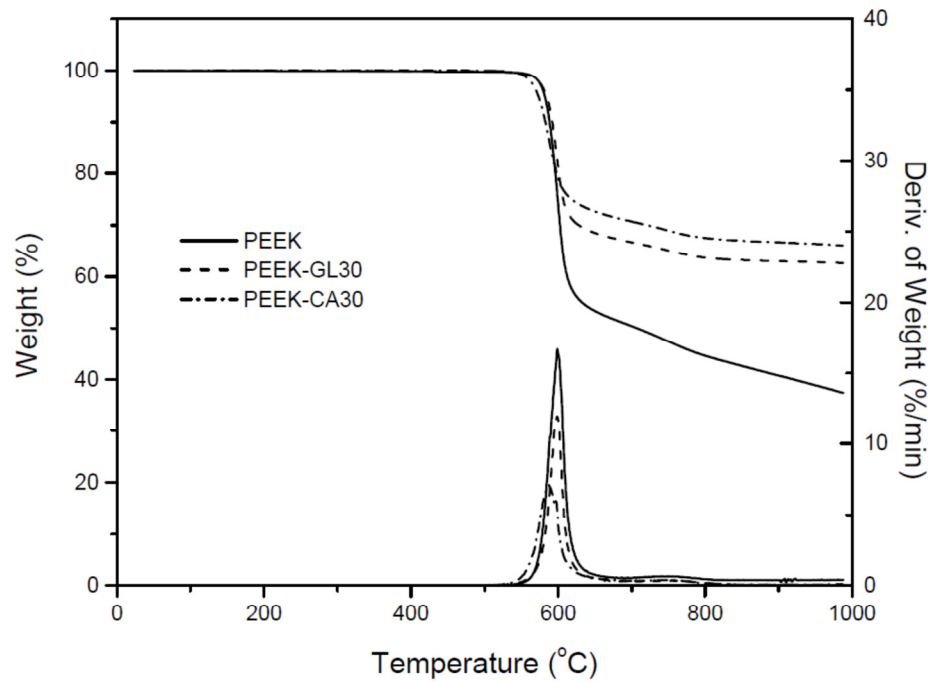


FIGURE 14. THERMAL DECOMPOSITION OF PEEK AND COMPOSITES IN N_2 [10]

Figure 14 shows a rapid and significant mass loss occurring just below 600°C resulting in the volatilisation of around 45% of the polymer mass. This has also been identified by other authors and has been attributed to the loss of phenol as a decomposition product [51] although carbon monoxide (CO) and carbon dioxide (CO_2) have also been identified as evolving rapidly over this temperature range [52], possibly as a by-product of phenol production. This is followed by a slower process of volatilisation of the residue, with over 35% present even at 1000°C . In the presence of 30% glass fibre (PEEK-GL30), rapid mass loss also occurs just below 600°C which results in the volatilisation of around 25% of the polymer retaining just under half as much polymer (in terms of mass) than the unmodified PEEK. This is also true with the presence of 30% carbon fibre (PEEK-CA30) where 20% of the mass is lost at the same temperature. At elevated temperatures, the presence of glass and carbon fibres have a similar effect with 65% and 70% of the polymer mass remaining, respectively.

Figure 15 shows the same materials and their decomposition processes in air. In this instance, the second decomposition step is attributed to the oxidation of the carbonaceous char formed as a result of the first decomposition step [10]. This step takes place at a lower temperature for PEEK-CA30 than for pure PEEK and PEEK-GL30 indicating that carbon fibre is more readily oxidised. Oxidation of pure PEEK and PEEK-GL30 occurs at around the same temperature although the latter ceases losing mass at around 700°C . In comparison to pure

PEEK and PEEK-CA30, PEEK-GL30 retains around 30% of its charred mass at elevated temperatures suggesting that PEEK reinforced with glass fibres has a stronger resistance to oxidation in an active environment than pure PEEK and PEEK-CA30.

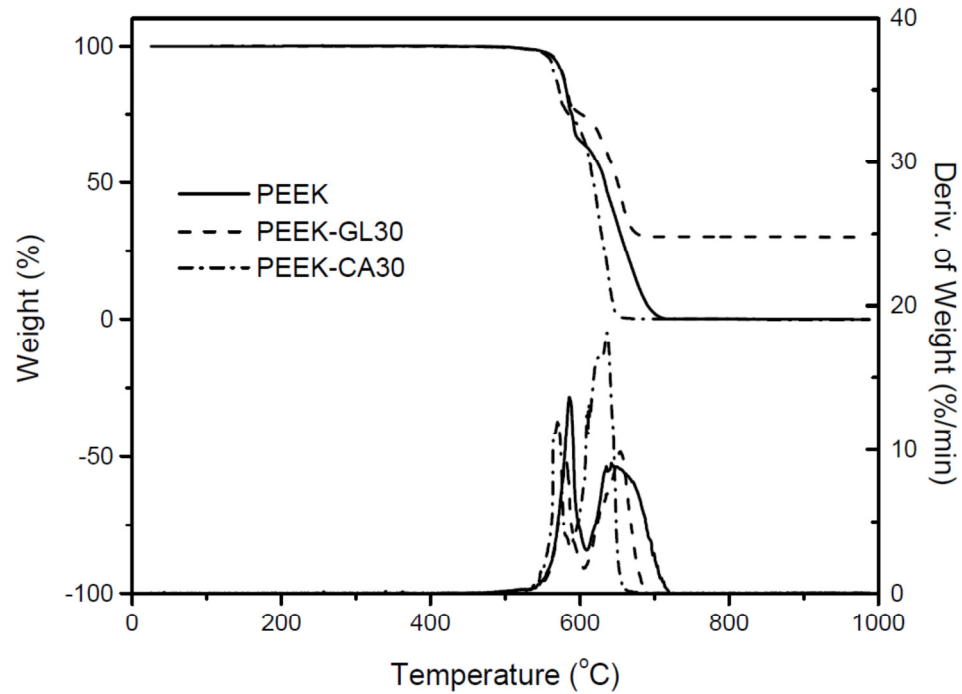


FIGURE 15. THERMAL DECOMPOSITION OF PEEK AND COMPOSITES IN AIR [10]

The flammability of PEEK and its composites differ in heat release rate and total heat released. This is depicted in Figure 16

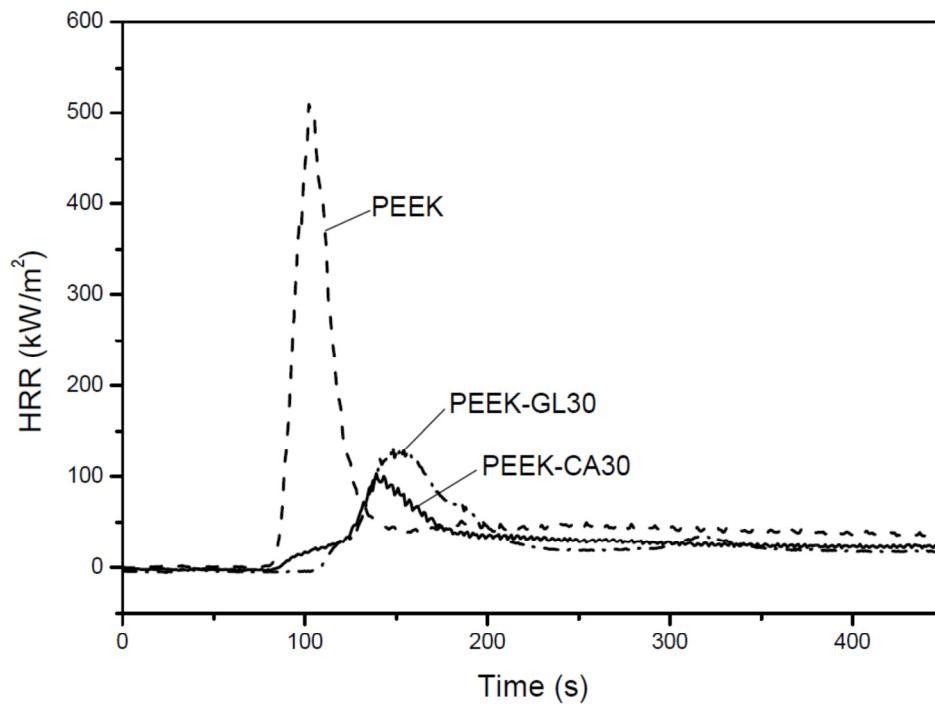


FIGURE 16. CONE CALORIMETER HEAT RELEASE CURVES OF PEEK AND COMPOSITES [10]

It can be seen that with 30% of the filler present, the heat release rate and total heat released is reduced by around 75% in the composites, however this reduction is greater for the carbon fibre filled composite. The lower heat release rate of filled PEEK is thought to be due to the mass-dilution effect, where the total amount of burning materials is reduced [10] giving a greater char yield as shown in Table 1. Conversely, it is believed that in charring systems, the presence of fillers can suppress heat radiation, melt viscosity and physical modification of the char [10]. As an example, the presence of glass fibre can reduce melt flow and dripping to prevent the spread of flames in a fire [10].

Polymer	Time To Ignition (s)	Char % (in N ₂)
PEEK	70	41
PEEK-CA 30	67	67
PEEK-GL 30	84	63

TABLE 1. CHAR YIELD (%) OF PEEK AND ITS COMPOSITES IN NITROGEN [10]

As seen in Table 1, the presence of glass fibre (PEEK-GL30) increases the time to ignition, although this is not significantly true for its carbon fibre equivalent where the time to ignition is lower but the increase to the peak heat release rate is more gradual.

1.4.3 PEEK Decomposition – Products and Mechanisms

It has been proposed that the decomposition of PEEK occurs through competing mechanisms. These are chain scission, leading to volatile fuel formation, and cross linking, leading to char formation [53]. PEEK decomposition is initiated by random homolytic scission of either the ether or the carbonyl bonds in the polymer chain [54] although there is disagreement with regards to which of these bonds is more stable. It is believed that as most of the products of PEEK decomposition contain terminal hydroxy groups and there are none with aldehyde units that the ether links are less thermally stable [51]. The main products of PEEK decomposition have been identified as CO, CO₂, phenols and some aromatic ethers [10]. Furthermore, work has been carried out on the initial decomposition of PEEK and its products using TGA-MS [50], pyGC/MS [52] as well as a combination of the two [55]. Table 2 shows the decomposition products of PEEK determined by stepwise pyGC/MS characterised by peak temperature of production.

Temperature	Decomposition Product
450°C	4-Phenoxyphenol
	1,4-Diphenoxybenzene
650°C	CO + CO ₂
	Diphenylether
750°C	Phenol
	Benzene
	Dibenzofuran
	Hydroquinone
	4-Dibenzofuranol
	4-Hydroxybenzophenone
	p-Benzoquinone
	Benzophenone
	Biphenyl
	Naphthalene
	Fluorene
1100°C	4-Hydroxybenzophenone
	1,4-Diphenoxybenzene
	4-Phenylphenol

TABLE 2. DECOMPOSITION PRODUCTS OF PEEK BY TEMPERATURE – PYGC/MS [52]

Using pyGC/MS has shown that the degradation of PEEK is initiated by cleavage at chain ends and branches to produce the following products at 450°C:

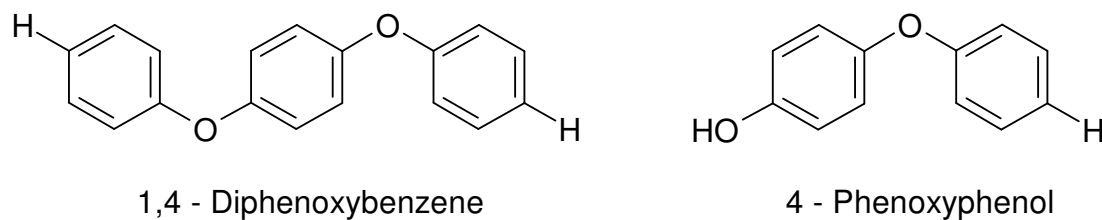
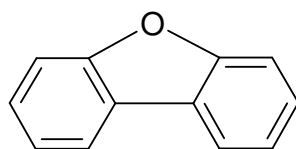


FIGURE 17. PEEK DEGRADATION PRODUCTS AT 450°C

At higher temperatures, decomposition products contain lower molecular weight volatiles as well as benzene and methylbenzene. As the randomness of the main chain scission increases, other volatile products are formed such as diphenylether and CO and CO₂ at 650°C and dibenzofuran, biphenyl and naphthalene at and above 750°C [52].

At temperatures above 650°C, chain cleavage at carbonyl ends is believed to be the primary pyrolysis pathway. Phenol has been named as a major decomposition product, its yield being greater than benzene at temperatures above 650°C [55]. As well as phenol and benzene, dibenzofuran has also been named as a major decomposition product, the structure of which (shown below) can easily be generated from the PEEK monomer unit.



Dibenzofuran

Dibenzofuran is produced at a peak pyrolysis temperature of 750°C, a high temperature environment which is believed to favour the recombination of adjacent radicals to form dibenzofuran derivatives, for which the following mechanism is proposed [52]:

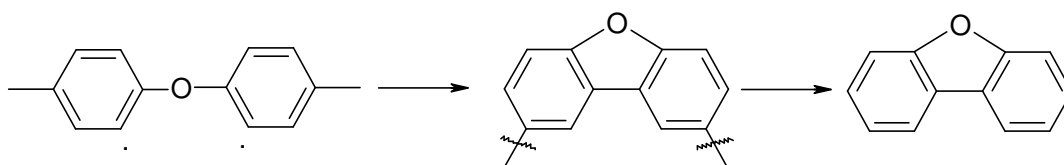
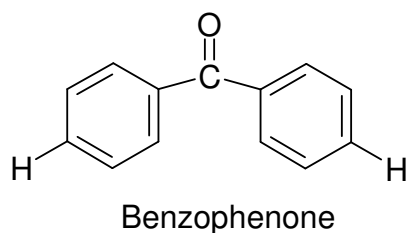


FIGURE 18. RECOMBINATION OF ADJACENT RADICALS TO FORM DIBENZOFURAN [52]

Dibenzofuran has been identified in the decomposition products of poly(1,4-phenylene oxide) and is commonly observed as a dimer [51]. The corresponding carbonyl derivative was not observed by the authors and therefore indicates that the ether group is more stable than the ketone group. However, work completed by Tsai et al finds benzophenone to be a minor product of PEEK decomposition with a peak pyrolysis temperature at 750°C. Its structure (shown below) could be linked to a dibenzofuran carbonyl derivative.



The yield of phenol has been detected as two to three times greater than that of benzene and dibenzofuran. This is increased to a yield twenty times greater under dynamic (10°C min⁻¹) TGA heating rates [55]. It is proposed that breaking the ether linkage produces phenolic end groups which, after hydrogen abstraction, leave phenol as the major decomposition product. Ether-linked molecules have been found to be present amongst the products of pyrolysis indicating that breakage of the carbonyl bond is also occurring [55]. It is believed that cleavage of the ether group occurs at lower temperatures to yield phenol as a major product of decomposition. In contrast, decomposition of the carbonyl group, occurring at higher temperatures, yields CO₂ as a major product of pyrolysis [50].

Species containing two aryl groups, such as biphenyl, naphthalene and fluorene show similar patterns of formation. All have a peak pyrolysis temperature of 650°C; reach maximum amounts at 750°C and decrease rapidly to trace amounts above 900°C [52]. This is similar to the pattern shown by dibenzofuran and indicates that all are formed by the recombination of free radicals produced by ether or carbonyl scission of the main polymer chain [52]. This process produces biphenyl as shown:

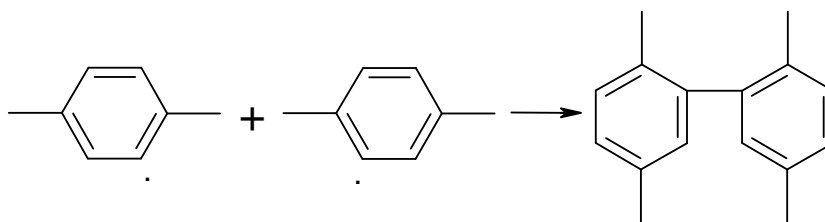


FIGURE 19. RECOMBINATION OF ADJACENT RADICALS TO FORM BIPHENYL [52]

Above 900°C, significant amounts of phenyl phenol have been detected in the pyGC/MS possibly due to the continuing pyrolysis of ether-containing species in the incompletely carbonised solid residue. The mechanism for this is shown below:

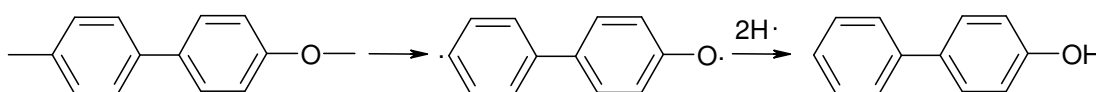


FIGURE 20. PYROLYSIS OF SOLID RESIDUES TO FORM PHENYL PHENOL [52]

A high char yield suggests that the random main chain scission is accompanied by carbonisation and pyGC/MS data indicates that carbonisation might be the dominant pyrolysis pathway at temperatures above 750°C [52].

Further analysis has been completed on PEEK which has been thermally aged to determine the early stages of the crosslinking mechanism which results in a char-like residue. It is believed that crosslinking occurs during the early stages of decomposition [51]. Using ^{13}C Nuclear Magnetic Resonance (NMR), PEEK samples heated for various periods of time in air were analysed. PEEK was thermally aged for 0.5, 4 and 6 hours at 400°C. Differences in NMR spectra were found and as the thermal aging process was increased, there was a slight reduction in the ratio of C-5 to C-6 and C-4 to C-7 [56] positions of which are seen in Figure 21.

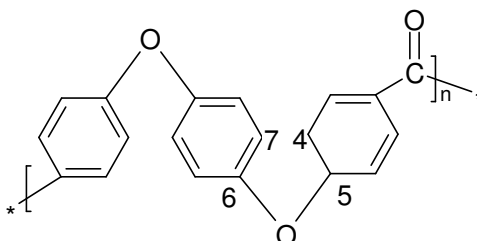


FIGURE 21. PEEK WITH INVOLVED CARBONS [56]

Figure 22 and Figure 23 show the crosslinking mechanisms determined by the changes in ratios of C-5 to C-6 and C-4 to C-7.

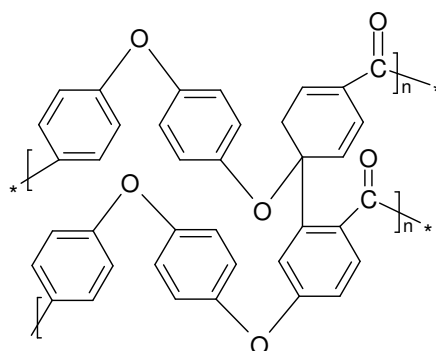


FIGURE 22. PEEK WITH CROSSLINKING AT C-5 [56]

These changes were found to be more significant for samples which were aged for longer periods of time suggesting that the effect is occurring to a greater extent [56].

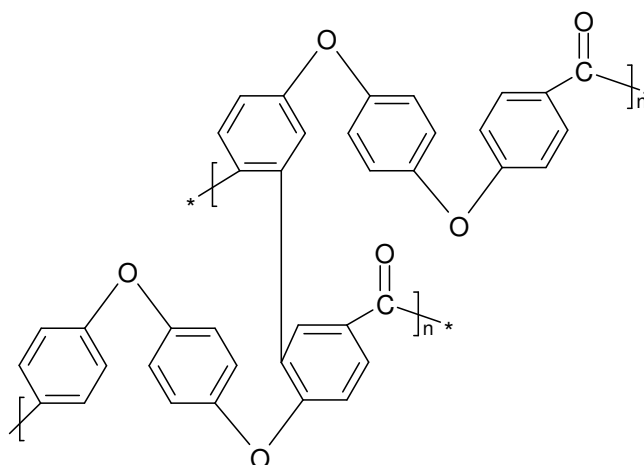


FIGURE 23. PEEK WITH CROSSLINKING AT C-4 [56]

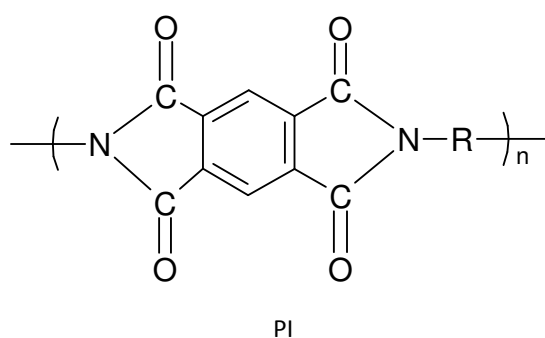
1.4.4 Comparison of Results of Flammability Tests for PEEK

In 2000, 150 million tonnes of plastic were produced on a global scale [57]. 12% of this was made up by engineering thermoplastics, totalling 18 million tonnes. Engineering thermoplastics are defined as 'high performance materials that provide a combination of high ratings for mechanical, thermal, electrical and chemical properties' [57]. As an engineering thermoplastic, PEEK is a rival of other polymers in the same class. Polymers such as polyimide, polyetherimide and polyphenylene sulphide have similar properties and therefore, tend to be

selected depending on their final application. These polymers, due to their better properties and specific applications incur a higher cost.

1.4.4.1 Polyimide (PI)

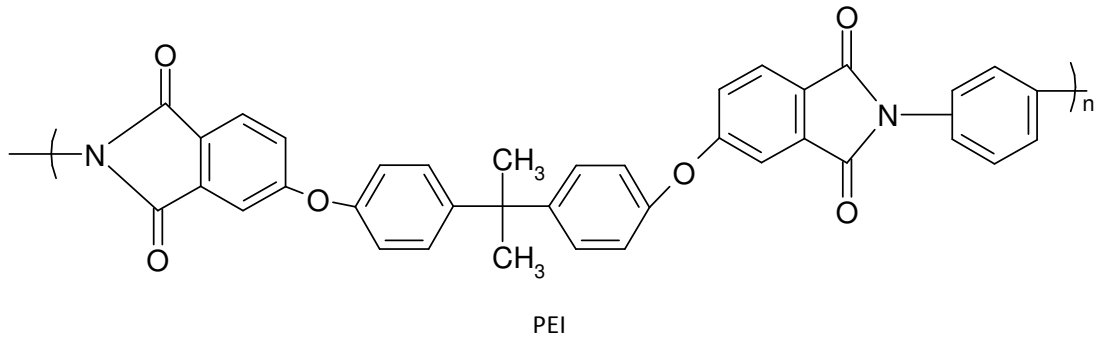
Polyimide (PI) is a high-temperature, linear thermoplastic. Similar to PEEK, PI is used in high performance applications as a replacement for glass and metal products. PI contains the sequence CO – NR – CO as part of a ring structure along the backbone, the presence of which gives the polymer its high temperature properties [58]. This sequence is depicted:



PI has high oxidative stability and therefore can withstand temperatures of up to 260°C [58]. They are resistant to weak acids and organic solvents but not bases. PI also resists ionising radiation and has good electrical properties, however, exposure to water or steam above 100°C may cause parts to crack rendering poor hydrolysis resistance [58]. Common uses for PI are appliance bearings, seals and abundant usage within the electronics industry.

1.4.4.2 Polyetherimide (PEI)

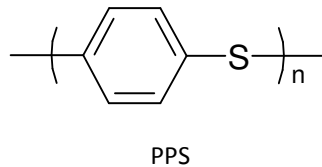
Polyetherimide (PEI) is an amorphous thermoplastic with high temperature resistance, rigidity and impact strength. PEI has similar properties to PI and although will burn, both have self-extinguishing properties [58]. The structure of PEI is as depicted:



PEI has low smoke emission and is resistant to alcohols, acids and hydrocarbon solvents however, dissolves in partially halogenated solvents. PEI is sold under the trade name of Ultem™ and similar to PI, the polymer is used widely thorough out the electronics industry. PEI is also used in the automotive industry for temperature sensors and lamp sockets and due to its dimensional stability is used for large, flat parts such as computer hard disks [58].

1.4.4.3 Polyphenylene Sulphide (PPS)

Poly(phenylene sulphide) (PPS) is a high temperature, high strength and highly chemically resistant thermoplastic. This is indicated by the presence of an aromatic benzene ring on the backbone of the structure linked with an electronegative sulphur atom [58]:



Due to its highly crystalline nature, PPS is brittle and is often reinforced with glass fibre. PPS has similar mechanical properties to other engineering thermoplastics and its intrinsic flame resistance allows for applications in the electronic industry and instances where the material's mechanical properties need to remain constant at elevated temperatures. As such, PPS is used for impellers and pump housings [58].

Polymer	T _d (°C)	T _p (°C)	T _{ig} (°C)
PEEK	570	600	570
PEI	527	555	528
PPS	504	545	575

TABLE 3. ONSET DECOMPOSITION (TD), PEAK MASS LOSS TEMPERATURE (TP), AND IGNITION (TIG) TEMPERATURES OF PEEK, PEI AND PPS [59]

The onset of decomposition (T_d) in PEEK occurs at a higher temperature (570°C) than in PEI and PPS as is shown in Table 3 [59]. In both PEEK and PEI, the peak mass loss temperature (T_p) occurs after ignition, in PPS this occurs before. PPS also ignites at a higher temperature than PEI and PEEK. From Table 4 it can be seen that PEEK, PEI and PPS have all been given a V-0 rating in UL-94 tests. PEI has the highest oxygen index value (47%) although the lowest ignition temperature of those considered. This is possibly due to the polymer's self-extinguishing properties [58] and the way the material behaves in the LOI test.

Polymer	LOI [O ₂] (%v/v)	UL 94 Rating
PEEK	35	V0
PI	37	V0
PEI	47	V0
PPS	44	V0

TABLE 4. LOI AND UL-94 RATING FOR PEEK, PI, PEI AND PPS [59]

The heat release rate of PEEK at ignition is 15 kW m⁻². This is similar to PEI and marginally lower than PI as is shown in Table 5. The values for heat release rate correspond to those of mass loss rate (MLR) at ignition.

Polymer	MLR (g m ⁻² s ⁻¹)	HRR (kW m ⁻²)	HR Capacity (J g ⁻¹ K ⁻¹)	Char Yield (In N ₂ %)
PEEK	0.72	15	163	46
PI	1.3	24	29	53
PEI	0.82	14	121	49

TABLE 5. MASS LOSS RATE (MLR) AND HEAT RELEASE RATE (HRR) AT IGNITION AND HEAT RELEASE CAPACITY AND CHAR YIELD OF PEEK, PI AND PEI [59]

1.5 Studies Aimed At Fire Retarding PEEK

From the previous section, it is clear that PEEK is a polymer with high thermal stability. From the literature, its onset of decomposition is around 570°C in an inert atmosphere [10]. Most commodity polymers have much lower thermal stability and to attain higher thermal decomposition temperatures, fire retardants and additives are incorporated. The decomposition temperatures of such polymers, in their unadulterated state are shown in Table 6, at a heating rate of 10°C per minute in an inert atmosphere.

Polymer	Decomposition Temperature
Polystyrene (PS)	163°C
Low Density Polyethylene (LDPE)	217°C
Nylon-6	310°C
Polymethylmethacrylate (PMMA)	325°C
Polypropylene (PP)	328°C
Polyetheretherketone (PEEK)	570°C

TABLE 6. DECOMPOSITION TEMPERATURES OF GENERAL POLYMERS [60]

From Table 6 it can be seen that many polymers decompose before PEEK has even melted ($T_m = 343^\circ\text{C}$) [60]. As a result of the polymer's high melting temperature, it is processed at 400°C, above the temperature of activity of most fire retardant systems. Anything which is incorporated into PEEK, be it to improve mechanical, thermal or any other properties, needs to be stable above 400°C. As a result, improving the fire safety of PEEK has concentrated mainly on blending (with other high temperature polymers), the incorporation of inert fillers and nano-materials. The attempts made to improve the thermal stability and flammability of PEEK are reviewed in this section.

1.5.1 Blending

PEEK has very good heat resistance and thermal stability. For a material to be classified in such a way, it should not decompose below 400°C and should retain its properties near the

decomposition temperature [47]. There has been some research into the prospect of further fire retarding PEEK through producing composites and blends. Blending PEEK with poly (aryl ether sulphone) (PES) has indicated that the presence of one polymer affects the properties of the other [54]. The blended product was found to have a lower thermal stability than either of the homopolymers and this was attributed to the interactions between the degradation products of PES (which degrades beforehand) with PEEK and also due to reduced viscosity of the blend.

PEEK has been blended with a thermotropic liquid crystalline polymer (TLCP) and the thermal properties of the blended material have been investigated. In the past, blending of TLCP with conventional thermoplastics has resulted in a reduced melt viscosity and improved processability [61]. The research found that the presence of TLCP influences the degradation behaviour of PEEK and also, that the presence of PEEK destabilises the TLCP. The degradation mechanism of each polymer was not altered through blending, however, the degradation process was accelerated as a result of the blend [61].

1.5.2 Fillers

Between 0-50% of aluminium nitride was loaded into PEEK to produce a series of high performance composites [62]. The presence of aluminium nitride (AlN) particles within the matrix acted as an effective nucleating agent which in turn increased the melting temperature of the material. It was reported that the presence of AlN at 50% increased the melting temperature of PEEK by 11°C. The percentage of char present at higher temperatures (900°C) also increased as the percentage of AlN increased. PEEK containing 50% AlN showed a 73% char yield at 900°C [62].

Reinforcing PEEK using metal carbonates has been undertaken using calcium carbonate (CaCO_3) at 0% - 30% mass [63]. The presence of the CaCO_3 filler increased the glass transition temperature (with between 5% and 30% filler present) but decreased the melting temperature over the same mass range. Similarly, reinforcing PEEK with hydroxyapatite (a calcium containing mineral) at 0%-40% mass caused a decrease in the melting temperature, proportional to the volume of hydroxyapatite [64].

1.5.3 Structural Modifications

Efforts to improve the fire retardancy of PEEK by means of modifying the main polymer chain have also failed. Synthesis of a series of PEEK materials containing a tertiary amine gave materials with thermal properties less favourable than those of PEEK. The glass transition temperature was found to be 119.6°C (well below that of PEEK at 144°C) and temperatures 386°C and 407°C were attributed to 5% and 10% mass loss in air, respectively [65]. Further structural modification has allowed for the synthesis of sulphonated poly ether ether ketone (SPEEK). Sulphonation appears to take place exclusively on the phenyl rings bordered by two ether linkages. Thermal degradation data of SPEEK has detailed that the introduction of the SO_3^- group significantly reduces the thermal stability of PEEK. The temperature corresponding to the onset of thermal decomposition decreases as the relative presence of the SO_3^- group increases [66].

PEEK samples have been modified with UV radiation as a means of increasing the material's mechanical properties. The report proposed that UV radiation promoted cross-linking and chain scission. Samples which had been irradiated showed a higher glass transition temperature although the melting temperature for the polymer decreased [67].

1.5.4 Nanocomposites

PEEK has also been reinforced with nano-sized particles of silica and alumina [44]. The resulting nanocomposites contained between 5-7.5% mass of SiO_2 or Al_2O_3 . Reinforcing PEEK in such a way increased the hardness and elastic modulus of the material as well as its tensile strength by 20-50%. The authors commented that there appeared to be no chemical reactions taking place between the nanoparticles and the polymer matrix. Analysis also found a higher crystallinity fraction and a 40°C increase in the degradation temperature of the filled material in comparison with the unfilled material. This however, had no effect on the melting temperature of PEEK which remained at 343°C [10]. Based on the results of this work, further modification of PEEK using nano-silica particles has been undertaken [68]. Some nano-silica (SiO_2) particles were pre-treated with stearic acid and both the modified and unmodified products were added at 2.5-10% mass. Addition of the nano-silica particles increased the melting temperature to 345°C for silica added at 10% mass. The silica products that underwent surface modification with stearic acid showed higher melting temperatures compared to the

unmodified products ($\pm 1^\circ\text{C}$) [68]. The authors conclude that the presence of nano-silica fillers significantly improves the thermal stability of PEEK. Decomposition temperatures increase with increasing filler content. For SiO_2 present at 10%, the decomposition temperature is determined as 600°C . Although this initially appears to be well over the value stated previously ($575\text{-}580^\circ\text{C}$ [10]), the reported value of decomposition corresponds not to onset temperature but to one equivalent to 10% mass loss. Similarly, TGA curves show that decomposition temperatures of pure PEEK also reach 600°C after 10% of the mass is lost [10].

Recent interests have centred on using nanoscale reinforcing fillers to make polymeric materials with exceptional properties [69]. Carbon nanotubes have been employed for this purpose and have been added to various polymers as a means of improving their thermal properties [70] [71] [72]. Inorganic fullerene-like tungsten disulphide (WS_2) nanoparticles (with a layered onion structure and a hollow core) have been incorporated into the PEEK matrix as method of improving its tribological properties. The nanoparticles were added at 0.01%-5% mass. Results showed that the WS_2 particles readily oxidised to WO_3 at elevated temperatures. Addition of 1% of the nanoparticles shifted the peak decomposition rate to $20\text{-}30^\circ\text{C}$ higher [73] than that of pure PEEK. The authors propose that this is due to the strong interactions and bonding between the PEEK matrix and the WS_2 nanoparticles.

Most recently, carbon nanotubes have effectively been distributed within the PEEK matrix by Diez-Pascual et al [74]. The authors used a dispersion method involving the addition of ethanol and subsequent sonication of the mixture to agitate the agglomerates present, as a better dispersion allows for more enhanced properties. The SWNT utilised in their study increased the onset of decomposition temperature of the resulting PEEK/SWNT nanocomposites by 25°C with the incorporation of 1% by mass, showing the potential of these materials.

1.6 Studies Aimed at Fire Retarding Other High Temperature Polymers

Additional high temperature polymers, such as those discussed in previous sections have also been modified in similar ways to PEEK to attain improved thermal properties. Analogous methods have been used i.e. fillers, blending and nanocomposites, and the effectiveness of these methods is discussed in the following sections.

1.6.1 Polyimide (PI)

Due to the presence of a conjugated electron system, triphenylamine groups have a high thermal stability [75]. Such groups have been attached to pyridine to produce a monomer containing heterocyclic pyridine and triphenylamine groups to produce a novel monomer: 4-(4, 4'-diaminotriphenylamine)-2, 6-bis-(4-methylphenyl) pyridine. This has then been incorporated into the polyimide chain [75]. The thermal decomposition temperature equivalent to 10% mass loss increased from 524°C-598°C and 527°C-614°C in both air and nitrogen, respectively. The glass transition temperature (T_g) increased from 316°C to 373°C. Also, due to the addition of the novel monomer the char yield in nitrogen increased from 59% to 73% [75]. The authors believed that the resulting polymers had a higher thermal stability and glass transition temperature was most likely due to the presence of the rigid pyridine group.

An additional polyimide structural modification technique allows for the incorporation of naphtha into the polymer backbone [76] to produce polynaphthalimides (PNI) which have superior chemical and thermal properties when compared to polyimide alone. The thermal decomposition temperature equivalent to 10% mass loss increased slightly in the PNI compounds and the glass transition temperature also increased to 386°C [76].

Nanodiamond particles are synthesised by the detonation of carbon-containing explosives and, as a result, such particles are stable, both chemically and mechanically and can withstand high temperature processing [77]. These particles have been dispersed into the polyimide matrix at 1-2% mass. The presence of nanodiamond at 1.5% increases the temperature for 5% mass loss in thermal decomposition from 545°C to just over 610°C [77]. One mechanism used to describe the increased stability is that the presence of nanodiamond increases the instances of crosslinking [78].

Polyimide has also been reinforced with plasma-modified carbon nanotubes with maleic anhydride at 0-3% mass [79]. As a result, the initial decomposition temperature increases with increasing carbon nanotube content. The dispersion of carbon nanotubes in the matrix appeared to enhance the thermal stability of the resulting compound as it has been found that the carbon nanotubes chemically or physically interact with the polyimide matrix [79].

Zinc borate has been incorporated into polyimide at loading levels of 1%, 5% and 10% [80]. The presence of zinc borate was found to decrease the decomposition temperature corresponding to 5% mass loss. The authors believe that the presence of zinc borate generally reduced the interactions between polymer backbones. They also reported that a reduction in polymer backbone interaction is seen to decrease the glass transition temperature of a polymer. In this case, the reduction in polymer backbone interaction is believed to have been supported by the rigid three-dimensional nature of zinc borate thus increasing the rigidity of the polymer chain and therefore increasing the glass transition temperature by around 40°C.

1.6.2 Polyetherimide (PEI)

Carbon nanofibres have been dispersed in the polyetherimide matrix at 1-3% [81]. Although other properties of the resulting compound were increased i.e. electrical and mechanical with increased loading, this was untrue for the thermal properties. As the carbon nanofibre content increased, the temperature for the onset of thermal decomposition decreased although there was an 8°C increase in T_g at 3%, attributed to the immobilising effect of carbon nanofibres at high temperatures [81].

Due to their excellent physical properties, multi-walled carbon nanotubes (MWNT) have also been incorporated into polyetherimide at 0.5% and 1% [82]. Thermally, the properties of the nanocomposite were enhanced with an increase in glass transition temperature of 11°C. The authors believe that this increase is due to the reduced mobility of the polymer chains caused by the presence of the MWNT.

The presence of fluorinated groups is believed to enhance hydrolytic resistance, solubility and more importantly, the thermal stability of polyetherimides [83]. Fluorinated copolyetherimides have been synthesised as a means of increasing such material properties. As the amount of fluorine in the copolymer increases, the glass transition temperature was found to decrease. In addition, TGA results showed that the fluorinated polyetherimides decomposed 5% by mass at a lower temperature (400°C) than pure polyetherimide (500°C). It was suggested by the authors that this effect was due to the addition of the fluorinated side chains and their relative stability.

Polyetherimide has been blended with acetylene-terminated monomer (ATM) structures [84]. The blends, 91% PEI and 9% ATM were cured prior to testing and held at various temperatures (150°C, 230°C and 270°C) for a period of 24 hours. The curing process was selected as a method to enable crosslinking to occur between the PEI and the ATM. Thermal analysis of the samples revealed the higher the curing temperature, the higher the temperature corresponding to 2% mass loss. Conversely, these temperatures were much lower than the pure PEI which shows a 2% mass loss at 490°C in air.

CHAPTER 2. EXPERIMENTAL PROCEDURES

2.1 Thermal Decomposition

The processes involved in the decomposition of polymers can be measured in various ways to obtain such information as rate of decomposition and identification of decomposition

products. Thermal stability is largely one of the most important factors for a high performance engineering plastic's service life [85]. Thermal decomposition is probably the single most important factor controlling the flammability of a polymer. Techniques commonly used are thermogravimetric analysis (TGA), differential thermal analysis (DTA) and differential scanning calorimetry (DSC) and techniques with analysis of volatiles such as pyrolysis gas chromatography – mass spectrometry (pyGC/MS) and thermogravimetric analysis coupled with infrared red (TGA-FTIR). Both methods are discussed in detail in the following sections.

2.1.1 Thermogravimetric Analysis (TGA)

2.1.1.1 Instrumentation

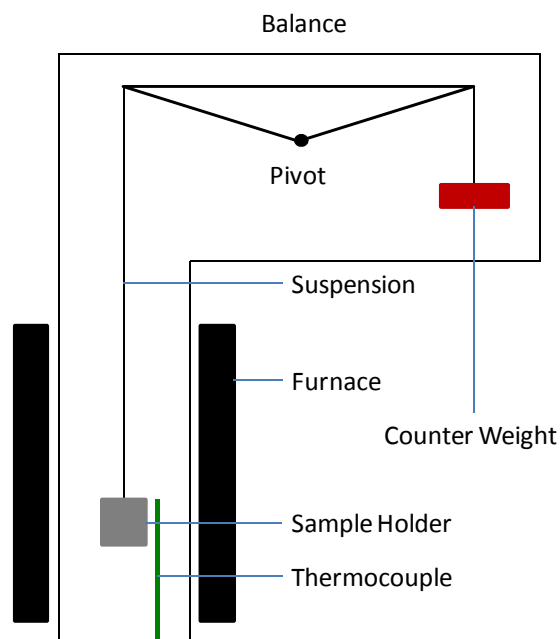


FIGURE 24. SCHEMATIC VIEW OF TGA APPARATUS

A Schematic view of a typical TGA is shown in Figure 22. The instrument consists of:

- A furnace;
- An electrobalance;
- A data acquisition device
- A computer/programmer.

2.1.1.2 Calibration

The TGA can be calibrated with a set of known masses to confirm that the recordings are accurate. The rate of airflow can also be calibrated using a bubble flow meter technique and a horizontal calibrated burette. As the airflow meter on the TGA 1000 instrument has markings but no scale, the rate of air flow was determined, by calibration, before experiments began. Temperature calibrations can also be undertaken.

2.1.1.3 Sample Preparation

The samples were cut from 2 mm pellets and were approximately 1.5 mm in length. The sample consisted of a single piece which weighed approximately $10 \text{ mg} \pm 0.5 \text{ mg}$.

2.1.1.4 Materials

For the TGA, samples of PEEK used were unfilled 90G, 150G and 450G, filled 450G with carbon fibre (CA) and glass fibre (GL) at 30%, filled 381G with talc (TL) at 30% and filled 150G with titanium dioxide (TI) at 30%.

2.1.1.5 Procedure

TGA experiments were performed in air and nitrogen on the TG1000 and the TGA-50 respectively, at heating rates ranging from 1 to $50^\circ\text{C min}^{-1}$ and between 20 and 900°C . It has been established that for PEEK materials, in particular at higher heating rates (such as $40^\circ\text{C min}^{-1}$) there may not be enough time for the sample to react with oxygen because there is inadequate time for the evolved decomposition products to diffuse away from the sample-oxygen interface [85]. Experiments were performed three times to ensure that the results were reproducible.

2.1.2 Simultaneous Thermal Analysis - Fourier Transform Infrared (STA-FTIR)

Simultaneous Thermal Analysis (STA) comprises of both thermogravimetry (TG) and differential thermal analysis (DTA) techniques. A Fourier Transform Infrared (FTIR) is coupled to the STA for the purpose of evolved gas analysis. This technique uses two sample crucibles which are heated or cooled at a precise and controlled rate. One crucible contains a sample whose thermal response is known or no sample, the other crucible contains a sample with unknown thermal response. Differences in the behaviour of the two materials caused by differences in specific heat, occurrence of an exothermic or endothermic reaction, or phase change can result in a temperature difference between the two crucibles. The coupling of STA with FTIR can provide information regarding changes in mass and their causes.

2.1.2.1 Instrumentation

The instrument consists of the following:

- STA
- FTIR Attachment

All STA-FTIR experiments completed in this thesis were done so on a STA 780 coupled with a Nicolet Magna IR Spectrometer 550.

2.1.2.2 Sample Preparation

The samples were cut from 2 mm pellets and were approximately 1.5 mm in length. The sample consisted of one quantity which weighed approximately $10 \text{ mg} \pm 0.5 \text{ mg}$.

2.1.2.3 Materials

For the TGA, samples of PEEK used were unfilled 450G, filled 450G with carbon fibre (CA) and glass fibre (GL) at 30%.

2.1.2.4 Procedure

STA-FTIR experiments were performed in air and nitrogen at heating rates ranging from 1 to 50°C min⁻¹ and between 20 and 900°C. The heated line was held at 220°C and the gas cell temperature was 280°C. Experiments were performed three times to ensure that the results were reproducible.

2.1.2.5 Data Interpretation

FTIR data at typical scan rate 20 scans per 20 seconds (averaging 60 scans per minute) were obtained for the full duration of each run. Data was analysed using the OMNIC software Version 7.2 and the HR Nicolet Vapour Phase library.

2.1.3 Pyrolysis Gas Chromatography - Mass Spectrometry (pyGC/MS)

The products of decomposition can be qualified and quantified through Pyrolysis Gas Chromatography coupled with Mass Spectrometry (pyGC/MS). It is believed that knowledge of the decomposition products could be used to put forward reaction mechanisms occurring during such processes [55]. Using this information, it may be possible to suggest the key features which limit a polymer's thermal stability and therefore identify potential areas which could lead to the development of a newer polymer with a greater thermal stability [55].

2.1.3.1 Instrumentation

The instrument consists of the following components:

- A pyrolyser;
- A gas chromatograph;
- A mass spectrometer.

A schematic of the pyGC/MS is shown in Figure 25. All pyGC/MS experiments shown in this thesis were completed on a Perkin Elmer Turbo Mass GC/MS system coupled with a CDS Pyroprobe 5200.

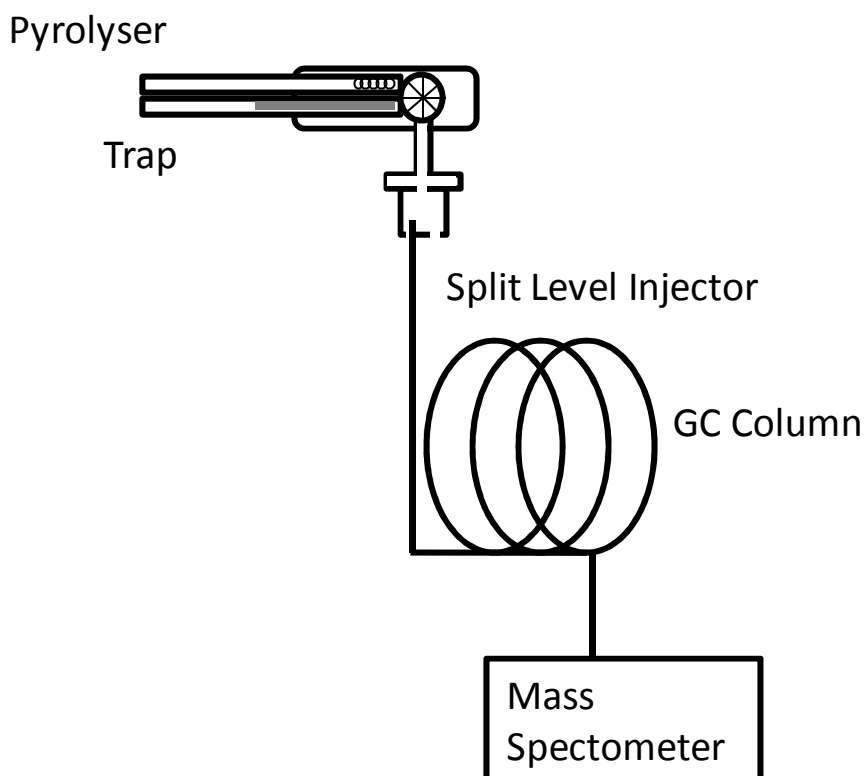


FIGURE 25. SCHEMATIC VIEW OF A pyGC/MS

2.1.3.2 Specifications

Pyrolyser

The pyrolyser can be programmed to perform single step or multistep analysis. The filament temperature can be set in 1°C increments up to 1400°C . The heating rate can be set in units of 0.01°C to 20°C per millisecond or 0.01°C to 999.99°C per second or minute. Initial and final times can also be set between 0.01 and 999.99 minutes. For flash pyrolysis, samples are held for 15 seconds at the final temperature. Decomposition gases were collected on a Tenax TA trap at 50°C . The trap was heated at 280°C for 2 minutes and the desorbed gases transported via a transfer line held at 310°C .

Gas Chromatograph

The GC column was a Perkin Elmer PE-5 30 m x 0.25 mm with a $0.25\ \mu\text{m}$ film thickness. The GC oven temperature was held initially at 50°C for 2 minutes and then heated to 280°C for 2 minutes and held for 5 minutes.

Mass Spectrometer

Mass spectra were recorded under EI positive mode with ionisation energy of 70 eV. The mass detector was set to scan from m/z 40 to 300.

2.1.3.3 Sample Preparation

Samples used were cut to size from sheets of PEEK film of 50 μm thickness. These were held in quartz capillary tubes 25 mm in length with a 1.9 mm inside diameter. The sample was held in the centre of the capillary tube with using quartz wool plugs positioned at each end.

2.1.3.4 Materials

Samples analysed were unfilled PEEK – 450G, 450G filled with carbon fibre (450CA30), glass fibre (450GL30) and talc (381TL30) all present at 30%.

2.1.3.5 Procedure

The quartz capillary tubes were placed within the platinum heating coil of the pyroprobe. The program was then set to the heating rate and time required. Temperatures were selected based on the decomposition of PEEK and the products of decomposition as detailed in previous work [50] [52] [55]. A flash pyrolysis method was used. With the flash pyrolysis method, separate samples are subjected to the temperature regime. Experiments were conducted three times to ensure repeatability.

2.1.3.6 Data Interpretation

The compounds with the chemical structure matched best to the volatile pyrolysates from the pyrolyser were searched using the NIST mass spectra library.

Flammability

The flammability of pure PEEK materials and filled PEEK materials have been assessed using the methods described in Chapter 1. Experimental procedures and instrumentation are described in detail in the following sections.

2.2 Ignitability

The ignitability of a material is defined as the ease of ignition, usually by a small flame or spark. Ignition is often characterised as the initiation of combustion. The combination of heat flux and time are factors governing the thermal exposure which causes ignition. Ignitability can also be related to flame spread as the spread of flame across a surface is due to progressive ignition along that surface.

2.2.1 Bunsen Burner Test (UL-94)

The most commonly used small-flame test for plastics is the Underwriters' Laboratory – 94 (UL-94) test, first issued in 1970 [86] and used for classifying how materials burn in different orientation and thicknesses. The standard [35] incorporates various test methods, using the same burner, in different orientations. The horizontal burn (HB) standard is provided for those specimens unable to meet the criteria for the more stringent vertical burn (VB) standard. The UL-94 is a 'realistic' test when small items are considered however, fire performance of larger items must be considered. The UL-94 standard rates only the material. For finished appliances, there is the UL-746 series [86].

2.2.1.1 Instrumentation

The instrument consists of the following components:

- Burner with a 50 W, 20 mm flame;
- Ring stand, clamp and wire gauze;
- Flow meter;
- Timing device; and
- Cotton wool pads (for the VB series).

The experimental set-up for the vertical burn test uses the same instrumentation, with the addition of cotton wool pads as shown in Figure 26. In the VB series of experiments, the burner is applied from below to measure the extent of burning after the flame has been removed [35].

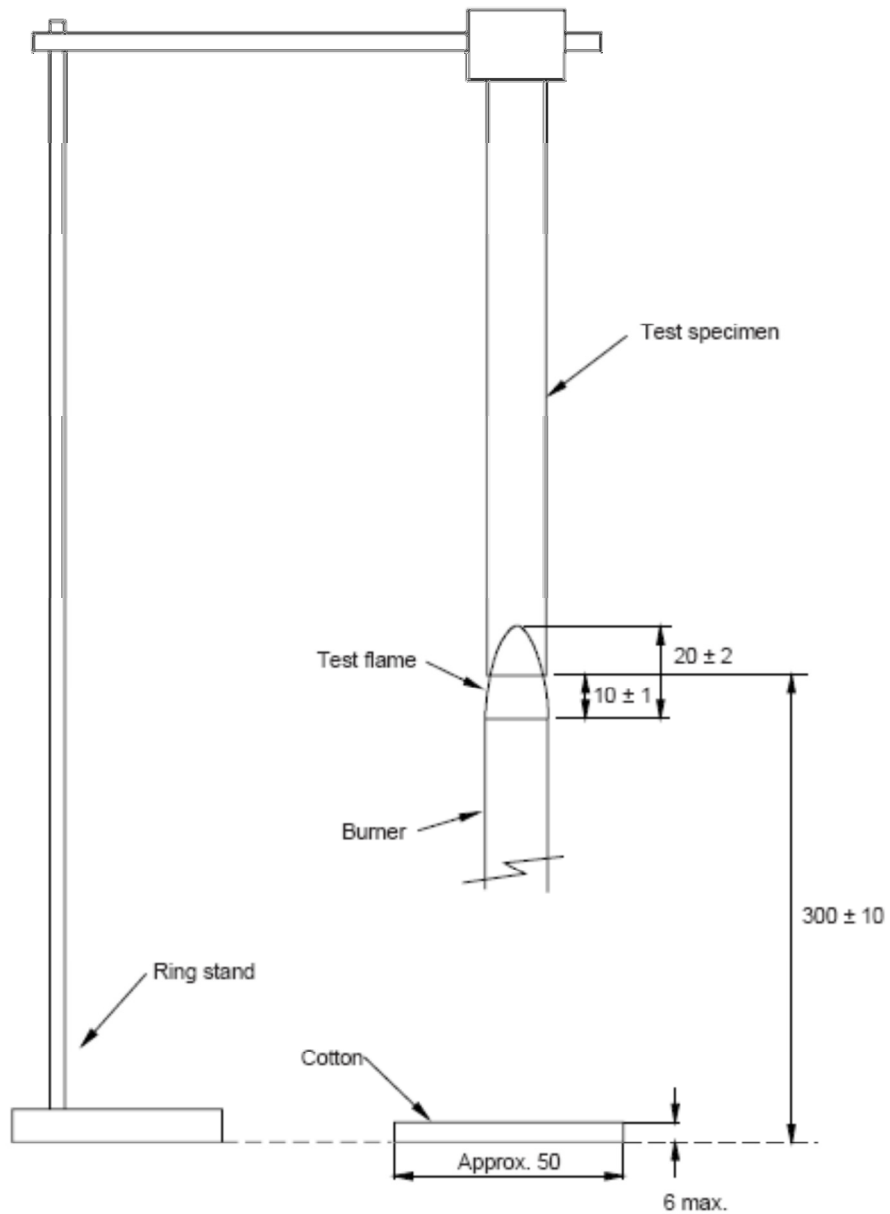


FIGURE 26. FRONT VIEW OF VB EXPERIMENTAL SET-UP [35]

2.2.1.2 Calibration

A flow meter can be used to calibrate the size of the flame. A copper block and thermocouple arrangement can be used to measure the temperature of the flame [87].

2.2.1.3 Sample Preparation

The sample size used was 13 mm x 125 mm x 1.6 mm. Samples were marked at 25 mm and 75 mm from the exposed end. According to the UL-94 standard samples are to be conditioned, half in a 70°C oven for a period of 168 hours and half in 50% humidity at 23°C ± 2 for 48 hours. As it was determined that moisture was having an effect on the results of flame, tests, samples were examined 'as received' to obtain true data.

2.2.1.4 Materials

For the UL-94, samples of PEEK used were unfilled 90G, 150G and 450G and filled 450G with carbon fibre (CA) and glass fibre (GL) at 30%.

2.2.1.5 Procedure

-Horizontal Burning

The sample was supported in the horizontal orientation and tilted to an angle of 45°. The flame was applied to the exposed end of the sample for a 30 second period (or until the flame reached the 25 mm mark). If the sample continued to burn once reaching the 25 mm mark, the time taken for the flame to travel between the 25 mm and 75 mm mark was recorded. If the flame did not reach the 75 mm mark, the time of combustion and length between these two marks was recorded.

-Vertical Burning

The sample was supported in the vertical orientation and the flame applied to the exposed end of the sample for a 10 second period. The flame was then removed, until flaming stops, and then reapplied for another 10 seconds and then removed. Factors such as dripping, flaming drips and ignition of the cotton were recorded. Both sets of samples were tested 10 times to obtain a reproducible result. This methodology is different to the actual UL-94 VB test

whereby 5 samples are initially tested, if 1 out of 5 samples fail, then 5 more samples are tested. 2 out of 10 samples are allowed to fail to obtain a specific rating.

2.2.1.6 Analysis

The criteria for the UL-94 VB experiments are expressed in Table 7.

Sample classified to the following criteria	V-0	V-1	V-2
After flame time for each individual specimen t_1 or t_2	$\leq 10s$	$\leq 30s$	$\leq 30s$
Total after flame for any set (t_1 plus t_2 for 5 specimens)	$\leq 50s$	$\leq 250s$	$\leq 250s$
After flame/glow time for each specimen after 2 nd appl ($t_2 + t_3$)	$\leq 30s$	$\leq 60s$	$\leq 60s$
After flame glow of any specimen up to clamp	No	No	No
Cotton indicator ignited by flaming drips	No	No	Yes

TABLE 7. UL-94 VB TEST CRITERIA

2.2.2 Single-Flame Source Test (ISO 11925)

2.2.2.1 Instrumentation

The instrument consists of the following components:

- Combustion chamber (see Figure 27);
- Ignition source (tilted at 45° vertically);
- Fuel (95% minimum purity);
- U-shaped specimen holder;
- Filter paper

A Fire Testing Technology (FTT) Single Flame Source Test was used for all data presented in this thesis and ISO 11925-2 [88] was adhered to throughout. A schematic view of the combustion chamber is shown in Figure 27.

Dimensions in millimetres

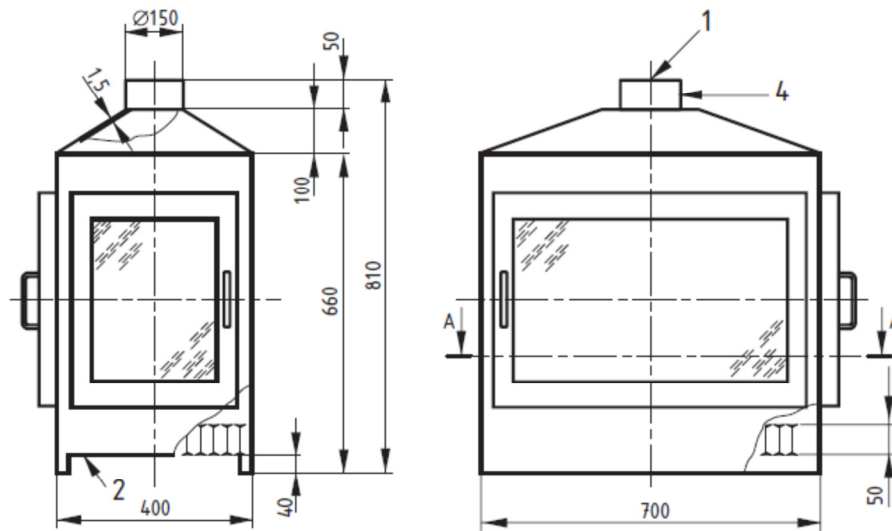


FIGURE 27. SCHEMATIC VIEW OF A CONTROLLED VENTILATION CHAMBER [88]

Figure 28 shows a diagram of the typical support and burner positioning. The numbered aspects of the diagram refer to the following:

- 1 – Specimen holder
- 2 – Test Specimen
- 3 – Support
- 4 – Burner base

A denotes the flame impingement point and is shown in greater detail in Figure 28. Here, the numbered aspects of the diagram refer to the following:

- 1 – Test specimen
- 2 – Burner spacer

d denotes the thickness of the test specimen.

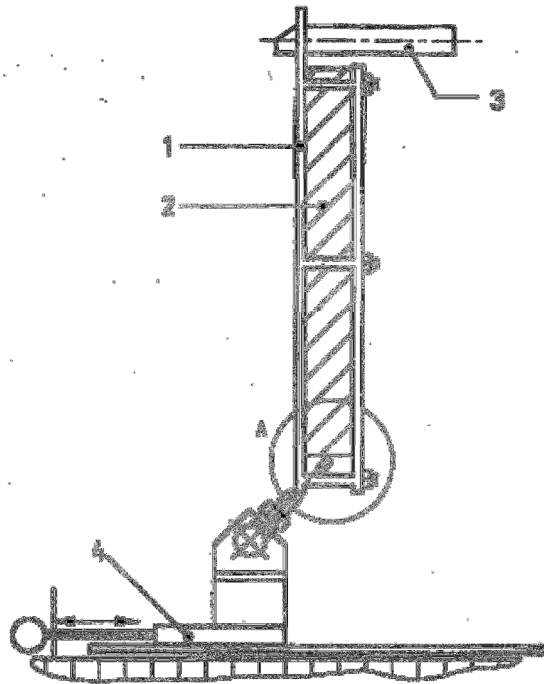


FIGURE 28. SCHEMATIC VIEW OF TYPICAL SUPPORT AND BURNER POSITIONING [88]

2.2.2.2 Calibration

Flame calibration should be completed prior to every experiment. A flame measuring device such as a metal plate should be used to produce a $20 \text{ mm} \pm 1 \text{ mm}$ flame. Removable spacers for both edge and flame impingement can be mounted at the burner orifice to check the distance between the burner edge and specimen surface.

2.2.2.3 Sample Preparation

The samples (90 mm x 250 mm) were cut from sheets of PEEK film which were 210 mm x 297 mm.

2.2.2.4 Materials

For ISO 11925, samples of PEEK used were natural (1000) and black – with the presence of 0.5% carbon black pigment (1300). The thicknesses ranged from $12 \mu\text{m}$ to $750 \mu\text{m}$.

2.2.2.5 Procedure

The burner was ignited in the vertical position and the flame allowed to stabilise. Using the flame height measuring device, the flame was adjusted to a height of 20 mm \pm 0.1 mm and the height checked prior to each application. There are two test methods which can be employed; both methods are described here and both methods were utilised. A flame application time can be chosen for the test procedure; either 15 seconds, with a total test duration of 20 seconds or 30 seconds, with a total test duration of 60 seconds.

2.2.2.6 Surface Exposure Method (Face Ignition)

The flame is applied to the centre line of the test specimen 40 mm above the bottom edge. In practice, each different surface which may be exposed should be tested.

2.2.2.7 Edge Exposure Method (Edge Ignition)

For specimens with a thickness of less than or equal to 3 mm (such as a film), the flame is applied to the midpoint on the bottom of the test specimen.

In both instances, if the test specimen melts or shrinks away from the flame without being ignited, the product should be tested in accordance to Annex A of ISO 11925-2.

Dimensions in millimetres

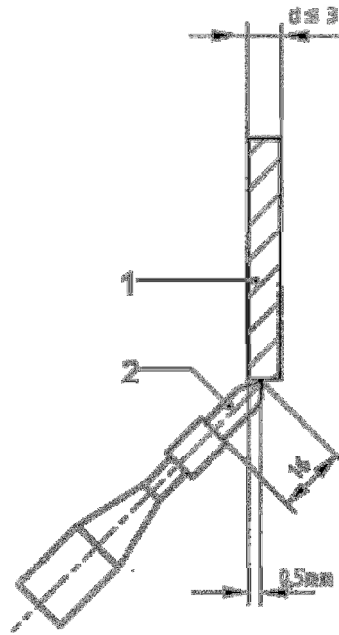


FIGURE 29. POINT OF FLAME IMPINGEMENT FOR TEST SPECIMENS LESS THAN OR EQUAL TO 3 MM THICK [88]

2.3 Ease of Extinction

The ease at which a fire can be extinguished is dependent on the material which is fuelling the fire and as a result, some materials are harder to extinguish than others. This characteristic provides a measure of fire hazard: a material that is harder to extinguish is more likely to prolong a fire than one which is easily extinguished, if all other factors are identical. A common method of determining the ease of extinguishment is the oxygen index where the oxygen concentration required to support continued burning is determined.

2.3.1 Limiting Oxygen Index (LOI)

All LOI measurements presented in this thesis were obtained using a Fire Testing Technology (FTT) Oxygen Index Control Unit and conform to BS EN ISO 4589-2 [31]. The sample size used was 13 mm x 125 mm x 1.6 mm.

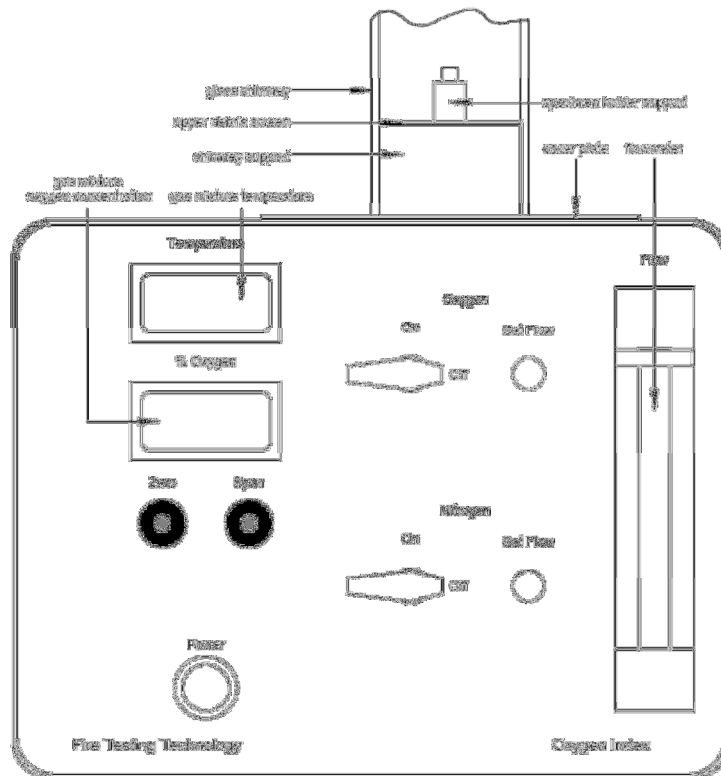


FIGURE 30. VIEW OF THE OXYGEN INDEX FRONT PANEL [31]

2.3.1.1 Instrumentation

As shown in Figure 30, the instrument consists of the following components:

- Control unit with oxygen analyser and flow meter;
- Specimen holder support (allowing for samples in a vertical orientation); and
- Glass chimney

2.3.1.2 Calibration

The instrument was calibrated using the following procedure. First the oxygen index was switched on and the oxygen cell was given 1 hour to warm up and stabilise before the calibration took place. The exhaust system was switched on and the oxygen and nitrogen cylinders were turned on. Adjusting the oxygen flow valve to the 'off' position allowed only nitrogen to flow through the system at 10.6 L min^{-1} . After the oxygen analyser had stabilised, the oxygen concentration was set at zero. The nitrogen valve was then switched to the 'off'

position and the oxygen valve to the 'on' position. The oxygen flow rate was then set to 10.6 L min⁻¹ and after the analyser had stabilised, the span was adjusted to 99.5%.

2.3.1.3 Sample Preparation

For the top surface ignition procedure used, the samples were marked 50 mm from the end to be ignited.

2.3.1.4 Materials

For the LOI, samples of PEEK used were unfilled 90G, 150G and 450G and filled 450G with carbon fibre (CA) and glass fibre (GL) at 30%.

2.3.1.5 Procedure

The oxygen flow rate was decreased and simultaneously, the nitrogen flow rate was increased until a reasonable oxygen percentage was obtained – for PEEK, the LOI is 34 - 35%. The total flow rate of the gases was maintained at 10.6 L min⁻¹ throughout the experiment.

The sample was then clamped into the specimen holder support in a vertical position (see Figure 7) and ignited with a propane flame measuring 16 mm ± 4 mm. The burn time of the sample was measured. If the oxygen concentration was insufficient to support candle-like burning (for at least 180 seconds or through 50 mm of the sample), the oxygen concentration was increased and the experiment was repeated on a fresh sample. This procedure was repeated until a minimum concentration of oxygen was established to support candle-like burning in an oxygen/nitrogen environment.

2.4 Heat Release

The temperature of the fire environment and the rate of fire spread can be influenced by both the amount of heat released from a burning material and the rate at which that heat is released. Both methods of determining heat release utilise the oxygen consumption method to provide heat release data at the bench scale (cone calorimeter) and the micro scale (PCFC).

2.4.1 Cone Calorimeter

The cone calorimeter is a bench-scale instrument developed by the National Institute of Standards and Technology (NIST) in 1982 [89]. The cone calorimeter is an effective method of measuring several of the parameters related to flammability [36], these include:

- Heat release rate;
- Total heat release rate;
- Effective heat of combustion;
- Mass loss rate;
- Ignitability;
- Smoke and soot; and
- Toxic gases and their ratios [37]

Among these, the total heat release rate is an important constraint as it defines the size and potential hazard of any resulting fire [90].

2.4.1.1 Instrumentation

A typical cone calorimeter consists of the following components:

- Conical-shaped cone heater;
- Spark ignition source;
- Load cell;
- Flow measuring instrument;
- Paramagnetic oxygen analyser;
- CO/CO₂ analyser;
- Laser photometer for smoke visibility measurements

A Fire Testing Technology (FTT) Cone Calorimeter was used for all the data presented in this thesis and ISO 5660-1 [36] was adhered to throughout. The sample size used was 100 mm x 100 mm with variable thicknesses.

2.4.1.2 Calibration

The cone calorimeter needs to be calibrated before running a set of samples. The procedure for doing so is detailed below. The silica gel and soda lime are inspected to see if they need renewing. The computer software 'Conecal' needs to be loaded. Any water which has collected in the refrigerated trap needs to be drained off. With the external extractor fan switched off, the differential pressure transducer (DPT) and methane need to be set to zero. The cold trap, load cell, pump and ignition buttons all need to be switched on at the front control panel of the cone calorimeter. The cone calorimeter extractor fan should then be switched on and adjusted so that the value for the mass flow rate measures 30 g s^{-1} at the duct and 24 L s^{-1} at the orifice plate.

Oxygen Analyser

The oxygen flow is reduced to zero manually using the flow meter valve. Nitrogen is then passed through the sample line at a flow rate of $200 \text{ cm}^3 \text{ s}^{-1}$. When the paramagnetic oxygen analyser has stabilised, both the analyser and the computer are set to zero. The nitrogen source is then turned off, allowing air to flow through the system. When the paramagnetic oxygen analyser has settled for the second time, the span is adjusted so that the reading shows 20.95%. The span button on the computer is selected and the calibration values are logged.

CO/CO₂ Analyser

Making sure that the cone calorimeter pump is switched off, the analyser should be set to zero by pressing the calibration (cal) button on the front control panel of the analyser. Zero should then be selected on the computer. The CO/CO₂ calibration gas is then switched on and adjusted to a flow rate of 1.6 L min^{-1} . After the reading stabilises, the calibration option is selected on the front control panel and the CO component is selected. When the analyser reads 'calibration ok', the span button is selected on the computer and an actual concentration (stored by the computer) is given. This calibration process is then repeated for CO₂.

Laser Smoke Photometer

An opaque card is inserted into the side of the photometer. The readings should be allowed to stabilise before the zero button is selected on the computer. The opaque card should then be removed and the shutter closed. The photometer should be calibrated by first inserting the 0.8 optical density (OD) interference filters and then repeating with the 0.3 OD filter and selecting the calibrate option on the computer.

Orifice Flow Constant - Methane Calibration

The methane burner is inserted into its holder and the spark igniter positioned over the centre of the burner outlet. Methane gas, of a high purity (99.9%) is then passed through the burner. The methane valve should be opened and the methane supply on the cone calorimeter switched on. The burner should ignite within 5 seconds. The flow of methane needs to be adjusted to 5 kW based on the net heat of combustion of methane 50×10 kJ/g. "Calibrate heat release" is then selected on the computer, allowing for the calculation of the C Factor - the orifice flow constant. This value should read between 0.040-0.046 and therefore be placed between the two red lines shown on the computer screen. The value is then recorded by selecting "accept" on the computer.

Cone Heater Irradiance

Ensuring that the shutters are closed and there is a piece of insulating backing board on the load cell, turn on the cone heater and increase the temperature in a step-wise manner (of 200°C) until the required temperature is reached and allow the reading to stabilise. Making certain that the heat flux meter has water running through it; remove the plastic cap and position into the holder. Open the shutters to obtain a reading on the computer.

Load Cell

The load cell should be calibrated with calibration weights to ensure that the readings on both the load cell and on the computer are comparable. The mass range of the load cell should be adjusted so that the maximum mass is slightly higher than the mass of the sample (with the holder). Select the menu button on the load cell control panel until it reads OT.SC.OF. Press the min button on the control panel to ensure that Read 1 has a value of 0000. Press the menu button on the load cell control panel until it reads OUTPUT1. This should have a value of

0000. Press menu again and adjust the value of Read 2 to the maximum mass. Press menu until it reads OUTPUT2 and adjust this to a value of 10.000 volts. Pressing the menu button again will store any adjustments which have been made. The mass range should also be adjusted on the computer.

PMMA Calibration

The procedures mentioned previously should be undertaken at the start of every set of cone calorimeter experiments. Calibration of the instrument with a standard sample of PMMA however is only required on a weekly basis. The cone heater should read approximately 730°C and by using the heat flux meter, an irradiance of 50 kW m⁻² should be determined. If this is not the case, the temperature of the cone heater should be adjusted until this value is obtained.

2.4.1.3 Sample Preparation

The 100 mm x 100 mm sample should be accurately weighed and its thickness measured. The sample should then be wrapped in a 0.040 mm aluminium foil, with the matt side of the foil facing outwards. The foil should wrap all except for the upper surface of the specimen. A layer of ceramic fibre blanket with a thickness of 13 - 20 mm should be placed in the sample holder. The foil wrapped specimen is then placed over the ceramic fibre blanket and a retainer frame over the sample holder. As a result, 0.0088 m² of the surface of the sample is exposed to the radiant cone heater.

2.4.1.4 Materials

For the cone calorimeter, samples of PEEK used were unfilled 90G, 150G, 450G and 600G, filled 450G with carbon fibre (CA) and glass fibre GL at 30%, filled 381G with talc at (TL) at 30% and 150G and 450G with the presence of <0.5% carbon black pigment (150903 and 450903, respectively). Samples used range from 2.5 mm to 10 mm in thickness.

2.4.1.5 Procedure

On the computer, “run” was selected and details central to the test such as file name, exposed area, mass, orientations etc were typed in. Ensuring that the shutters were closed, the sample holder (with specimen) was placed on the load cell and the mass shown was checked to see if was comparable to that which was recorded. The spark igniter was placed over the centre of the sample surface. On the computer the ‘perform pre-run calibration’ option was selected. When the instrument was ready, the shutter was opened thus exposing the sample to the radiant cone heater. Simultaneously, button 1 on the handset was pressed to indicate ‘start of test’. When ignition occurred, button 2 was pressed on the handset to indicate ‘sample ignition’. Button 3 on the handset can be used to record the time of any observations made such as swelling, char formation, char splitting etc, the comments for which can be inputted manually at the end of the test. When flaming ceased, button 4 on the handset was pressed to indicate ‘end of test’. Keeping the shutters open, a further two minutes worth of data was collected and button 1 was pressed on the handset to indicate ‘finish’. The ‘Conecalc’ software then processed the data which was stored as a comma separated variable (CSV) file and analysed using packages such as Microsoft Excel.

All experiments were conducted in a similar manner to that described for the PMMA calibration. The experiments were performed in a horizontal orientation and initially at an irradiance of 50 kW m^{-2} , typical of a well-ventilated fully developed fire. The recommended heat flux for exploratory testing, 35 kW m^{-2} did not result in sample ignition after 10 minutes and so the irradiance was increased. All samples were tested at least 3 times to ensure reproducibility. Other irradiances were explored ranging from 45 kW m^{-2} to 70 kW m^{-2} .

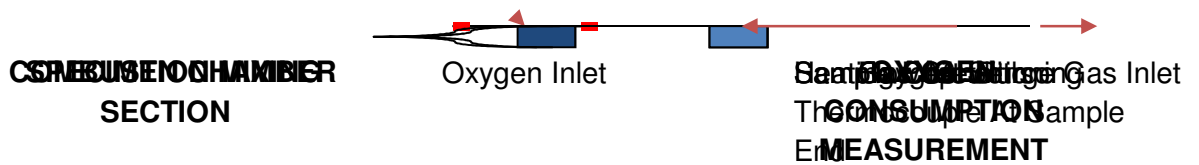
2.4.1.6 Data Interpretation

Data from the ‘Conecalc’ software was converted to CSV and can then be analysed on Microsoft Excel.

2.4.2 Pyrolysis Combustion Flow Calorimeter

2.4.2.1 Instrumentation

The PCFC apparatus is shown in Figure 31. A sample is placed within the sample cup. The specimen chamber is heated at a constant heating rate (1K per second) in a flow of nitrogen. Any volatile products enter the combustion mixing chamber, held at 900°C where a flow of oxygen is introduced, to ensure the complete combustion of these products.



Exhaust

FIGURE 31. SCHEMATIC VIEW OF A PYROLYSIS COMBUSTION FLOW CALORIMETER

2.4.2.2 Sample Preparation

Samples were obtained from the centre of cone calorimeter plaques. Approximately 5 mg of sample was utilised. Samples were weighed prior to, and after the experiment.

2.4.2.3 Materials

The materials investigated were the three viscosities of PEEK – 90G, 150G and 450G and PEEK filled with carbon and glass fibre at 30%.

2.4.2.4 Procedure

The heating rate was $60^{\circ}\text{C min}^{-1}$ in an $80\text{ cm}^3\text{ min}^{-1}$ stream of nitrogen; the maximum pyrolysis temperature was 900°C . The anaerobic thermal degradation products in the nitrogen gas stream were mixed with a $20\text{ cm}^3\text{ min}^{-1}$ stream of oxygen prior to entering the combustion furnace at 900°C . The heat release was determined by oxygen consumption calorimetry.

2.5 Char Analysis

Although char formation, by nature, is a chemical process, its significance is largely due to the polymer's physical properties. The structure and composition of char can indicate a decomposition pathway. The elemental composition of a char may also be of assistance when looking at filled polymeric materials to determine whether the filler material is lost during pyrolysis or retained within the structure. For this purpose, a scanning electron microscope with energy dispersive x-ray (SEM/EDAX) analysis was used.

2.5.1 Scanning Electron Microscope/Energy Dispersive X-Ray (SEM/EDAX) Analysis

Scanning electron microscopy is a surface imaging technique and, as with any microscope technique, its main objective is for magnification and focus for clarity. An SEM uses electrons to form an image: an electron beam follows a vertical path through the column of the microscope and through electromagnetic lenses which focus and direct the beam down towards the samples. Once the beam hits the sample, backscattered or secondary electrons are ejected from the sample and converted to a signal which produces an image. This process is carried out within a vacuum chamber to prevent:

- The filament, which produces the electron beam, from burning out;
- Gas molecules colliding with the electron beam; and
- Different compounds forming and being deposited on the sample if gas molecules do collide with the electron beam.

Energy dispersive x-ray (EDAX) analysis can be used for elemental examination or chemical characterisation of a sample. A high energy electron beam is focused onto the sample. At rest, atoms within a sample contain ground state (unexcited) electrons within electron shells. The electron beam can excite electrons on the surface to a higher excited state, ejecting it from its shell thus leaving an electron hole. An electron from an outer shell then fills the hole; the difference in energy (between the higher energy and lower energy shell) is released in the form of an x-ray. The x-ray is then detected and analysed and is characteristic of the atomic structure of the element from which it was emitted [91].

The two techniques combined together can provide a magnified image of the surface with information regarding the elements which are present and their ratios.

2.5.1.1 Instrumentation

The instrument consists of the following components:

- Electron Source
- Scanning Electron Microscope (SEM)
- EDAX Analysis Software

A schematic diagram of a SEM is shown in Figure 32.

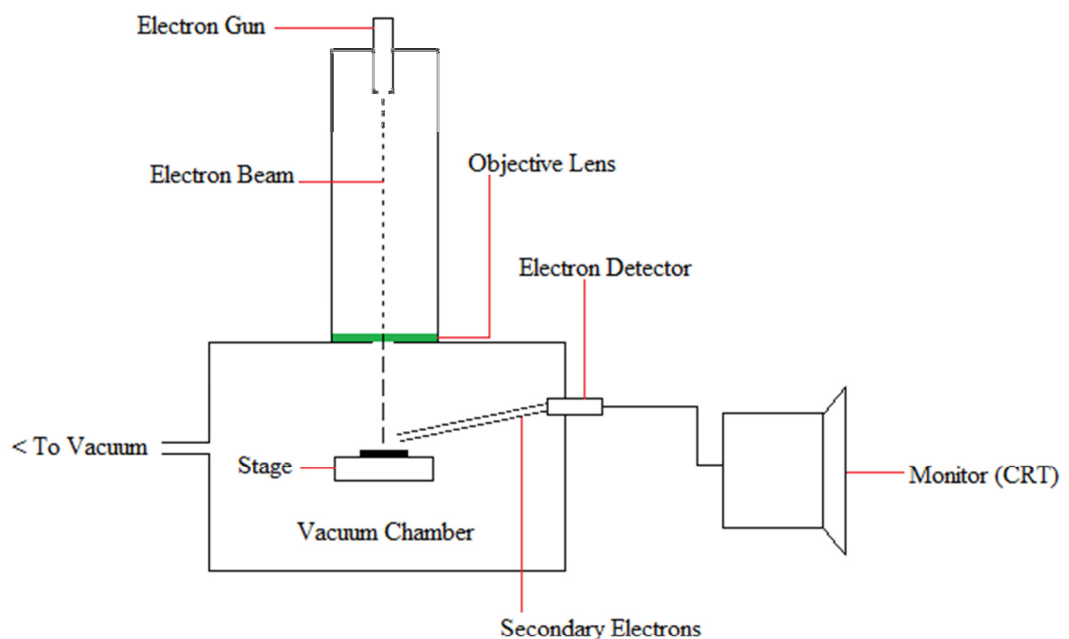


FIGURE 32. SCHEMATIC VIEW OF A SEM

2.5.1.2 Sample Preparation

Samples of PEEK char were obtained from the residues formed with the ISO 5660 test [36]. The samples had undergone Cone Calorimeter analysis at a 50 kW m^{-2} heat flux as described previously. These were cut to fit onto a specimen holder which measured 1 cm in diameter. A piece of carbon tape (also measuring 1 cm in diameter) was adhered to the surface of the sample holder and the PEEK sample was placed on top.

2.5.1.3 Procedure

The sample was placed onto a black adhesive surface which is mounted onto the sample holder. Any excess sample was removed and the sample holder was placed onto the stage within the SEM. The vacuum chamber was closed and the pressure set at 0.5 torr.

2.5.1.4 Data Interpretation

Data can be analysed on screen using the SEM software and images can be created from the 'online' screen and viewed as .jpg files.

2.5.2 Diamond Attenuated Total Reflectance/Fourier-Transform Infrared (dATR-FTIR)

Attenuated Total Reflectance/Fourier Transform Infra Red (ATR-FIR) is a technique which analyses the surfaces of materials. The foundation of this technique focuses on passing infrared radiation through an infrared transmitting crystal such as zinc selenide, germanium, or diamond – with a high refractive index. This allows the infrared radiation to reflect within the ATR element many times. A schematic diagram of the interaction of the ATR crystal with infrared radiation is shown in Figure 33.

Pressure is applied to the sample thus enabling it to come into intimate optical contact with the top surface of the ATR element – the crystal. Infrared radiation is then administered to the crystal and this penetrates through the sample infinitely along with each reflection along the top of the crystal surface by means of the evanescent wave. An evanescent wave is a

penetrating electromagnetic field whose intensity quickly decays as it moves away from its source. The evanescent wave protrudes merely a few microns ($0.5 - 5 \mu\text{m}$) beyond the crystal surface into the sample. At regions within the infrared spectrum where the sample absorbs energy, the evanescent wave becomes altered or attenuated. This attenuated energy from each evanescent wave is passed back to the infrared beam. At the output end of the ATR element, the infrared radiation is directed towards a detection source.

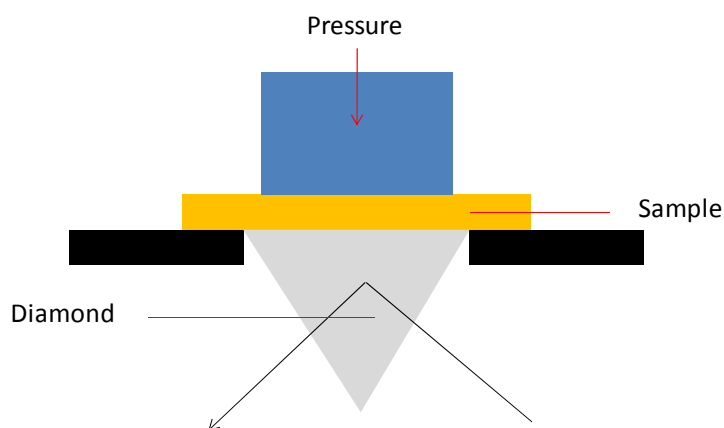


FIGURE 33. SCHEMATIC DIAGRAM OF THE INTERACTION OF THE ATR CRYSTAL WITH INFRARED RADIATION

2.5.2.1 Instrumentation

The instrument consists of the following components:

- ATR with diamond crystal
- FTIR

2.5.2.2 Sample Preparation

Samples of PEEK were obtained from the thinner products of ISO 11925 [88]. These had been subjected to varied temperatures in an oven for different periods of time.

2.5.2.3 Procedure

The sample was placed onto the stage; the pressure arm then lowered down onto the sample to ensure maximum contact with the ATR crystal.

2.5.2.4 Data Interpretation

The ATR-FTIR software processes the data which can be stored as a comma separated variable (CSV) file and therefore analysed using packages such as Microsoft Excel.

2.6 Materials

The materials studied in for the preparation of this thesis were all supplied by Victrex plc. They consist of three base materials 90G, 150G and 450G (in order of increasing melt viscosity). 381G (a medium melt viscosity grade) and 600G (a high melt viscosity grade) are also studied. 450G is filled with 30% carbon fibre to produce 450CA30 and 30% glass fibre to produce 450GL30. 381G is filled with 30% talc to produce 381TL30. 150G is filled with 30% titanium dioxide to produce 150TI30. Both 150G and 450G are filled with small amounts of carbon black, usually for colouring purposes. Further information about the base grade commercial polymers can be obtained from Technical Data Sheets available from Victrex.

RESULTS AND DISCUSSION

CHAPTER 3. THERMAL DECOMPOSITION

The thermal decomposition processes of PEEK and its products of decomposition are examined in this chapter. Thermogravimetric analysis has been employed to determine the kinetic parameters of PEEK and its carbon and glass-fibre filled composites. The technique was also utilised to investigate the thermal decomposition of PEEK, of different viscosities and with varying additives. Differential thermogravimetric analysis was employed to determine the effect of fillers on the virgin polymer. Simultaneous thermal analysis coupled with Fourier transform infrared analysis of gas phase products was employed to determine the volatile products of the decomposition of PEEK and its fibre-filled composites. Similarly, pyrolysis gas chromatography mass spectrometry was utilised to determine the gas phase products of a flash pyrolysis scenario – whereby the temperature of the polymer increases rapidly, as subsequently does the rate of decomposition.

These experiments were completed to provide a better understanding of the processes occurring during the thermal decomposition of PEEK and its fibre-filled composites and the sensitivity of these processes to environmental conditions, particularly atmosphere (such as the presence or absence of an oxidative environment) and heating rate.

3.1 Thermogravimetric Analysis

3.1.1 Thermogravimetric Analysis in Air

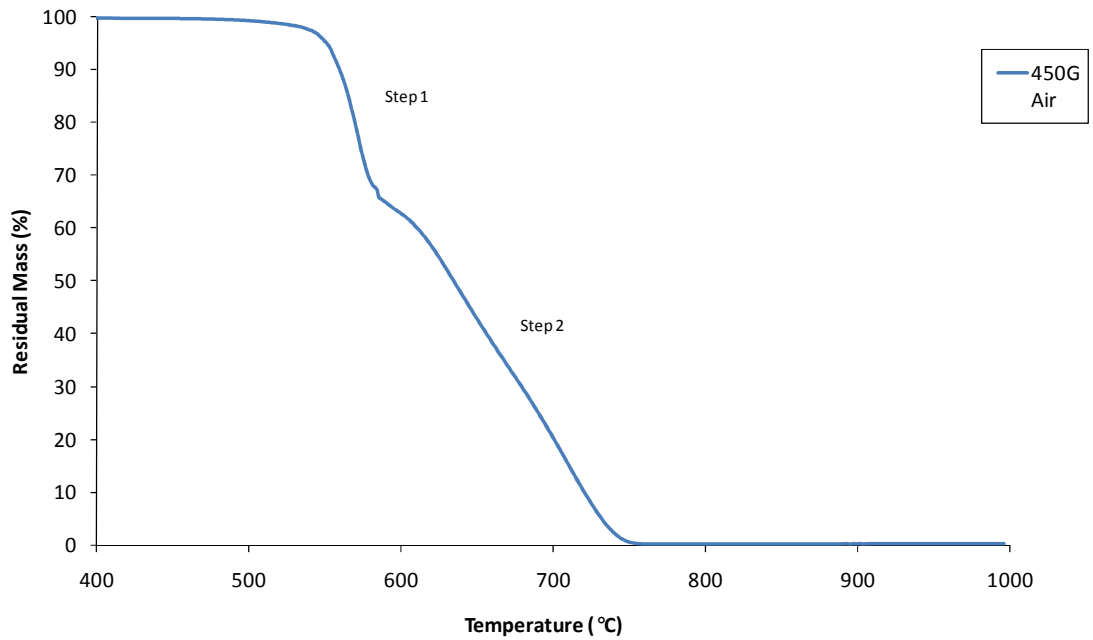


FIGURE 34. TGA OF 450G IN AIR

Initial TGA experiments were carried out and it was determined that the decomposition process of PEEK in an oxidative environment occurred in two separate steps. These are labelled on Figure 34. The first step of decomposition is attributed to the random chain scission of the ether and ketone bonds [52] [10]. The second decomposition step is attributed to the oxidation of the carbonaceous char formed as a result of the first decomposition step [10]. Between the two stages there appears to be a 'bump' in the mass loss curve. This is not part of the decomposition of PEEK and is an artefact of the experiments.

Initial TGA experiments were also carried out to determine which heating rate would be suitable for conducting further experiments. Figure 35 shows that a heating rate between $5^{\circ}\text{C min}^{-1}$ and $20^{\circ}\text{C min}^{-1}$ would be the best. A heating rate of $50^{\circ}\text{C min}^{-1}$ does not give total decomposition as the samples are being heated too quickly with mass remaining at 1000°C . Although during the first decomposition step the effect of heating rate is insignificant, the second decomposition step appears to rely on a slower heating rate for effective char oxidation. It was determined that $10^{\circ}\text{C min}^{-1}$ would provide the most informative data. In studies on chlorinated polyvinylchloride (PVC) [92], the char appeared more stable at higher heating rates, however this was not shown to be the case. At high heating rates, less stable char results but the access of oxygen is limited. At lower heating rates, more stable char is

formed but more oxygen impinges on the char during heating. The use of a high heating rate to the end of the first stage, followed by a low heating rate showed that the char resulting from rapid heating was less thermally stable.

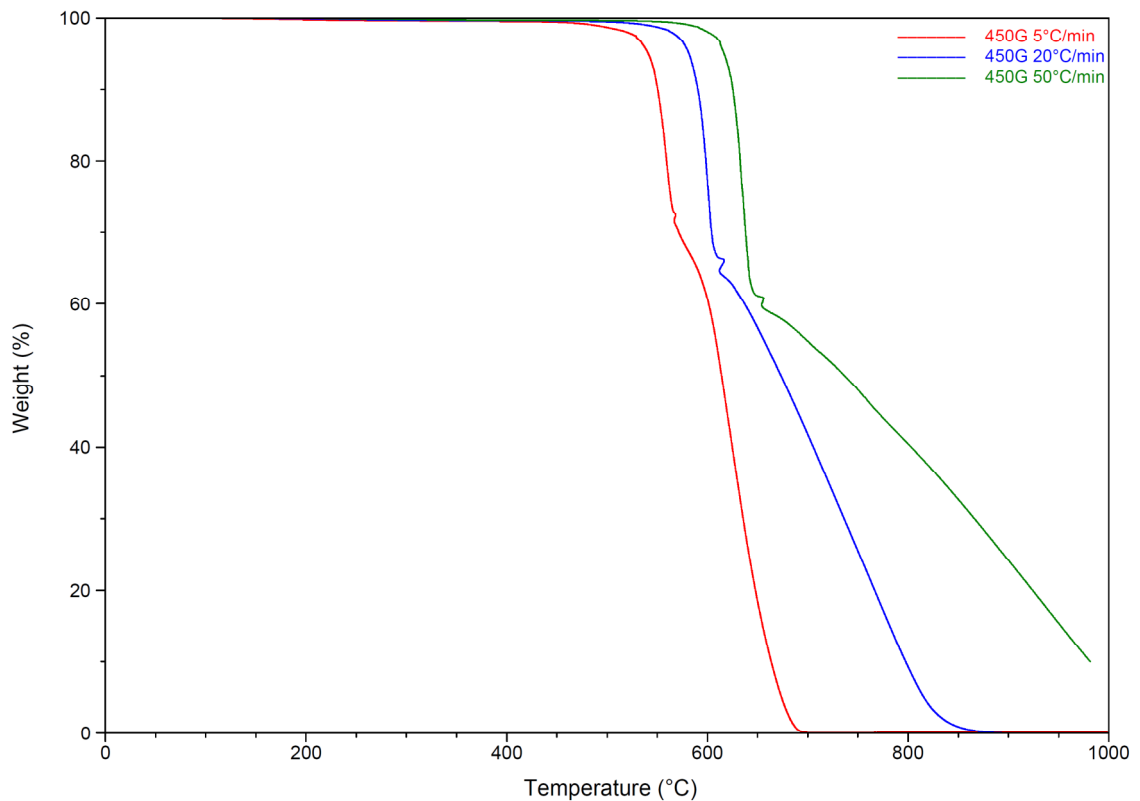


FIGURE 35. TGA WITH DIFFERENT HEATING RATES IN AIR

3.1.1.1 *Effect of Polymer Viscosity*

Experiments were conducted in air on the different viscosities of PEEK in order to determine whether a difference in the material's intrinsic viscosities would manifest itself as a difference in decomposition behaviour. The results of this experiment are shown in Figure 36. All three materials display very similar behaviour during the first step of decomposition, losing around 35% mass within a 30°C window. Scission and release of both the ether and ketone groups would result in 21% mass loss, based on the repeat unit of PEEK. 35% mass loss indicates that some aromatic compounds, such as phenol, as suggested from the pyrolysis products of PEEK [52], are also being released. In the second step of decomposition, 450G appears to be the most stable and then in turn the 90G and 150G samples. Repeat testing

shows this apparent difference to be experimental error. The remaining mass is lost in the second decomposition stage with total mass lost by 750°C.

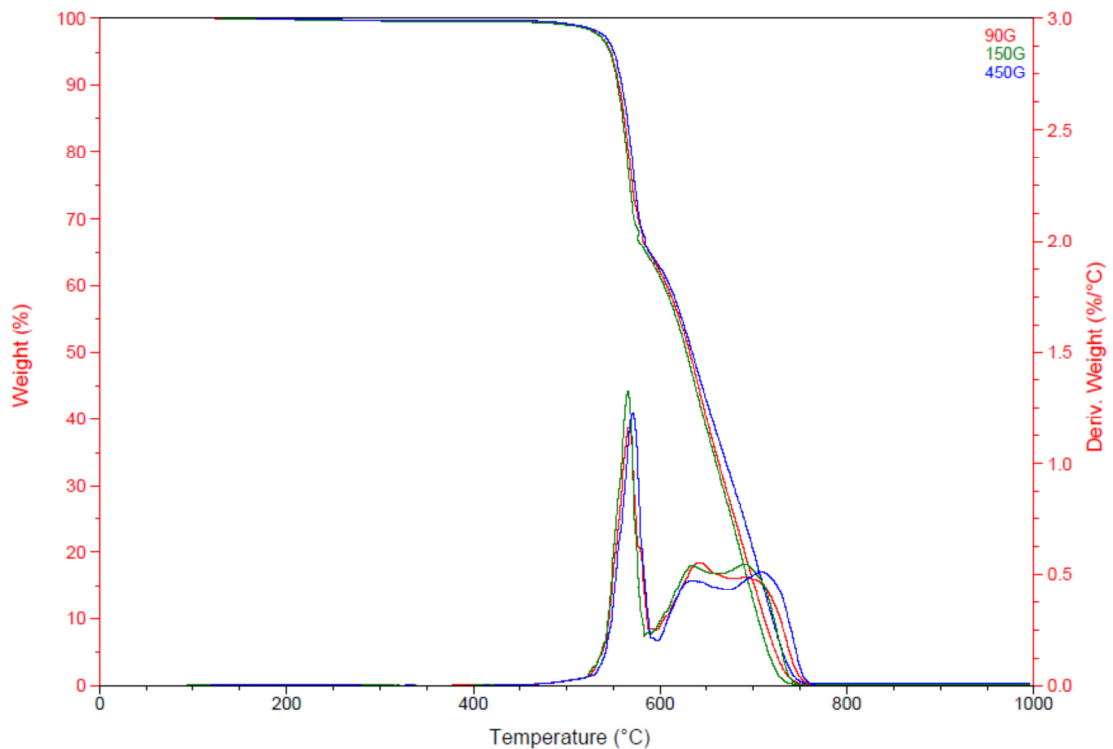


FIGURE 36. TGA AND DTG OF 90G, 150G AND 450G IN AIR

Differential mass curves for 90G, 150G and 450G are also shown in Figure 36. All three materials begin to lose mass at a similar temperature with an almost identical rate of mass loss. Of the three viscosities, it appears that 150G loses the most mass and 90G loses the least in the first decomposition step. During the second decomposition step, 450G loses less mass per °C but mass loss occurs over a longer period of time – ceasing at 775°C. 90G and 150G lose more mass per °C however for both these samples, total mass loss occurs at a lower temperature – 150G being the lowest at just before 750°C. This lower total mass loss temperature for 150G could account for the higher final mass in the TGA curves. Interestingly, during the second step of decomposition, both 150G and 450G show two significant peaks of mass loss - one at ~640°C and one at ~710°C, the latter being greater in height. Conversely, the 90G samples show only the first peak at ~640°C and subsequently, mass loss begins to decrease gradually. The second peak is evident; however, this peak is not larger than the first as it is for 150G and 450G samples.

3.1.1.2 Experiments on Fillers

Experiments were conducted in air on PEEK containing fillers to investigate if there were differences between the fibre-filled samples and between the fibre-filled and unfilled samples. Material data sheets show that in the LOI and UL-94, PEEK reinforced with carbon and glass fibre has better flammability properties than the unfilled virgin polymer. The results of this experiment are shown in Figure 37. During the first step of decomposition, the onset of decomposition for 450GL30 (~560°C) occurs at a higher temperature than pure PEEK (535-540°C) and the polymer appears to be more stable than PEEK filled with carbon fibre. This may be due to the oxidation of carbon fibre which causes the material to lose more mass at an earlier stage. However, the presence of carbon fibre gives greater thermal stability than the pure PEEK alone. 450CA30, although having a similar onset of decomposition, loses mass at a steadier rate. At around 650°C, there is a 3% difference in mass loss between the fibre-filled samples. During the second step of decomposition, 450GL30 loses mass in a similar manner to pure PEEK and 450CA30 until around 800°C when the material remains at around 35% up to 1000°C. 450G loses all its mass at 750°C and 450CA30 at 775°C.

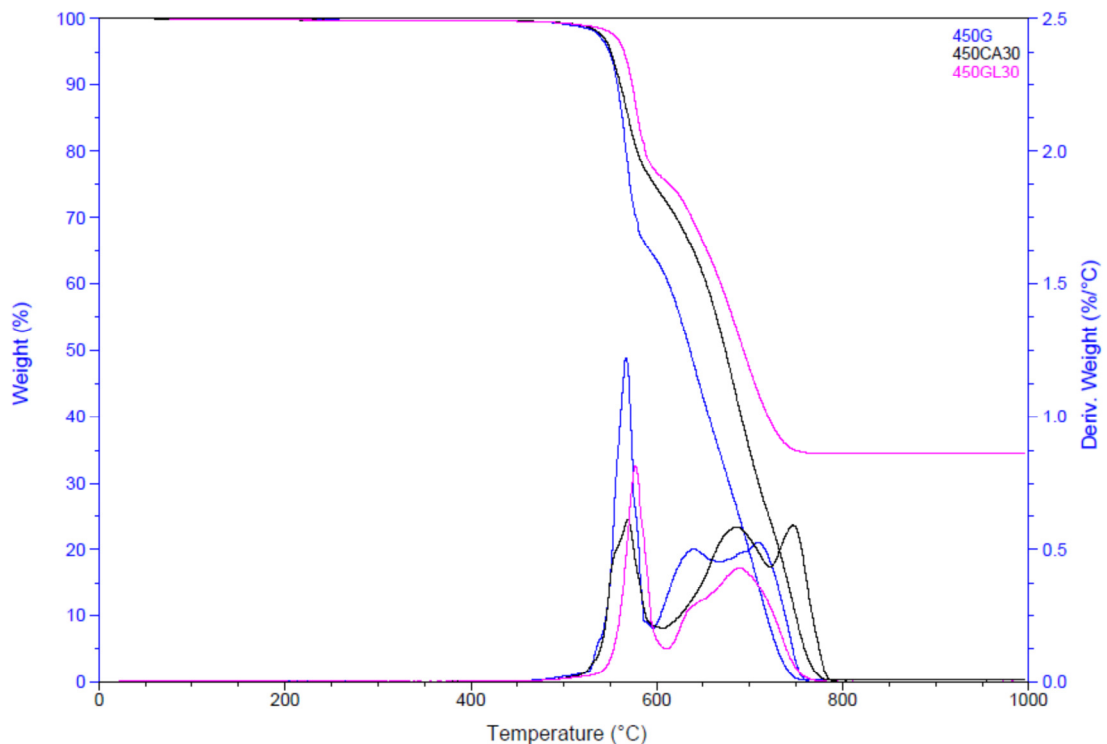


FIGURE 37. TGA AND DTG OF 450G, 450CA30 AND 450GL30 IN AIR

Derivative mass loss curves for 450G, 450CA30 and 450GL30 can be seen in Figure 37. Both 450CA30 and 450GL30 show a lower peak during the first major period of mass loss at around 550°C. The onset of mass loss for 450GL30 is later and this is also indicated in the TGA curves. In the second step of decomposition – between 600°C and 800°C 450GL30 appears to lose the least mass, followed by 450G and 450CA30. 40CA30 shows mass loss up to 50°C after 450G and 450GL30 cease to lose mass. No mass is lost by any of the materials after 800°C.

PEEK reinforced with talc at 30% (381TL30) was also investigated. The results of this are shown in Figure 38. The onset of decomposition for 381TL30 occurs at a similar temperature to the unfilled PEEK however, during the first step of decomposition, the total amount of material lost is considerably less – around 20% compared to the 35% for unfilled PEEK. The second step of decomposition for 381TL30 is similar to that of unfilled PEEK although this process occurs at a higher temperature. At 750°C where all material is lost in the unfilled PEEK, around 30% of the 381TL30 remains stable up to 1000°C. The 30% remaining mass is attributed, as expected, to the inert talc filler.

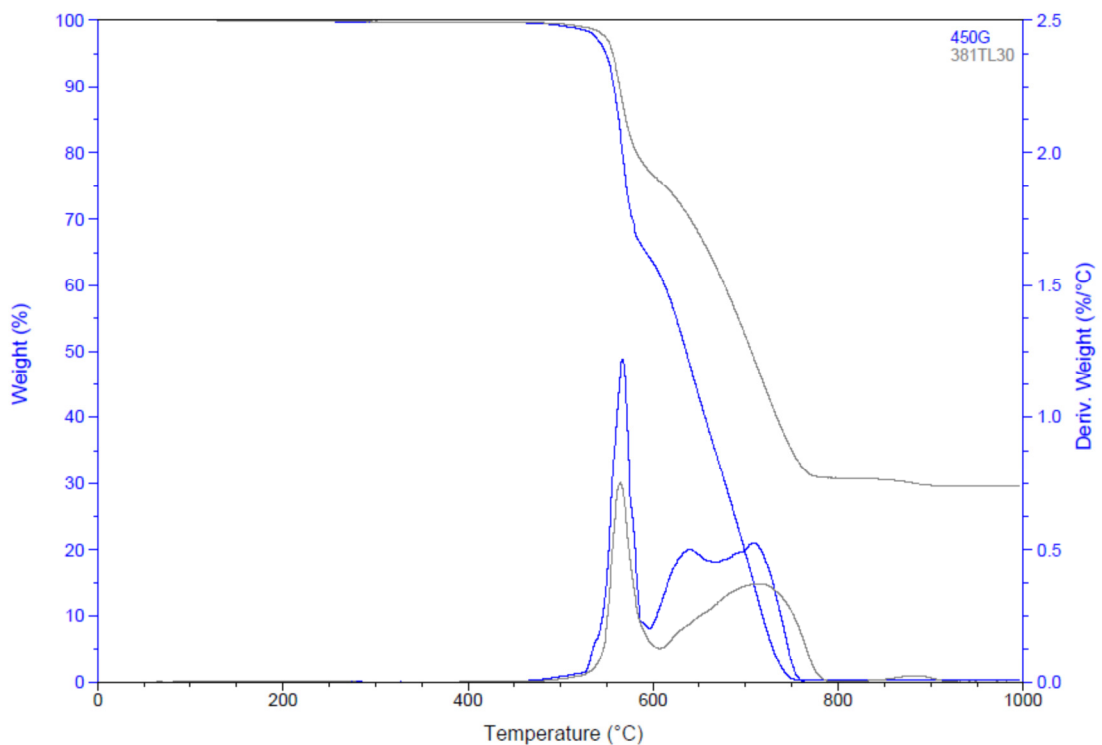


FIGURE 38. TGA AND DTG OF 450G AND 381TL30 IN AIR

Derivative mass loss curves are shown for 450G and 381TL30 in Figure 38. Both 450G and 381TL30 being to lose mass at a similar time. During the first decomposition step, 450G loses more mass than 381TL30. For the second decomposition step, 450G again loses more mass than the talc filled composite however, total mass loss occurs earlier for 450G – at around 760°C compared to 900°C for 381TL30. For the talc filled composite, there is a small but significant loss of mass which occurs between 800°C and 900°C. This loss of mass is due to the remaining water that is driven off between 800°C and 840°C, resulting in the transformation of talc to enstatite ($Mg_2Si_2O_6$) and amorphous silica [93].

Similarly, experiments have also been conducted on PEEK reinforced with titanium dioxide (TiO_2) at 30% (150TI30) as seen in Figure 39 . Again, the onset of decomposition for 150TI30 occurs at a similar temperature to unfilled PEEK. During the first step of decomposition around 25% mass loss occurs in the filled PEEK compared to a 35% mass loss in the unfilled PEEK. During the second step of decomposition, 150TL30 shows greater thermal stability than the unfilled PEEK after 650°C. In the unfilled PEEK, total mass loss occurs at around 750°C. In the filled PEEK, mass loss occurs until around 800°C when 30% mass remains up to 1000°C. The 30% remaining mass is attributed, as expected, to the inert titanium dioxide filler.

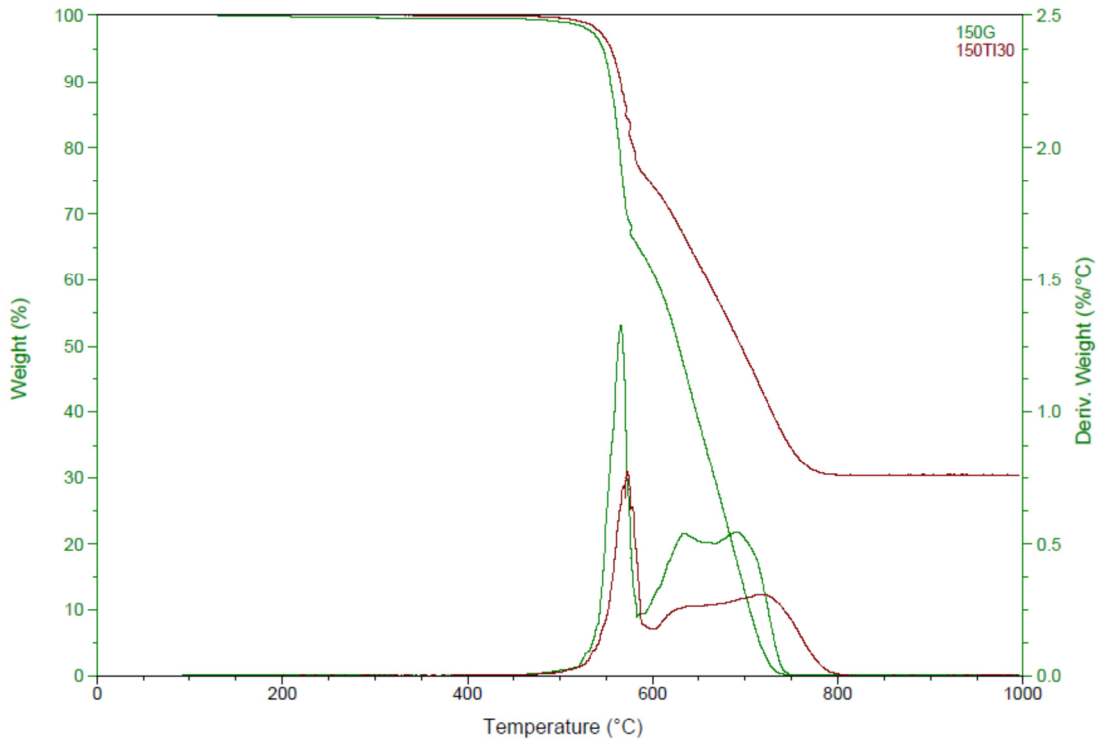


FIGURE 39. TGA AND DTG OF 150G AND 150TI30 IN AIR

The derivative mass curves for 150G and 150TI30 in air are shown in Figure 39. As indicated by the first major mass loss peak – at around 550°C, it can be seen that 150G loses more mass per °C than 150TI30. Additionally for 150TI30, the mass loss experienced in the second major peak – between 600°C and 800°C is also less than 150G however extends over a slightly longer period of time. Whereas 150G ceases to lose mass above 750°C, the titanium dioxide filled composite continues to lose mass till around 800°C.

In air, the thermal stability of the fillers used in PEEK varies. A greater variation is seen in the second step of decomposition.

Sample	T _{40%} (°C)
450G	660
450CA30	700
450GL30	740
381TL30	720
150TI30	740

TABLE 8. TEMPERATURE CORRESPONDING TO 40% RESIDUE

The first step results in a reduction of mass loss by 30%, as expected with the presence of 30% less polymer. However, during the second step, the thermal stability of the glass and titanium dioxide filled samples is higher, as seen by the temperatures corresponding to 40% residue in Table 8. This temperature is higher for all filled materials compared to 450G which reach 60% mass loss at 660°C.

3.1.1.3 Conditioned Samples

Experiments conducted in the cone calorimeter investigated the effects of conditioning on heat release rate (as described later in Figure 99). This experiment was mirrored in the TGA using samples of the same material – unfilled 450G. The samples were placed in an oven at 400°C for 2, 4 and 6 hours. The results of this experiment are shown in Figure 40.

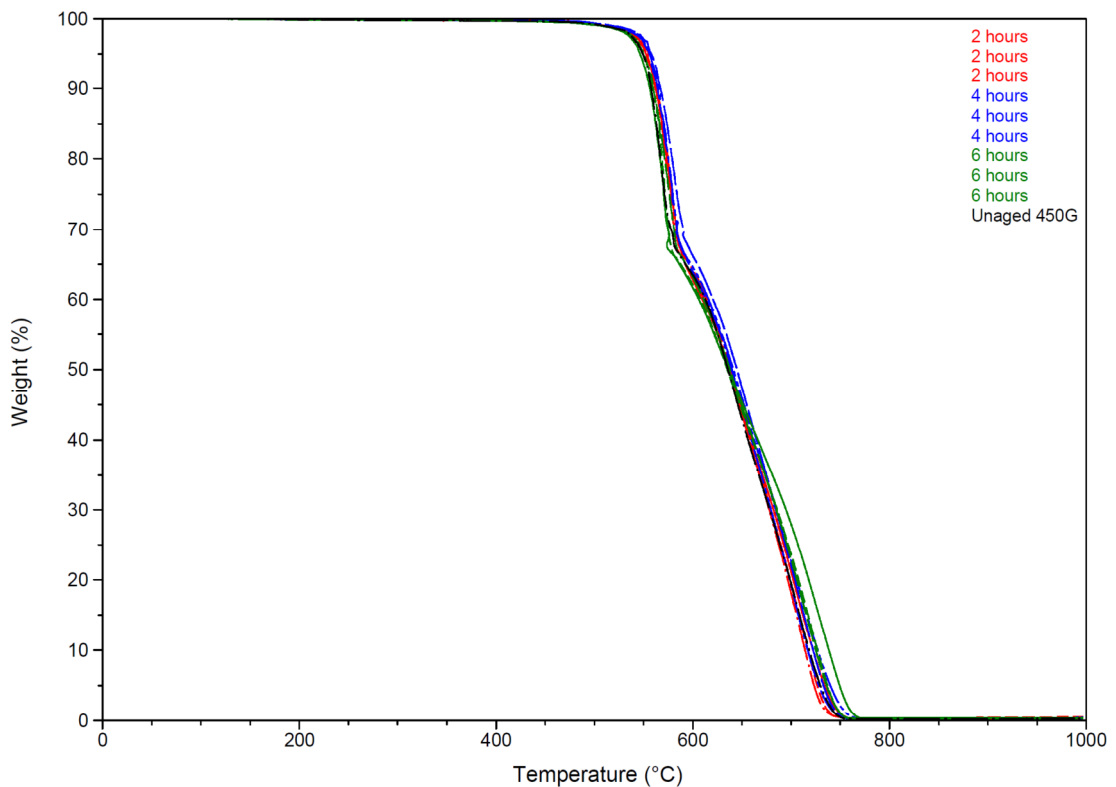


FIGURE 40. TGA OF 450G CONDITIONED IN AIR

As seen in Figure 40, samples conditioned for 2, 4 and 6 hours at 400°C show the same two step decomposition as the unaged 450G polymer. There appear to be slight differences in both the first and second decomposition steps as seen in Figure 41 and Figure 42, respectively.

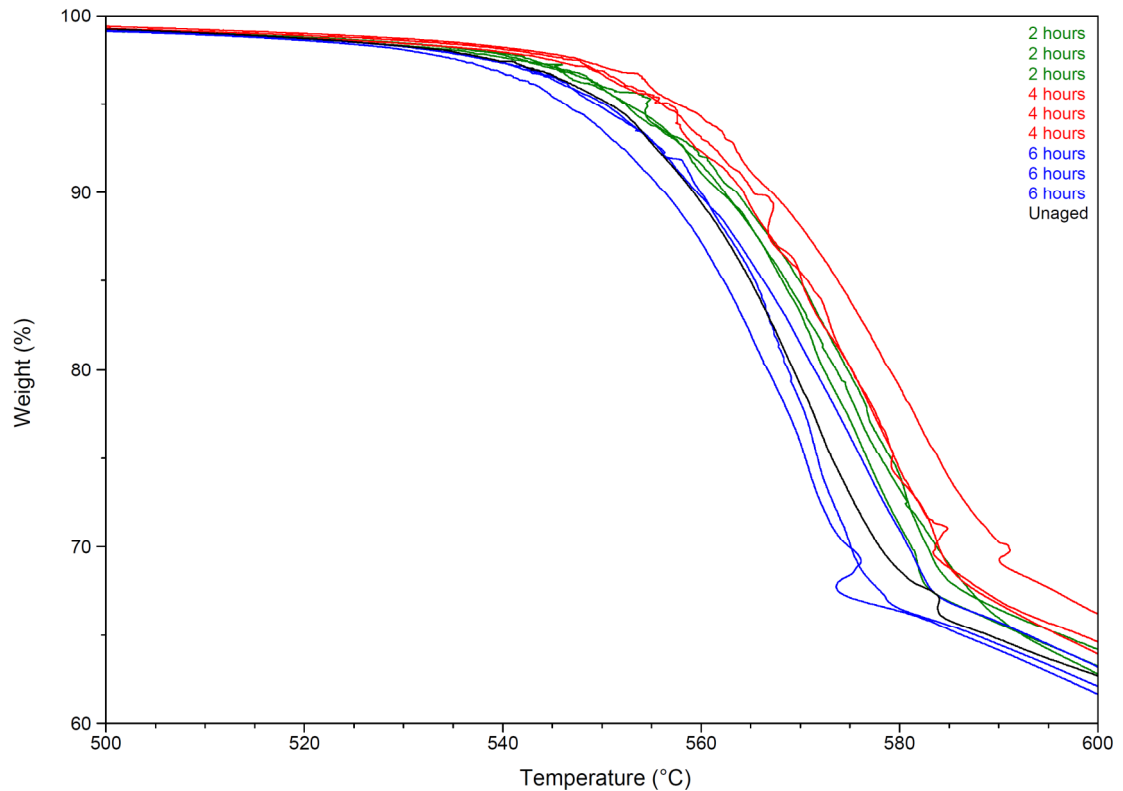


FIGURE 41. TGA OF 450G CONDITIONED IN AIR – FIRST DECOMPOSITION STEP

During the first step of decomposition as shown in Figure 41, it is evident that pre-conditioning the samples increases the material's thermal stability although this is a highly magnified portion of the TG curve and shows noise in the instrumental data. This is true for the samples aged for 2 and 4 hours but not for the samples aged for 6 hours where the effect of pre-conditioning seems to lower the material's thermal stability, as seen by the lower temperature for the onset of decomposition and for 30% mass loss. The temperature corresponding to 30% mass loss is 575°C for samples conditioned for 6 hours compared to 595°C for samples conditioned for 4 hours.

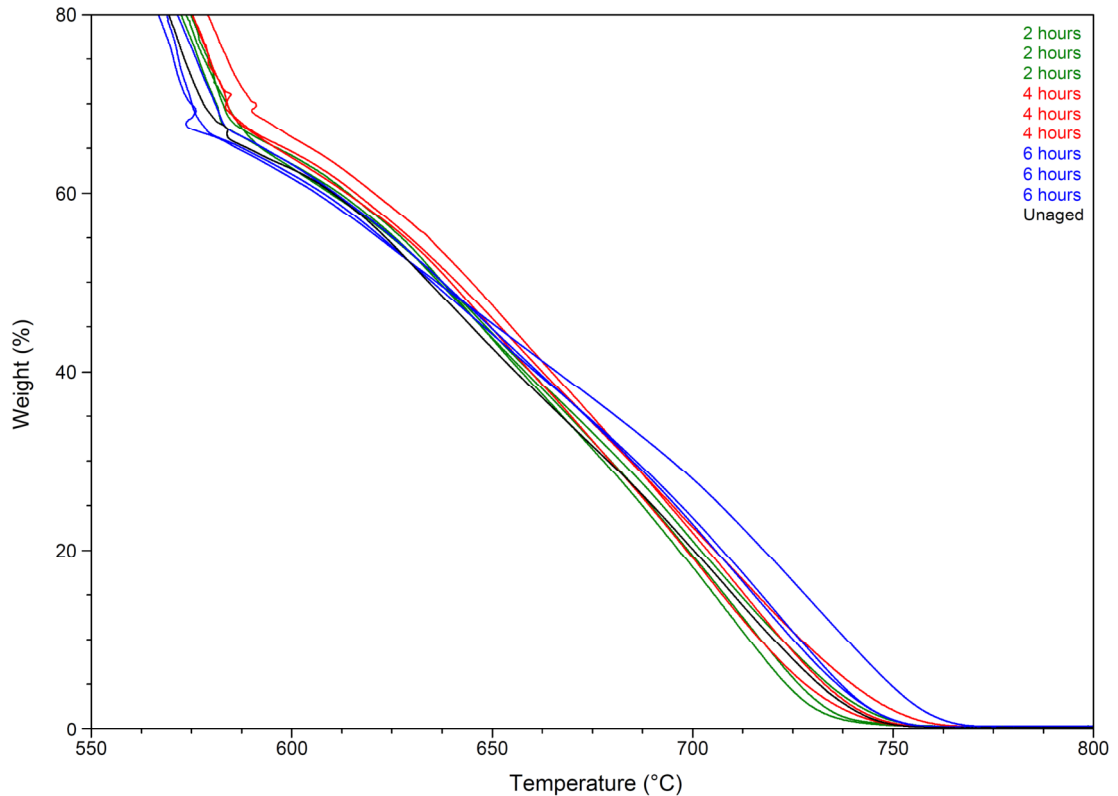


FIGURE 42. TGA OF 450G CONDITIONED IN AIR – SECOND DECOMPOSITION STEP

In the second step of decomposition shown in Figure 42, the opposite effect is observed. The samples aged for 6 hours show a greater thermal stability (with more mass present at a higher temperature) than those aged at 2 hours. It appears that the conditioning at 6 hours causes an earlier onset of decomposition and therefore, this earlier onset makes the sample more thermally stable in the second decomposition step. The earlier onset of decomposition may be due to degradation occurring during the conditioning process, the longer sample are conditioned for, the more degradation occurs and therefore, the earlier decomposition occurs in the TGA. Alternatively, this instead of degradation, the samples aged for 6 hours may be showing signs of crosslinking, as described in section 1.4.3, an occurrence that is necessary for effect char formation. If decomposition is occurring at a lower temperature, the decomposition mechanism may be altered, leading to enhanced thermal stability at higher temperatures.

3.1.1.4 Calculated Thermogravimetric Curves

A TGA curve in air has been calculated by proportional addition of the mass loss of the individual curves to investigate the effect of carbon fibre on the decomposition of PEEK. This is shown in Figure 43. The experimental and calculated curves for 450CA30 are similar up to about 50% mass loss where the calculated curve shows greater thermal stability. In addition, the calculated curve also shows a distinct third step of decomposition which is not present in the experimental curve, indicating that this slower oxidation process of carbon fibre is eliminated in the presence of PEEK and suggesting that PEEK enhances the oxidation of carbon fibre.

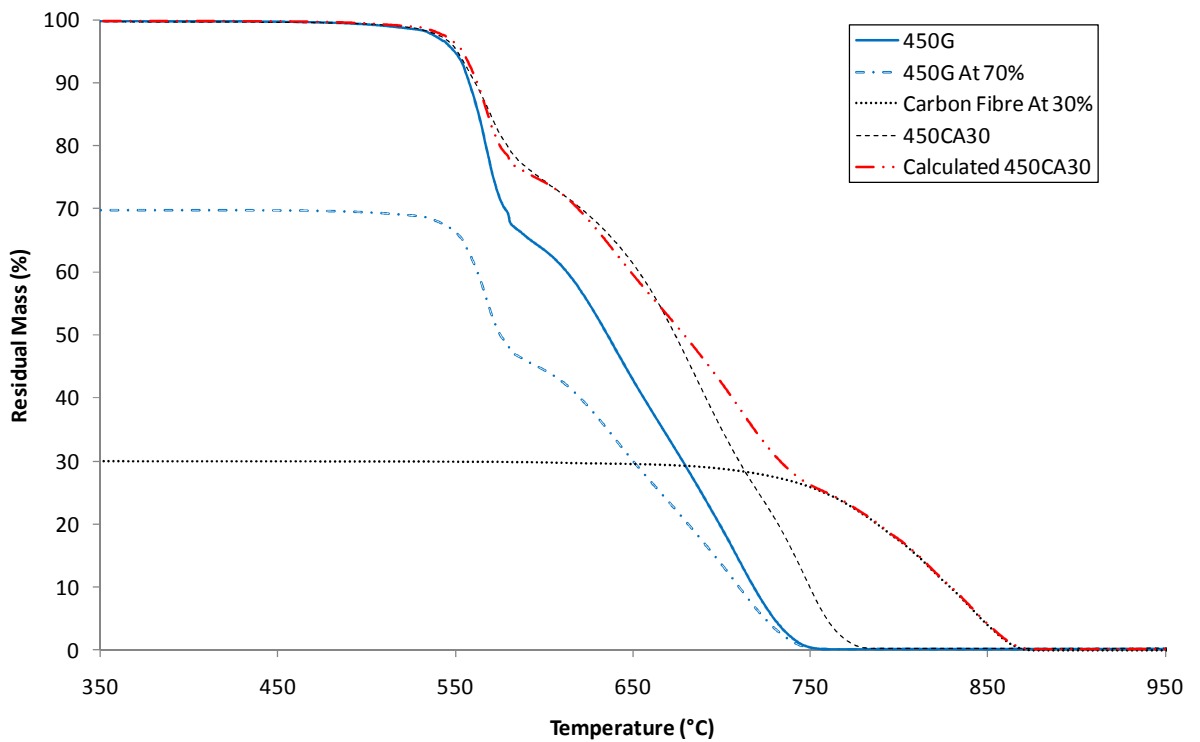


FIGURE 43. TGA CALCULATED CURVES 450CA30 FROM CONSTITUENTS IN AIR

Similarly, a calculated curve had been created for the decomposition of 450GL30 from its constituent parts as shown in Figure 44. The first and second steps of decomposition do not mirror each other as closely as they do in the case of 450CA30. The presence of glass fibre in the experimental curve inhibits the onset of decomposition compared to the calculated curve. In Figure 44, the calculated curve and experimental curves both show a 30% residue.

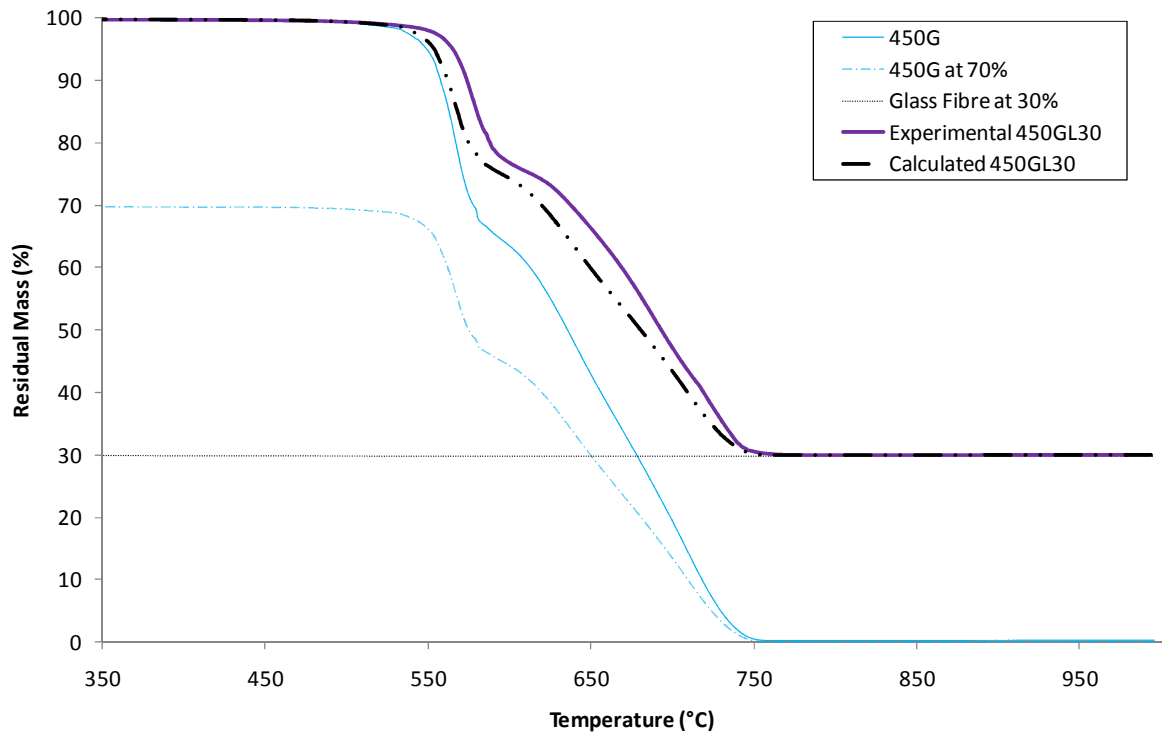


FIGURE 44. TGA CALCULATED CURVES 450GL30 FROM CONSTITUENTS IN AIR

3.1.2 Thermogravimetric Analysis in Nitrogen

Experiments were completed in nitrogen to determine further thermogravimetric information about PEEK. Similarly, experiments were completed on PEEK of different viscosities and filled PEEK.

Figure 45 shows a three step decomposition incomparable to the results determined from experiments completed in air, which show a two step decomposition. The onset of

decomposition occurs at around 585°C and the first step presents a 40% mass loss – this is around 5% greater than the equivalent decomposition step in air, with 10% attributed to the second step. This therefore indicates that the processes occurring during the first step of decomposition – random chain scission of the ether and ketone bonds [50] [106] – is not dependent on the atmosphere. In fact, this process seems to be slightly enhanced in the presence of nitrogen. Again, 30% mass loss occurs within a 30°C window indicating that scission of the ether and ketone bonds do not require, or are not enhanced by an oxidative atmosphere. The second step of decomposition which is attributed to the oxidation of carbonaceous char occurs to a lesser extent with only 10% mass lost. During the third step, there is little mass loss after 800°C and at 900°C; the material is stable with 50% mass remaining.

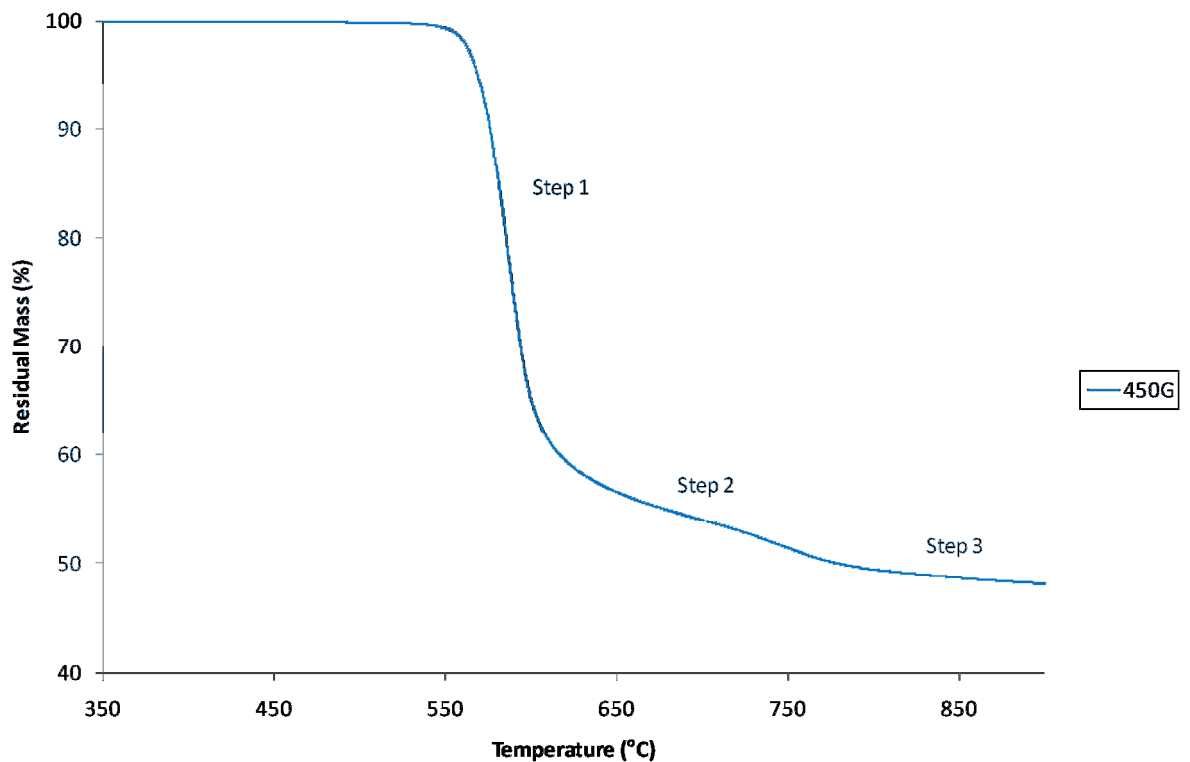


FIGURE 45. 450G TGA IN NITROGEN

3.1.2.1 Effect of Variation of PEEK Viscosity on Thermal Decomposition

The results of experiments conducted on PEEK with different viscosities are shown in Figure 46. It is apparent that 450G, the most viscous of the materials is the most thermally

stable during the first step of decomposition, followed by 150G (a medium viscosity material) and then followed by 90G (a low viscosity material).

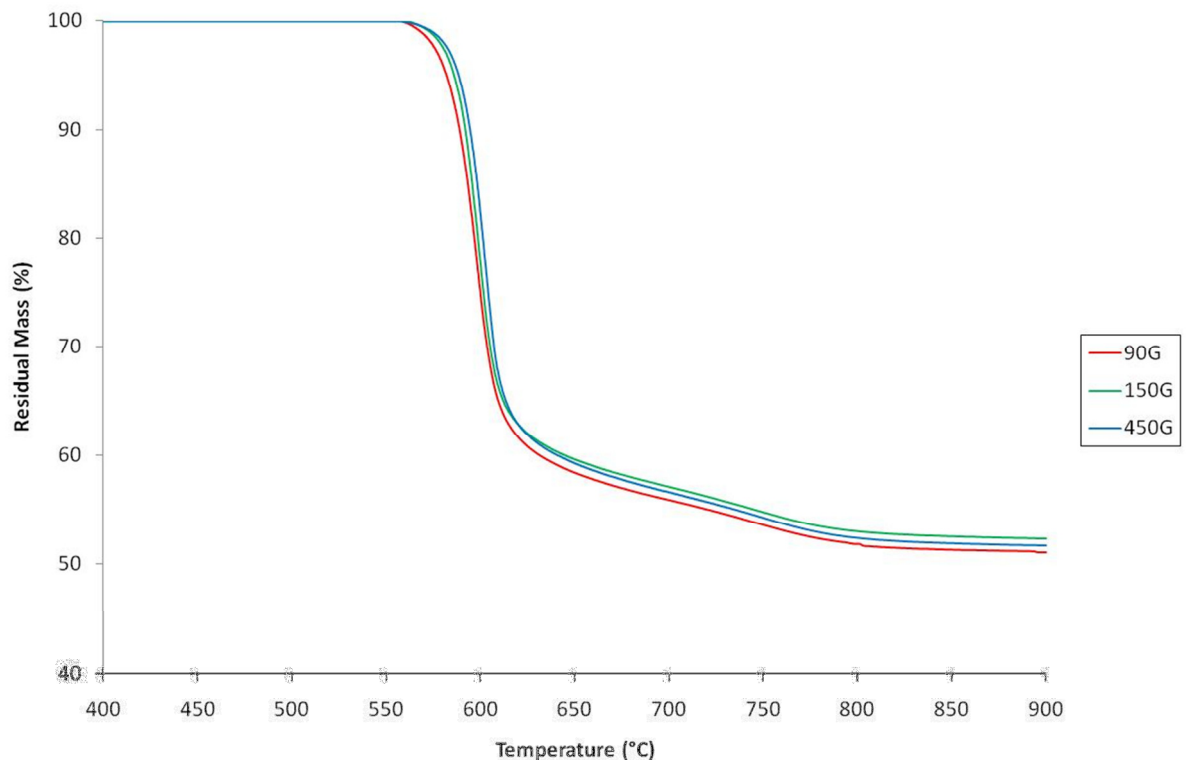


FIGURE 46. TGA OF 90G, 150G AND 450G IN NITROGEN

During the second step of decomposition, the order of stability changes whereby the 150G exhibits a higher final mass than the 450G. The value corresponds to around 1% mass and therefore could be due to experimental error.

3.1.2.2 *Effect of Various Additives on Thermal Decomposition*

Experiments were completed on PEEK reinforced with carbon fibre (450CA30) and glass fibre (450GL30) at 30%. The results of this experiment are shown in Figure 47. From this it can be seen that 450GL30 has a higher onset of decomposition temperature. In the first step of decomposition, 450GL30 is also more thermally stable. 450CA30 decomposes at a lower temperature but loses less mass than 450GL30 – typically around 5% less. It may be assumed that a process occurs at 600°C which either slows down 450GL30 decomposition or accelerates 450CA30 decomposition. After 600°C, both materials enter the second step of decomposition with 450CA30 continuing to decompose at a faster rate than 450GL30. Due to the 5% less mass

lost by 450CA30, the material appears to be more thermally stable than 450GL30. After 800°C little mass loss is shown and the final mass of material remaining for 450CA30 and 450GL30 is 65% and 68% respectively. In an inert atmosphere, the presence of filler increases the thermal stability of pure PEEK and 450GL30 appears to be the more thermally stable of the fibre-filled materials.

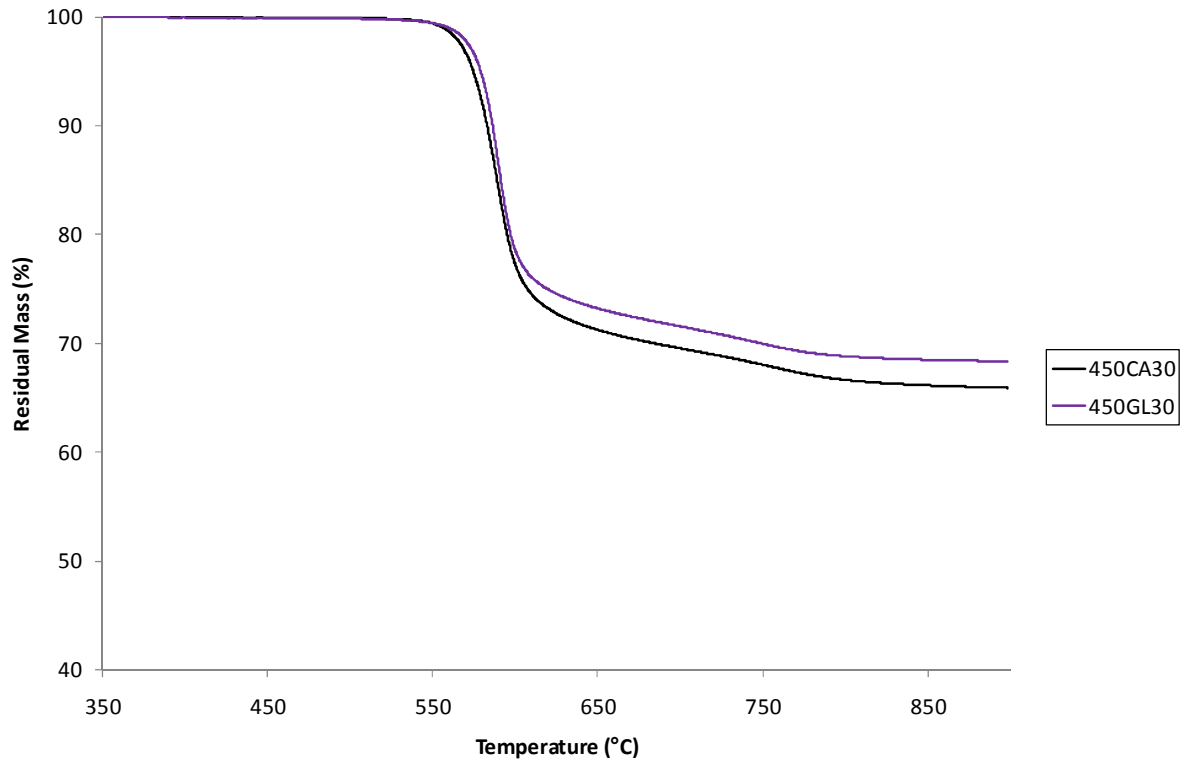


FIGURE 47. TGA OF 450G, 450CA30 AND 450GL30 IN NITROGEN

Experiments have also been conducted on PEEK filled with talc and titanium dioxide as shown in Figure 48. Both materials show a similar decomposition temperature and behaviour during the first step of decomposition although 150TI30 exhibits a greater mass loss – around 5%. During the second step of decomposition both materials decompose at a similar rate between 600°C and 800°C. After 800°C little mass loss is shown and the final mass of material remaining for 381TL30 and 150TI30 is 68% and 66%, respectively.

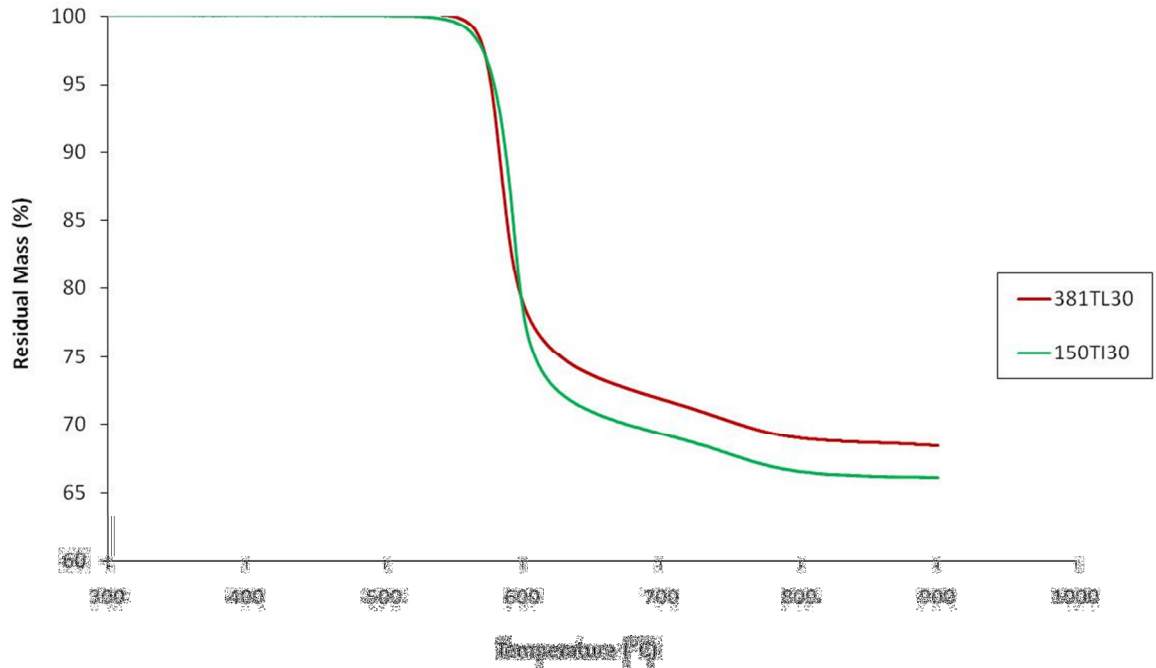


FIGURE 48. TGA OF 381TL30 AND 150TI30 IN NITROGEN

3.1.3 Comparisons between 450G in Air and Nitrogen

Comparisons were made between results obtained from thermogravimetric analysis in air and nitrogen. The results for unfilled PEEK (450G) are shown in Figure 49. The difference in atmosphere increases the onset of decomposition temperature in nitrogen by around 100°C. In both atmospheres, the first step of decomposition is similar although a greater mass loss – around 10% – is exhibited in a nitrogen atmosphere. The second steps of decomposition are different: in air, the material continues decomposing at a rapid rate up to 750°C when all of the material has decomposed. In comparison, in nitrogen, after 600°C the material decomposes steadily till around 800°C and then little mass loss is shown up to 900°C where 52% residue remains. For samples of differing viscosities, shown in Figure 50, there is a greater difference in the first stage of decomposition in nitrogen between the different viscosities whereby 90G begins decomposing at a lower temperature than 150G and 450G. This is not evident in the samples tested in air.

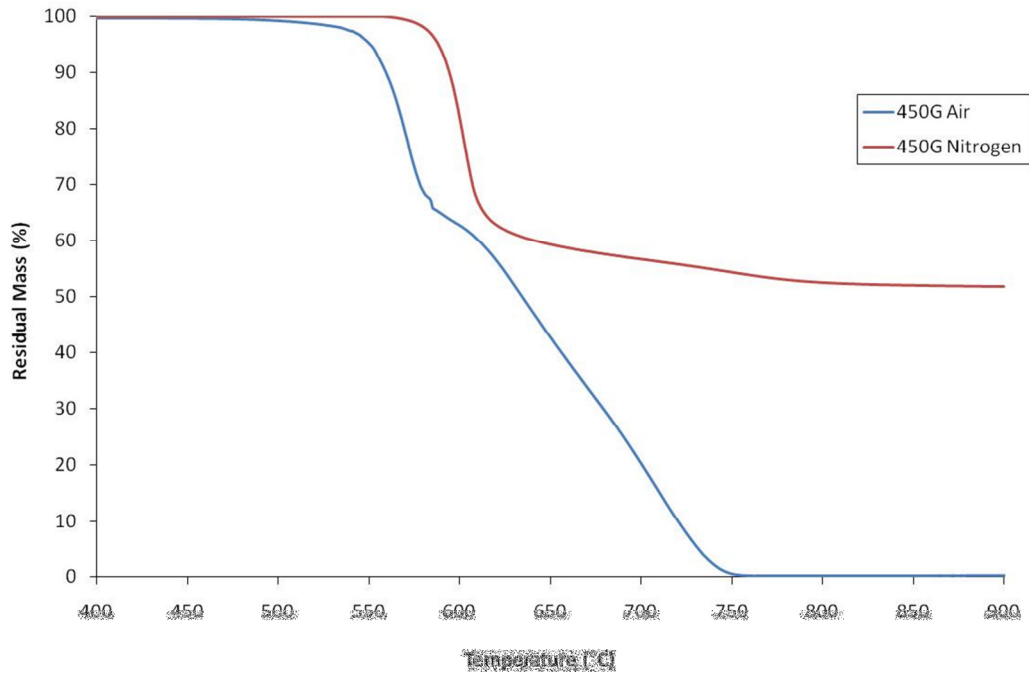


FIGURE 49. 450G TGA IN AIR AND NITROGEN COMPARISON

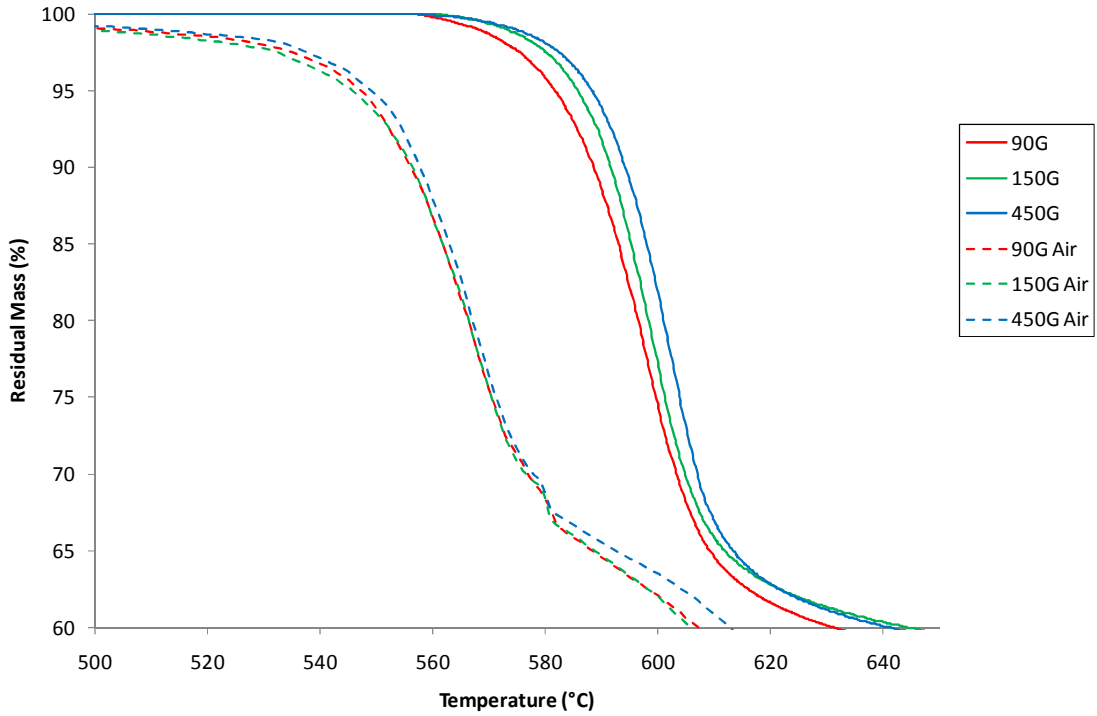


FIGURE 50. DIFFERENT VISCOSITY TGA IN AIR AND NITROGEN COMPARISON

3.1.4 Activation Energy and Arrhenius Factor Determination

The kinetic properties of PEEK and its fibre-filled composites have been determined using two methods: the ASTM method [20] (utilising Kissinger's equations) and the iso-conversion method [21]. The results of the ASTM method are shown in Figure 51 and Figure 52 and the values are outlined in Table 9. An activation energy of 222 kJ mol^{-1} has been determined for 450G with an Arrhenius factor of $1.1 \times 10^{13} \text{ s}^{-1}$. For 450CA30, these values are higher for both the activation energy and Arrhenius factor, at 243 kJ mol^{-1} and $2.5 \times 10^{14} \text{ s}^{-1}$, respectively. For 450GL30, values are much higher with 380 kJ mol^{-1} for the activation energy and $2.7 \times 10^{22} \text{ s}^{-1}$ for the Arrhenius factor.

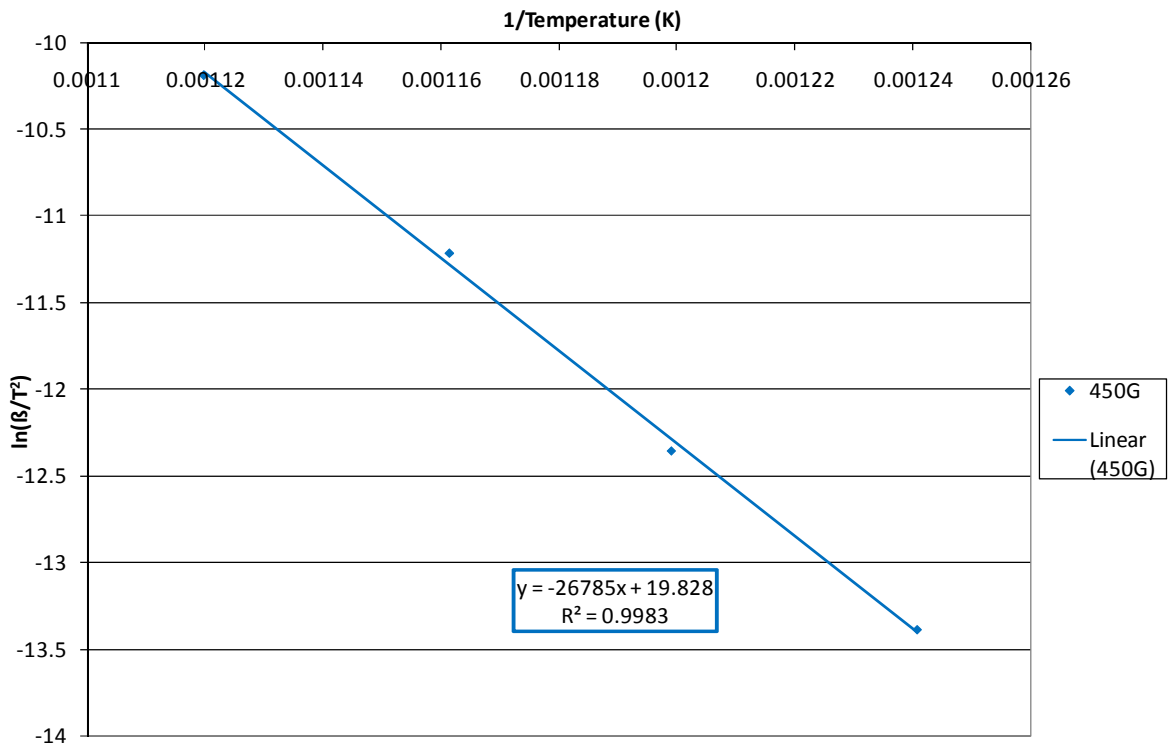


FIGURE 51. ASTM KINETICS METHOD 450G

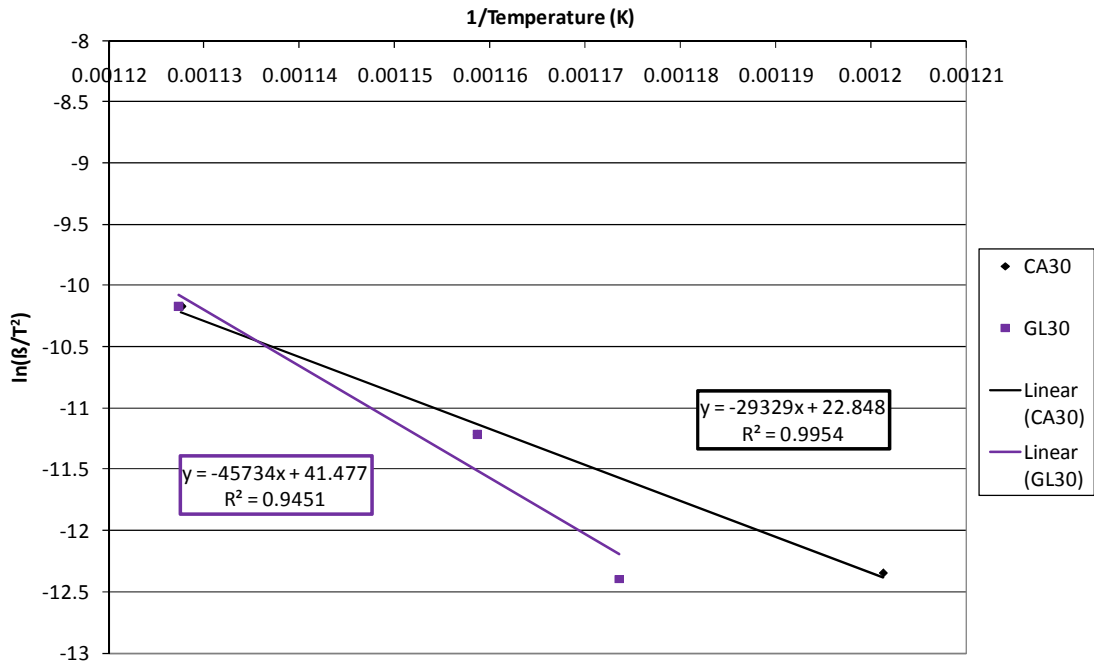


FIGURE 52. ASTM KINETICS METHOD 450CA30 AND 450GL30

SAMPLE	Ea (kJ mol ⁻¹)	A (s ⁻¹)
450G	222	1.1 x 10 ¹³
450CA30	243	2.5 x 10 ¹⁴
450GL30	380	2.7 x 10 ²²

TABLE 9. 450G, 450CA30 AND 450GL30 ASTM KINETICS

The results of the iso-conversion method are shown in Figure 53. PEEK and its carbon and glass-fibre filled composites all show a similar activation energy up to around 70% conversion (or mass loss) with a value just over 250 kJ mol⁻¹. After 70% conversion, the values for all three increase at different rates with 450G having an activation energy at 90% conversion of 474 kJ mol⁻¹. For 450CA30 and 450GL30, the activation energies are 744 kJ mol⁻¹ and 559 kJ mol⁻¹, respectively. These high values would be expected at high degrees of conversion as the main mechanism here is one of char formation. Interestingly, there are differences in the rank order of activation energies of PEEK and its composites which are not expressed identically by both methods.

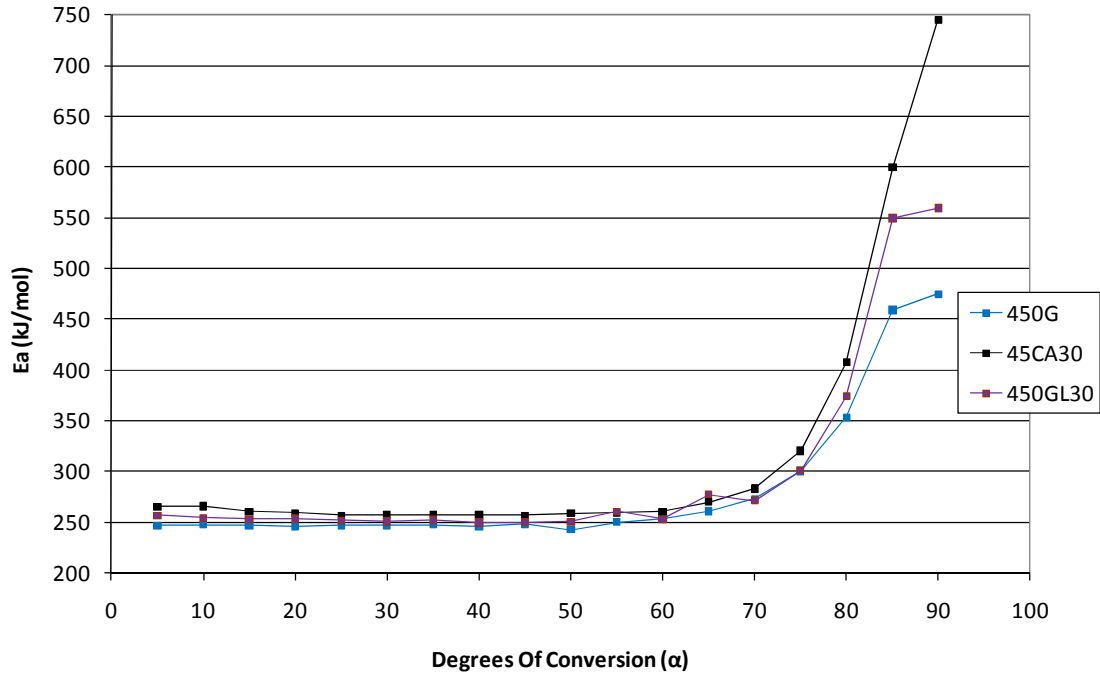


FIGURE 53. 450G, 450CA30 AND 450GL30 ISO-CONVERSION COMPARISON

3.2 Simultaneous Thermal Analysis – Fourier Transform Infrared (STA-FTIR)

Simultaneous thermal analysis coupled with Fourier transform infrared (STA-FTIR) was completed on PEEK samples to determine the gas phase products of PEEK decomposition in both an oxidative and inert atmosphere.

3.2.1 STA-FTIR in Air

As determined from TGA experiments, the onset of decomposition of PEEK in an oxidative environment occurs at around 550°C. The major decomposition products from literature have been determined to be phenol, benzene, CO and CO₂ [50] [52] [55]. The presence of these products occurs between 550°C and 750°C. Carbon dioxide, one of the major decomposition products in an oxidative environment is shown in Figure 54 at ~670°C. The library spectra are denoted by the name of the compound.

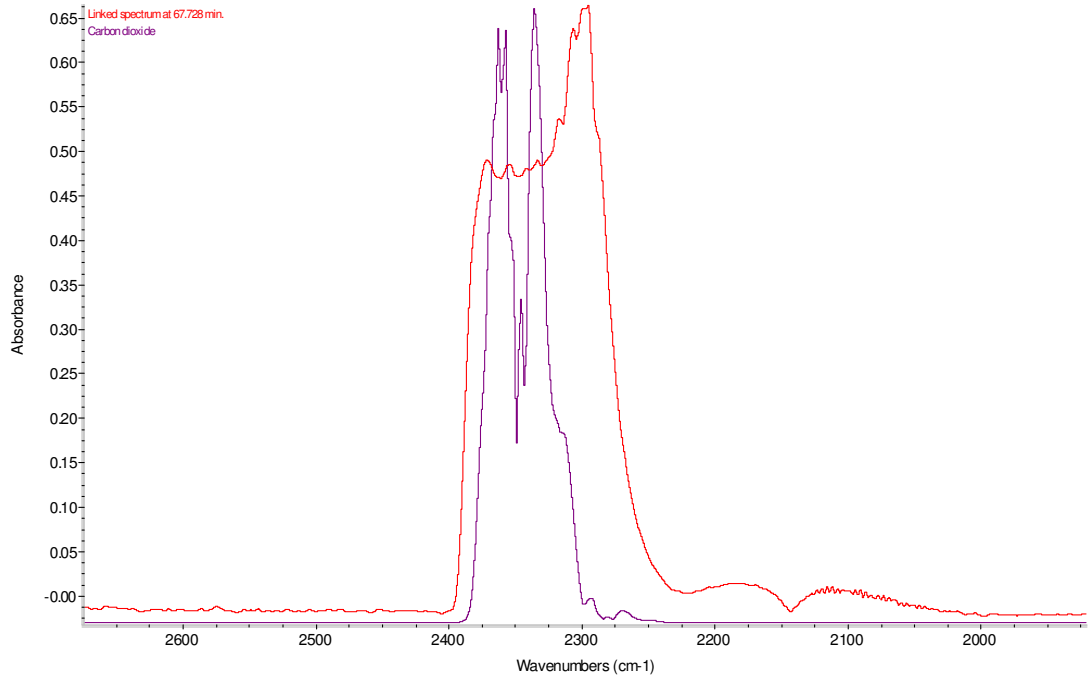


FIGURE 54. CARBON DIOXIDE FROM 450G PEEK IN AIR TO 900°C

The presence of benzene (and possibly other aromatics) is seen in Figure 55 at around 570°C.

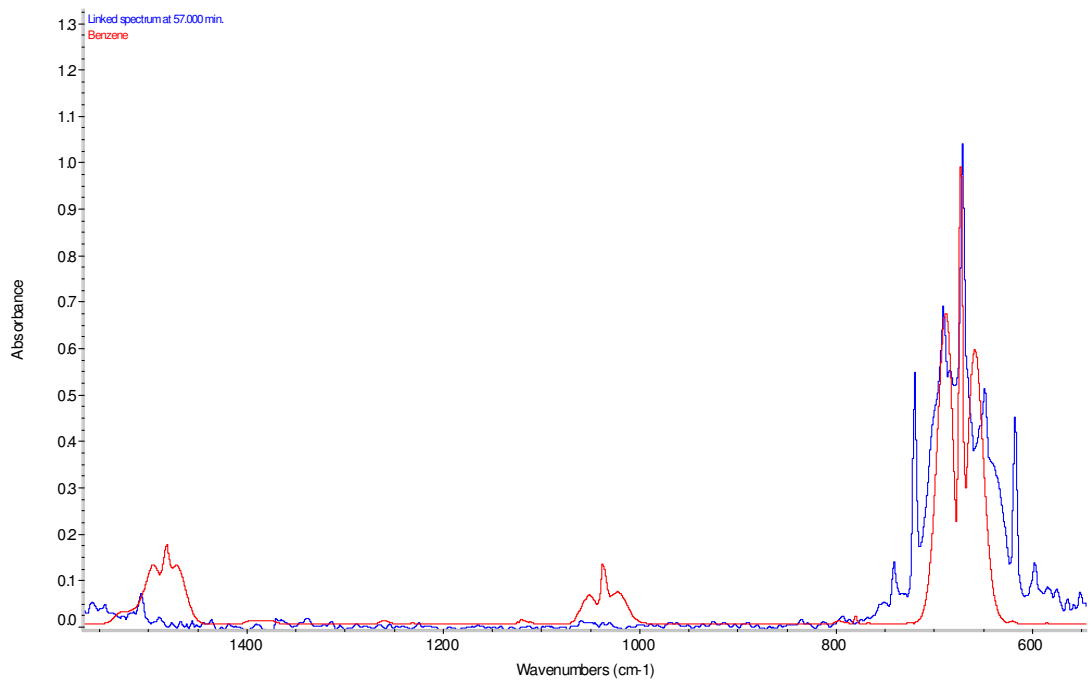


FIGURE 55. BENZENE FROM 450G PEEK IN AIR TO 900°C

3.2.2 STA-FTIR in Nitrogen

In an inert atmosphere, CO a major product of PEEK decomposition is observed throughout the experiments.

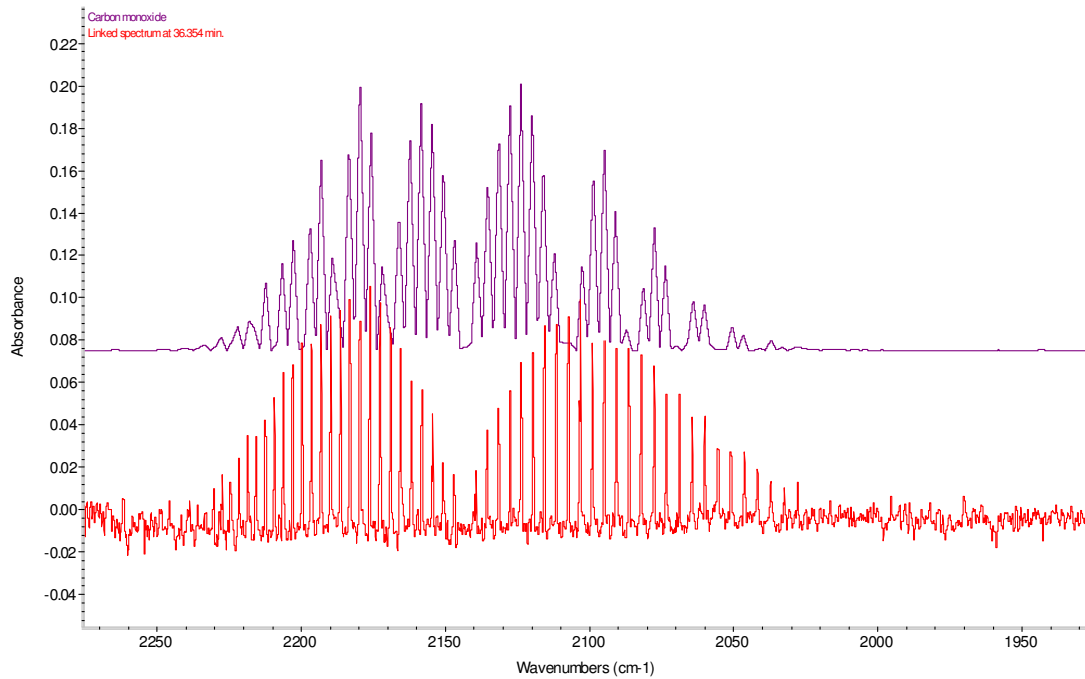


FIGURE 56. CARBON MONOXIDE FROM 450G PEEK IN N₂ TO 900°C

After initial analysis of the data, it was determined that there may be a leak in the heated line of the FTIR, as a result, further experiments could not be completed.

3.3 Pyrolysis Gas Chromatography – Mass Spectrometry (pyGC/MS)

Pyrolysis gas chromatography coupled with mass spectrometry was utilised to determine the gas phase products of the decomposition of PEEK and its filled composites in an inert atmosphere.

3.3.1 PEEK 450G

A flash pyrolysis technique was used and samples of 450G were heated to 750°C. The results are shown in Figure 57.

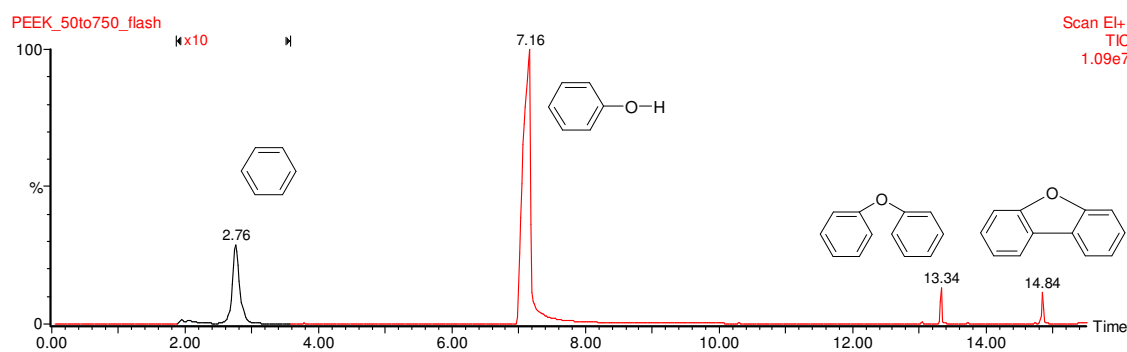


FIGURE 57. pyGC/MS FLASH PYROLYSIS OF 450G AT 750°C

One large peak is present at 7.16 minutes corresponding to phenol. Two smaller peaks are shown at 13.34 and 14.84 minutes which are consistent with diphenylether and a dibenzofuran-type structure. Both phenol and diphenylether production, from the main PEEK chain is detailed in Figure 58.

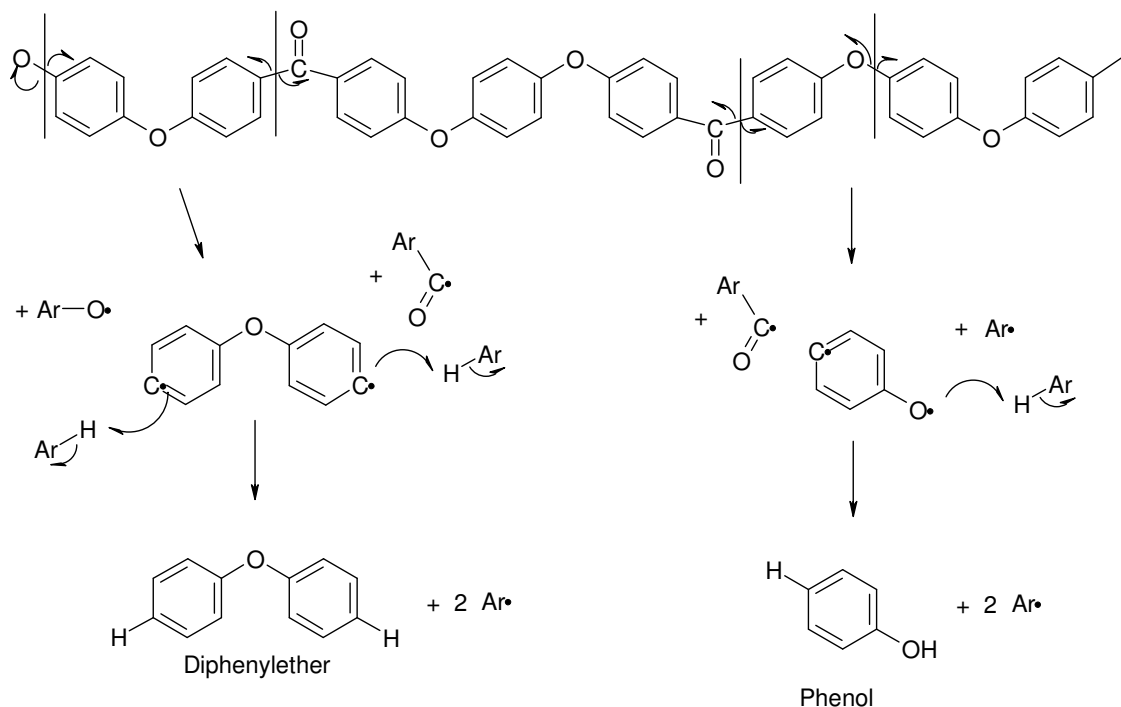


FIGURE 58. DIPHENYLETHER AND PHENOL PRODUCTION

A final small peak, which has been enlarged by a factor of 10 for clarity, is shown at 2.76 minutes, corresponding to benzene.

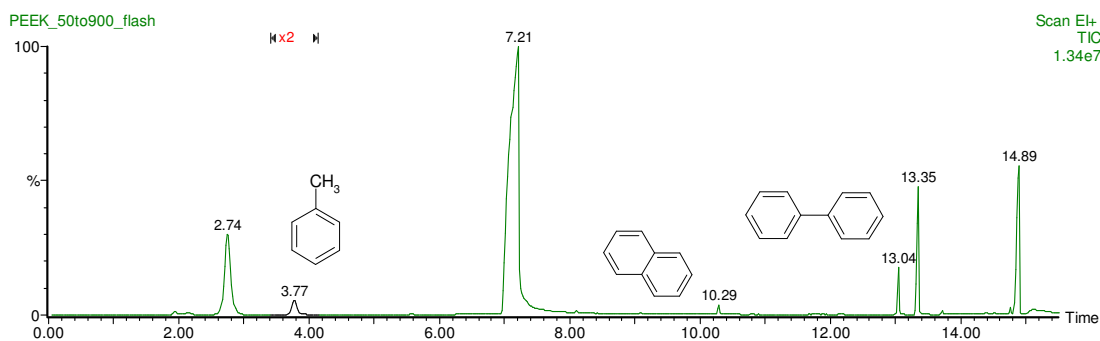


FIGURE 59. pyGC/MS FLASH PYROLYSIS OF 450G AT 900°C

450G has also been heated to 900°C as seen in Figure 59. More peaks are present, as would be expected with a higher temperature. In addition to the peaks mentioned previously, a peak is present at 13.04 minutes with mass spectrum corresponding to biphenyl, the production of which is detailed in Figure 60. There are also two smaller peaks, one at 3.77 minutes (which has been enlarged by a factor of 2 for clarity) and one at 10.29 minutes which correspond with methyl benzene and possibly naphthalene.

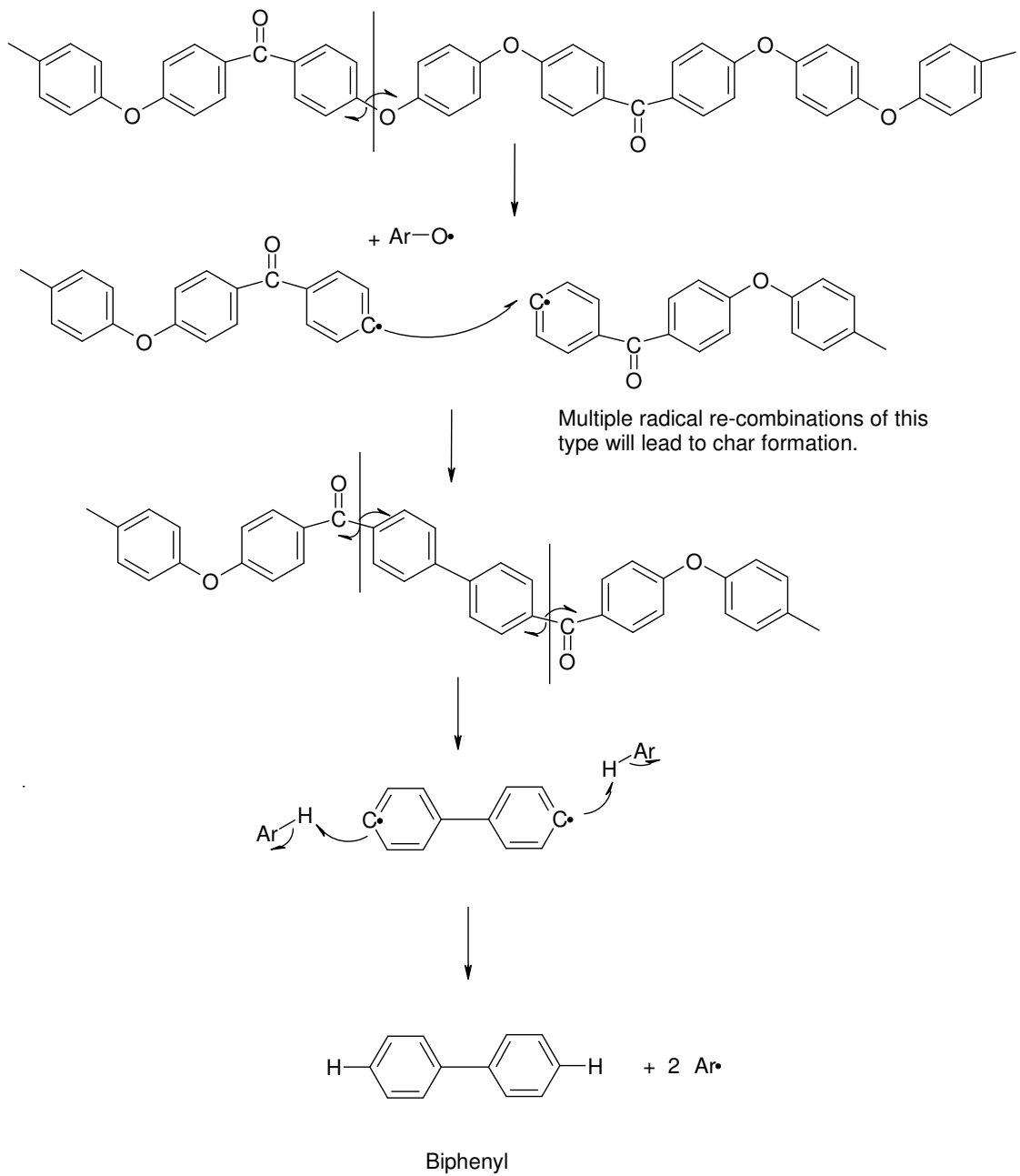


FIGURE 60. BIPHENYL PRODUCTION

3.3.2 Filled Materials

The carbon fibre, glass fibre and talc filled composites of PEEK were analysed using the flash pyrolysis technique at 900°C. The results for carbon fibre are shown in Figure 61. The peaks are similar in terms of the products that they represent in the mass spectrum, however they are shifted slightly. This is also true for the 450GL30 sample, shown in Figure 62 and the 381TL30 sample shown in Figure 63.

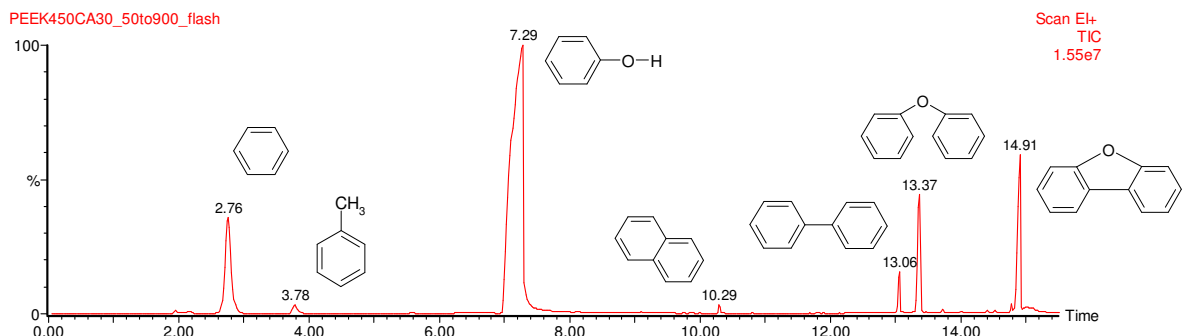


FIGURE 61. pyGC/MS FLASH PYROLYSIS OF 450CA30 AT 900°C

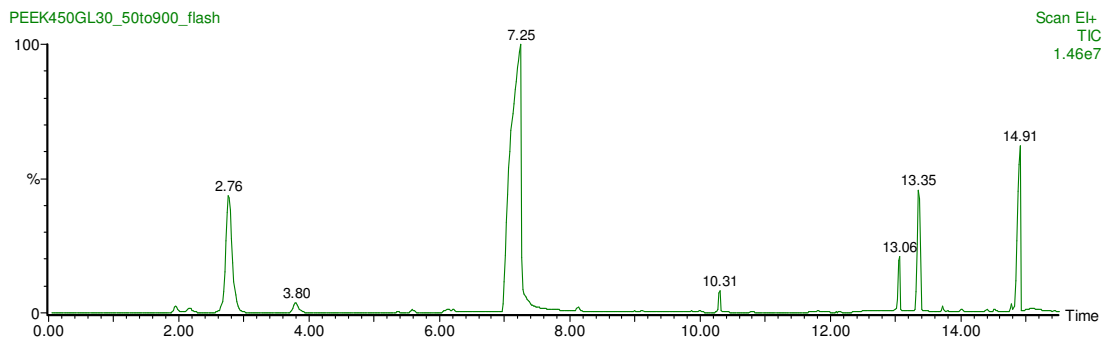


FIGURE 62. pyGC/MS FLASH PYROLYSIS OF 450GL30 AT 900°C

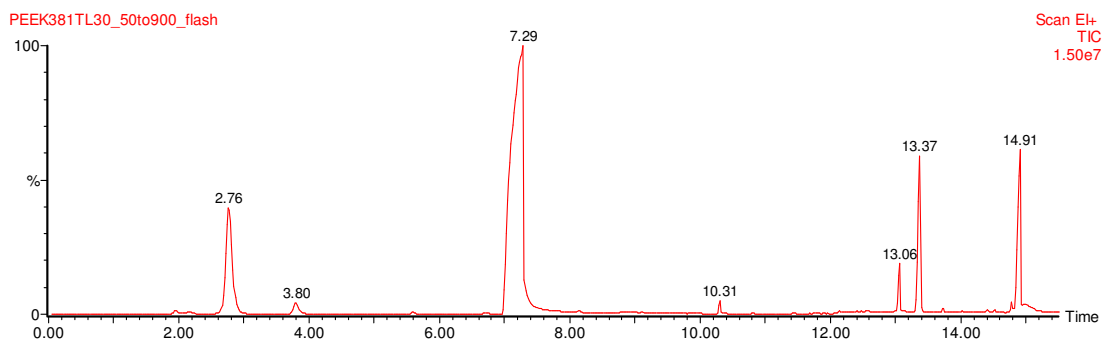


FIGURE 63. pyGC/MS FLASH PYROLYSIS OF 381TL30 AT 900°C

A comparison of PEEK and its filled composites is shown in Figure 64. The peak at 3.80 minutes for the filled samples is not so prominent in the unfilled 450G sample. The differences found in the thermal decomposition of PEEK and its composites, as shown in TGA experiments are not observed as differences in their decomposition products.

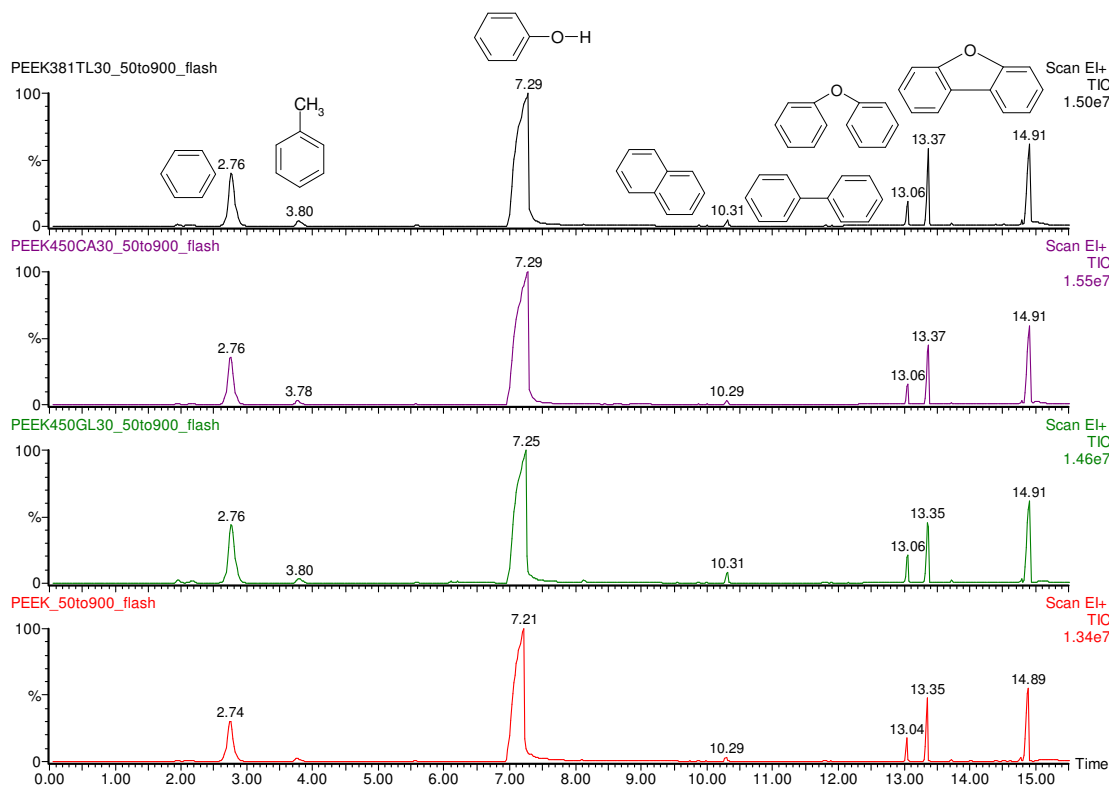


FIGURE 64. pyGC/MS FLASH PYROLYSIS OF PEEK AND ADDITIVES AT 900°C

3.4 Summary

The decomposition of PEEK in air and nitrogen occurs via a two and three-step process, respectively. The resultant carbonaceous residue decomposes much more slowly, particularly in nitrogen where two distinct steps are apparent. The third step in an inert atmosphere is attributed to the decomposition of the char which is subsequently formed as a result of the previous two steps. The first step of decomposition, in both atmospheres, results in the rapid loss of around 30% mass within a 30°C range. This loss is attributed to the production of

phenol, benzene, CO and CO₂, as determined by pyGC/MS and TGA-FTIR. The thermal decomposition of PEEK in nitrogen is delayed by about 100°C.

In air, the effect of viscosity is less apparent than it is in nitrogen. In nitrogen, during the first step of decomposition, 450G the most viscous and highest molecular weight material is more thermally stable than 150G and 90G as it begins to decompose at a higher temperature. Decomposition of the lowest molecular weight 90G material with shorter chains of around ~ 60 repeat units is more rapid in the inert atmosphere as random chain scission is accelerated by the presence of oxygenated species. This suggests the influence of the number of end groups on the decomposition process in the absence of oxygen. Viscosity appears to have no effect on the resulting decomposition products in the pyGC/MS.

The presence of filler in PEEK enhances the thermal decomposition in both an oxidative and inert atmosphere. Both the activation energy and Arrhenius factor of filled materials is increased compared to the unfilled materials, this increase is more apparent at higher degrees of conversion where the mechanism is primarily char oxidation, but there are significant differences between the data when different methods are used to calculate the decomposition kinetics of PEEK and its filled materials. Carbon fibre, glass fibre, titanium dioxide and talc all affect the thermal stability of PEEK with glass fibre and titanium dioxide being the most effective as both delay the onset of decomposition and produce a more thermally stable residue during the second stage of decomposition. The presence of filler does not appear to affect the subsequent products of decomposition with the exception that relatively more methylbenzene is present in the decomposition products of filled materials than unfilled materials, as determined from the pyGC/MS.

CHAPTER 4. FLAMMABILITY

The flammability of PEEK of various viscosities and incorporated with fillers has been investigated. The UL-94 test has been utilised to determine the ignitability and flame spread of the materials detailed above. The limiting oxygen index apparatus was used to determine the ability of the material to sustain candle-like burning. The pyrolysis combustion flow calorimeter was employed as a micro-scale flammability test as a means of determining the heat release rate of a material at this scale. The apparatus can also be used to determine the temperature of the polymer at ignition and at steady surface burning. The cone calorimeter has been utilised to determine a variety of properties related to flammability such as ignitability, heat release rate, total heat released and mass loss rate. The cone calorimeter provides such data at the bench-scale and therefore is useful for comparing with the data obtained from the pyrolysis combustion flow calorimeter which provides many of the same parameters at a micro-scale. The single-source flame test was adopted as a means of determining flammability properties of samples containing small amount of carbon black – for colouring purposes – without the use of the cone calorimeter, as said samples created scatter in the data.

These experiments were completed to relate the measured thermal decomposition behaviour of PEEK and its composites (as investigated in Chapter 4) to their performance in industry standard tests as well as to investigate the sensitivity of industry standard tests to various physical and material properties such as thickness, presence of fillers, presence of moisture and absorption of infrared radiation.

4.1 UL-94

4.1.1 Horizontal and Vertical Burn

Unfilled PEEK of different viscosities and PEEK filled with glass and carbon fibre were examined in the UL-94. The results of the horizontal burn experiment are shown in Table 10 with all samples passing the horizontal burn criteria. Filled PEEK samples tend to have a lower average time to extinction than unfilled PEEK samples although the average burn lengths were about 14 mm, similar to the unfilled samples.

PEEK	H-B	Average Time for Extinction (s)	Average Burn Length (mm)
90G	√	6.2 (±4.0)	14 (±1.6)
150G	√	3.2 (±3.0)	14 (± 2.5)
450G	√	6.3 (±2.0)	11 (±2.7)
450CA30	√	3.6 (± 1.9)	14 (±2.0)
450GL30	√	4.1 (±2.8)	15 (±2.3)

TABLE 10. UL-94 HORIZONTAL BURNING

The results of the vertical burn test for the different viscosities are shown in Table 11. Both the medium to high viscosity PEEK samples passed the UL-94 criteria. 90G samples were spread across the V-0 and V-2 criteria due to the formation of flaming drips. Dripping has been quantified in terms of the pyrolysis mechanism and polymers which decompose through random chain scission, such as PEEK, tend to exhibit small size wax-like dripping, compared to polymers which decompose through unzipping, such as PMMA, which exhibit larger drips which correspond to structural collapse of the bulk [94].

PEEK	V-0	V-1	V-2	Average Total Time(s)	Average Burn Length (mm)	UL-94 V - Rating
90G	√√√√√√		√√√√	13.2 (±4.0)	31.1 (±11.9)	V-2
150G	√√√√√√√√√√			6.9 (±1.9)	26.7 (±5.6)	V-0
450G	√√√√√√√√√√			6.5 (±1.1)	30.9 (±7.9)	V-0

TABLE 11. UL-94 DATA 90G, 150G AND 450G

As seen in Table 12, both the filled samples also passed the V-0 rating. Differences exist in the burn times t_1 and t_2 of the filled and unfilled polymers, for 450G, t_1 is on average greater than t_2 ; for both 450CA30 and 450GL30, the opposite is true. Once ignited, the unfilled polymer char is less easy to reignite while the filled polymer char is easier to reignite. There also appears to be a greater burn length and a shorter total burn time (the sum of t_1 and t_2) for the filled samples— although there is uncertainty due to the scatter present in the data.

	t ₁	t ₂	Average Total Time	Average Burn Length
Sample	(s)	(s)	(s)	(mm)
450G	3.7	2.7	6.5 (±1.1)	30.9 (±7.9)
450CA30	4.0	2.7	6.0 (±2.4)	34.0 (±6.4)
450GL30	2.2	3.5	5.7 (±1.0)	39.4 (±26.0)

TABLE 12. UL-94 DATA FOR 450G, 450CA30 AND 450GL30

It is interesting that although there are clear differences between the filled and unfilled polymer in terms of burning behaviour, these differences are not evident within the UL-94 V-0 test criterion. Correlations have been found between cone calorimeter peak heat release rate data and UL-94 V-ratings although due to the nature of the UL-94 experiments, the closest correlations were observed at low heat fluxes (30 kW m^{-2}), close to the ignitability limits for many materials [95]. The critical heat flux for ignition of PEEK has been calculated as 27 kW m^{-2} and is quoted experimentally at between 30 and 40 kW m^{-2} [96] and therefore a correlation at 30 kW m^{-2} would not to apply to PEEK.

4.1.2 Wet, Dry and Humid Conditions

The UL-94 standard [35] suggests that materials should be exposed to two separate conditions prior to testing. Five samples should be stored in an oven at 70°C for 168 hours and five samples should be stored at 50% relative humidity (RH) for a period of 48 hours. In the past, relatively little has been known about the effect of moisture on PEEK flammability. It is however, known that 0.5% moisture is absorbed by PEEK 450G at saturation as per ASTM D570 [97].

Condition	Temperature ($^\circ\text{C}$)	Average (%)	Standard Deviation
'Wet'	12	+0.366	0.119
	25	+0.334	0.008
50% RH	21	+0.261	0.007
'Dry'	70	-0.124	0.007
	100	-0.130	0.005

TABLE 13. WET, DRY AND HUMID CONDITIONS SAMPLE MASS LOSSES AND GAINS

The effect of moisture on the UL-94 experiments was investigated using five material conditions. These were a 12°C water bath for 168 hours, a 25°C water bath for 168 hours, 50% relative humidity for 48 hours, a 70°C oven for 168 hours and a 100°C oven for 168 hours. The mass losses and gains for 10 samples placed in each condition are shown in Table 13.

It might be expected that samples exposed to a wet condition in a higher temperature scenario (25°C) would absorb more moisture than those exposed to a lower temperature scenario (12°C). From Table 13, it can be seen that there is a large value for the standard deviation for the samples placed in the 12°C scenario and therefore this cannot be inferred. In the case of samples exposed to the 'dry' condition, those at 70°C lost less moisture than those at 100°C, as would be expected. There was a difference of 0.49% in moisture content between the wet (12°C) and dry (100°C) conditions.

Condition	Average		Total Flame Time (s)	Rating	
	1st Appl Time (s)	2nd Appl Time (s)		V-0	V-1
12°C	1.19 (±1.2)	4.76 (±2.3)	59.5	10	0
25°C	2.35 (±1.8)	7.7 (±4.0)	100.5	3	7
50% RH	1.56 (±0.8)	6.38 (±3.0)	79.4	9	1
70°C	0.95 (±0.7)	4.39 (1.0)	53.3	10	0
100°C	1.07 (±0.2)	3.92 (±0.8)	49.9	10	0

TABLE 14. WET, DRY AND HUMID CONDITIONS RESULTS

The UL-94 results for samples in the 'wet', 'dry' and 'humid' conditions are shown in Table 14. The presence of moisture appears to have a lesser consequence on the application times than on the subsequent UL-94 V-ratings. Moisture content appears to be disadvantageous to the UL-94 rating. This is the opposite to what would be expected as usually, something which is wet, is harder to burn than something which is dry. Samples which have been dried (at both temperatures) all show a V-0 rating, with the exception of one; however those exposed to moisture – either placed in a water or in a humid condition show some V-1 ratings. As this is not evident from the average application times, with samples in a 12°C water bath and 70°C oven showing similar application times and different V-ratings, this may be a physical sample effect. Following testing, the burned samples were examined carefully and the presence of small bubbles on the surface of 'wet' samples was noticed, as seen in Figure 65.



FIGURE 65. WET AND DRY SAMPLES POST UL-94

These were not present on the surface of 'dry' samples and therefore, it may be concluded that the presence of bubbles was promoting the surface spread of flame up the sample.

In support of this, the total flame time was established for all ten samples in each condition. Samples which were dry (in the 100°C oven) showed 50% lower flame times than those which were wet (in a 25°C water bath). It is also interesting to note that samples which were drier showed lower standard deviations in burning time and therefore, more consistency.

4.1.3 Higher Flame Temperature

The idea that for a high decomposition temperature polymer such as PEEK, the amount of energy produced by a 50 W flame may not be enough to form the char the polymer requires after each flame application to cause self extinction was investigated. For that reason, samples were tested with a 50 W flame and a 60 W flame (with the heat fluxes determined using a copper slug technique [98]) to determine if this had an effect on the resulting UL-94 ratings.

TEST #	FLAME TIME (SEC)		FLAME/GLOW 2 nd APPL T2 + T3	RESULT Rating
	1 st APPL T1	2 nd APPL T2		
1	1.2	6.0	6.0	V0
2	2.8	2.7	2.7	V0
3	2.0	3.6	3.6	V0
4	2.1	5.2	5.2	V0
5	1.4	12.3	12.3	V1
6	1.2	2.8	2.8	V0
7	1.4	7.0	7.0	V0
8	2.5	8.5	8.5	V0
9	2.5	10.7	10.7	V1
10	1.5	13.4	13.4	V1

TABLE 15. UL-94 450G 50 W FLAME RESULTS

The results of this experiment are shown in Table 15 and Table 16. From these results, it can be seen that a hotter flame produces lower flaming times and therefore, more V-0 ratings. Interestingly, for samples exposed to the hotter flame, the burn time after the first flame application is longer – possibly allowing the polymer to become hotter, reach a higher temperature for the production of char and therefore causing self extinction earlier during the second flame application. In addition, the total flame times ($t_1 + t_2$) for both flames show a 23% reduction between the 50 W flame and the 60 W flame from 91 seconds (shown in Table 15) to 70 seconds (shown in Table 16).

TEST NO	FLAME TIME (SEC)		FLAME/GLOW 2 nd APPL T2 + T3	RESULT Rating
	1 st APPL T1	2 nd APPL T2		
1	1.6	4.4	4.4	V0
2	1.7	1.3	1.3	V0
3	4.8	3.8	3.8	V0
4	1.7	11.5	11.5	V1
5	3.7	4.5	4.5	V0
6	5.2	2.2	2.2	V0
7	1.1	4.8	4.8	V0
8	3.5	4.7	4.7	V0
9	2.3	3.3	3.3	V0
10	1.8	1.6	1.6	V0

TABLE 16. UL-94 450G 60 W FLAME RESULTS

4.2 Limiting Oxygen Index (LOI)

The results of the LOI experiments are shown in Table 17.

Sample	LOI (%)	Comments
90G	38.9	Dripping gives self extinguishing behaviour
150G	37.3	Some dripping
450G	37.3	No dripping
450CA30	45.5	Bends during burning (see Figure 66)
450GL30	44.7	Bends during burning (see Figure 67)

TABLE 17. LOI OF FILLED AND UNFILLED PEEK

The 90G samples gave a higher LOI value than the higher viscosity materials as the samples dripped away from the flame during the test causing the remaining sample to self extinguish and pass that particular oxygen concentration. Some dripping was noted with the 150G sample, while there were no drips with the 450G samples. 450G exhibited a lower LOI value than both filled materials as expected from the TGA data whereby filled composites have a greater thermal stability than unfilled samples.



FIGURE 66. 450CA30 POST LOI

Again there were differences between the filled materials – 450CA30 had a slightly higher LOI than 450GL30. There were also differences in the ways the materials behaved during the tests. 450CA30 samples would curl in on themselves – thus enclosing the flame and causing the sample to extinguish (see Figure 66). Similarly, 450GL30 samples twist round

themselves and enclose the flame (see Figure 67) – although this occurred to a lesser extent than for the carbon fibre-filled samples.



FIGURE 67. 450GL30 POST LOI

A possible reason for this outcome is the residual stress present from injection moulding the polymer samples which exists to a greater extent in the fibre-filled samples. These differences in physical behaviour may account for the differences in the LOI values of the fibre-filled composites; the ‘curling’ seems to be quite effective at enclosing a flame and promoting self extinguishing behaviour however should be seen as an artefact of the LOI test in terms of quantifying flammability.

4.2.1 Wet and Dry Conditions

The effect of wetting and drying samples was investigated in the LOI. Samples were exposed to two conditions: 25°C in a water bath and 100°C in an oven.

Condition	Moisture (%)	Standard Deviation
Wet	+ 0.19	0.033
Dry	- 0.32	0.086

TABLE 18. SAMPLE MASS LOSSES AND GAINS

The mass losses and gains for both conditions are shown in Table 18 and the results for the wet and dry samples are shown in Table 19. The wet samples show a higher LOI value than the dry samples, by about 1% point. This is opposite to what has been observed in the UL-94 but is what would be expected with samples which are exposed to wetting and drying whereby the presence of moisture is advantageous. This may be due to the heating effect of a flame on the different orientations of samples in these two tests. In the UL-94, where samples are ignited at the bottom and the flame is allowed to spread up, more of the sample above is pre-heated to create a bubbled surface. In the LOI, the sample is ignited from above and the flame is expected to travel down the sample. As the heat from the flame rises, there is less heat applied to the sample below and as a result, bubbles were not seen on the surface of burnt LOI samples.

450G	%
Wet	36.7
Dry	35.6

TABLE 19. 450G WET AND DRY LOI RESULTS

4.3 Pyrolysis Combustion Flow Calorimeter (PCFC)

4.3.1 Effect of Viscosity

Samples of 90G, 150G and 450G were examined in the PCFC. The results are shown in Figure 68 and a summary of the data is presented in Table 20. As observed in the TGA experiments, in an inert atmosphere, 90G is less thermally stable than 150G and 450G and begins losing mass at a lower temperature. This is also observed in the PCFC experiments, whereby 90G releases heat at a lower temperature. The threshold for 50 W g^{-1} is reached by 90G at around 580°C , by 150G at 587°C and 450G at 590°C .

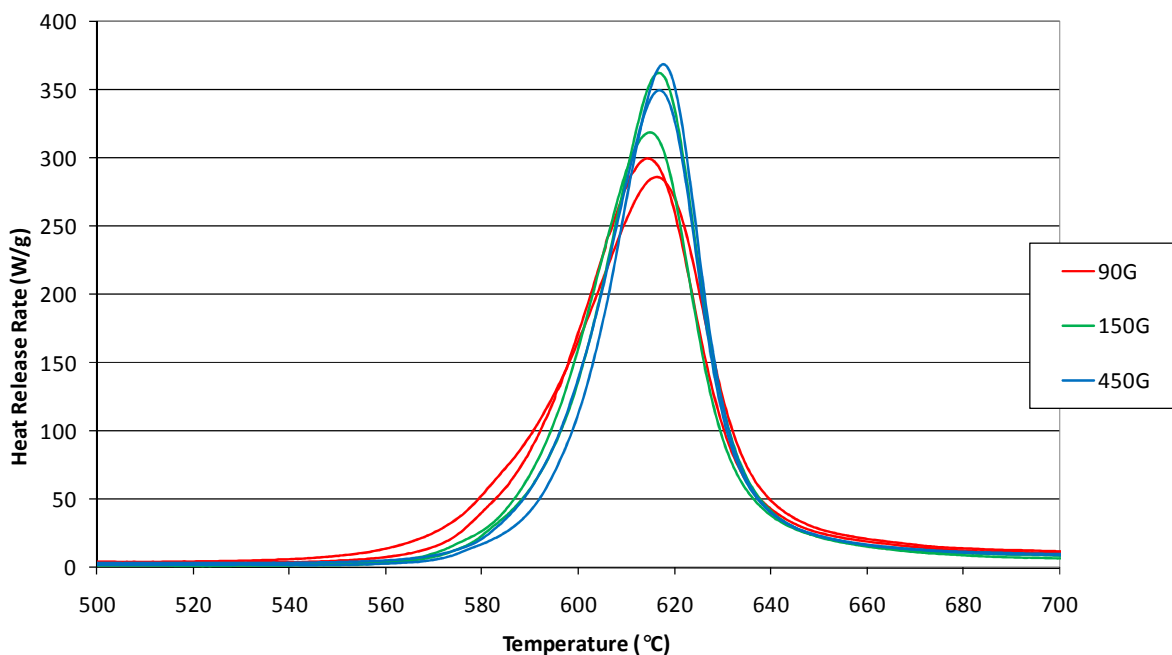


FIGURE 68. PCFC VISCOSITY EXPERIMENTS HEAT RELEASE RATES

Differences also exist in the peak sample temperature, although all samples reach a peak temperature of around 616°C, the temperature for 450G is slightly higher than for 90G. The peak of heat release for 90G is 287 W g⁻¹ as seen from Table 20. For 150G this value is 332 W g⁻¹ and for 450G, 356 W g⁻¹. It appears that the lower viscosity material, although having an earlier onset of heat release temperature produces the smallest peak of heat release however, all samples produce the same amount of total heat. The earlier onset of heat release for the lower viscosity 90G may be due to the shorter lengths of chain present within the polymer. These chains require slightly less energy than longer chains for volatile formation to occur and at a linear heating rate, this will occur at a lower temperature. Alternatively, if decomposition is initiated at chain ends, there will be more initiating sites in the lower viscosity polymer.

	Onset Temperature (°C)	Peak Temperature (°C)	PHRR (W g ⁻¹)	Char (%)	THR (kJ/g)
90G	571 ± 2.6	615.2 ± 1.6	287.2 ± 10.1	51.5 ± 2.3	11 ± 0.5
150G	575.4 ± 0.8	616.5 ± 2.2	332.7 ± 25.2	48.4 ± 1.0	10.7 ± 0.4
450G	580.6 ± 1.3	617.2 ± 0.8	356.1 ± 14.2	50.3 ± 0.9	10.9 ± 0.1

TABLE 20. PCFC VISCOSITIES EXPERIMENTS SUMMARY OF DATA

4.3.2 Effect of Fillers

Samples of 450G, 450CA30 and 450GL30 were tested in the PCFC. The results are shown in Figure 69 and a summary of the data is presented in Table 21.

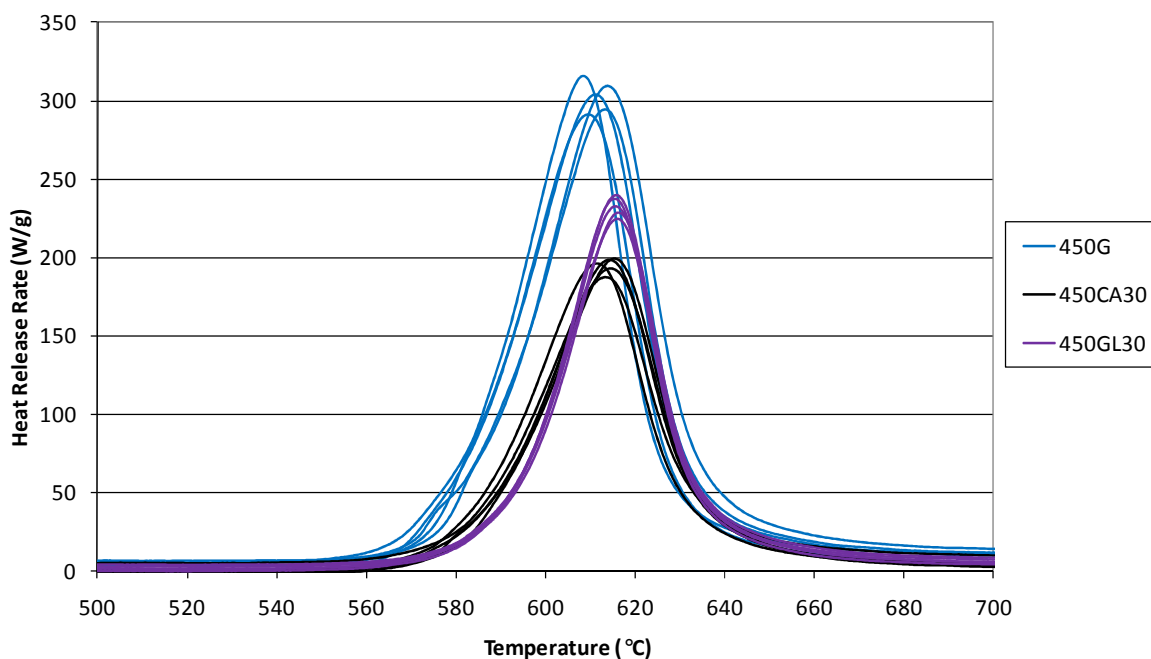


FIGURE 69. PCFC ADDITIVES EXPERIMENTS HEAT RELEASE RATES

The unfilled polymer begins releasing heat prior to the filled polymers; this is expected as 450G decomposes earlier than the filled polymers as seen in the TGA experiments. The average peak heat release rate of the unfilled samples is 302 W g^{-1} and therefore higher than the filled samples. Again there are differences between the filled materials. 450GL30 gives a higher average peak heat release rate (232 W g^{-1}) than 450CA30 (195 W g^{-1}). However, both reduce the peak heat release rate when compared to the unfilled material with a 35% reduction for 450CA30 and a 23% reduction for 450GL30. Interestingly, the presence of 30% filler does not reduce the peak heat release rate uniformly. In the glass fibre-filled composite a more rapid pyrolysis rate, and hence the release of flammable material occurs more sharply compared to the carbon-fibre composite. The temperature of the onset of heat release rate in the PCFC corresponds to the ignition temperature of the polymer. The average temperature for 450G is 594°C , for 450CA30 is 596°C and for 450GL30 is 605°C . In the TGA, it has been

argued that the temperature that corresponds to around 10% mass loss in air corresponds to the piloted ignition temperature [18]. In an inert atmosphere, 450G reaches this mass loss at 576°C, 450CA30 at 583°C and 450GL30 at 586°C. This pattern correlates with the TGA data, with 450G having a lower ignition temperature than the filled composites although all temperatures are lower than the ignition temperatures determined from the PCFC data. These differences are possibly due to the higher heating rate (60°C min⁻¹) in the PCFC, if the TGA were to be run at 60°C min⁻¹, better agreement would be expected. The residue yields show good agreement between the PCFC and TGA data.

	Onset Temperature (°C)	Peak Temperature (°C)	PHRR (W g ⁻¹)	Char (%)	THR (kJ/g)
450G	594 ± 1.8	611.2 ± 2.2	302.8 ± 10.3	51.6 ± 2.6	10.7 ± 0.3
450CA30	596.4 ± 0.9	613.6 ± 1.5	194.9 ± 4.8	68.5 ± 3.8	7.0 ± 0.2
450GL30	605.6 ± 0.5	615.7 ± 0.3	232.5 ± 6.1	65.9 ± 1.5	7.2 ± 0.1

TABLE 21. PCFC ADDITIVES EXPERIMENTS SUMMARY OF DATA

4.4 Cone Calorimeter

4.4.1 Effect of Thickness on Burning Behaviour

Experiments were completed in the cone calorimeter on the thickness of medium viscosity samples ranging from 2.5 mm to 10 mm. The results for the experiments completed with 2.5 mm thick samples are shown in Figure 70. The curves typically show thermally thin burning. On average, a sharp increase in heat release rate is observed between 200 and 275 seconds which reaches a peak heat release rate of 325 kW m^{-2} at 275 seconds. A sharper decrease in heat release rate is shown between 300 and 350 seconds. Typically, a 150 second burn time is observed.

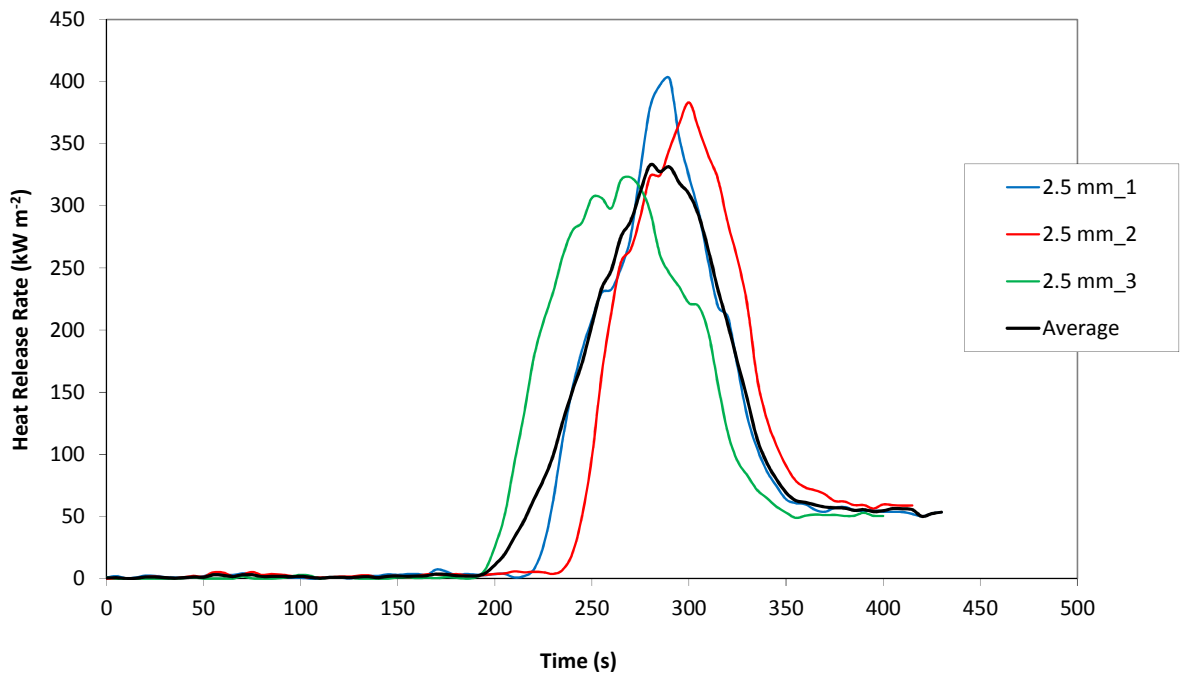


FIGURE 70. 150G 2.5 MM HEAT RELEASE RATE

The results for the experiments completed with 3.2 mm thick samples are shown in Figure 71. A steady increase in heat release rate is observed between 150 and 240 seconds followed by a second steadier increase in heat release rate between 250 and 275 seconds with a peak heat release rate of 290 kW m^{-2} at 275 seconds. There is a steady decrease in the heat release rate between 280 and 350 seconds.

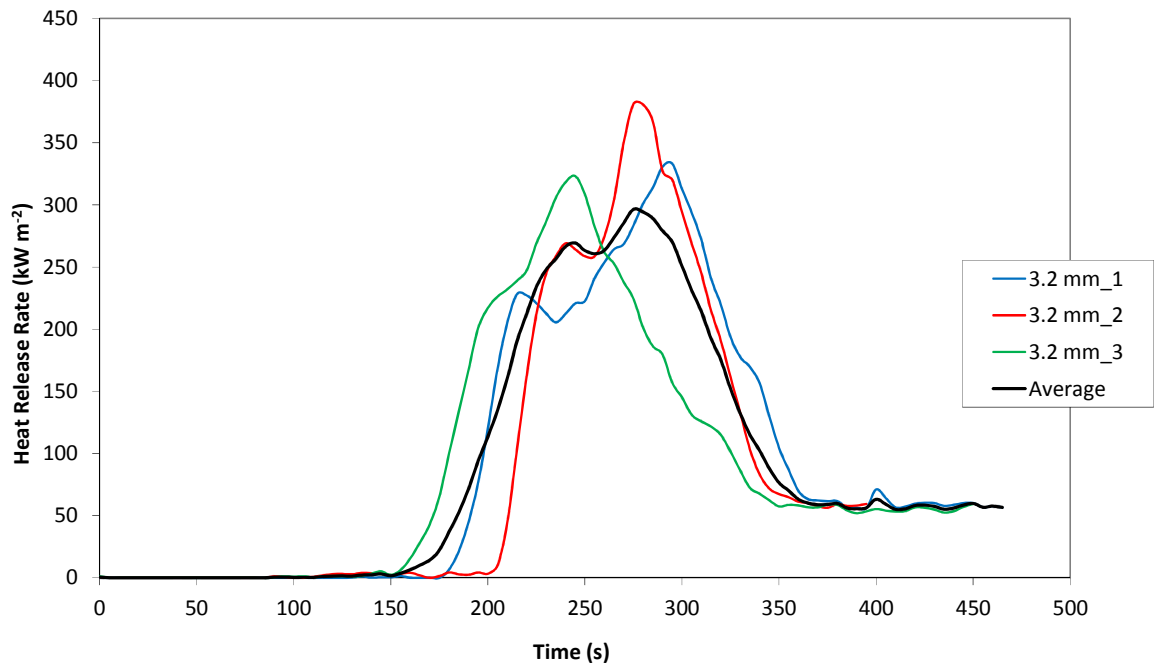


FIGURE 71. 150G 3.2 MM HEAT RELEASE RATE

The results for the experiments completed with 3.5 mm thick samples are shown in Figure 72. The samples used show a very large difference of around 100 seconds between the ignition times of samples 1 and 3. Therefore, the 'average' shows three separate instances where the heat release rate increases steadily. An 'average' peak heat release rate of 240 kW m^{-2} is observed at 380 seconds. A steady decrease in heat release rate is seen between around 400 and 500 seconds. It is acknowledged that with such large scatter in the data, taking an average from only 3 points is not statistically valid.

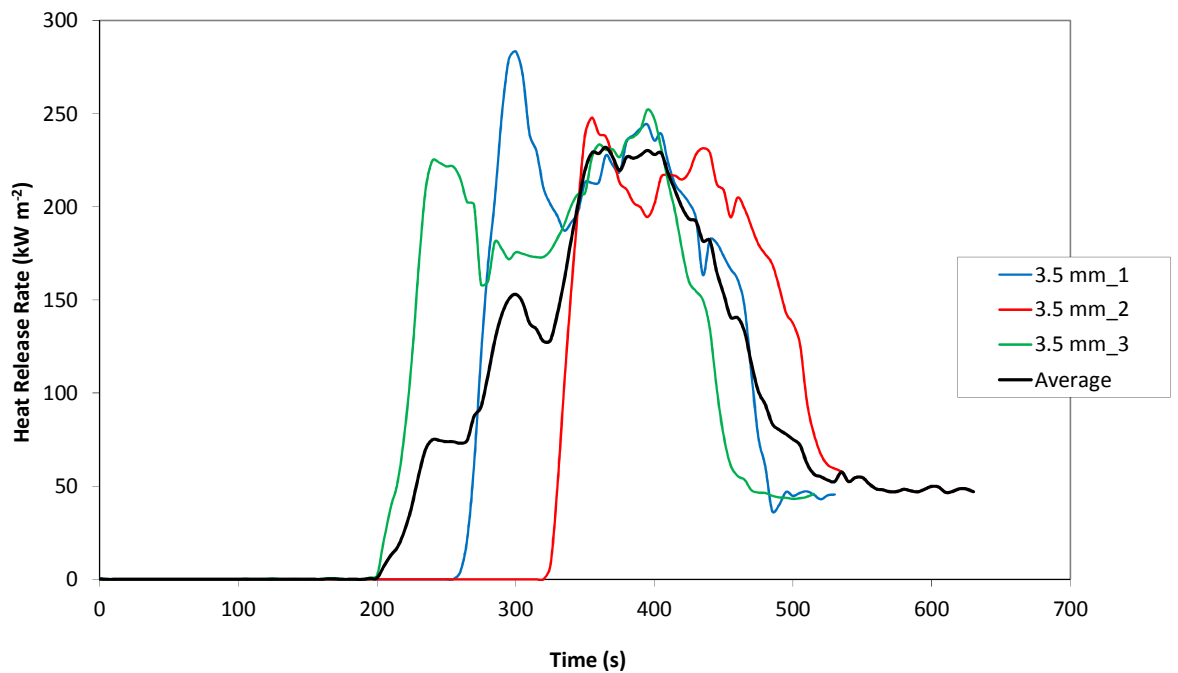


FIGURE 72. 150G 3.5 MM HEAT RELEASE RATE

The results for the experiments completed with 6 mm thick samples are shown in Figure 73. All curves show a similar pattern with a sharp increase in heat release rate followed by a sharp decrease in heat release rate and then a small period of steady burning. This is followed by slight increase in heat release rate and then a slight decrease. A peak heat release rate of 210 kW m^{-2} is observed at 390 seconds. Typically, a 1000 second burn time is observed.

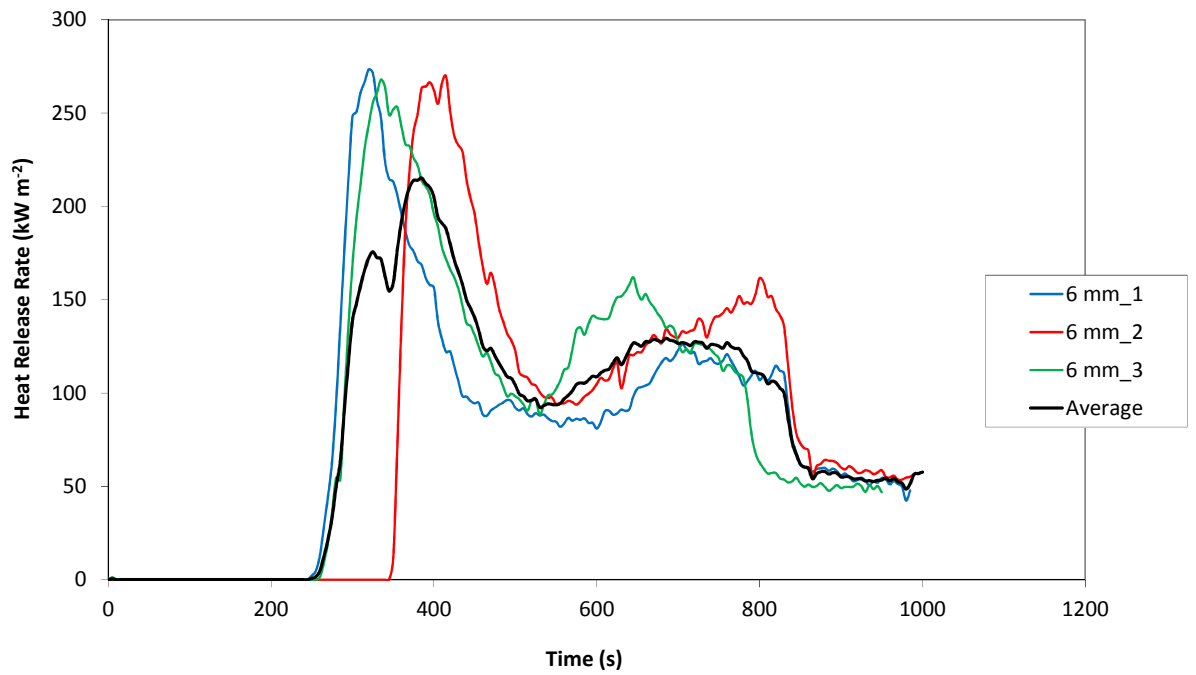


FIGURE 73. 150G 6 MM HEAT RELEASE RATE

The results for the experiments completed with 10 mm thick samples are shown in Figure 74. Similarly to Figure 73, there are two distinct peaks of heat release rate separated by a period of steady burning. On average, there is a sharp increase in heat release rate between 300 and 350 seconds with a peak heat release rate of 170 kW m^{-2} . This is followed by a period of steady burning with a second increase in heat release rate between 1000 and 1150 seconds which results in a second peak heat release rate of 170 kW m^{-2} at 1150 seconds.

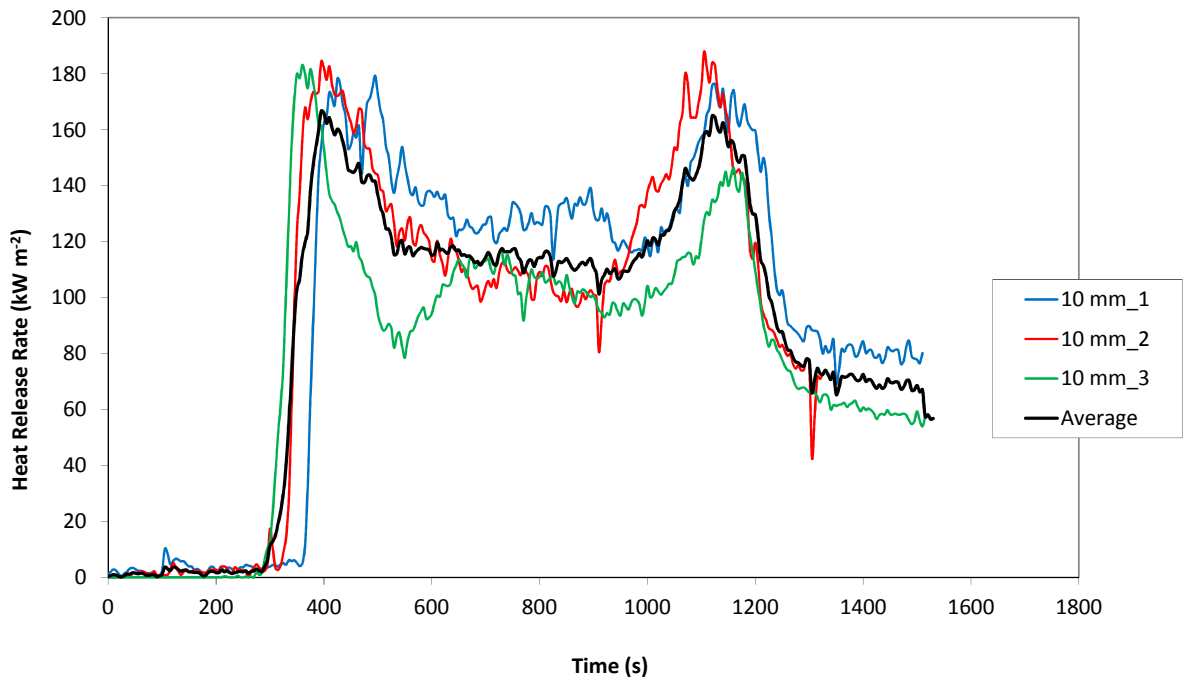


FIGURE 74. 150G 10 MM HEAT RELEASE RATE

Thermally thin behaviour, as exhibited by the 2.5 mm and 3.2 mm thick samples is shown typically by a short time to ignition, followed by a very sharp increase in heat release rate with one peak of heat release rate reached quite rapidly as all the sample is pyrolysed at once. There is a sharp decrease in heat release rate as the entire sample has been burned and burn times tend to be short due to the amount of fuel present. The peak heat release rate achieved is also dependent on the total fire load.

In comparison, thermally thick samples show a longer time to ignition as thermal equilibrium is reached. When the sample ignites the heat release rate increases steadily but reaches a lower peak in comparison to the thermally thin samples. This process occurs prior to any charring of the sample. This is followed by a long period of steady state burning and then a

second peak in heat release rate as the final few millimetres of the sample burn – acting as a thermally thin sample. This peak can also be attributed to the breakup of the char or an increase in effective rate of pyrolysis.

The averages of each thickness experiment have been plotted in Figure 75. As expected, thinner samples show thermally thin burning behaviour and thicker samples show thermally thick burning behaviour.

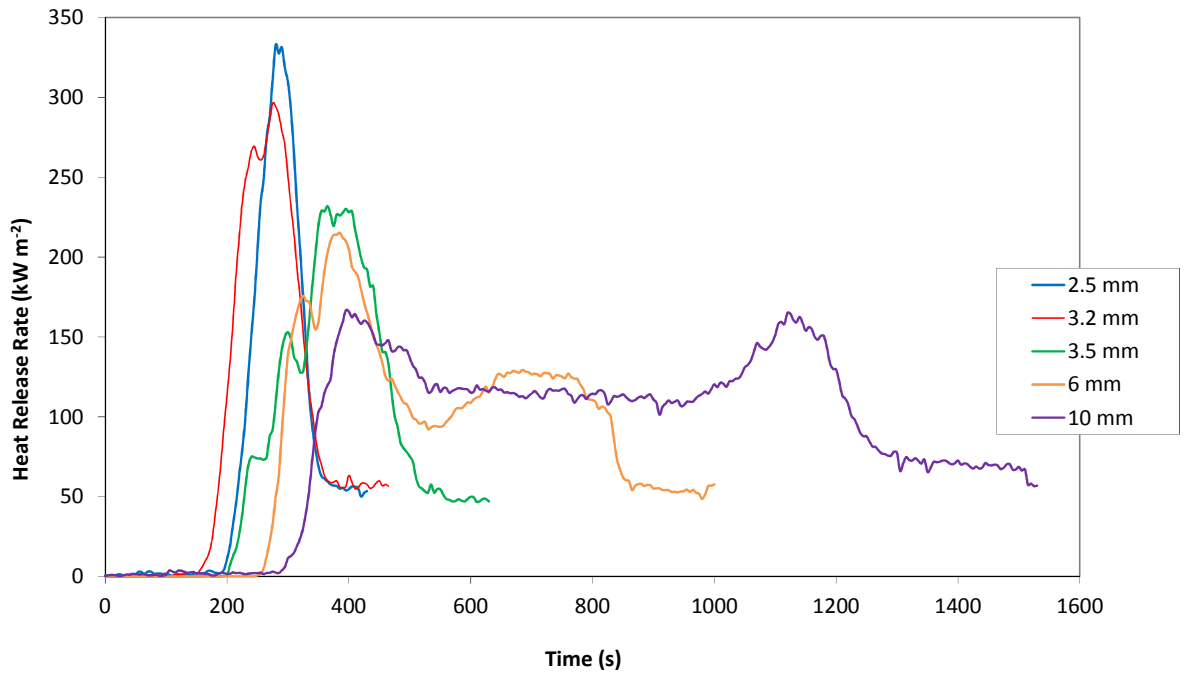


FIGURE 75. 150G AVERAGE HEAT RELEASE RATE OF VARIED THICKNESSES

4.4.2 Effect of Viscosity on Burning Behaviour

Experiments were completed on the different viscosities of PEEK – 90G, 150G and 450G and the effect of these on heat release rate. For 90G, shown in Figure 76, on average a sharp increase in heat release rate occurs at around 160 seconds reaching a peak heat release rate at around 240 kW m⁻². A period of steady burning is achieved between 250 and 320 seconds. A sharp decrease in heat release rate is seen between 350 and 400 seconds. The differences in the shapes and distributions of the curves are attributed to the intumescent behaviour of PEEK in the cone although this is discussed later (Section 4.4.13, Page 167).

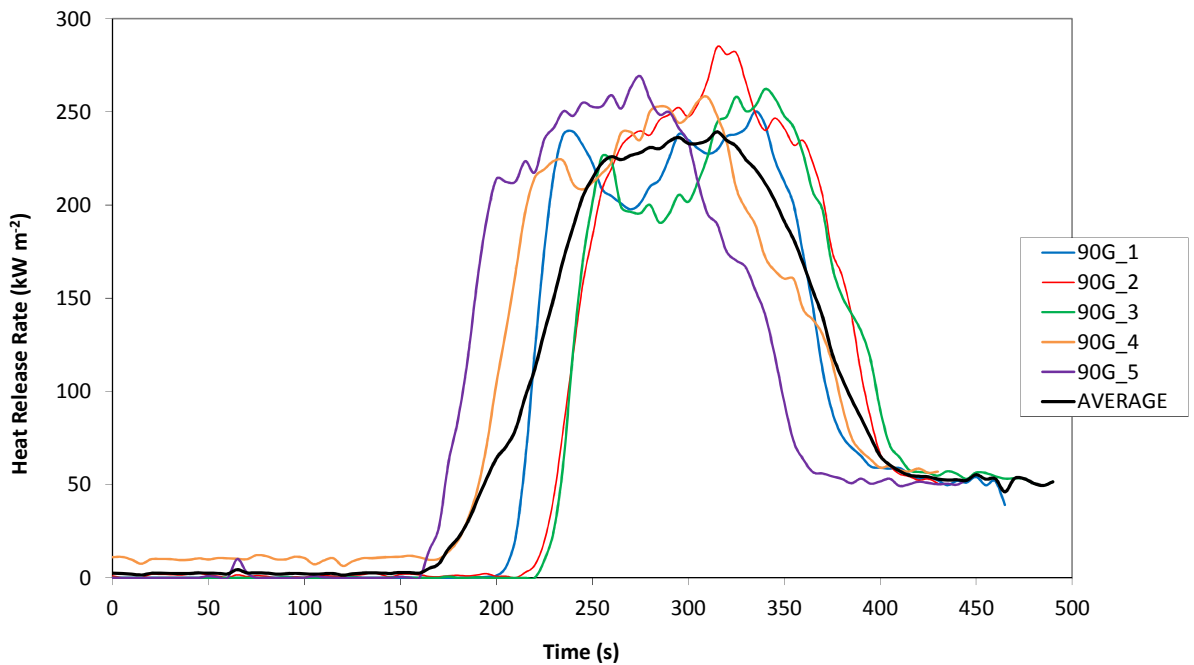


FIGURE 76. 90G 3.2 MM HEAT RELEASE RATE

For 150G samples, shown in Figure 77, on average a sharp increase in heat release rate occurs similarly to the 90G samples at around 160 seconds reaching a peak heat release rate at around 280 kW m^{-2} . A period of steady burning is achieved between 230 and 300 seconds. A sharp decrease in heat release rate is seen between 350 and 400 seconds.

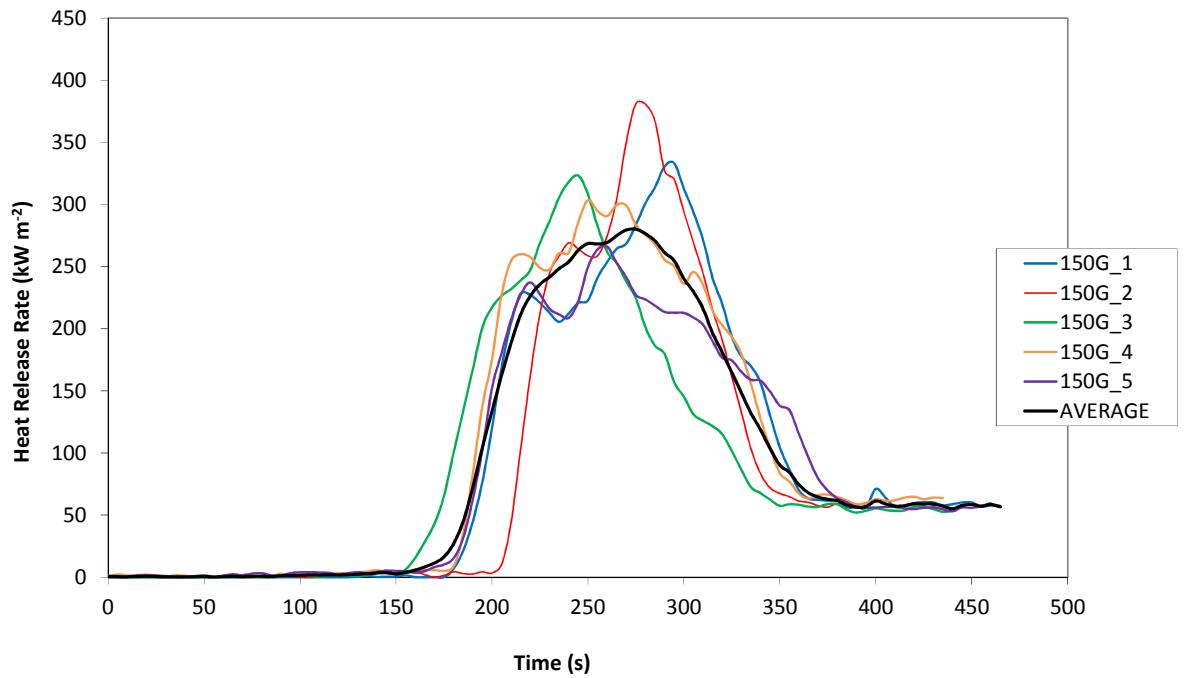


FIGURE 77. 150G 3.2 MM HEAT RELEASE RATE

For 450G, shown in Figure 78, on average a sharp increase in heat release rate occurs similarly to the 90G and 150G samples at around 180 seconds, reaching a peak heat release rate of 300 kW m^{-2} at around 290 seconds. A second steadier increase in heat release rate is observed between 210 and 280 seconds. A steady state of burning is achieved between 275 and 290 seconds. A sharp decrease in heat release rate is seen between 300 and 330 seconds.

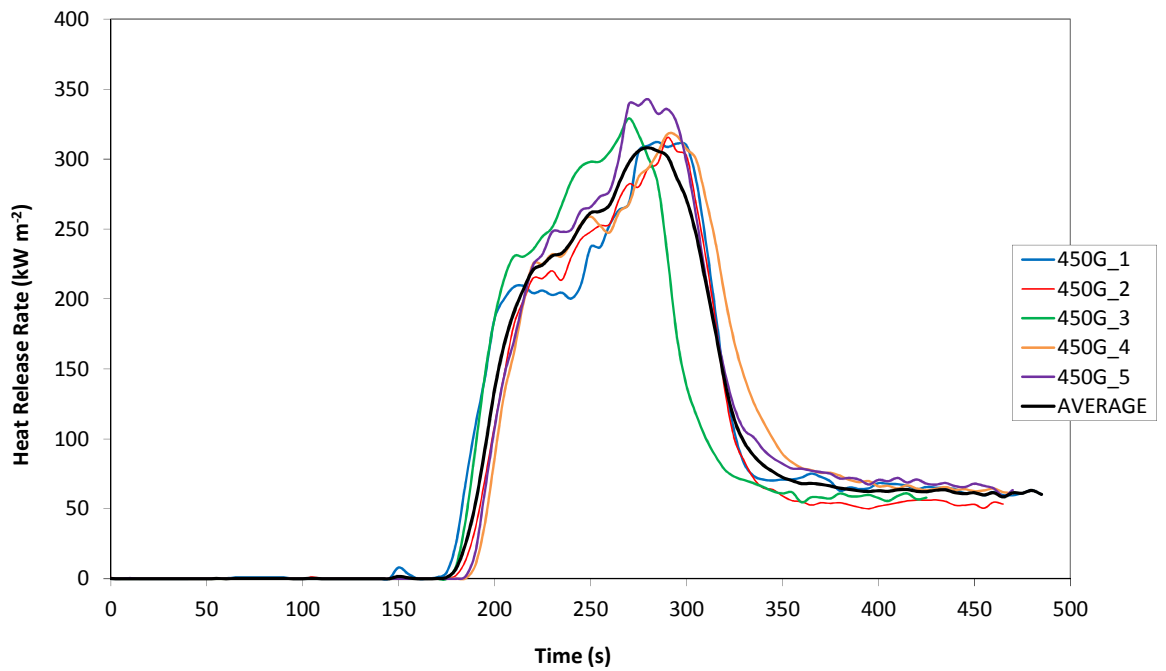


FIGURE 78. 450G 3.2 MM HEAT RELEASE RATE

The averages of each viscosity experiment have been plotted in Figure 79.

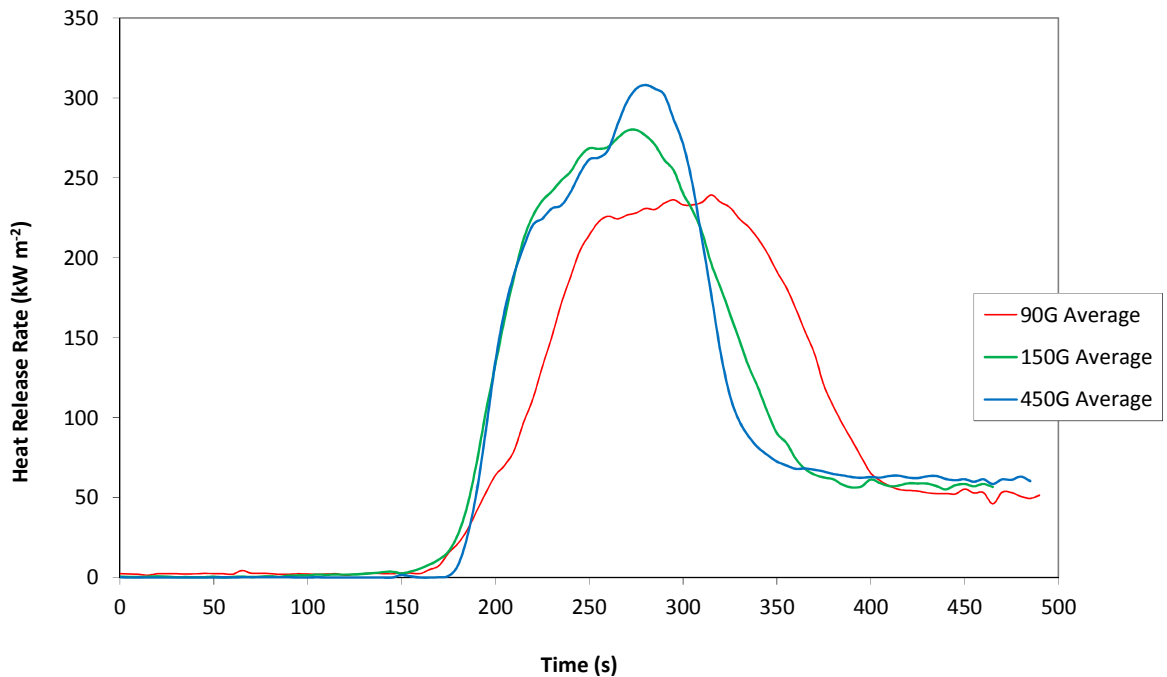


FIGURE 79. VISCOSITY 3.2 MM AVERAGE HEAT RELEASE RATES

The curves show a similar time to ignition – identified by a sharp increase in heat release rate. There are differences with regards to the gradient of the curves, 90G, being the least viscous of the samples shows a steadier increase up to the peak heat release rate whereas 150G and 450G samples show a similar pattern. A lower average peak heat release is also observed for the 90G samples. It is believed a more viscous sample, such as 450G, will take longer to heat up and in doing so, will release more energy when it ignites, therefore giving a higher peak heat release rate and a faster initial heat release rate.

4.4.3 Effect of Fillers on Burning Behaviour

Experiments were completed on the additives commonly incorporated within PEEK – carbon and glass fibre – to look into the results shown in literature (see Figure 16) in greater detail. The results for PEEK incorporated with 30% carbon fibre (CA30) are shown in Figure 80. There is a great difference in ignition times between the five samples which were tested shown by a 400 second difference in ignition times between sample 3 and sample 5. Due to these inconsistencies, the average heat release rate which has been plotted shows a steady

increase in heat release rate between 300 and 550 seconds with a peak heat release rate of 70 kW m^{-2} at 580 seconds and a steadier decrease in burning between 600 and 1000 seconds. The long times to ignition, and the large amount of scatter in the data show that for the 450CA30 samples, 50 kW m^{-2} is close to the critical heat flux for ignition (in one case, ignition occurs after 11 minutes).

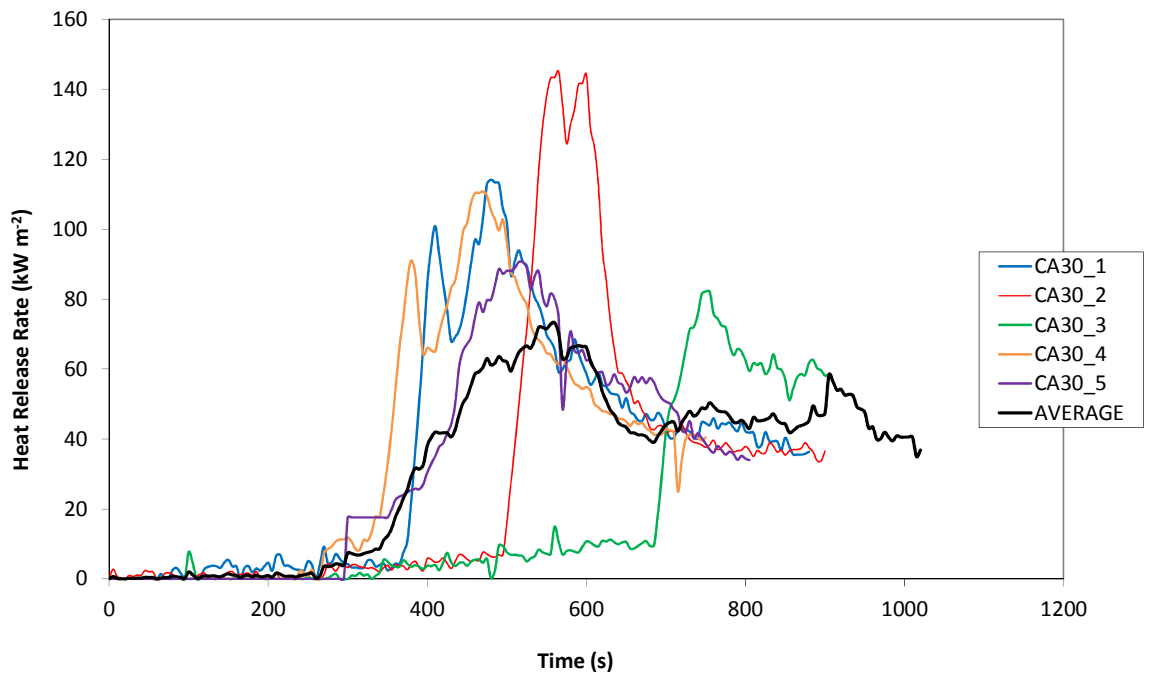


FIGURE 80. 450CA30 3.2 MM HEAT RELEASE RATE

The results for PEEK incorporated with 30% glass fibre (GL30) are shown in Figure 81. There is less inconsistency with the ignition times compared to the carbon fibre-reinforced samples with a 100 second difference in the ignition times of samples 1 and 5. The average plot shows a steady increase in heat release rate between 200 and 430 seconds with a peak heat release rate of 80 kW m^{-2} at 430 seconds and a steadier decrease in heat release rate between 460 and 900 seconds. The smaller amount of scatter and shorter time to ignition is consistent with the 450GL30 samples having a lower critical heat flux for ignition than the 450CA30, however, the 450GL30 samples appear to have a higher thermal stability in the TGA experiments in both and inert and oxidative atmosphere.

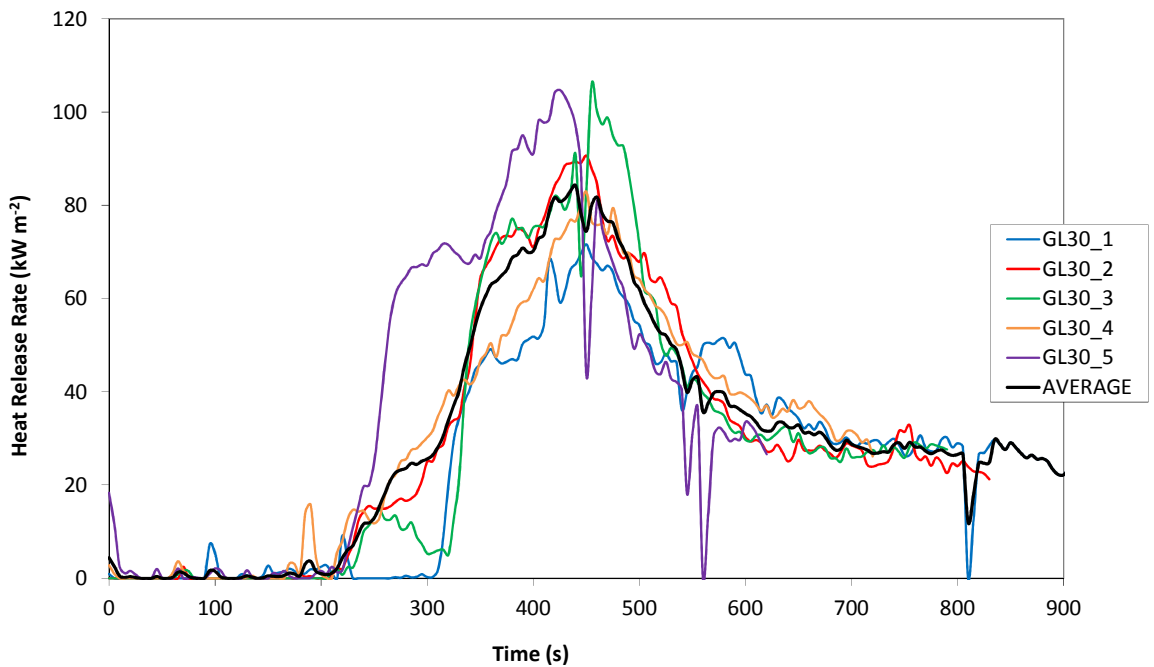


FIGURE 81. 450GL30 3.2 MM HEAT RELEASE RATE

The average of each of the experiments with filled PEEK has been plotted in Figure 82. There are similarities with work completed previously (see Figure 15) whereby on average, PEEK filled with glass fibre ignites earlier than PEEK filled with carbon fibre but both delay time to ignition (t_{ig}) compared to the virgin 450G. There are significant differences in peak heat release rate between the filled and unfilled polymer and these are also observed in Figure 16. However, the gradual increase in heat release rate is the result of scatter in the results and not the burning behaviour of the individual samples.

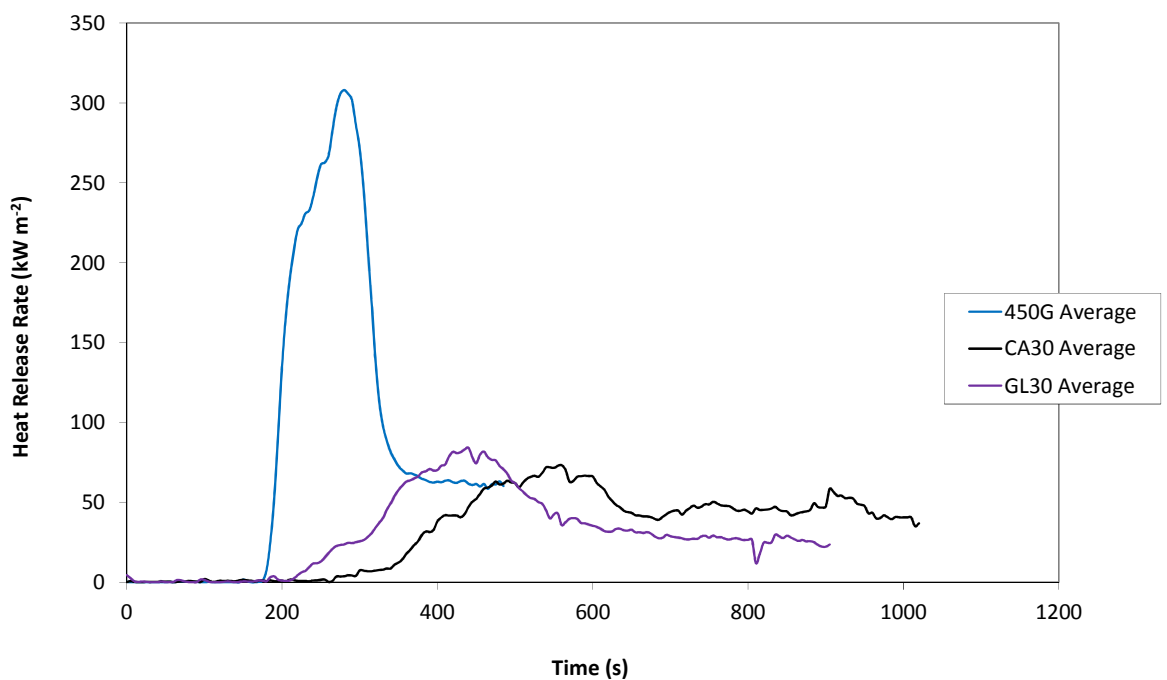


FIGURE 82. ADDITIVES EXPERIMENTS 3.2 MM AVERAGE HEAT RELEASE RATES

4.4.4 Scatter in the Cone Calorimeter

From the previous sections (4.4.1, 4.4.2 and 4.4.3) it is evident that there is a large amount of scatter present in the data. From section 4.4.1 which deals with the thickness of samples in the cone calorimeter, it can be seen that as the thickness of the sample increases, the difference between the ignition times of individual samples also increases. The thinnest sample (2.5 mm), shown in Figure 70 shows a 40 second difference in time to ignition

compared to a thicker sample (6 mm), shown in Figure 73 which shows difference of 100 seconds and therefore more scatter. From Section 4.4.2, which deals with the viscosity of samples in the cone calorimeter, it is evident that a lower viscosity sample (90G) shown in Figure 76 gives a larger difference in the time to ignition of individual samples (70 seconds) compared to higher viscosity sample (450G) shown in Figure 78 which shows a smaller difference (15 seconds). In section 4.4.3 which looks at the effect of filler on burning behaviour, the carbon fibre-filled samples, 450CA30, show a 400 second difference in time to ignition of individual samples (Figure 80), compared to the unfilled 450G PEEK at the same thickness, which shows a 50 second difference, as seen in Figure 78. The presence of scatter within the data is problematic, both in terms of assessing the flammability of these materials and drawing effective conclusions, and as a result will be investigated further in the following section. As the time to ignition is increased, it is expected that the peak of heat release will also increase due to the sample being exposed to the radiant heat flux for a longer period of time and therefore absorbing more heat, which in turn is released when the material finally ignites. As a result, it would be expected for there to be a correlation between these two parameters in the cone calorimeter. As it was determined that the 2.5 mm samples showed the least scatter in the time to ignition, this thickness was investigated using a four different viscosities – 90G, 150G, 450G and 600G and a variety of fillers - carbon fibre, glass fibre, carbon black and talc.

4.4.4.1 Effect of PEEK Viscosity on t_{ig} and PHRR

It is expected that varying the viscosity of the samples will vary the scatter in the time to ignition. The results for 90G – the least viscous of the samples are shown in Figure 83.

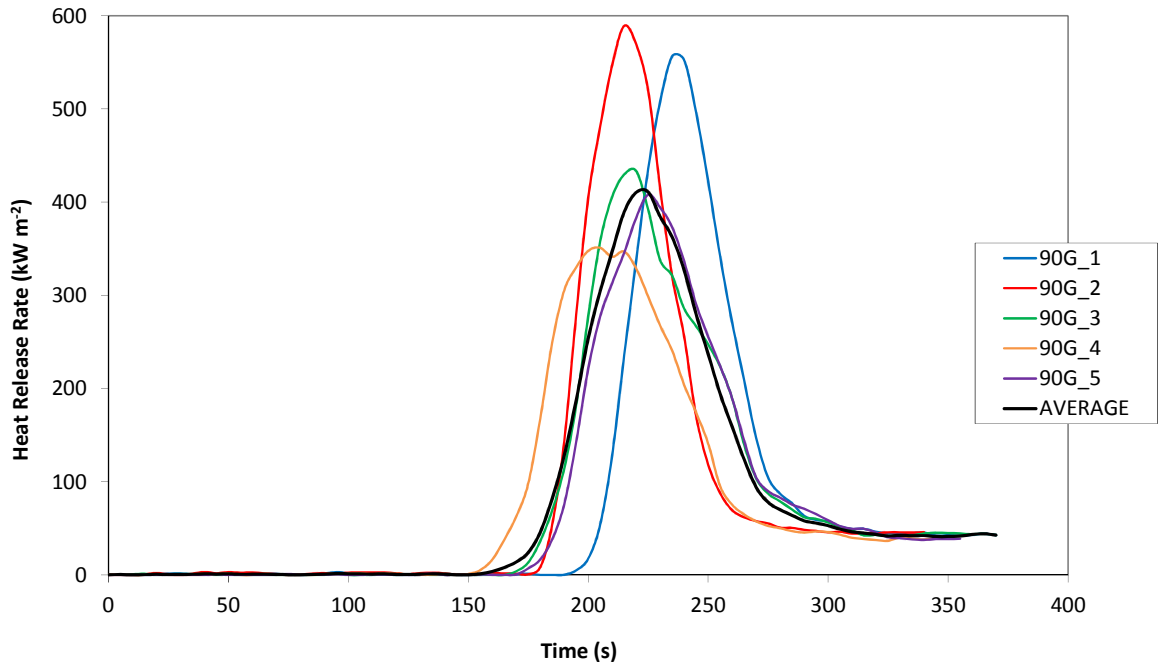


FIGURE 83. 90G 2.5 MM HEAT RELEASE RATE

Table 22 shows the data obtained from the cone calorimeter. It can be seen that the total heat released is around the same value for all five samples indicating that the same amount of sample was burned. There are differences in the time to ignition, peak heat release rate and time to peak heat release rate. From Table 22, it can be deduced that as the time to ignition increases, so does the peak heat release rate. This can be seen in Figure 84.

Sample	t_{ig} (s)	PHRR (kW/m ²)	tPHRR (s)	THR (MJ m ⁻²)
90G_1	194	556.5	235	29.0
90G_2	181	589.1	215	29.2
90G_3	168	433.5	220	29.3
90G_4	151	350.9	205	26.4
90G_5	170	408.1	225	27.2
Average	172 (±16.0)	467.6 (±101.2)	220 (±11.2)	28.2 (±1.3)

TABLE 22. 90 G 2.5 MM CONE CALORIMETER PROPERTIES

Figure 84 shows the relationship between the time to ignition and the peak heat release rate for the least viscous of the samples tested. It is clear that as the time to ignition increases so does the peak heat release rate which supports the explanation that the longer the samples

are exposed to the 50 kW m^{-2} cone irradiance, the more heat is being absorbed and therefore, when the sample finally ignites, more heat is released.

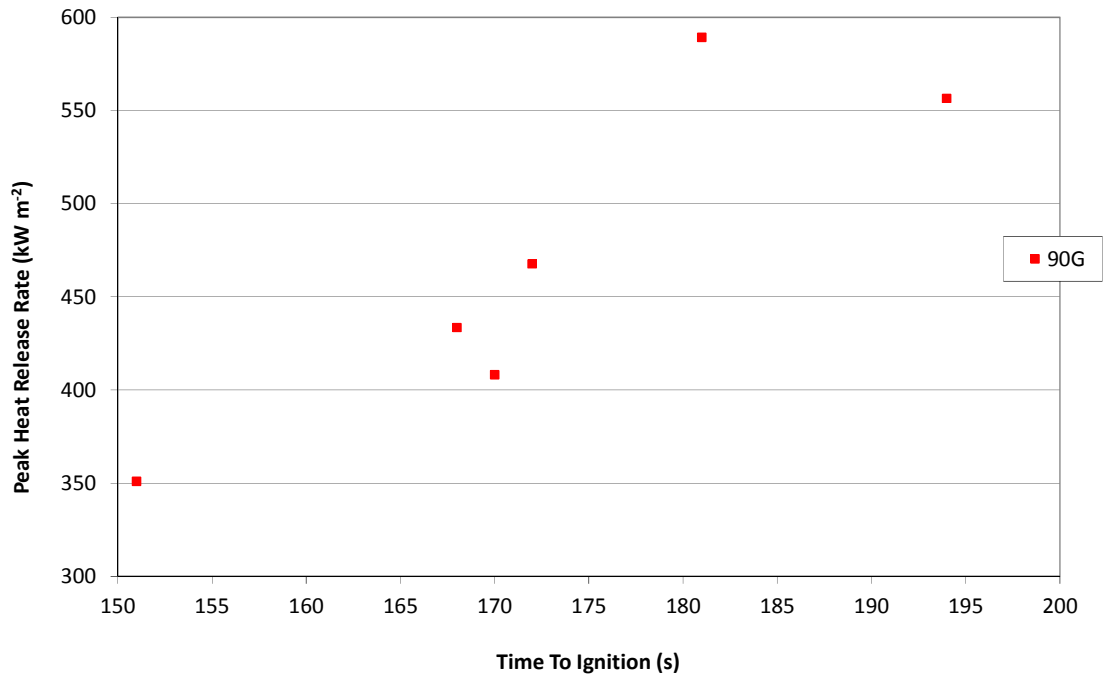


FIGURE 84. RELATIONSHIP BETWEEN 90G t_{ig} AND PHRR

The results for 150G – a sample of low-medium viscosity – are shown in Figure 85.

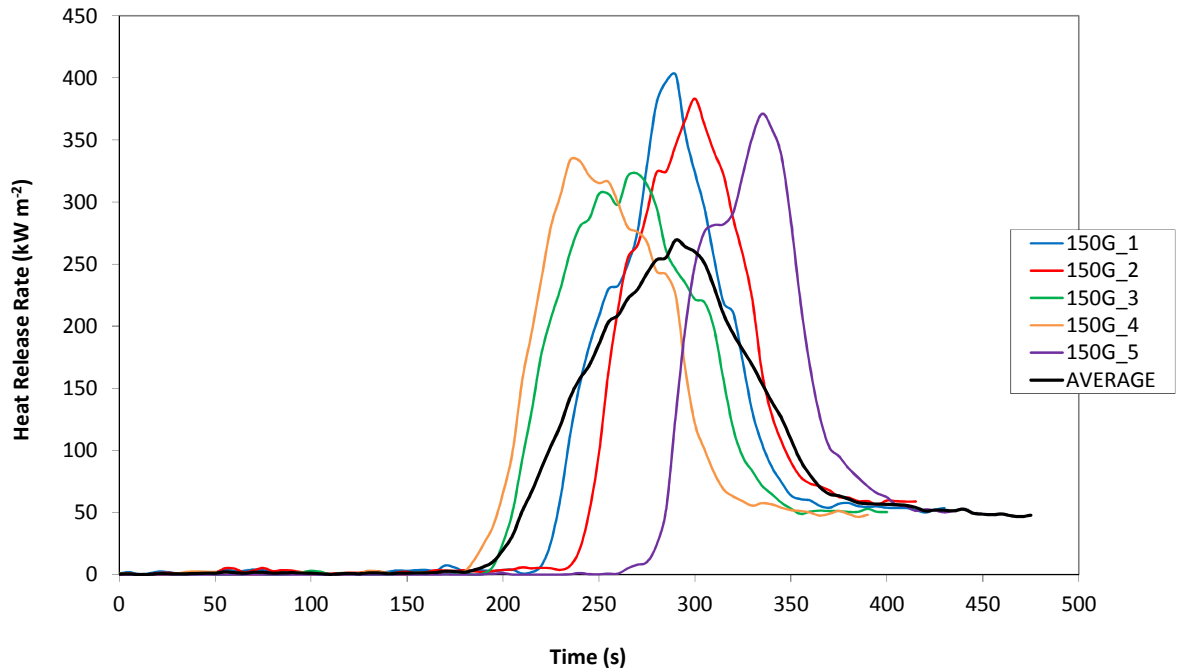


FIGURE 85. 150G 2.5 MM HEAT RELEASE RATE

Table 23 shows the data obtained from the cone calorimeter. Similar to the 90G samples, the THR of all experiments is around 31 MJ m⁻² indicating that the same amount of sample was burned in each instance. There appears to be little correlation between the t_{ig} and PHRR. This suggests the formation of a protective layer reducing the flammability of the pre-heated sample. There is a larger difference in the time to ignition of these samples compared to the 90G samples.

Sample	t_{ig} (s)	PHRR (kW m ⁻²)	t_{PHRR} (s)	THR (MJ m ⁻²)
150G_1	219	402.3	290	32.4
150G_2	236	383.2	300	31.4
150G_3	192	322.3	270	32.4
150G_4	182	333.8	235	31.1
150G_5	269	371.1	335	28.3
Average	219 (±34.9)	362.7 (±36.6)	286 (±36.9)	31.1 (±1.7)

TABLE 23. 150G 2.5 MM CONE CALORIMETER PROPERTIES

The results for 450G – a sample of medium-high viscosity – are shown in Figure 86. The results seem more consistent, with similar shaped curves, and a difference of 20 seconds between ignition of samples 1 and 3.

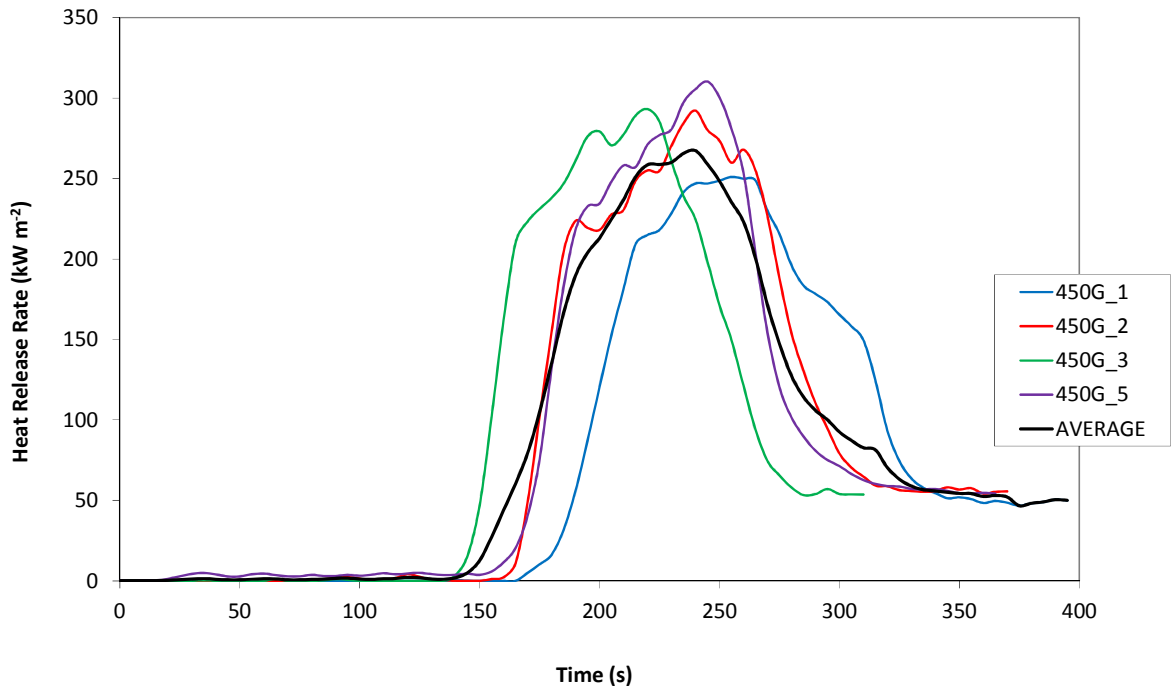


FIGURE 86. 450G 2.5 MM HEAT RELEASE RATE

Table 24 shows the data obtained from the cone calorimeter. Again there appears to be little or no correlation between the parameters t_{ig} and PHRR. The THR is around 30 MJ m^{-2} indicating that the same amount of sample was burned. Here there is a smaller amount of scatter in the time to ignition compared to both the 90G and 150G samples indicating that the scatter in the time to ignition is reduced with higher viscosity samples. To determine whether this is the case or not, the 600G samples would have to show a smaller amount of scatter in the time to ignition.

Sample	t_{ig} (s)	PHRR (kW m^{-2})	tPHRR (s)	THR (MJ m^{-2})
450G_1	166	250.9	255	29.5
450G_2	161	292.2	240	31.9
450G_3	136	393.2	220	28.4
450G_5	154	310.3	245	31.1
Average	154 (± 13.1)	311.7 (± 59.8)	240 (± 14.7)	30.2 (± 1.6)

TABLE 24. 450G 2.5 MM CONE CALORIMETER PROPERTIES

The results for 600G – a sample of high viscosity – are shown in Figure 87. The results seem more consistent than the lower viscosity samples with similar shaped curves and a difference of 20 seconds between ignition of samples 2 and 4, and therefore less scatter in the times to ignition than the lower viscosity samples.

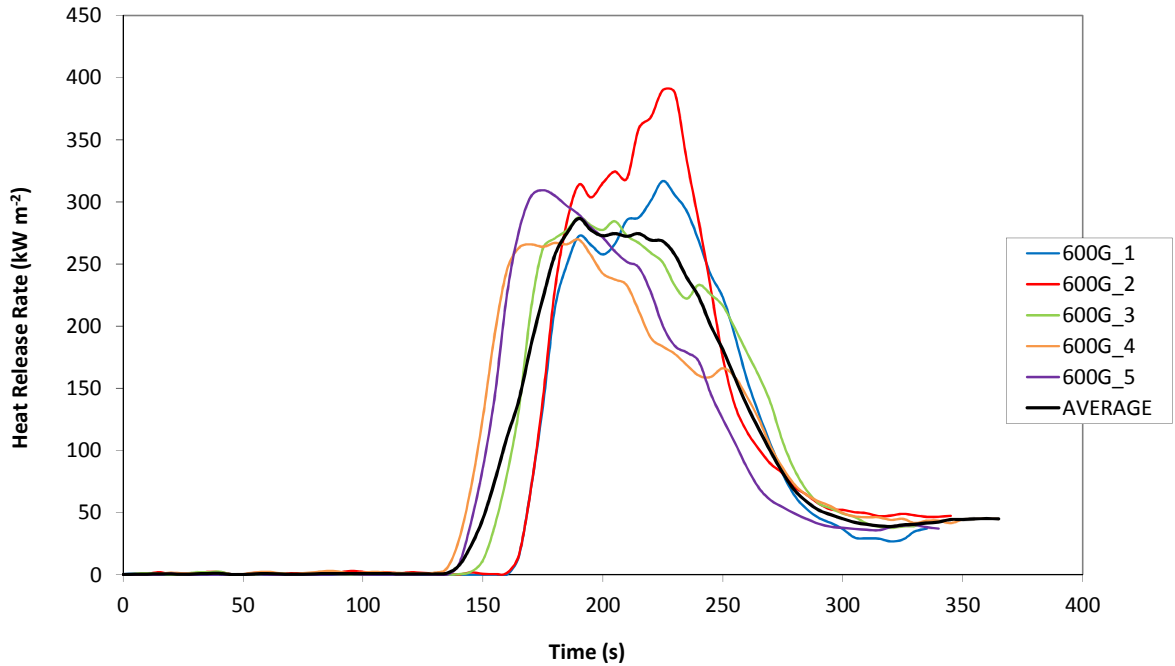


FIGURE 87. 600G 2.5 MM HEAT RELEASE RATE

Table 25 shows the data obtained from the cone calorimeter. Again there appears to be little or no correlation between the parameters t_{ig} and PHRR. The THR is around 29 MJ m^{-2} indicating that the same amount of sample was burned.

Sample	t_{ig} (s)	PHRR (kW m^{-2})	t_{PHRR} (s)	THR (MJ m^{-2})
600G_1	161	316.8	225	26.9
600G_2	165	389.9	225	30.5
600G_3	147	287.6	190	29.9
600G_4	137	269.6	190	30.8
600G_5	139	309.4	175	28.5
Average	149 (± 12.7)	314.7 (± 45.9)	201 (± 22.7)	29.3 (± 1.6)

TABLE 25. 600G 2.5 MM CONE CALORIMETER PROPERTIES

The t_{ig} and PHRR for all samples of each viscosity have been plotted in Figure 88. It is apparent that with low to mid viscosity samples – such as 90G and 150G, there is a definite correlation between the parameters plotted although this is true to a lesser extent in 150G samples. With the mid to high viscosity samples – such as 450G and 600G, there is no correlation between the parameters. This supports the idea that a lower molecular weight sample which is exposed to the cone irradiance for a greater amount of time prior to ignition will release its energy more quickly when the material finally ignites. As there is no correlation between the higher viscosity samples, it may be that something other than the differences in time to ignition is causing the scatter in the data.

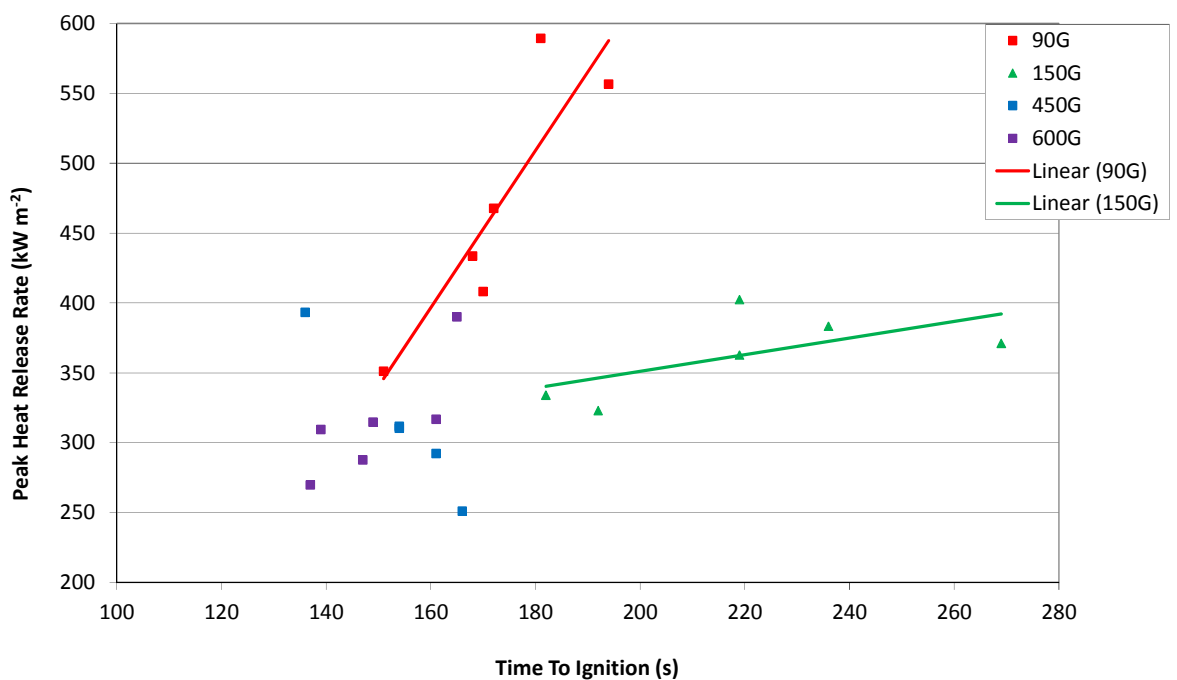


FIGURE 88. t_{ig} AND PHRR CORRELATION BETWEEN ALL VISCOSITIES

4.4.4.2 Effect of Additives on Scatter

It was previously thought that the presence of filler increased the amount of scatter in the time to ignition of repeat samples. The results for 450CA30 – PEEK filled with 30% carbon fibre are shown in Figure 89.

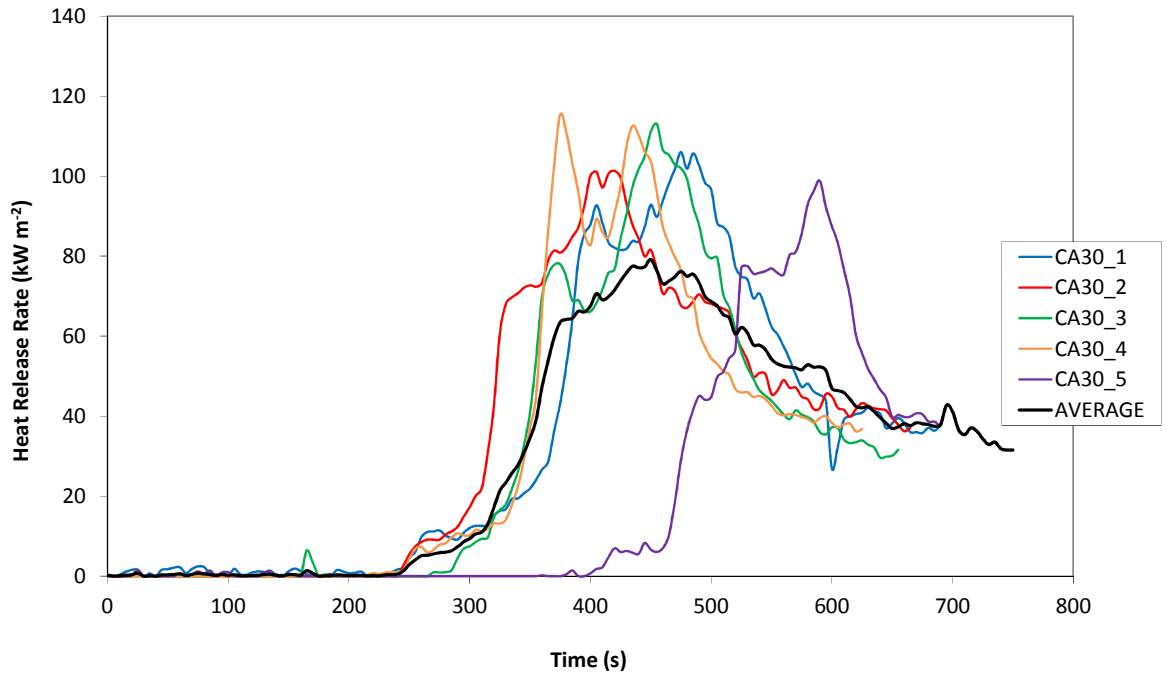


FIGURE 89. 450CA30 2.5 MM HEAT RELEASE RATE

The samples tested show similarities in the shape of the curves but significant differences in the times to ignition with 150 second interval between samples 1-4 and 5. This is much higher than the unfilled 450G which shows around a 30 second difference between all samples igniting.

Table 26 shows the data obtained from the cone calorimeter. Again there appears to be little or no correlation between the parameters t_{ig} and PHRR indicating another cause for this scatter. The THR is around 20 MJ m^{-2} suggesting that the same amount of sample was burned with the exception of sample 5. It may be that due to this sample's longer time to ignition, a protective barrier prevented more of the sample being burned.

Sample	t_{ig} (s)	PHRR (kW m^{-2})	t_{PHRR} (s)	THR (MJ m^{-2})
450CA30_1	246	105.7	485	23.0
450CA30_2	242	101.3	420	23.9
450CA30_3	283	113.0	455	20.5
450CA30_4	241	115.4	375	19.6
450CA30_5	424	98.8	590	15.9
Average	287(± 78.4)	106.8 (± 7.2)	465 (± 81.0)	20.6 (± 3.2)

TABLE 26. 450CA30 2.5 MM CONE CALORIMETER PROPERTIES

The results for 450GL30 – PEEK filled with 30% glass fibre are shown in Figure 90. The samples tested show similarities in the shape of the curves but significant differences in the times to ignition with 100 second interval between samples 1 and 5.

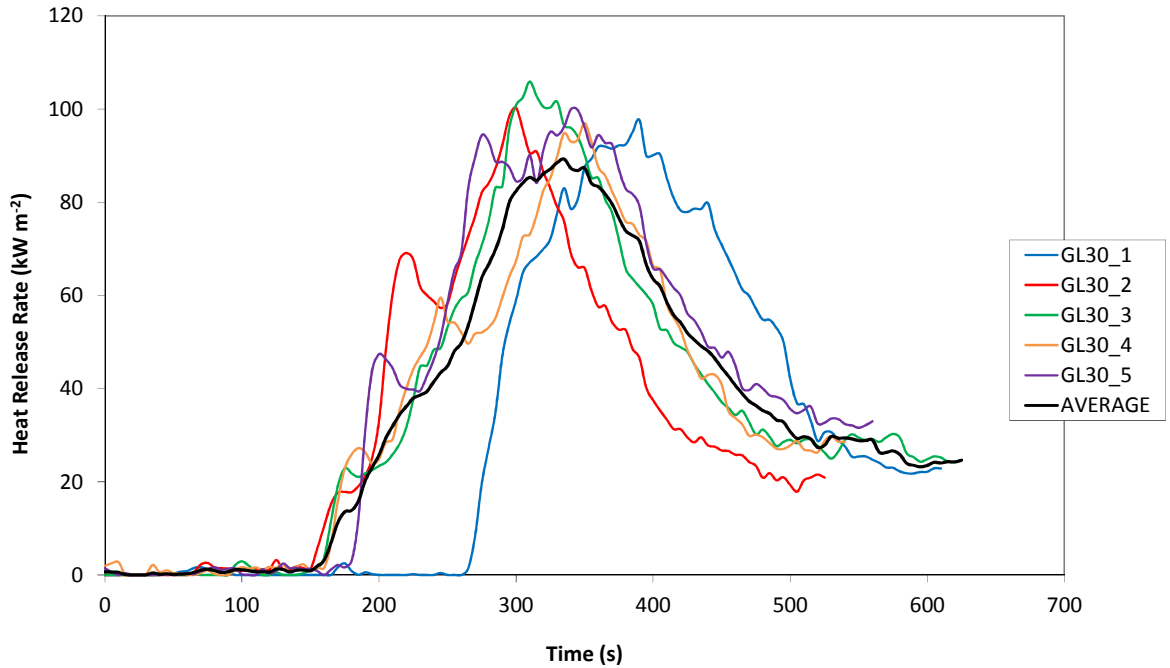


FIGURE 90. 450GL30 2.5 MM HEAT RELEASE RATE

Table 27 shows the data obtained from the cone calorimeter for the 450GL30 samples. There appears to be little or no correlation between the parameters t_{ig} and PHRR. The THR is around 20 MJ m^{-2} indicating that the same amount of sample was burned. These samples show less scatter than the carbon-fibre filled samples suggesting that the type of filler is important in terms of the extent of scatter.

Sample	t_{ig} (s)	PHRR (kW m^{-2})	t_{PHRR} (s)	THR (MJ m^{-2})
450GL30_1	271	97.7	390	19.3
450GL30_2	153	100.3	300	17.9
450GL30_3	163	105.9	310	22.3
450GL30_4	164	96.9	350	19.3
450GL30_5	181	99.9	340	22.9
Average	186 (± 48.3)	100.14 (± 3.5)	338 (± 35.6)	20.33 (± 2.2)

TABLE 27. 450GL30 2.5 MM CONE CALORIMETER PROPERTIES

The results for 381TL30 – PEEK filled with 30% talc are shown in Figure 91. The samples tested show similarities in the shape of the curves with no significant difference in the times to ignition. There is a steady increase in heat release rate observed between 185 to 290 with an average peak heat release rate of 110 kW m^{-2} . This is followed by a steady state period of burning between 290 and 350 seconds and steady decrease in heat release rate between 350 and 500 seconds.

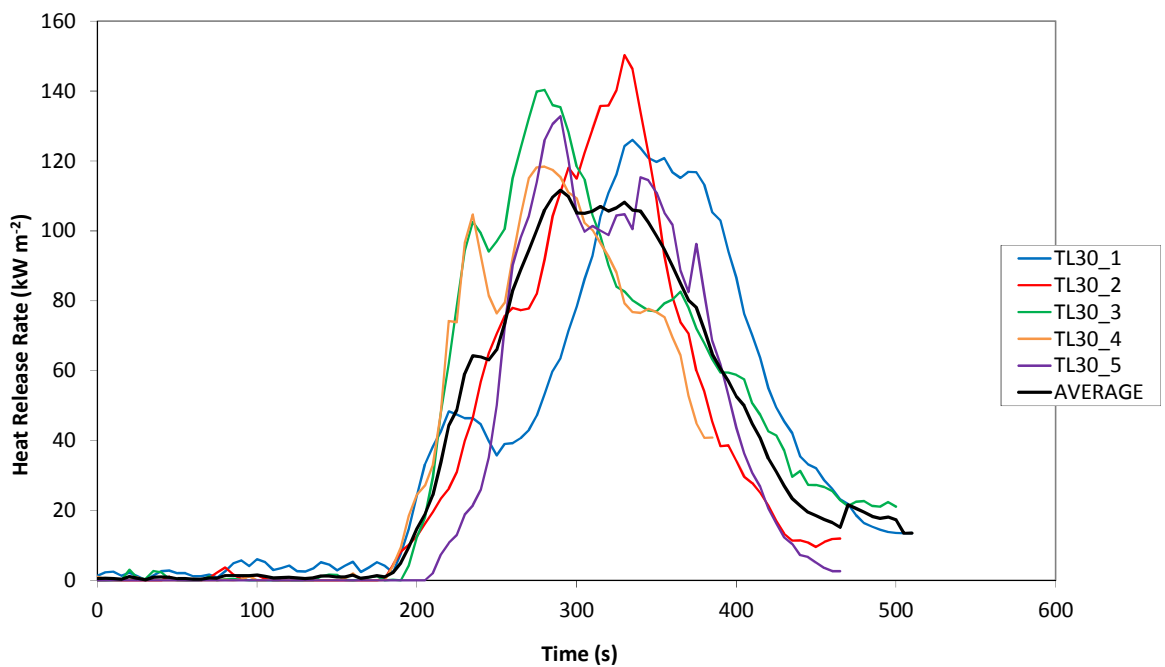


FIGURE 91. 381TL30 2.5 MM HEAT RELEASE RATE

Table 28 shows the data obtained from the cone calorimeter. There appears to be little or no correlation between the parameters t_{ig} and PHRR. The THR is around 18 MJ m^{-2} indicating that the same amount of sample was burned.

Sample	t_{ig} (s)	PHRR (kW m^{-2})	tPHRR (s)	THR (MJ m^{-2})
381TL30 1	185	126.1	335	20.2
381TL30 2	177	150.3	330	17.5
381TL30 3	189	135.9	285	21.1
381TL30 4	177	118.4	280	17.4
381TL30 5	196	138.8	290	16.5
Average	185 (± 8.1)	133.9 (± 12.2)	304 (± 26.3)	18.5 (± 2.0)

TABLE 28. 381TL30 2.5 MM CONE CALORIMETER PROPERTIES

The results for 450G903 – PEEK with <0.5% carbon black pigment are shown in Figure 92. Carbon black is added to the polymer commercially to change the colour of the resulting material from natural to black. The samples tested show little similarity in the shape of the curves and a significant difference in the times to ignition with a difference of 200 seconds between samples 1 and 2. It is interesting to note that the samples which are showing the most scatter in the time to ignition are the carbon fibre-filled samples and the samples containing carbon black pigment. There could be two conclusions drawn from this. One is that the presence of carbon-containing fillers is causing this effect, the other is that the difference in colour is causing this effect, as both carbon fillers cause a colour change in the resulting composite from natural to black.

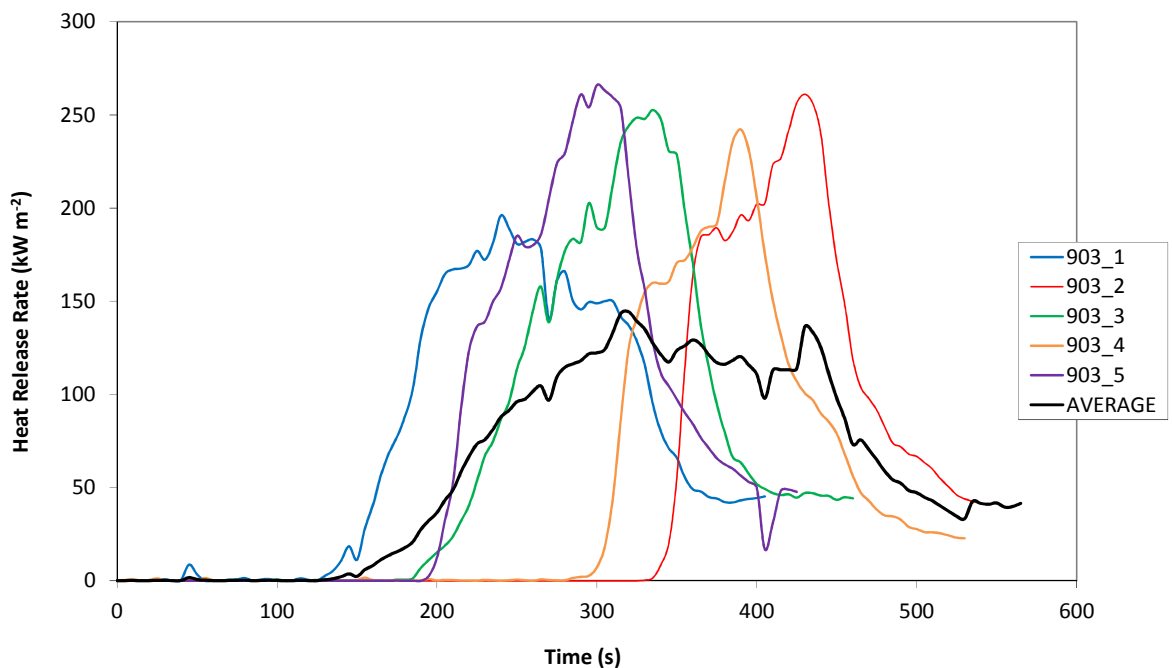


FIGURE 92. 450903 2.5 MM HEAT RELEASE RATE

Table 29 shows the data obtained from the cone calorimeter. There appears to be little or no correlation between the parameters t_{ig} and PHRR. The THR is around 28 MJ m^{-2} indicating that the same amount of sample was burned.

Sample	t_{ig} (s)	PHRR (kW m ⁻²)	tPHRR (s)	THR (MJ m ⁻²)
903 1	133	196.1	240	29.7
903 2	338	261.1	430	28.4
903 3	182	252.6	335	31.0
903 4	309	242.2	390	24.9
903 5	191	265.9	300	30.5
Average	230 (±88.2)	243.6 (±28.0)	339 (±75.5)	28.9 (±2.4)

TABLE 29. 450903 2.5 MM CONE CALORIMETER PROPERTIES

The averages of all experiments have been plotted in Figure 93 which shows a general overview of filled and unfilled PEEK materials and their heat release behaviour in the cone calorimeter. It is evident that filled PEEK materials generally give a longer time to ignition and a lower peak heat release rate which leads to a longer burn time. Interestingly, there are significant differences between the heat release curves of 450G and the 450G903 – the only difference is the presence of <0.5% carbon black pigment. Both samples ignite at around the same time but whereas 450G gives a sharp initial increase in heat release rate, the increase shown by 450G903 is steadier.

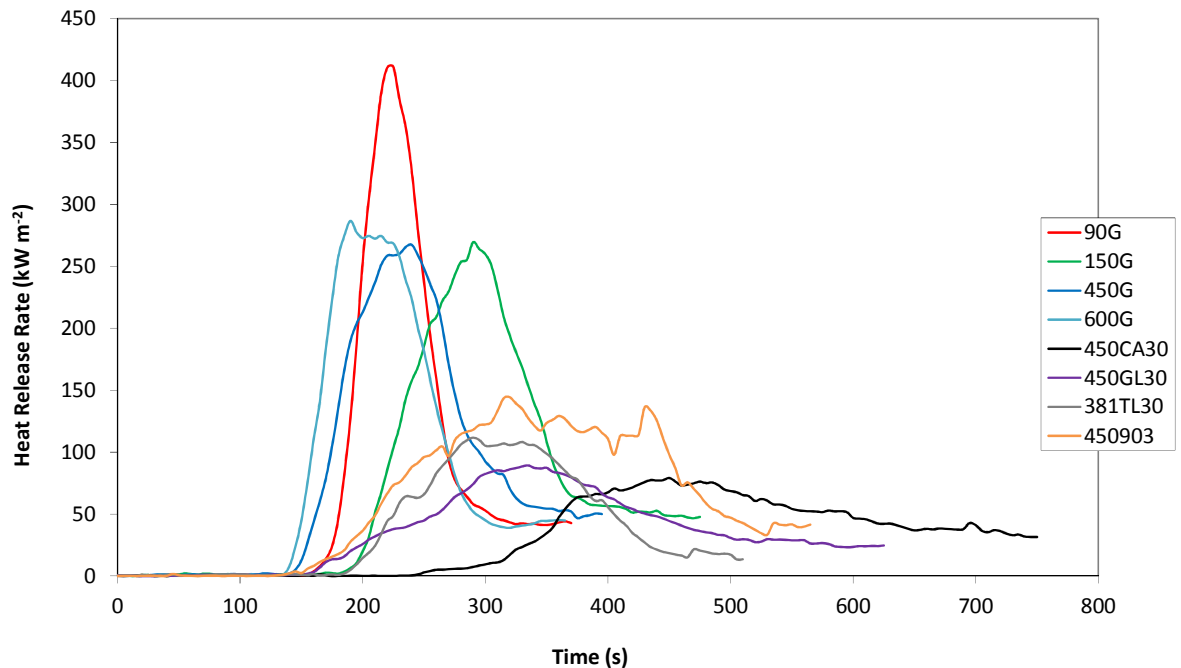


FIGURE 93. VISCOSITY AND ADDITIVES 2.5 MM AVERAGE HEAT RELEASE RATES

From these experiments it was determined that an effect other than the difference in time to ignition is causing significant amounts of scatter in the data. During these tests it was observed that samples were intumescent in the cone calorimeter. This intumescence may be the cause of scatter in the data in terms of peak heat release rate and time to peak heat release rate and therefore will be examined in the following section.

4.4.4.3 Char Heights Experiments

Experiments were conducted on the behaviour of PEEK as it intumesces in the cone calorimeter. In order to investigate the often large degree of scatter in the results, it was proposed that the height of the char may exert a strong influence on the burning behaviour. It was also proposed that there may be a correlation between the height of the char produced and the viscosity of the sample or the influence of presence of fillers.

Figure 94 shows the relationship between the char heights recorded for each sample (after they were removed from the cone calorimeter at the end of the test) against the peak heat release rate.

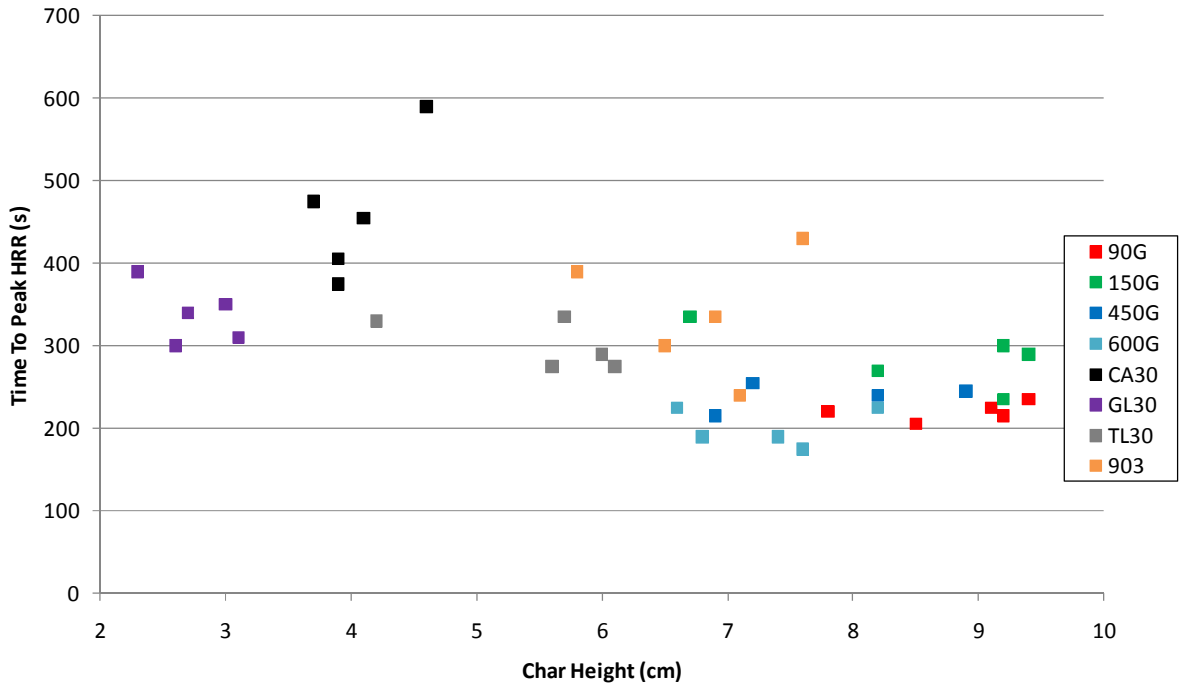


FIGURE 94. CHAR HEIGHT VS. PHRR CORRELATION

It is clear that there is little or no correlation between the char heights of the samples where viscosity is a variable. Conversely, there appears to be some grouping where the carbon and glass filled PEEK is concerned. The 450G903 samples show similar behaviour to the varied viscosity samples. The actual recorded heights can be seen in Table 30. The char heights for the unfilled samples are larger than those for the filled samples. It appears that the presence of filler is effective in reducing the intumescence of samples; this is more effectively achieved with the glass fibre samples, which reduce the height of intumescence from 8.0 cm to 2.7 cm, on average.

Sample	Run					Average (cm)
	1	2	3	4	5	
90G	9.4	9.2	7.8	8.5	9.1	8.8 (±0.7)
150G	9.4	9.2	8.2	9.2	6.7	8.5 (±1.1)
450G	7.2	8.2	6.9	8.6	8.9	8.0 (±0.9)
600G	8.2	6.6	6.8	7.4	7.6	7.3 (±0.6)
450CA30	3.7	3.9	4.1	3.9	4.6	4.0 (±0.3)
450GL30	2.3	2.6	3.1	3	2.7	2.7 (±0.3)
381TL30	5.7	4.2	6.1	5.6	6	5.5 (±0.8)
450903	7.1	7.6	6.9	5.8	6.5	6.8 (±0.7)

TABLE 30. CHAR HEIGHTS

In addition, the lower viscosity materials show a greater char height than the higher viscosity materials which may be due to the fact that in the melt, these materials have a higher flow rate. As intumescence occurs after the samples ignite, it would be expected that these materials have reached their melting temperatures. It is apparent from this data that both the time to ignition and height of the char may be playing a role in the scatter that is observed. There also appear to be other factors involved as the time to ignition and peak heat release do not correlate however, the peak heat release and height of the char show some correlation, as the height of the char increases, so does the peak of heat release as shown in Figure 95.

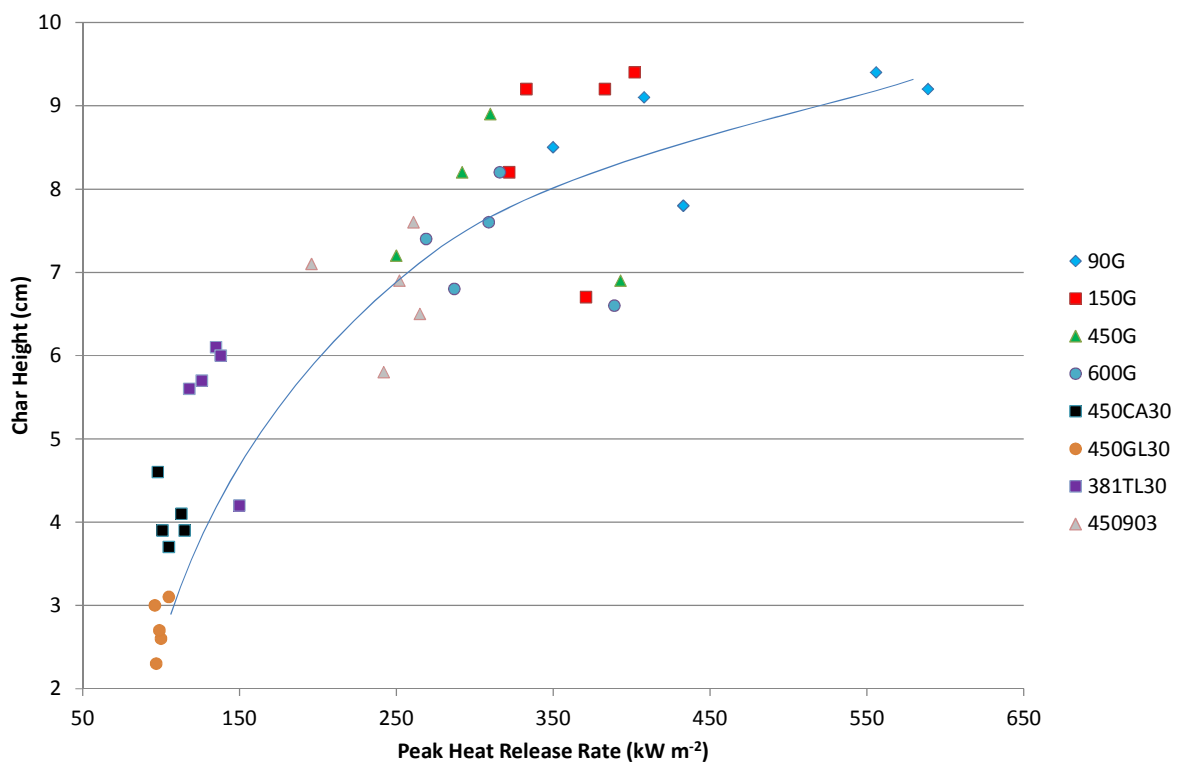


FIGURE 95. CORRELATION BETWEEN PHRR AND CHAR HEIGHT

4.4.5 Varied Heat Flux Experiments

Experiments were completed on varied heat fluxes within the cone calorimeter as a means of controlling or lessening the variation in data obtained. Increasing the external heat flux would ultimately decrease the material's time to ignition and increase its peak heat release rate. Therefore, if all samples ignited around or at the same time, there may be

similarities in the curves when overlaid. The critical heat flux for ignition of PEEK has been calculated as 27 kW m^{-2} and is quoted experimentally as between 30 and 40 kW m^{-2} [96]. This value was determined experimentally, as seen in Figure 96 and Figure 97. In Figure 96, samples were exposed to a 30 , 35 and 40 kW m^{-2} external heat flux as the predicted experimental critical heat flux for ignition was determined to be between these values. Samples were subjected to the heat flux for 10 minutes. If they ignited within 10 minutes, the time to ignition was recorded, if not, then 600 seconds was recorded. From this figure, it can be seen that the critical heat flux for ignition for 450G lies between 35 and 40 kW m^{-2} .

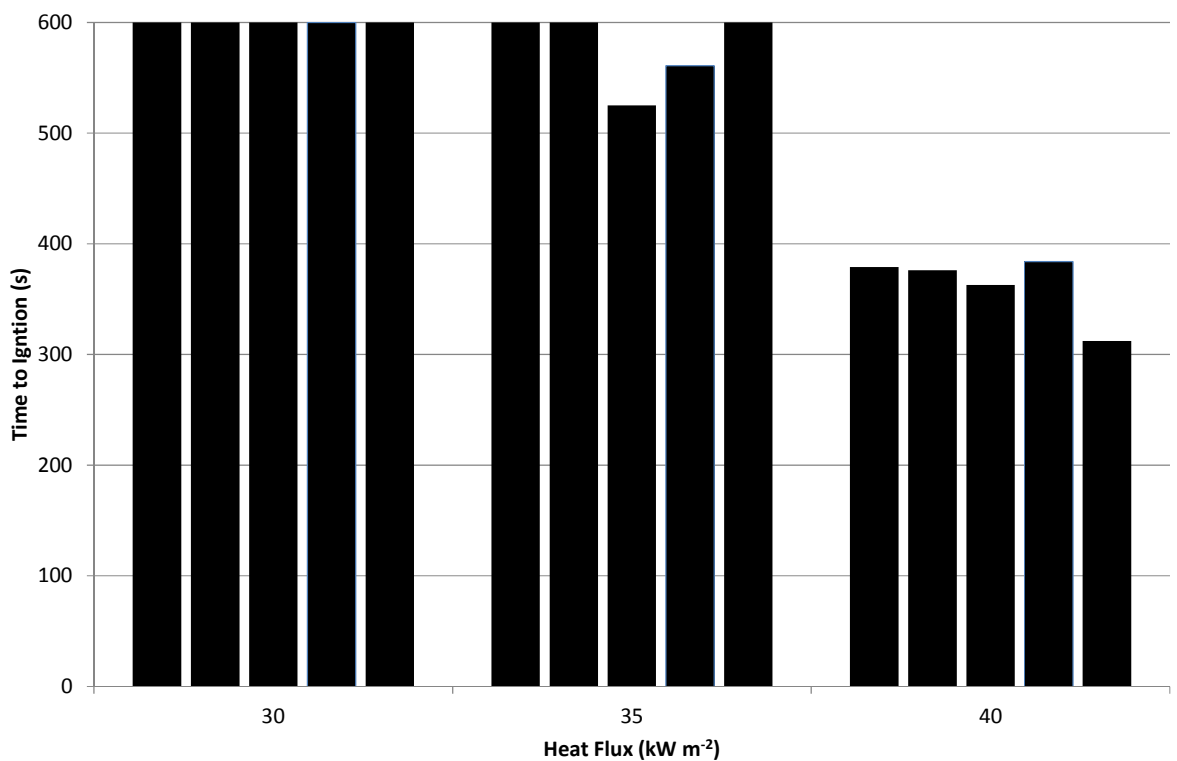


FIGURE 96. PEEK 450G CRITICAL HEAT FLUX FOR IGNITION 30-40 kW m^{-2}

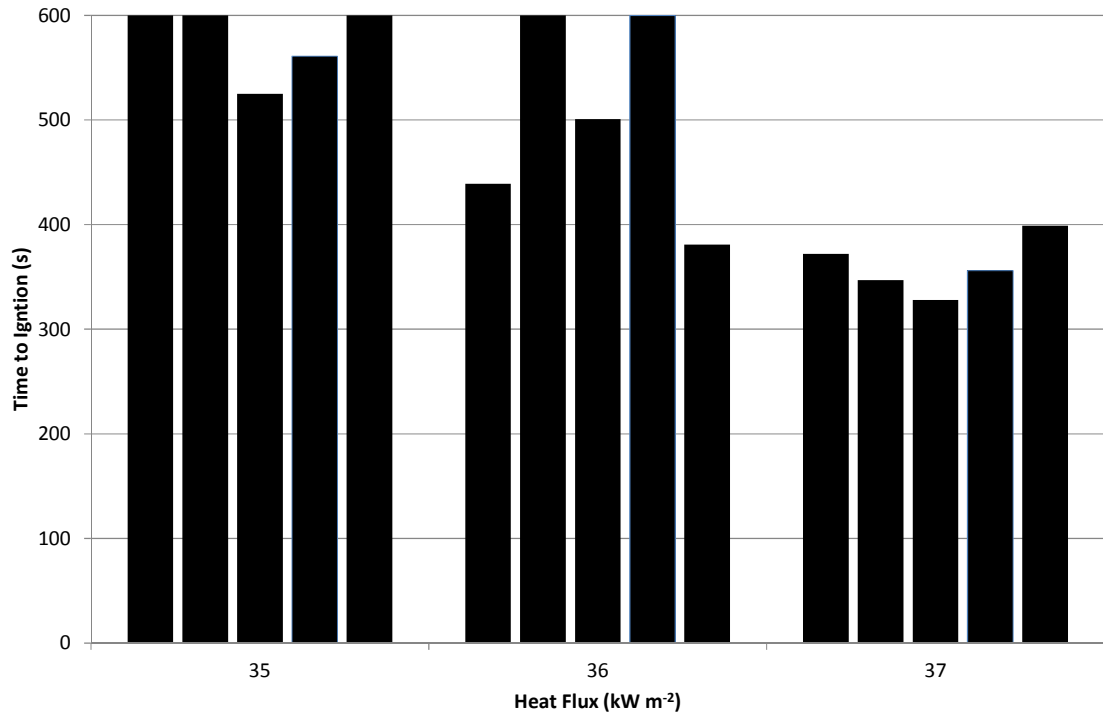


FIGURE 97. PEEK 450G CRITICAL HEAT FLUX FOR IGNITION 35-37 kW m⁻²

The range of heat fluxes was reduced to between 35 and 40 kW m⁻² as shown in Figure 97. Again the same approach was used. At 36 kW m⁻², two out of five samples did not ignite. At 37 kW m⁻² all samples ignited and so the critical heat flux for ignition of 450G is 36 kW m⁻². The lowest value for the varied heat flux samples was 45 kW m⁻² as it is accepted that samples tested in the cone calorimeter at up to 10 kW m⁻² above the critical heat flux for ignition will produce inconsistent data.

For the varied heat flux experiments, samples of 450G at 2.5 mm tested at heat fluxes varying from 45 kW m⁻² to 70 kW m⁻².

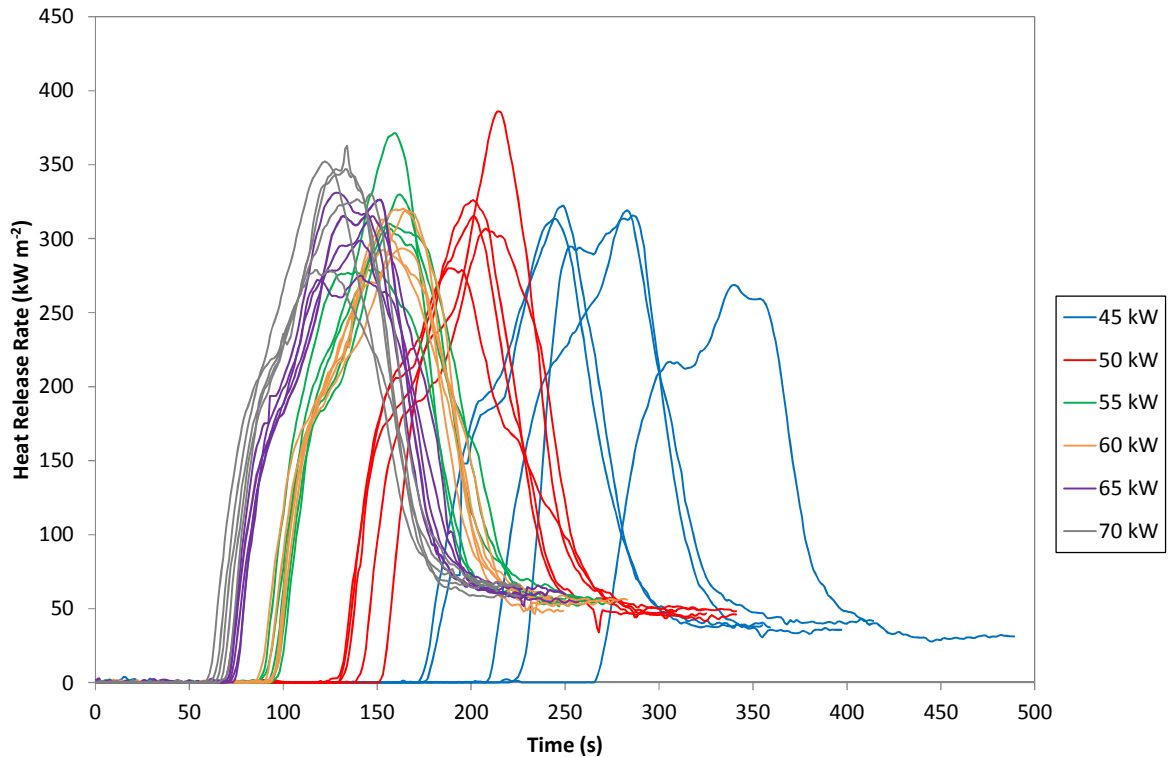


FIGURE 98. 450G 2.5 MM VARIED HEAT FLUX HEAT RELEASE RATES (GROUPED DATA)

These experiments have been grouped and plotted in Figure 98 to show the trends which exist as the external heat flux is increased. These values are also outlined in Table 31. As the external heat flux increases, it is apparent that the time to ignition decreases from 208 seconds for samples exposed to 45 kW m^{-2} to 64 seconds for those exposed to 70 kW m^{-2} . There is also an increase in the peak heat release rate as external heat flux increases; however, due to the presence of scatter, this is not as obvious. As expected, the time to peak heat release rate increases as the external heat flux increases, mirrored by the decrease in time to ignition.

Sample	t_{ig} (s)	PHRR (kW m^{-2})	tPHRR (s)	Char Yield (%)	THR (MJ m^{-2})
45 kW/m^2	208 (± 38)	307.9 (± 22)	281 (± 38)	45.2 (± 2)	25.4 (± 1)
50 kW/m^2	130 (± 4)	322.9 (± 39)	202 (± 10)	47.9 (± 3)	26.9 (± 1)
55 kW/m^2	92 (± 4)	319.6 (± 34)	156 (± 6)	48.5 (± 2)	27.2 (± 1)
60 kW/m^2	91 (± 3)	307.7 (± 14)	160 (± 7)	44.6 (± 2)	26.7 (± 1)
65 kW/m^2	72 (± 3)	309.3 (± 23)	142 (± 8)	43.4 (± 2)	27.5 (± 1)
70 kW/m^2	64 (± 4)	334.3 (± 33)	132 (± 10)	43.2 (± 2)	27.8 (± 1)

TABLE 31. 450G 2.5 MM VARIED HEAT FLUXES CONE CALORIMETER PROPERTIES

4.4.6 Conditioned Experiments

Samples of PEEK were conditioned in an oven to look at the effect this had on the heat release rate in the cone calorimeter.

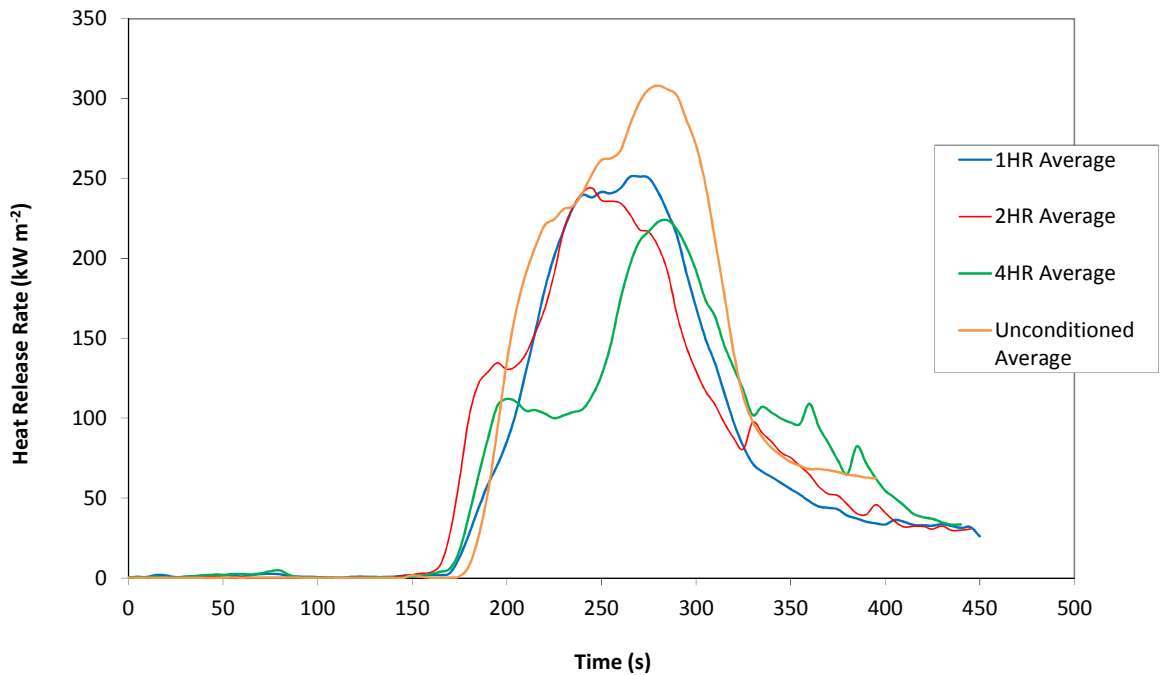


FIGURE 99. 450G 2.5 MM CONDITIONED PLAQUES – AVERAGE HEAT RELEASE RATES

Samples were heated at 400°C for 1, 2 and 4 hours. Figure 99 shows the average heat release rate curves of the conditioned cone calorimeter samples. The samples which had been conditioned for 1 hour show behaviour similar to a 450G unconditioned samples although a lower peak heat release rate is observed. The samples conditioned for 2 hours show a rapid increase in heat release rate followed by a slight shoulder which appears at 125 kW m⁻². This is emphasised by the samples conditioned for 4 hours where the size of the shoulder increases.

After burning, all samples show a rapid decrease in heat release rate up to 330 seconds where the rates of decreasing heat release rate change. Samples which have been conditioned for 4 hours show a more gradual decrease than samples which have been conditioned for 1 hour. In addition, the samples which have not been conditioned show a rapid decrease in heat release rate up to 330 seconds and then show a steady rate at around 60 kW m⁻². The average results for these experiments are shown in Table 32. The average time to ignition is not shown to

increase or decrease with conditioning time. The peak of heat release is higher for samples which have been conditioned for 1 hour although there is a lot of scatter in the data. Interestingly, the total heat released decreases with increased conditioning indicating that degradation of the samples may be occurring during this conditioning period. This is further emphasised by the large shoulder which is present after ignition, as shown in Figure 99. In addition, conditioning the samples has no effect on the amount of scatter present in the data.

Sample	t_{ig} (s)	PHRR (kW m ⁻²)	tPHRR (s)	Char Yield (%)	THR (MJ m ⁻²)
1 Hour	183 (±21)	269.3 (±6.2)	270 (±22.9)	47.9 (±4.1)	30.3 (±2.6)
2 Hours	180 (±26)	245.6 (±25.5)	247 (±7)	45.3 (± 1.4)	29.1 (±0.1)
4 Hours	180 (± 33)	233.0 (±21.0)	303 (± 28)	47.3 (±2.0)	26.7 (±0.3)

TABLE 32. AVERAGE PROPERTIES FOR 2.5 MM CONDITIONED SAMPLES

4.4.7 0.5% Carbon Black (CB) Pigment Experiments

As evidenced from the experiments on scatter, the presence of 0.5% carbon black (CB) had a great effect on reducing the flammability of samples tested in the cone calorimeter, albeit only being used commercially as a pigment to change the colour of the polymer from natural to black. The carbon black also increases the scatter of samples in the cone calorimeter. As a means of investigating the effect of carbon black further, lower viscosity samples (150G) were supplied filled with 0.5% CB to determine whether this effect was dependent on viscosity and the extent to which the presence of 0.5% CB reduced the flammability.

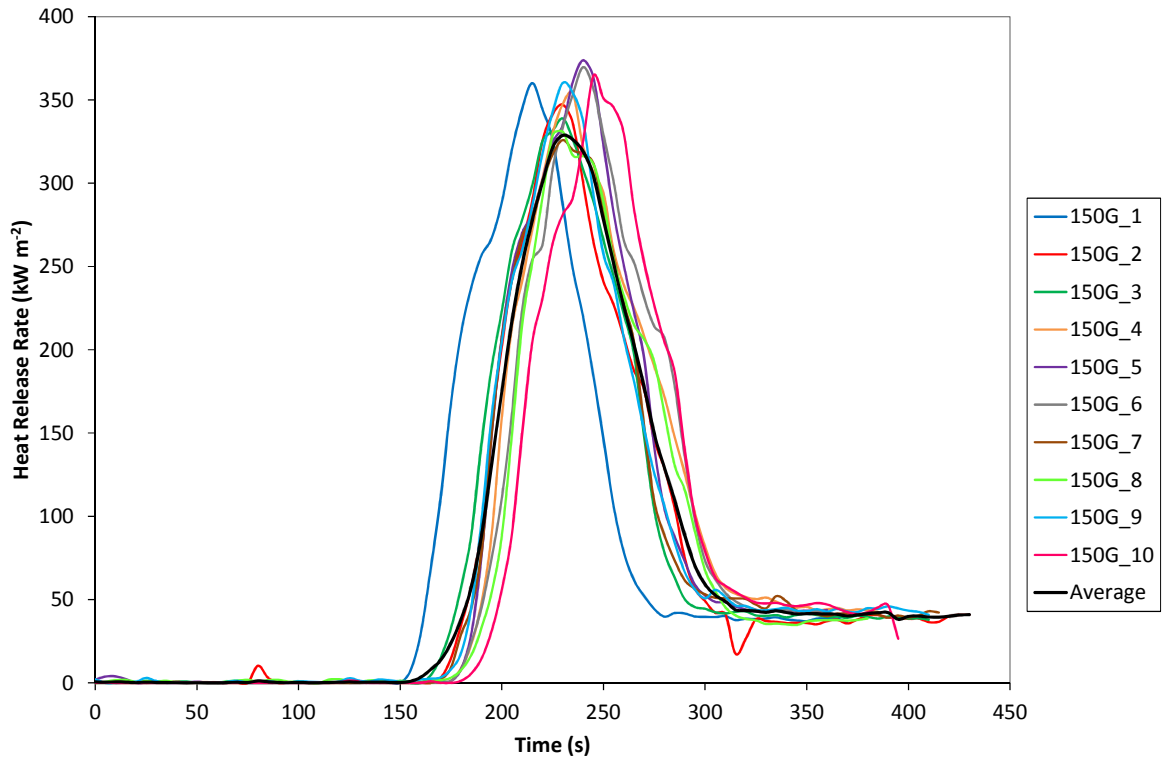


FIGURE 100. 150G 2.5 MM HEAT RELEASE RATE

Figure 100 shows the heat release rate curves for 150G. Although samples of 2.5 mm 150G samples have been shown previously (Figure 70) these samples are of the same batch with regards to the 0.5% CB samples. There is some variation in the samples times to ignition with an average time to ignition ranging from 150 seconds to 180 seconds. All samples ignite with a steady increase in heat release rate to around 350 kW m⁻². The heat release rate then decreases steadily to around 50 kW m⁻² at 300 seconds.

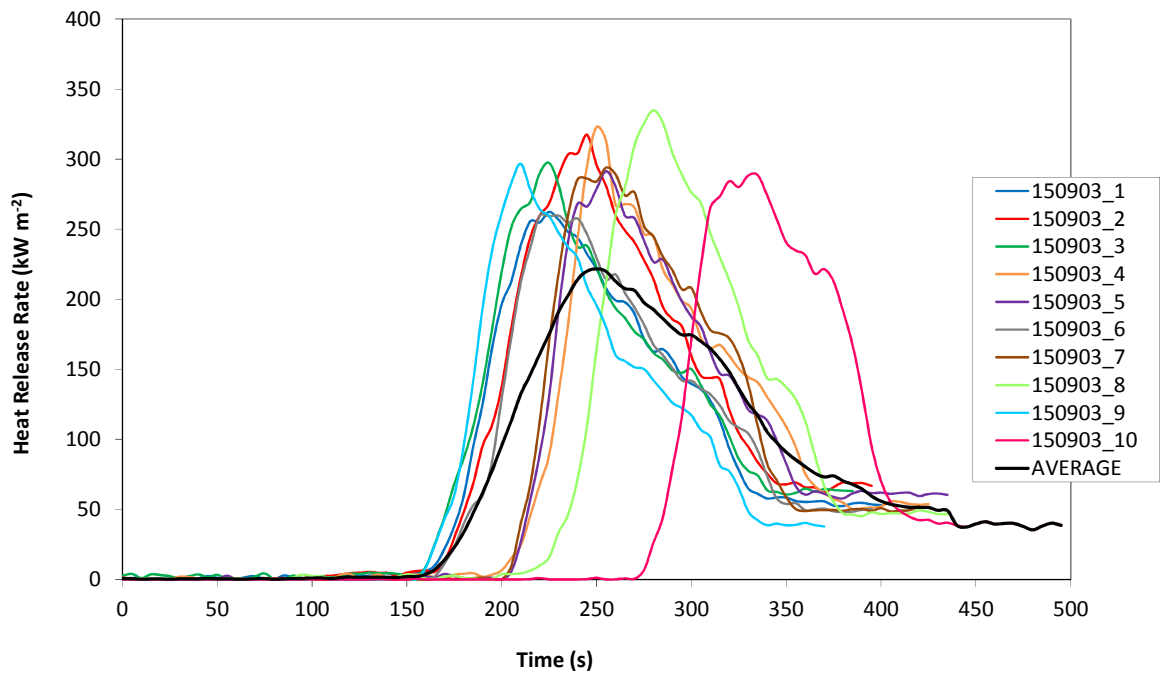


FIGURE 101. 150903 2.5 MM HEAT RELEASE RATE

Figure 101 shows the heat release rate curves for 150G filled with 0.5% CB (150903). There is variation in the samples times to ignition with an average time to ignition ranging from 150 seconds to 275 seconds. All samples ignite with a steady increase in heat release rate to around 300 kW m⁻². The heat release rate then decreases steadily to around 50 kW m⁻² at 300 seconds. Compared to the 150G samples shown previously, there is a lot more scatter in this data, as observed in previous experiments. The flammability of these samples also changes, the 150G samples show thermally thin burning. With the addition of 0.5% CB, after the peak of heat release rate, the 150903 samples show a steady decrease in heat release.

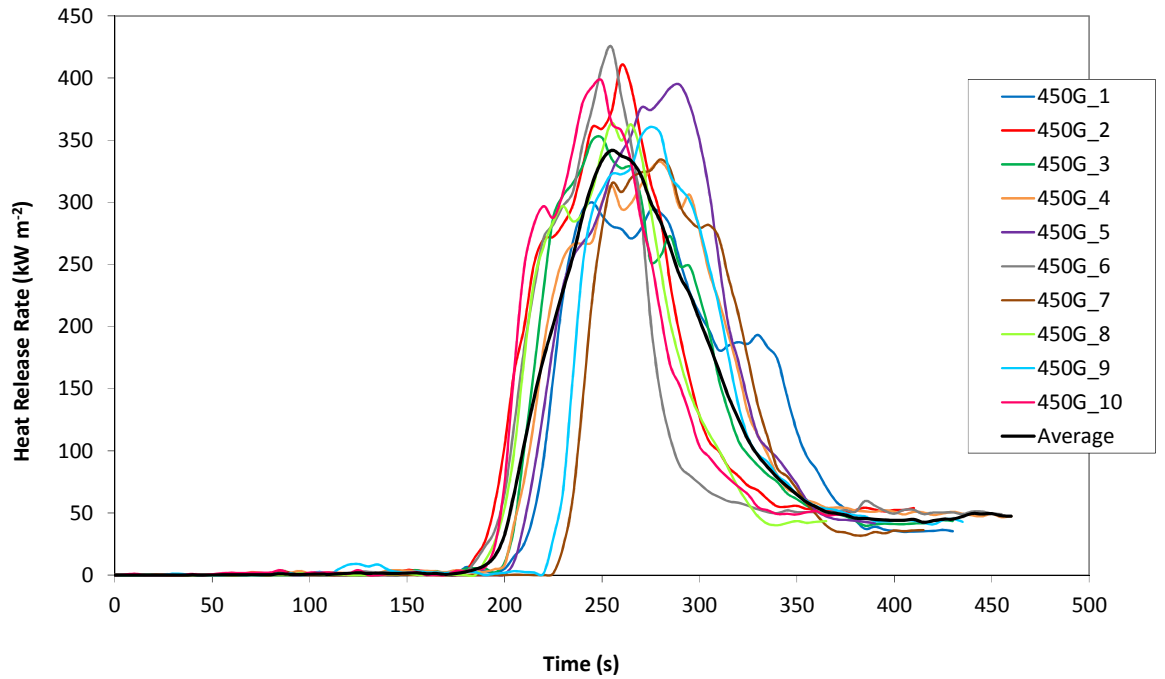


FIGURE 102. 450G 2.5 MM HEAT RELEASE RATE

Figure 102 shows the heat release rate curves for 450G. Again, there is variation in the samples times to ignition with an average time to ignition ranging from 180 seconds to 225 seconds. All samples ignite with a steady increase in heat release rate to around 350 kW m⁻². The heat release rate then decreases steadily to around 50 kW m⁻² at 350 seconds.

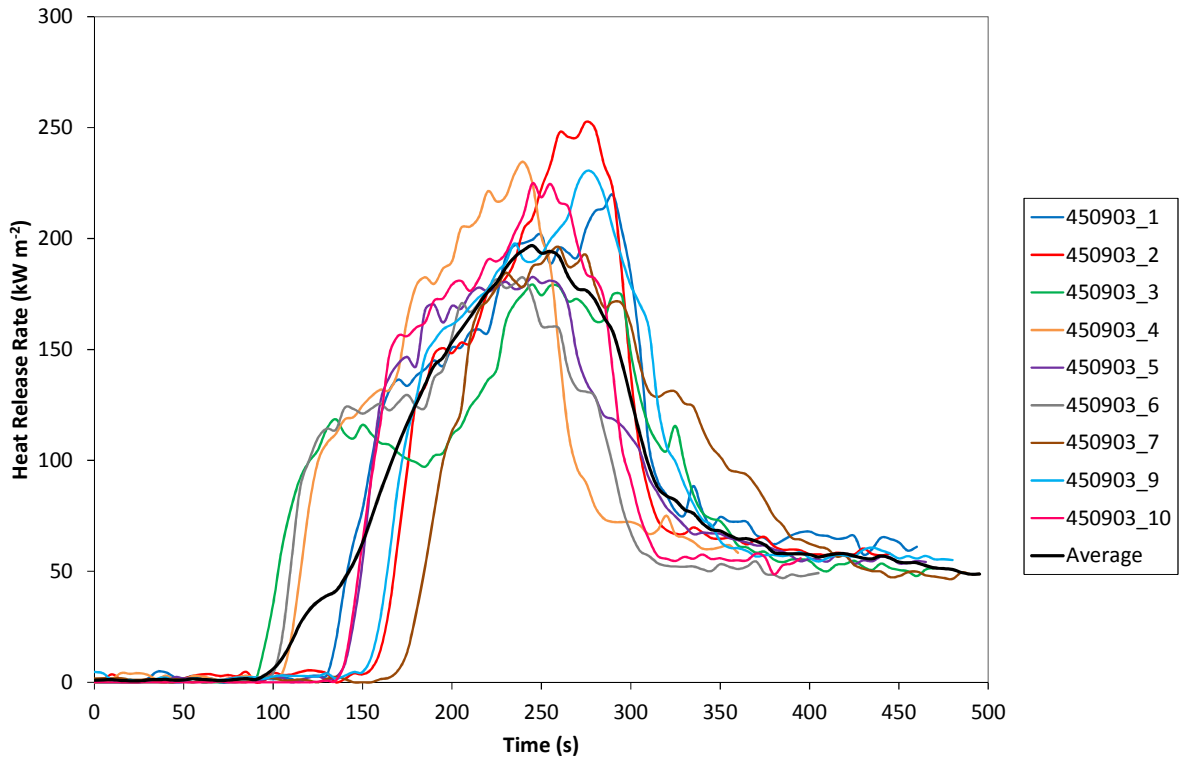


FIGURE 103. 450903 2.5 MM HEAT RELEASE RATE

Figure 103 shows the heat release rate curves for 450G filled with 0.5% CB (450903). Again, there is a large variation in the samples times to ignition with an average time to ignition ranging from 90 seconds to 160 seconds. All samples ignite with a steady increase in heat release rate to around 125 kW m⁻² where there is a shoulder present. The heat release rate increases steadily again to around 250 kW m⁻². The heat release rate then decreases steadily to around 50 kW m⁻² at 350 seconds. These samples vary with the 450G in terms of flammability. The presence of 0.5% CB appears to reduce the time to ignition causing an initial shoulder and more gradual increase to the peak heat release rate.

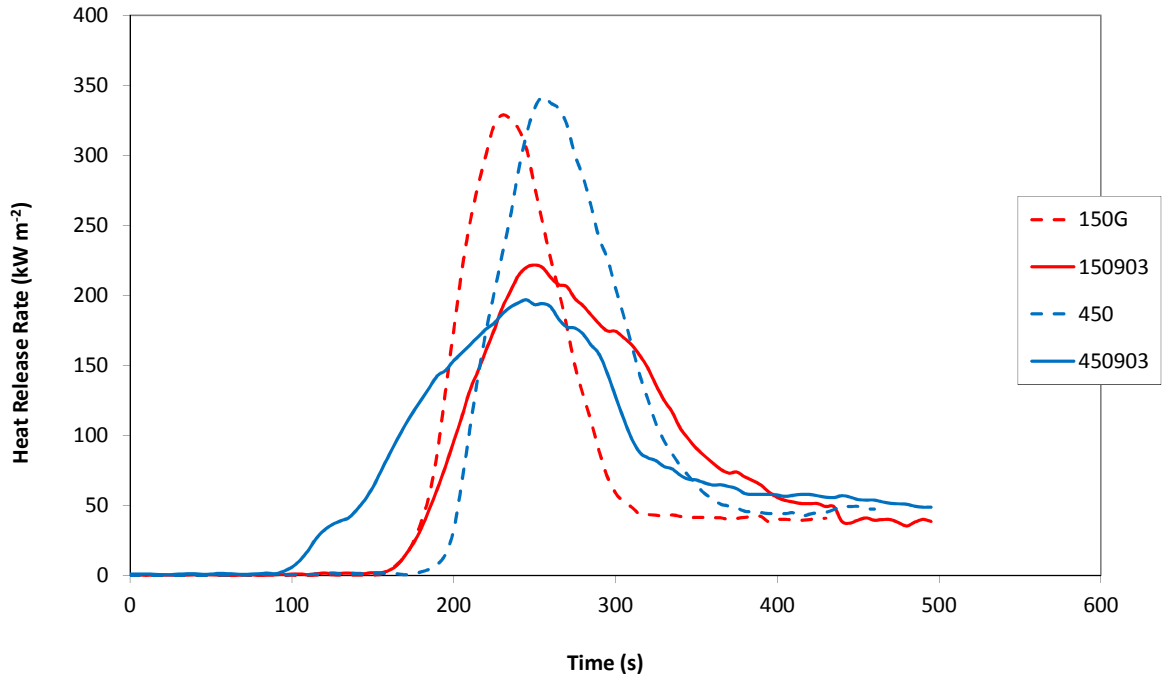


FIGURE 104. 150G, 150903 450G AND 450903 2.5 MM HEAT RELEASE RATE AVERAGES

The average curve for 150903 has been plotted against the average curves for 150G, 450G and 450903. These curves are shown in Figure 104, values from which are outlined in Table 33. As is evident from Figure 104, the presence of 0.5% CB in both 150G and 450G appears to reduce the peak of heat release by around 100 kW m^{-2} . It is difficult to come to this conclusion, as the presence of 0.5% CB creates more scatter in the data. Table 33 shows the extent of the scatter and numerically the difference between samples with and without small amounts of CB. The peak heat release rate for 150G samples drops from around 321.9 kW m^{-2} to 220.9 kW m^{-2} , with the addition of CB. Similarly, the values for 450G drop from 333.3 kW m^{-2} to 196.1 kW m^{-2} .

Sample	t_{ig} (s)	PHRR (kW m^{-2})	tPHRR (s)	THR (MJ m^{-2})
150G	171 (± 9)	321.9 (± 16)	232 (± 8)	28.6 (± 1)
150903	192 (± 37)	220.9 (± 24)	252 (± 36)	31.2 (± 2)
450G	199 (± 17)	333.4 (± 35)	265 (± 15)	36.2 (± 1)
450903	133 (± 25)	196.1 (± 27)	257 (± 9)	34.8 (± 3)

TABLE 33. 150G AND 450G CB PIGMENT CONE CALORIMETER PROPERTIES

There appears to be no correlation between the two viscosities of PEEK with regards to time to ignition. The presence of CB, albeit at 0.5% changes the colour of the samples from natural to black. In the 150G samples, the presence of CB increases the time to ignition of the sample, as would be expected due to the presence of carbon increasing a material's thermal conductivity. This is not true for the 450G samples where the presence of CB decreases the materials time to ignition. The thermal conductivity of the unfilled 450G is 0.25 W/m K which increases to 0.29 W/m K with the addition of 0.5% CB.

4.4.8 Presence of 0.1, 0.5 and 1 % CB Experiments

Continuing from the previous section, experiments were completed on samples with varying amounts of CB to determine whether it was the amount of CB present or merely the presence that was having an effect on the flammability.

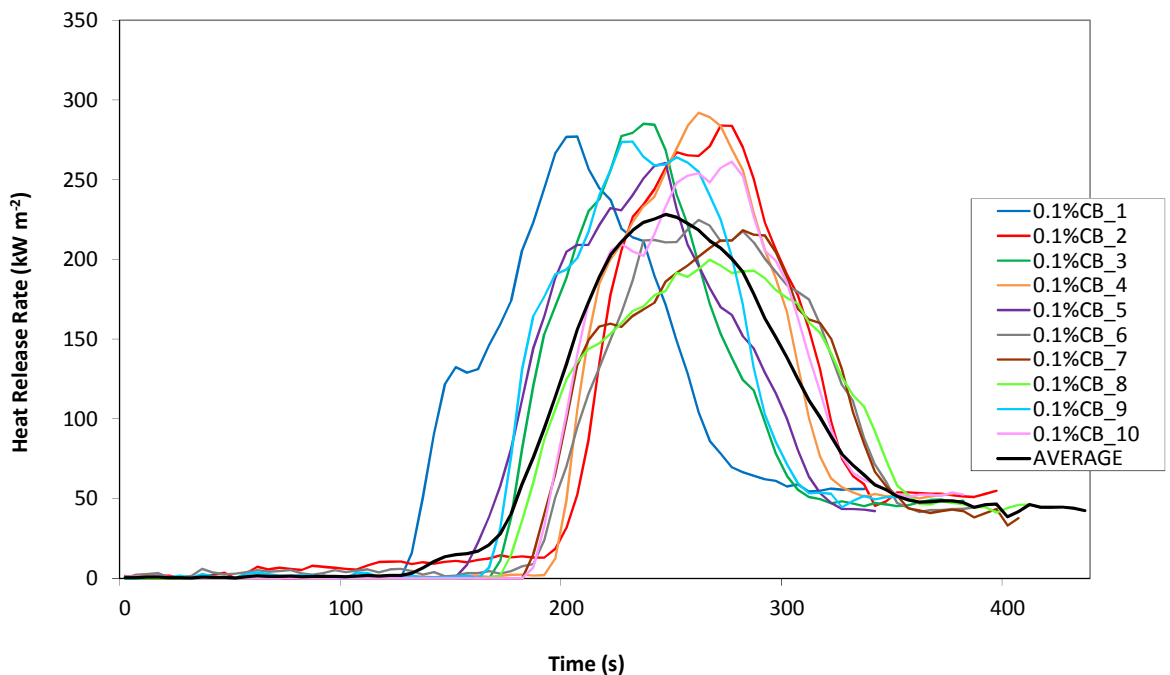


FIGURE 105. 450G 2.5 MM WITH 0.1 % CB HEAT RELEASE RATE

Samples with 0.1% CB were examined, the results of which are shown in Figure 105. As expected from previous experiments, there is a lot of scatter present in the data, with the time

to ignition ranging from 125 seconds to 200 seconds. The average peak heat release rate lies at around 250 kW m^{-2} and the heat release rate decreases to around 50 kW m^{-2} at around 350 seconds.

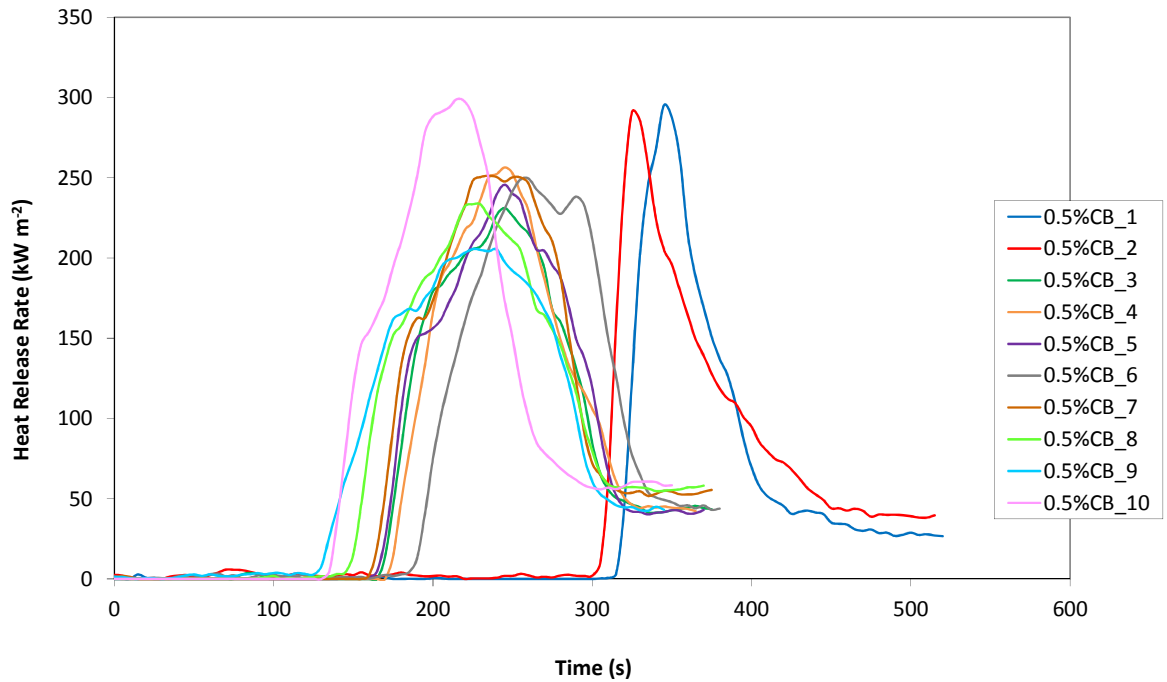


FIGURE 106. 450G 2.5 MM WITH 0.5% CB HEAT RELEASE RATE

Samples with 0.5% CB were examined, the results of which are shown in Figure 106. There is some scatter present in the data with two samples igniting much later than others at around 300 seconds. For the remainder of the samples, the time to ignition ranges from 120 seconds to 190 seconds. The average peak heat release rate lies at around 250 kW m^{-2} and the heat release rate decreases to around 50 kW m^{-2} at around 300 seconds.

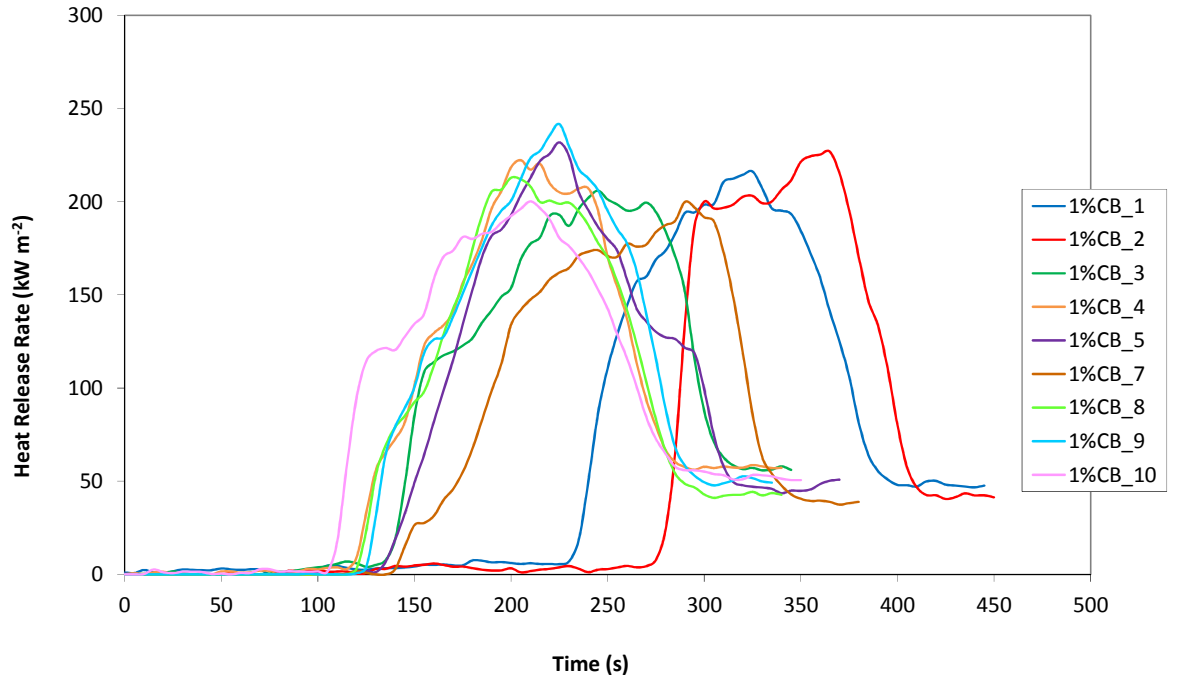


FIGURE 107. 450G 2.5 MM WITH 1% CB HEAT RELEASE RATE

Samples with 1% CB were examined, the results of which are shown in Figure 107. There is a lot of scatter present in the data and the time to ignition ranges from 100 seconds to 270 seconds. The average peak heat release rate lies at around 200 kW m⁻² and the heat release rate decreases to around 50 kW m⁻² at around 350 seconds.

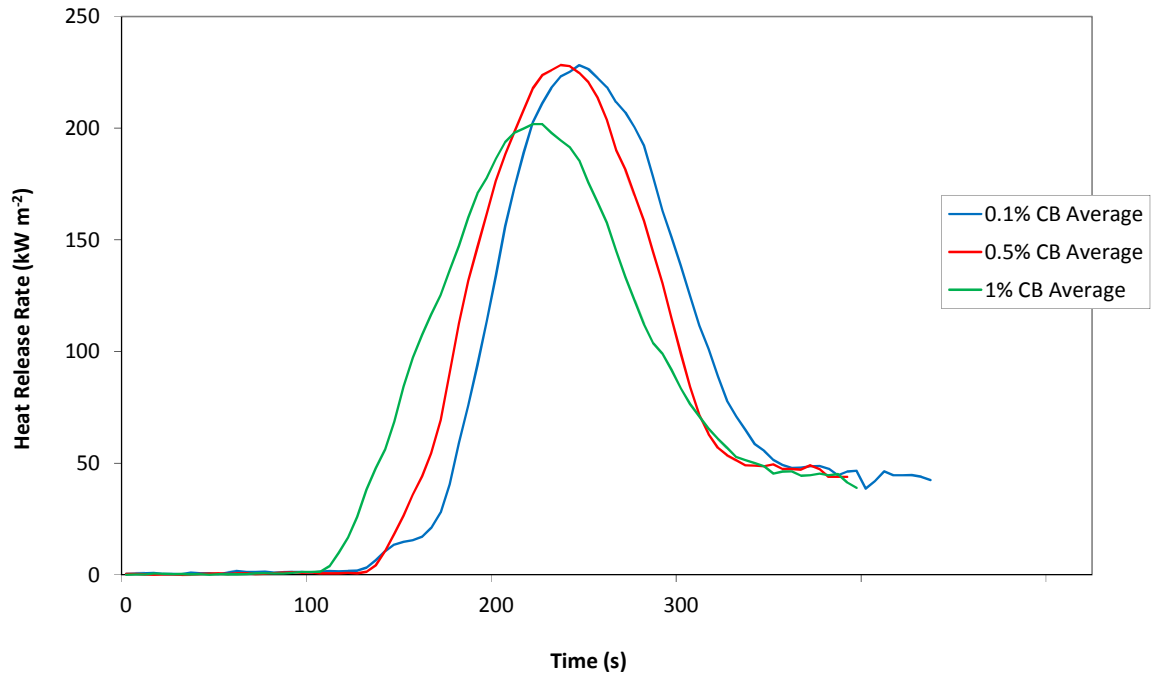


FIGURE 108. 450G 2.5 MM VARIED CB EXPERIMENTS AVERAGE HEAT RELEASE RATES

The average heat release rates of the three CB filled samples are shown in Figure 108, with results outlined in Table 34. Due to amount of scatter in the data, it is difficult to determine a hierarchy in terms of time to ignition and peak heat release rate although it seems that as the amount of CB increases, the scatter in the time to ignition also increases. As would be expected, the char yield increases with increasing CB content. In addition the time to reach the peak of heat release also increases with increasing CB content, possibly due to the presence of the shoulder which occurs after the initial ignition peak.

Sample	t_{ig} (s)	PHRR (kW m^{-1})	t_{PHRR} (s)	Char Yield (%)
0% CB	199 (± 17)	333.4 (± 35)	265 (± 15)	46.2 (± 1)
0.1% CB	174 (± 19)	256.8 (± 32)	251 (± 22)	46.1 (± 2)
0.5% CB	191 (± 68)	255.4 (± 31)	258 (± 43)	48.9 (± 2)
1% CB	157 (± 58)	217.5 (± 14)	254 (± 59)	47.4 (± 2)

TABLE 34. 450G VARIED CB PIGMENT CONE CALORIMETER PROPERTIES

4.4.9 Presence of 0.5% Filler Experiments

To determine whether other fillers incorporated at 0.5% would aid in reducing the flammability of PEEK, ketjan black (KJBLK) and zeospheres (ZS) were examined. Ketjan black is another pigment utilised for colouring purposes and zeospheres are inert, ceramic-based fillers incorporated for hardness and durability.

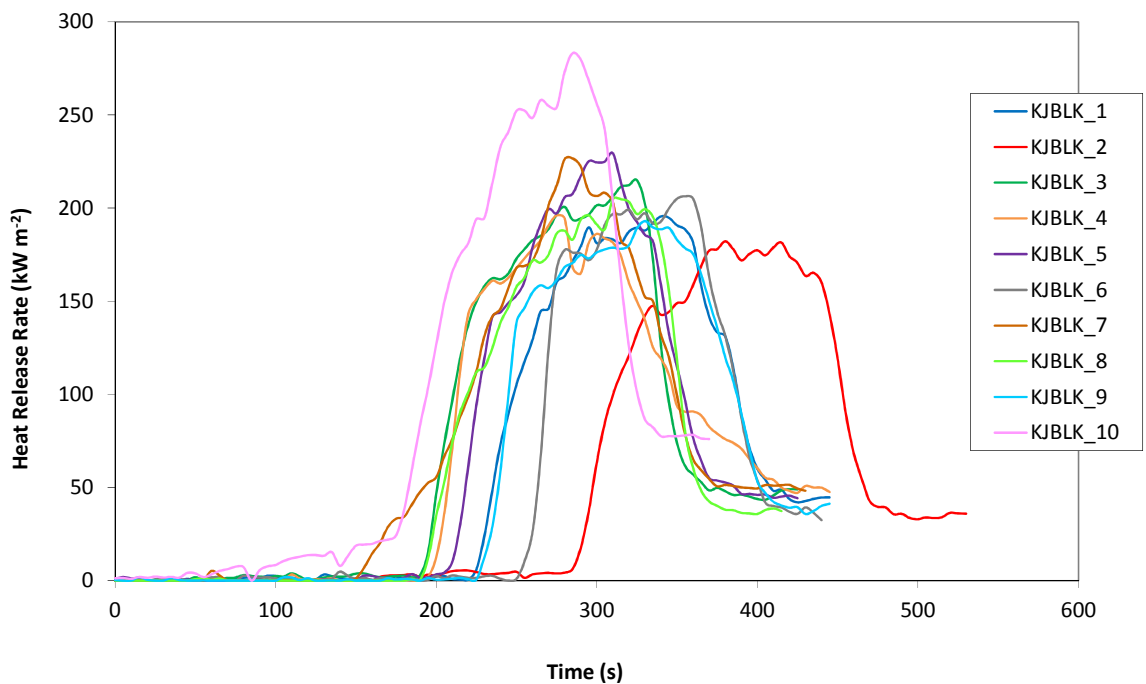


FIGURE 109. 450G 2.5 MM WITH 0.5% KETJAN BLACK

Samples with 0.5% ketjan black were investigated. The results are shown in Figure 109. The presence of ketjan black also increases the scatter present in the data. The time to ignition ranges from 150 seconds to 290 seconds. The peak of heat release rate varies with time to ignition – an earlier time to ignition gives a higher peak heat release rate. Samples decrease in heat release rate to 50 kW m⁻² at around 400 seconds.

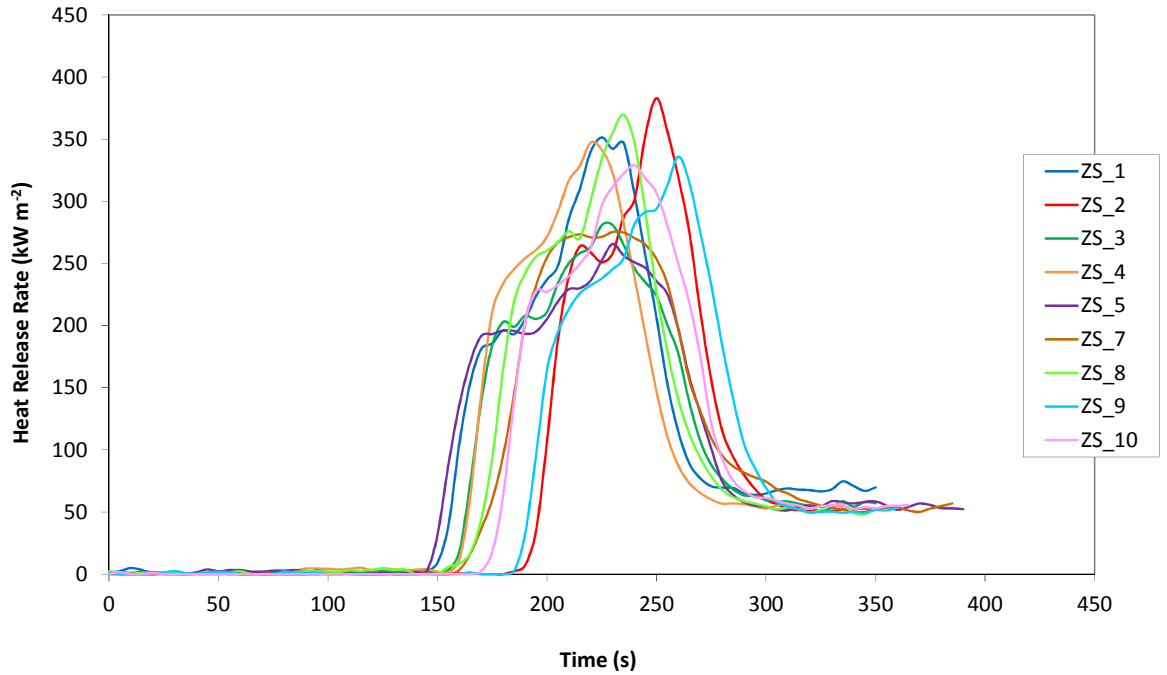


FIGURE 110. 450G 2.5 MM WITH 0.5% ZEOSPHERES

Samples with 0.5% zeospheres were investigated. The results are shown in Figure 110. The presence of zeospheres does not scatter the data as much. The time to ignition ranges from 150 seconds to 190 seconds. There is a rapid increase in heat release rate to a shoulder around 200 kW m⁻². The heat release then increases more steadily to a peak of heat release rate around 350 kW m⁻². Samples decrease in heat release rate to 50 kW m⁻² at around 290 seconds.

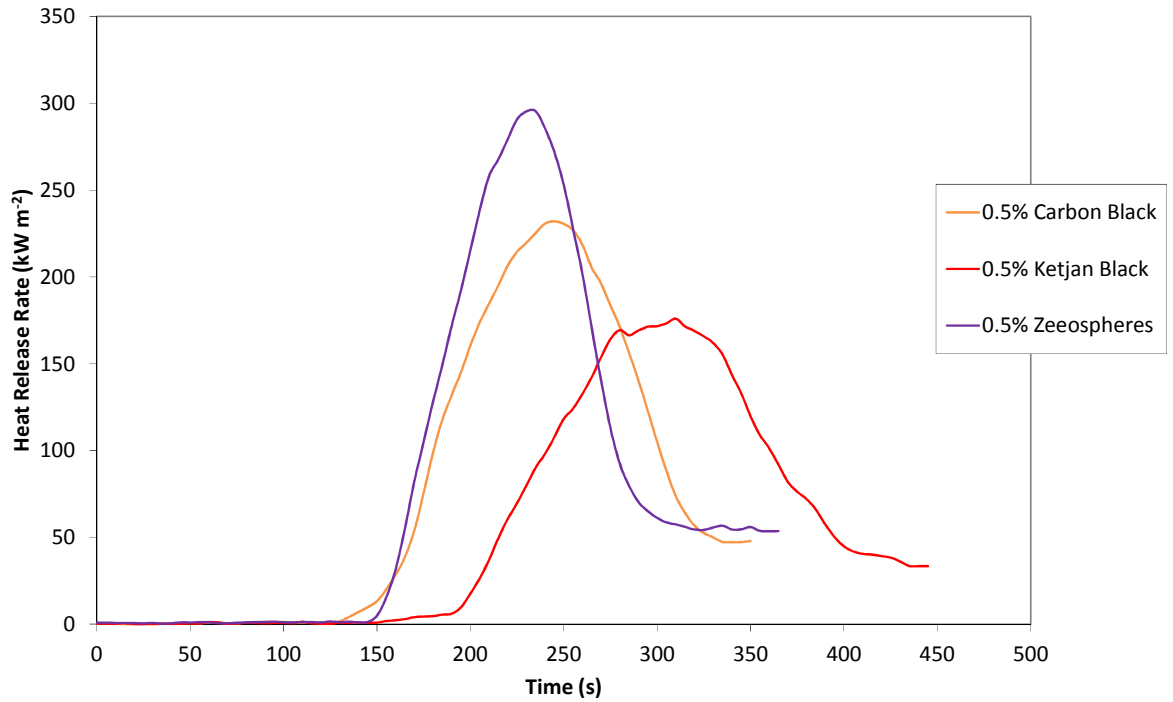


FIGURE 111. 450G 2.5 MM 0.5% FILLER EXPERIMENTS AVERAGE HEAT RELEASE RATES

The averages of the 0.5% filler experiments are plotted in Figure 111 and outlined in Table 35. The presence of zeeospheres decreases the time to ignition compared to the samples filled with black pigment. This would be as expected due to the difference in colour of these materials. Zeeospheres also increase the peak heat release rate from 255 kW m⁻² for 0.5% CB and 213 kW/m⁻² for 0.5% KJBLK to 317 kW m⁻². This value is similar to 333 kW m⁻², that which is quoted for 450G in Table 33. The presence of zeeospheres reduces the scatter in the data with regards to time to ignition.

Sample	t _{ig} (s)	PHRR (kW m ⁻²)	tPHRR (s)	Char (%)
450G	199 (±17)	333.4 (±35)	265 (±15)	46.2 (±1)
0.5% CB	191 (±68)	255.4 (±31)	258 (±43)	48.9 (±2)
0.5% KJBLK	214 (±39)	213.0 (±29)	320 (±33)	45.7 (±3)
0.5% ZS	167 (±16)	316.8 (±44)	232 (±15)	44.7 (±2)

TABLE 35. 450G 0.5% FILLER CONE CALORIMETER PROPERTIES

From this section, it can be assumed that the presence of carbon black (either CB or KLBLK) increases the scatter in the data with regards to time to ignition. However, the presence of carbon black is reducing the peak of heat release rate of the unfilled polymer from around 330

kW m^{-2} to 250 kW m^{-2} for 0.5% CB. It is interesting to note that the addition of fillers that subsequently change the colour of PEEK from natural to black increase the scatter in the time to ignition compared to those which do not discolour the unfilled material. This can be seen more clearly in Table 36 whereby the standard deviation for the time to ignition increases by more than four times for the 450CA30 (black) compared to the 450G (natural).

Sample	t_{ig} (s)
450G	199 (± 17)
450CA30	287 (± 78)
450903 (0.5%)	191 (± 68)
450903 (1%)	157 (± 58)

TABLE 36. EFFECT OF BLACK SAMPLES ON t_{ig} SCATTER

4.4.10 Surface Moisture Experiments

Experiments were completed on the effect of moisture on the flammability of PEEK. The presence of moisture on the surface may be causing the scatter in the time to ignition, seen in the cone calorimeter. In a previous section, it was detailed that the presence of moisture had a detrimental effect on UL-94 ratings – causing flames to spread faster up the sample. For this experiment, samples were ‘wetted’ by placing in a 12°C water bath for 120 hours. Samples which were ‘dry’ were placed in a 100°C oven for the same period of time. The absorption of moisture on samples in terms of mass gained or lost is shown in Table 37. On average, samples placed in the wet condition gained 0.1% in mass, while samples placed in the dry condition lost 0.2%; overall there is a 0.3% difference between samples which are wet and samples which are dry. The difference in these numbers indicates that there was moisture present in these samples ‘as received’.

450G Wet	Difference (%)
1	+0.1223
2	+0.1092
3	+0.0819
4	+0.1018
Average	+0.1038
Standard Deviation	0.0169
450G Dry	Difference (%)
1	-0.1926
2	-0.2011
3	-0.2055
4	-0.1647
Average	-0.1910
Standard Deviation	0.0183

TABLE 37. 450G 2.5 MM 'WET' AND 'DRY' SAMPLE GAINS AND LOSSES

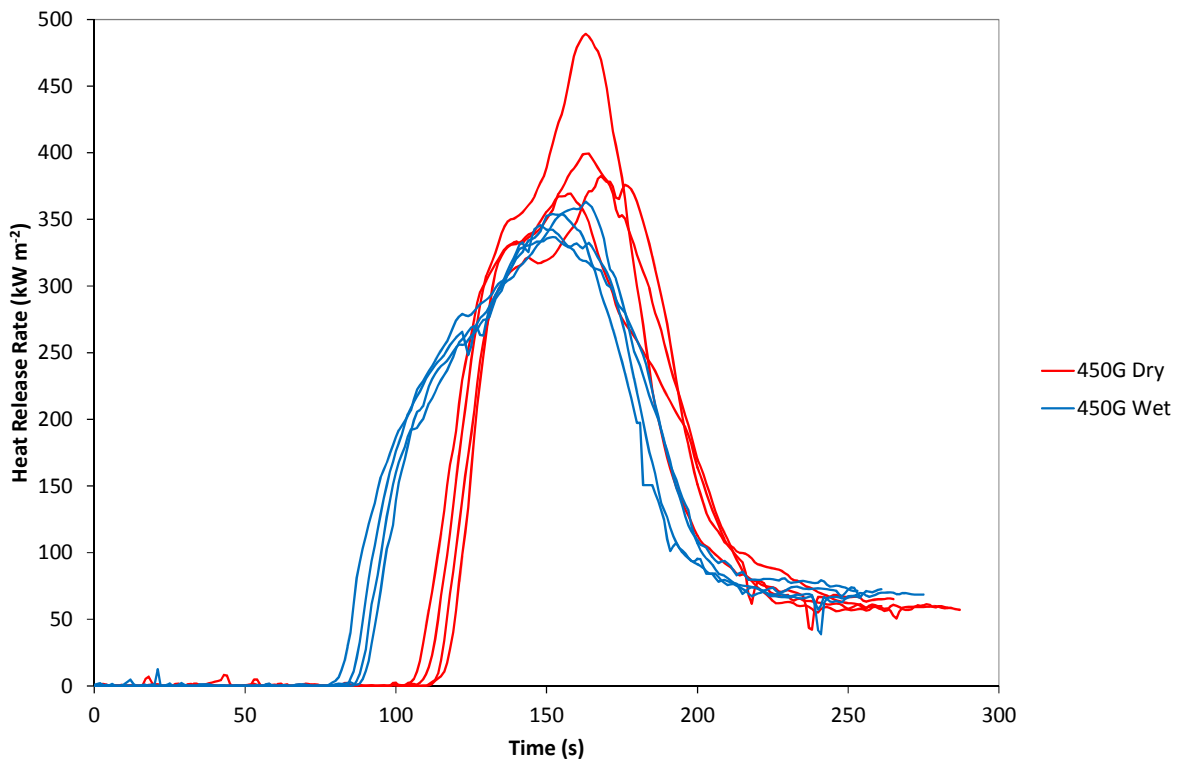


FIGURE 112. 450G 2.5 MM 'WET' AND 'DRY' CONDITION HEAT RELEASE RATES COMPARISON AT 60 kW m⁻²

Samples were burned in the cone calorimeter at 60 kW m⁻² to minimise scatter close to the critical heat flux for ignition – the results of this are shown in Figure 112 and outlined in

Table 38. Wet samples ignite at around 80 seconds and there appears to be very little scatter in the data. There is a steady increase in heat release rate to around 250 kW m⁻² where there appears to be a shoulder present. The heat release rate increases further to a peak heat release rate of around 350 kW m⁻². Heat release rate then begins to decrease to 60 kW m⁻² at around 225 seconds. Total heat released remains constant, at around 31 MJ m⁻².

Sample	t _{ig} (s)	PHRR (kW m ⁻²)	tPHRR (s)	Char (%)	THR (MJ m ⁻²)
Wet_1	81	353.9	115	46.7	x
Wet_2	86	363.3	163	44.7	31.8
Wet_3	83	345.6	148	45.9	30.8
Wet_4	88	336.8	152	41.7	32.2
Average	85 (±3)	349.9 (±11.4)	155 (±6)	44.0 (±2.4)	31.6 (±0.7)
Dry_1	111	399.4	164	45.9	30.6
Dry_2	111	382.7	168	42.3	31.2
Dry_3	108	489.2	163	44.4	31.5
Dry_4	102	369.3	158	49.8	29.5
Average	108 (±4)	410.1 (±54.1)	163 (±4)	45.1 (±3.7)	30.7 (±0.9)

TABLE 38. 450G 2.5 MM 'WET' AND 'DRY' CONE CALORIMETER PROPERTIES

Dry samples ignite at around 110 seconds and there is a steady increase in the heat release rate up to the peak at around 410 kW m⁻². Heat release rate decreases to 60 kW m⁻² at 250 seconds. The char yield remains at around 45% and the total heat released at around 31 MJ m⁻². The earlier time to ignition observed for the samples in the 'wet' condition shows a clear difference, whereas the scatter in the 'dry' peak heat release rates makes it difficult to determine whether, and by how much, this parameter is higher for 'dry' samples than for 'wet' samples. An earlier and steadier increase in heat release rate may be accounted for by the behaviour of these samples when exposed to a radiant heat source. Figure 113 shows a 'wet' sample – removed from the cone calorimeter after being subjected to a 60 kW m⁻² heat flux for 60 seconds. The presence of small bubbles can clearly be seen on the surface of the samples.

The presence of a bubbled surface increases the surface area of the sample, and as a result, more of the radiant heat from the cone calorimeter is absorbed, causing ignition to occur earlier. It may also be that these bubbles are created by the moisture within the polymer which attempts to evaporate as it is subjected to rapid heating. As a result, the bubbles create a thin layer which separates from the bulk of the polymer.



FIGURE 113. 450G 2.5 MM 'WET' CONDITION 60 kW M⁻² REMOVED AFTER 60 SECONDS

Due to its low thermal mass, this layer will heat up quickly and ignite earlier. After ignition, heat is fed back to the bulk of the polymer to sustain burning. Figure 114 shows a sample which was placed in the 'dry' condition also subjected to a 60 kW m⁻² heat flux for 60 seconds. In this case, there are no bubbles and this effect does not occur.



FIGURE 114. 450G 2.5 MM 'DRY' CONDITION 60 kW M⁻² REMOVED AFTER 60 SECONDS

The samples showing bubbles on the surface were cut to determine whether or not they were present throughout the bulk of the sample or not. Figure 115 shows a cross-sectional view of the cone calorimeter sample shown in Figure 113. The bubbles are present at the surface and transcend to all but the final 1 mm where it appears the heat front has not reached.

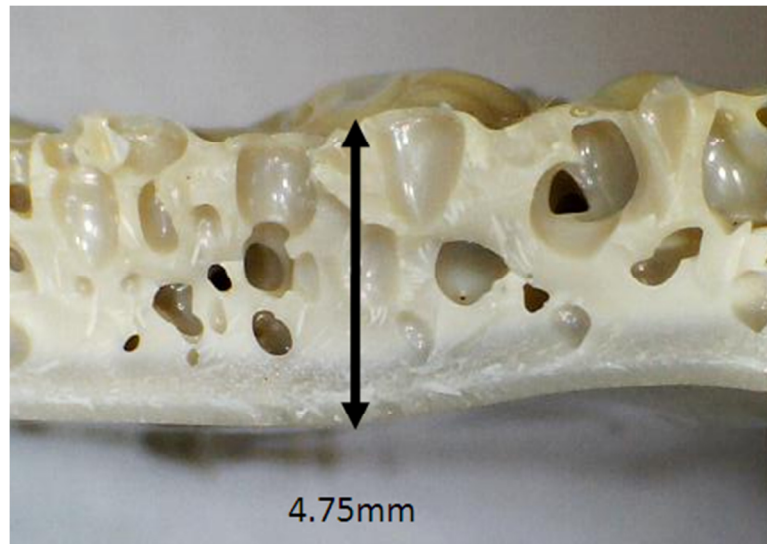


FIGURE 115. CROSS SECTION OF BUBBLED CONE CALORIMETER SAMPLES

Here another effect may be apparent. The original samples were 2.5 mm in thickness; this sample has increased to 4.75 mm after heating, and as a result has almost doubled in both thickness and volume. By doubling the volume of a sample, the density is halved and the sample effectively becomes a foam.

450GL30 Wet	Difference (%)
1	+ 0.122
2	+ 0.168
3	+ 0.116
Average	+ 0.135
Standard Deviation	0.028
450G Dry	Difference (%)
1	- 0.186
2	- 0.179
3	- 0.198
Average	- 0.188
Standard Deviation	0.010

TABLE 39. 450GL30 2.5 MM 'WET' AND 'DRY' SAMPLE GAINS AND LOSSES

The presence of the voids hinders heat transfer, causing the heat to be concentrated on the polymer surface and ignition to occur earlier.

“Wet and dry” samples containing filler were also burned in the cone calorimeter to investigate the effect conditioning the samples was having on flammability. The conditions used were identical to those used for the 450G samples. The absorption of moisture, in terms of mass gained or lost from the samples is shown in Table 39. Again there is a 0.3% difference between samples which are wet and samples which are dry indicating that the presence of glass fibre in the matrix is not hindering or accelerating the absorption of moisture. The results of cone calorimeter experiments completed at 60 kW m^{-2} are shown in Figure 116 and the data is shown in Table 40.

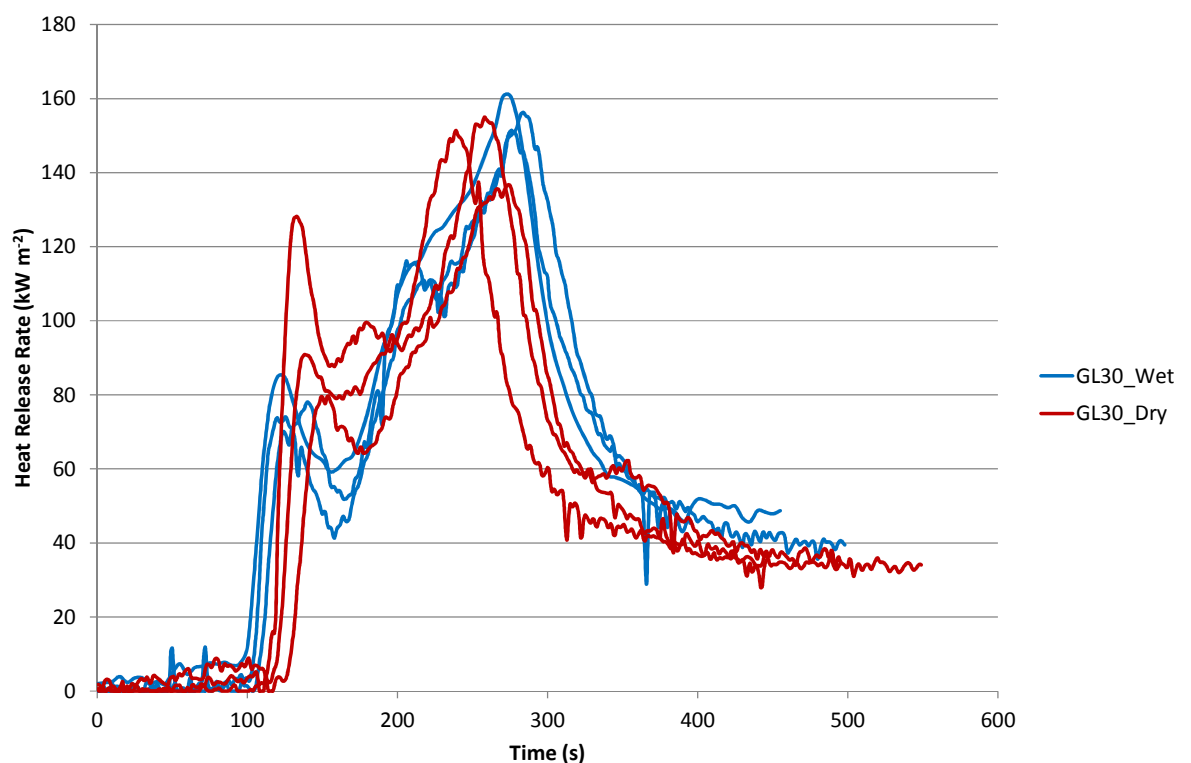


FIGURE 116. 450GL30 2.5 MM ‘WET’ AND ‘DRY’ CONDITION HEAT RELEASE RATES COMPARISON AT 60 kW M^{-2}

Whereas the 450G samples show a difference of 23 seconds between the average time to ignition for wet and dry samples, the 450GL30 samples show only a 16 second difference, indicating that the effect which is occurring on the surface of the samples is occurring to a lesser extent in the glass fibre-filled samples with the same amount of moisture absorbed. This may be due to the higher density of the 450GL30 samples (1510 kg m^{-3}) compared to the 450G samples (1300 kg m^{-3}) which may be restricting the bubble formation throughout the bulk.

Sample	t _{ig} (s)	PHRR (kW m ⁻²)	tPHRR (s)	Char (%)	THR (MJ m ⁻²)
Wet_1	87	160.8	275	64.7	29.5
Wet_2	94	150.9	278	69.6	24.7
Wet_3	88	156.2	284	66.4	29.7
Average	90 (±4)	156.0 (±5.0)	279 (±5)	66.9 (±2.5)	27.9 (±2.8)
Dry_1	98	151.4	239	64.1	25.3
Dry_2	113	136.5	275	68.2	24.4
Dry_3	108	155.0	258	63.7	24.3
Average	106 (±8)	147.6 (±9.8)	257.3 (±18)	65.3 (±2.5)	24.7 (±0.6)

TABLE 40. 450GL30 2.5 MM 'WET' AND 'DRY' CONE CALORIMETER PROPERTIES

4.4.11 Wet, Dry and Humid Conditioning Experiments

The experiments detailed above were extended to include a 'humid' condition – samples which had been subjected to 50% relative humidity, to observe if there were any differences in behaviour between these and the 'wet' samples – as observed in the UL-94 experiments. The conditions and their details are shown in Table 41.

Condition	Details
Wet	25°C water bath for 168 hours
Dry	100°C oven for 168 hours
Humid	50% relative humidity for 168 hours

TABLE 41. WET, DRY AND HUMID CONDITIONS AND DETAILS

The data for 'wet', 'dry' and 'humid' samples has been grouped and plotted in Figure 117. Wet samples ignite between 65 and 90 seconds and reach a peak heat release rate at around 350 kW m⁻². Heat release rate decreases steadily to 60 kW m⁻² at around 225 seconds. Dry samples ignite between 110 seconds and 115 seconds and increase steadily in heat release rate to around 550 kW m⁻². There is a decrease in heat release rate to 60 kW m⁻² at 225

seconds. Humid samples ignite between 75 seconds and 95 seconds and increase steadily in heat release rate to around 350 kW m⁻².

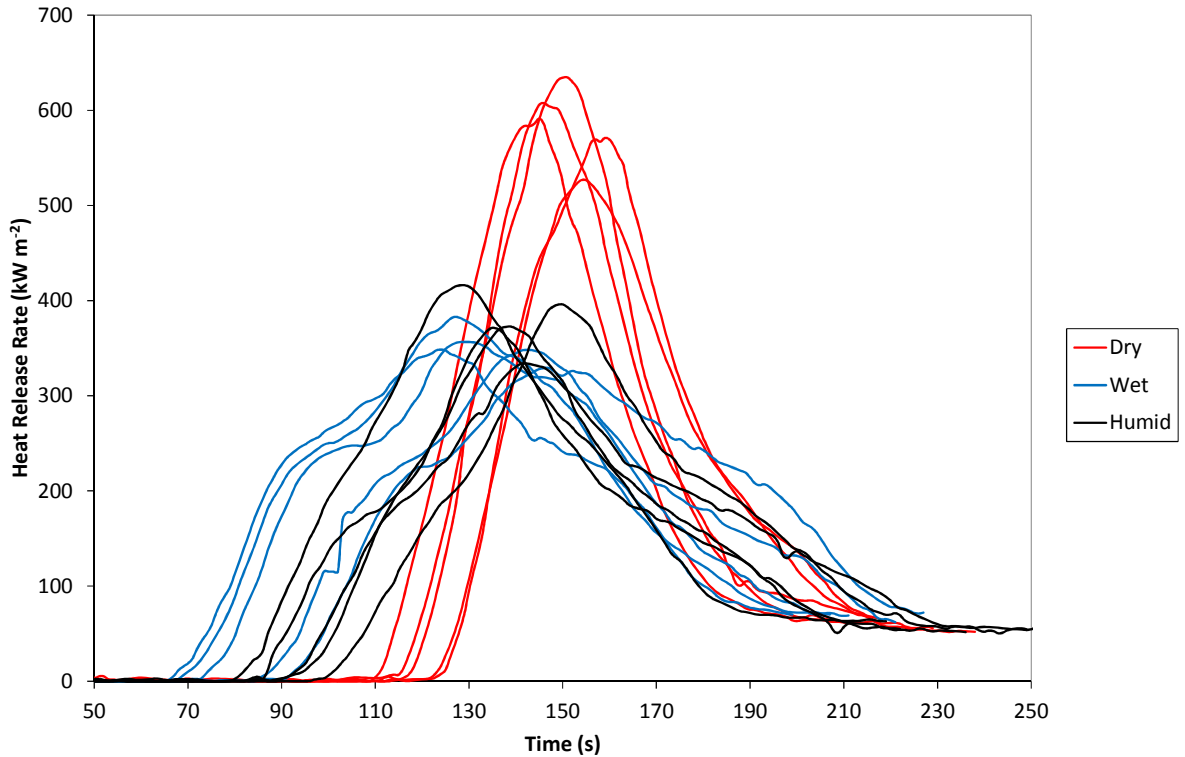


FIGURE 117. 150G 2.5 MM ALL CONDITIONS COMPARISON HEAT RELEASE RATE AT 60 kW M⁻²

	t _{ig} (s)	PHRR (kW m ⁻²)	tPHRR (s)	Mass Loss (%)	THR (kW m ⁻²)
Dry	118 (±5)	586.3 (±41)	151 (±6)	49.1 (±2)	25.9 (±1)
Wet	75 (±9)	353.2 (±20)	134 (±10)	53.5 (±1)	27.9 (±1)
Humid	88 (±7)	378.1 (±31)	139 (±8)	51.1 (±6)	25.3 (±2)

TABLE 42. 150G ALL CONDITIONS CONE CALORIMETER PROPERTIES

There is a decrease in heat release rate to 60 kW m⁻² at 225 seconds. ‘Wet’ samples ignite prior to ‘humid’ samples which ignite prior to ‘dry samples’. Both ‘wet’ and ‘humid’ samples have a similar peak of heat release rate – at around 350 kW m⁻²: lower than ‘dry’ samples which have a peak heat release rate at around 550 kW m⁻². This data is summarised in Table 42.

4.4.12 Crystalline and Low Crystallinity Surface Experiments

The 'wet', 'dry' and 'humid' study has been expanded to include different degrees of crystallinity to determine the effect of moisture on these samples. Moisture absorbed into a semi-crystalline polymer such as PEEK can only occur in the amorphous phase as the densely packed crystalline phase will resist the penetration of water. The normal state of PEEK – used for all cone calorimeter experiments – has a crystallinity of around 35%. A low crystallinity sample can be obtained by utilising a cold tool when moulding – the resulting samples have a crystallinity of ~10%. In addition, annealed samples can also be created, using the same hot tool at the standard samples, and then further annealing PEEK at 250°C for 12 hours, giving samples with a crystallinity of 40%. The effects of varied crystallinity and moisture on flammability are described in the following section.

Low crystallinity 150G samples exposed to the same conditions as those detailed in Table 41 were tested at 60 kW m⁻² and results are shown in Figure 118. 'Wet' and 'humid' samples show similar heat release curves – both show an earlier average time to ignition (76 seconds and 73 seconds compared with 114 seconds) than 'dry' samples and a lower average peak heat release rate (320 kW m⁻² and 323 kW m⁻² compared to 497 kW m⁻²). The results are outlined in Table 43.

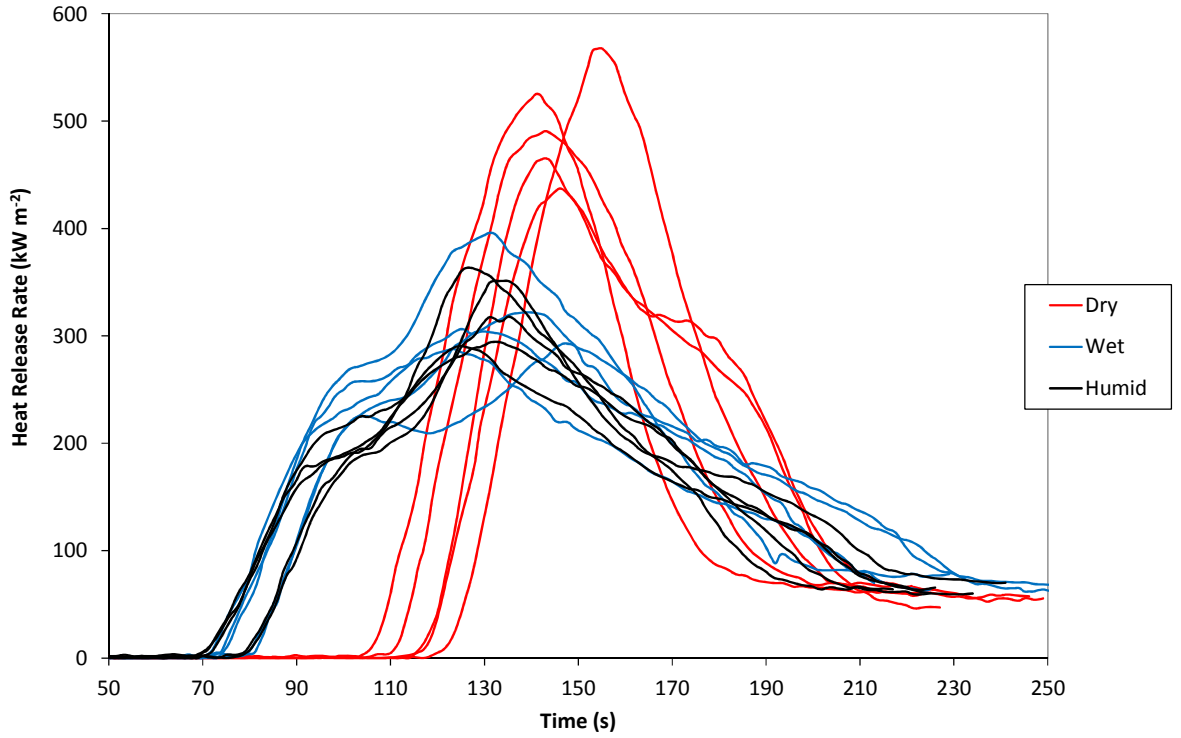


FIGURE 118. 150G 2.5 MM LOW CRYSTALLINITY SAMPLES WITH VARIED CONDITIONS HEAT RELEASE RATE AT 60 kW m⁻²

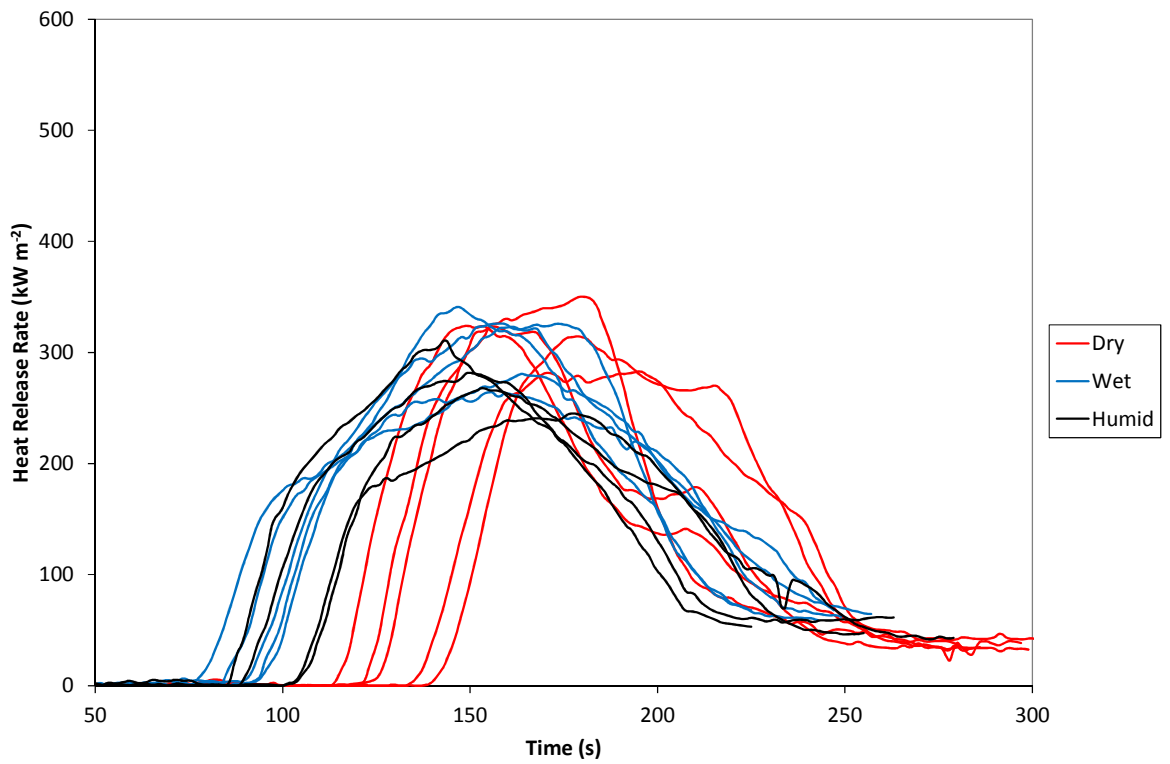


FIGURE 119. 450G 2.5 MM LOW CRYSTALLINITY SAMPLES WITH VARIED CONDITIONS HEAT RELEASE RATE AT 60 kW m⁻²

		t_{ig} (s)	PHRR (kW m ⁻²)	tPHRR (s)	Mass Loss (%)	THR (MJ m ⁻²)
150G	Dry	114 (±7)	497.2 (±51)	146 (±5)	51.2 (±3)	26.5 (±2)
	Wet	76 (±4)	320.4 (±44)	134 (±9)	55.3 (±1)	29.1 (±3)
	Humid	73 (±4)	323.5 (±33)	130 (±4)	56.1 (±3)	26.9 (±1)
450G	Dry	130 (±10)	318.9 (±24)	172 (±19)	55.2 (±2)	25.44 (±1)
	Wet	86 (±7)	307.0 (±33)	157 (±7)	55.5 (±1)	30.5 (±1)
	Humid	96 (±9)	276.3 (±27)	156 (±15)	56.7 (±4)	26.0 (±1)

TABLE 43. 150G AND 450G LOW CRYSTALLINITY SAMPLES WITH VARIED CONDITIONS CONE CALORIMETER PROPERTIES AT 60 kW M⁻²

Interestingly, in both cases, the wet samples show a higher value for total heat released (29.1 and 30.5 MJ m⁻² compared to around 25 MJ m⁻²). The cone calorimeter curves for amorphous 450G samples tested at 60 kW m⁻² are shown in Figure 119. All samples show a similar peak of heat release with 'dry' samples igniting after 'wet' and 'humid' samples.

Crystalline 150G samples exposed to the same conditions as those detailed in Table 41 were tested at 60 kW m⁻² and results are shown in Figure 120.

		t_{ig} (s)	PHRR (kW m ⁻²)	tPHRR (s)	Mass Loss (%)	THR (MJ m ⁻²)
150G	Dry	113 (±4)	584.5 (±44)	142 (±4)	49.0 (±2)	25.5 (±1)
	Wet	89 (±6)	401.5 (±20)	143 (±10)	55.5 (±2)	30.4 (±1)
	Humid	85 (±3)	406.5 (±26)	131 (±2)	48.7 (±3)	24.5 (±1)
450G	Dry	142 (±3)	352.4 (±18)	171 (±8)	52.2 (±3)	26.3 (±1)
	Wet	86 (±5)	428.2 (±47)	146 (±8)	55.4 (±3)	31.9 (±1)
	Humid	92 (±10)	409.7 (±53)	145 (±11)	55.0 (±1)	25.9 (±1)

TABLE 44. 150G AND 450G CRYSTALLINE SAMPLES WITH VARIED CONDITIONS CONE CALORIMETER PROPERTIES AT 60 kW M⁻²

'Wet' and 'humid' samples show similar heat release curves – both show an earlier time to ignition (89 seconds and 85 seconds compared with 113 seconds) than 'dry' samples and a lower peak heat release rate (402 kW m⁻² and 407 kW m⁻² compared to 584 kW m⁻²). The

results are outlined in Table 44 for both 150G and 450G samples. It is interesting that the humid samples show an earlier time to ignition, although this cannot be seen from the average due to the scatter present in the data.

Crystalline 450G samples were tested at 60 kW m^{-2} and results are shown in Figure 121. Both 'wet' and 'humid' samples showed an earlier time to ignition (86 seconds and 92 seconds compared with 142 seconds) than 'dry' samples, however, 'dry' samples showed a lower peak heat release rate (352 kW m^{-2} compared to 428 kW m^{-2} and 410 kW m^{-2}) which would not be expected for a sample which had been subjected to the radiant heat of the cone calorimeter for a longer period of time. It is also expected that wetting and drying crystalline samples would have a lesser effect on flammability due to there being less space within the polymer for moisture to be absorbed, compared with amorphous samples.

However, this is not the case in the 150G samples where the effect of moisture is similar to that seen in the low crystallinity and standard samples.

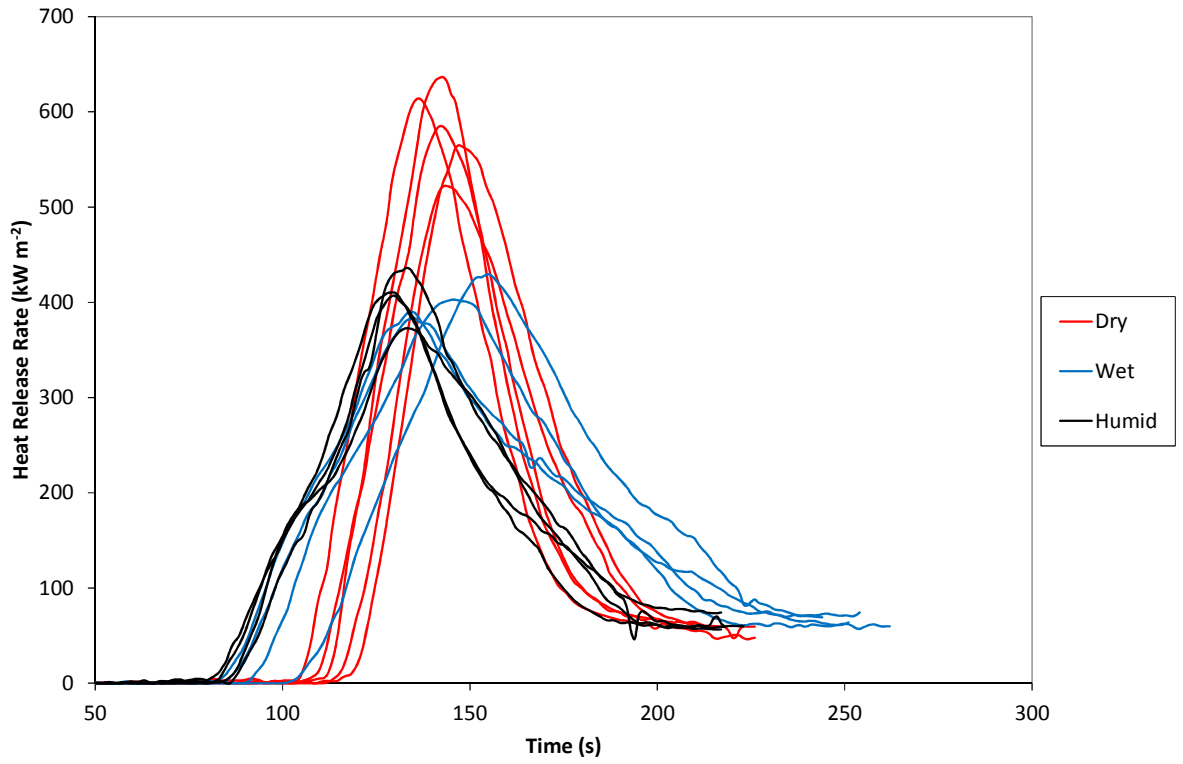


FIGURE 120. 150G 2.5 MM CRYSTALLINE SAMPLES WITH VARIED CONDITIONS HEAT RELEASE RATE AT 60 kW M^{-2}

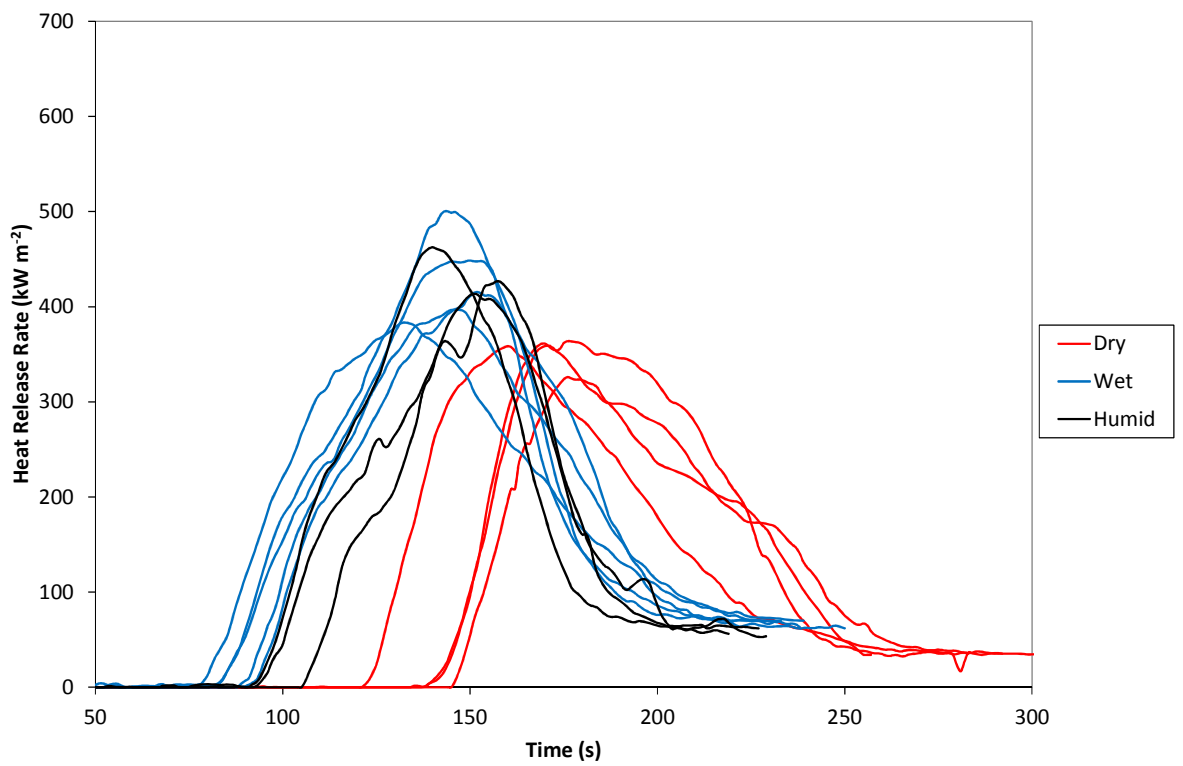


FIGURE 121. 450G 2.5 MM CRYSTALLINE SURFACE WITH VARIED CONDITIONS HEAT RELEASE RATE AT 60 kW M^{-2}

4.4.13 Problems with PEEK in the Cone Calorimeter

Several problems have been experienced with PEEK samples in the cone calorimeter. A major problem was the intumescing of samples. For samples of lower viscosity, intumescence occurred to a greater extent, as seen in the char heights experiments (Section 4.4.4.3). Figure 122 and Figure 123 are images of 3.2 mm cone calorimeter samples of 90G and 450G PEEK respectively.

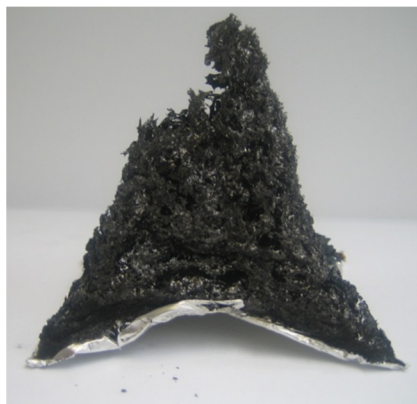


FIGURE 122. 90G 3.2 MM CONE CALORIMETER SAMPLE AFTER 50 kW m⁻²



FIGURE 123. 450G 3.2 MM CONE CALORIMETER SAMPLE AFTER 50 kW m⁻²

These images show the extent of intumescence. Figure 124 shows a 3.2 mm cone calorimeter sample of 450CA30. There is considerably less intumescence and the remains of carbon fibre

can be seen on top of the sample. Figure 125 shows a 3.2 mm cone calorimeter sample of 450GL30, again with less intumescence and what appears to be a barrier layer created by the glass fibre.



FIGURE 124. 450CA30 3.2 MM CONE CALORIMETER SAMPLE AFTER 50 kW/m⁻²



FIGURE 125. 450GL30 3.2 MM CONE CALORIMETER SAMPLE AFTER 50 kW/m⁻²

Due to the samples intumescing, it was possible that the external heat flux of the radiant cone heater was not uniform throughout the surface of the sample. The intumesced parts were closer to the heater and therefore being heated to a greater extent than those parts near the edge of the sample which had remained relatively static. It is suggested in ISO 5660-1 [36] to use a grid constructed from 1.9 mm diameter stainless steel rod with samples that intumesce as a means of preventing this occurrence. Figure 126 shows a 450G cone calorimeter sample with the suggested grid after subjecting to 35 kW m⁻² irradiance in the cone. The sample forms a glassy char on its upper surface which appears to have prevented the sample from igniting.

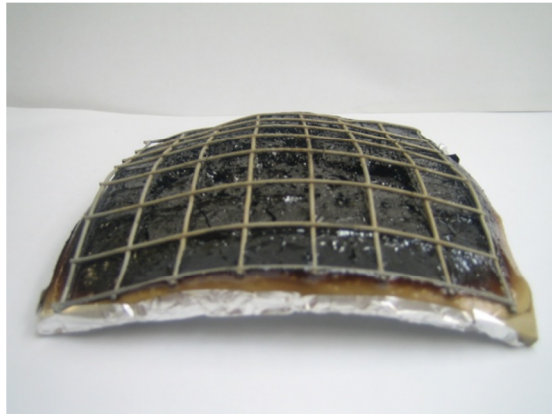


FIGURE 126. 450G WITH GRID CONE CALORIMETER SAMPLE AFTER 35 kW m⁻²

Samples of 450G PEEK were tested in the cone calorimeter at 50 kW m⁻² with the stainless steel grid. The results of this experiment are shown in Figure 127.

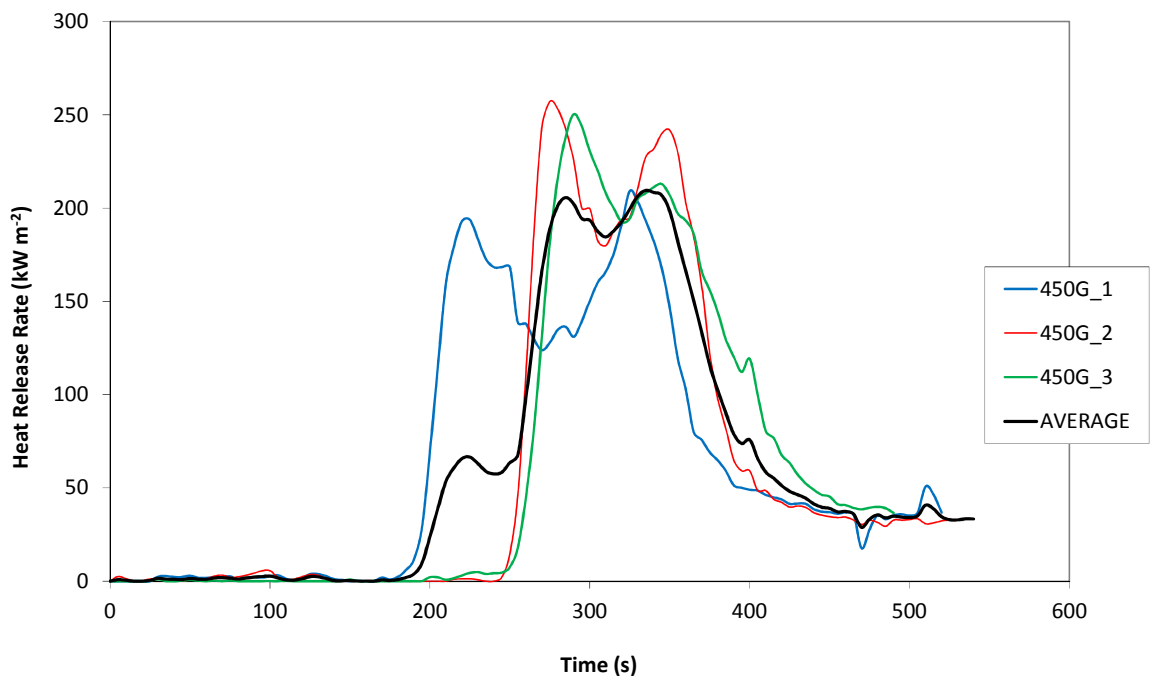


FIGURE 127. 450G 3.2 MM WITH GRID HEAT RELEASE RATE

It is evident that there are some differences in burning behaviour between the samples which were tested. There appear to be two distinct peaks of heat release rate with a slight period of steady state burning. This is masked by the average due to the difference in ignition times.

These values were then plotted with 450G samples where a grid was not present. This is shown in Figure 128. There are significant differences between the samples with and

without a grid. The average plots show that the presence of a grid increases the time to ignition and reduces the peak heat release rate – in this instance by 100 kW m^{-2} . A reduction in the time to ignition with the presence of a grid may be due to the volatiles formed upon heating of the sample being unable to escape and therefore ignite. The intumescence which occurs is possibly due to the formation of volatile products of decomposition such as CO and CO₂ which ‘push’ the polymer up as they are formed, hence intumescence is greater with a lower viscosity sample.

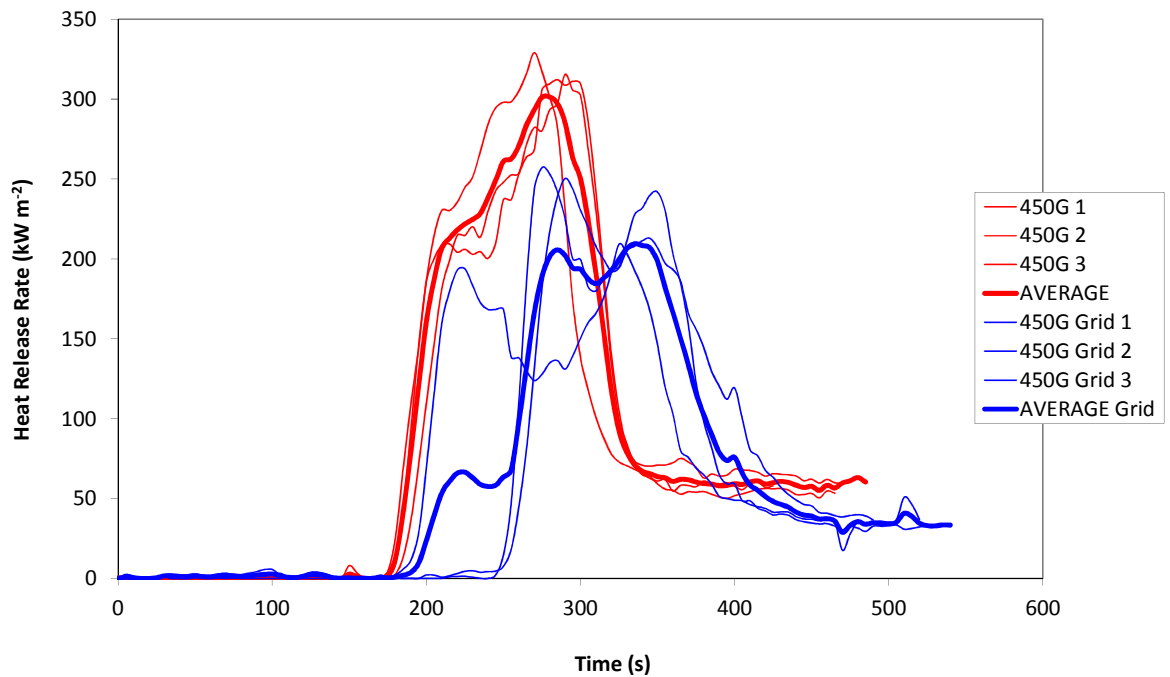


FIGURE 128. 450G 3.2 MM WITH AND WITHOUT GRID HEAT RELEASE RATE (GROUPED DATA)

4.5 Single-Flame Source Test (ISO 11925)

The single-source flame test was adopted as a means of determining flammability properties of samples containing small amount of carbon black – for colouring purposes – without the use of the cone calorimeter, as these samples resulted in excessively scattered data. Natural and black PEEK (with small amounts of carbon black) were used in this experiment. The results are outlined for natural samples in Table 45. As the thickness of the film increases, the time taken for the flame to reach the top of the sample increases – due to

the presence of a greater amount of sample. For samples of 25, 50 and 100 μm , the entirety of the sample is consumed, however for samples of 250 μm , a shorter burn length is observed.

Sample Thickness (μm)	Time of Test (s)	Time to Top (s)	Burn Length (mm)
25	33 ± 8.8	15.9 ± 2.2	250 ± 0 (Maximum)
50	80.1 ± 26.7	25.5 ± 10.0	250 ± 0 (Maximum)
100	138.1 ± 13.7	113.5 ± 10.6	250 ± 0 (Maximum)
250	110 ± 115.0	249.7 ± 31.6	109.7 ± 71.4

TABLE 45. ISO 11925 FOR 'NATURAL' PEEK AT VARIED THICKNESSES

The results are outlined for black samples in Table 46. Similarly, as the sample thickness increases, the time taken for the flame to reach the top increases due to the presence of a greater amount of sample. Interestingly, the burn length between the natural and black samples is different. The black samples do not burn completely (248.3 mm out of 250 mm) at 25 μm where as the natural samples do.

Sample Thickness (μm)	Time of Test (s)	Time to Top (s)	Burn Length (mm)
25	23 ± 6.5	12.9 ± 3.6	248.3 ± 5.4
50	38.3 ± 21.6	28.9 ± 11.9	221.1 ± 55.7
100	94.9 ± 54.5	110.3 ± 12.1	193.8 ± 90.5
250	28.6 ± 3.6	n/a	46 ± 3.8

TABLE 46. ISO 11925 FOR 'BLACK' PEEK AT VARIED THICKNESSES

The same is true for samples of 50 μm , which burn 221.1 mm out of 250 mm and samples of 100 μm which burn 193.8 mm out of 250 mm. It appears that the presence of small amounts of carbon black is preventing the extent of upward flame spread in the black samples. This is not as expected as a sample which is black would be better at absorbing radiation than one which is a light brown/tan colour. Additionally, the small amounts of carbon black present in the polymer may be aiding in the production of a char which ultimately prevents flame propagation.

4.6 Summary

Changing the viscosity of PEEK affects its flammability. In the ignitability and ease of extinction tests, the occurrence of dripping has opposite effects. In the UL-94 test, dripping causes the lowest viscosity material to fail both the V-0 and V-1 ratings. In the LOI test, dripping allows the 90G material to pass a particular oxygen concentration and subsequently achieve a higher rating than the 150G and 450G materials. In the cone calorimeter, the sample with the lowest viscosity has the lowest peak of heat release and the earliest time to ignition. This implies that 90G, due to its shorter chain lengths or greater number of chain ends decompose more quickly in the anaerobic conditions below the polymer surface (this is consistent with TGA data), allowing fuel production and the criteria required for ignition to be met earlier. Similarly, the lower viscosity samples begin releasing heat earlier in the PCFC also consistent with decomposing at a lower temperature in the TGA in nitrogen.

The thickness of samples affects the materials burning behaviour, as observed in the small-flame ignitability test and the cone calorimeter. In the small flame ignitability test, the rate of flame spread is reduced as the thickness of the sample is increased. In the cone calorimeter, burning behaviour shifts from thermally thin, characterised by a rapid heat release and a high peak of heat release, to thermally thick, where the heat release is gradual as the surface burns from the top down and a thermal gradient exists within the sample.

The presence of filler in PEEK reduces the material's flammability. In the ignitability and ease of extinction tests, the presence of filler results in shorter burn times in the UL-94 and exposure to higher oxygen concentrations in the LOI. In the cone calorimeter, filled materials show a lower peak of heat release, a longer time to ignition and a lower total heat release. In particular for samples containing glass fibre, this effect is greater in the cone calorimeter due to the enforcement and whitening of char by glass fibre. These samples also show less swelling towards the cone heater. This effect is not observed in the PCFC due to the nature of this experiment and the relatively small sample sizes.

The presence of moisture in PEEK during flammability tests has been seen to be detrimental to the material's flammability. In both the UL-94 and cone calorimeter, the presence of moisture (at less than 0.5%) increases the flammability. In the UL-94, this is characterised by a 50% increase in total flame time compared to samples which have been dried. In the cone calorimeter, an earlier time to ignition is observed for samples which are wet. In both cases, the presence of small bubbles was noted on the surface of samples, these bubbles are believed

to be forming when the PEEK reaches its melting point and causing earlier ignition or allowing for ease of flame spread (a series of successive ignitions) due to either the increases surface area of the bubbled surface, the lifting of the bubbled layer from the bulk of the surface or the insulation of the foam-like structure of the resulting polymer.

The problem of scatter within the data has been observed with many flammability tests. In the cone calorimeter, increasing the external heat flux at which tests were completed appeared to reduce the scatter in the time to ignition. The critical heat flux for ignition of PEEK was determined to be 36 kW m^{-2} suggesting that samples being tested at lower heat fluxes ($45\text{-}60 \text{ kW m}^{-2}$) may be too close to the limits of flammability for PEEK and causing scatter. This effect has also been observed in the UL-94 tests whereby using a hotter flame allows for a 23% reduction in the total burning time. The behaviour of PEEK in both these tests could be a result of the material's method of fire protection (char formation) and its high decomposition temperature. The presence of carbon (as fibre or powder) appears to increase the scatter in terms of the time to ignition and peak of heat release in the cone calorimeter. This may be merely due to the presence of carbon (promoting oxidation) or due to the subsequent colour change caused in the composite material and the way that black materials interact with the cone calorimeter's radiation source.

CHAPTER 5. CHAR ANALYSIS

Char analysis of PEEK was completed using the diamond attenuated reflectance accessory coupled with Fourier-transform infrared (dATR-FTIR) on films of 450G to determine the processes occurring during the early stages of decomposition. Scanning Electron Microscope/Energy Dispersive X-Ray (SEM/EDAX) was utilised to observe the char formed during the cone calorimeter experiments, with respect to filled samples. Nuclear Magnetic Resonance (NMR) was also employed to determine the processes occurring during the early stages of decomposition.

These experiments were completed to understand the processes occurring during the thermal decomposition of 'standard' PEEK.

5.1 Diamond Attenuated Total Reflectance/Fourier-Transform Infrared (dATR-FTIR)

The dATR-FTIR spectra for 'standard' PEEK – of 100 μm is shown in Figure 129.

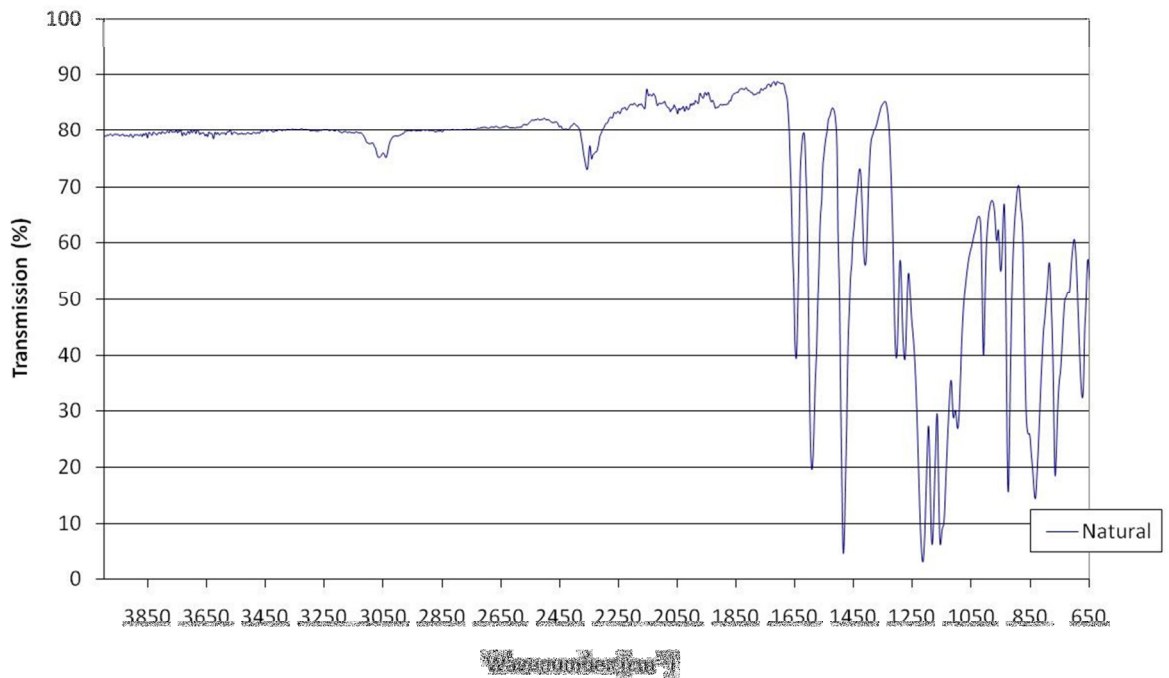


FIGURE 129. DATR-FTIR OF NATURAL PEEK FILM

The presence of CO₂ is evident at around 2354 cm⁻¹. The infrared spectra of PEEK has been interpreted elsewhere[99].

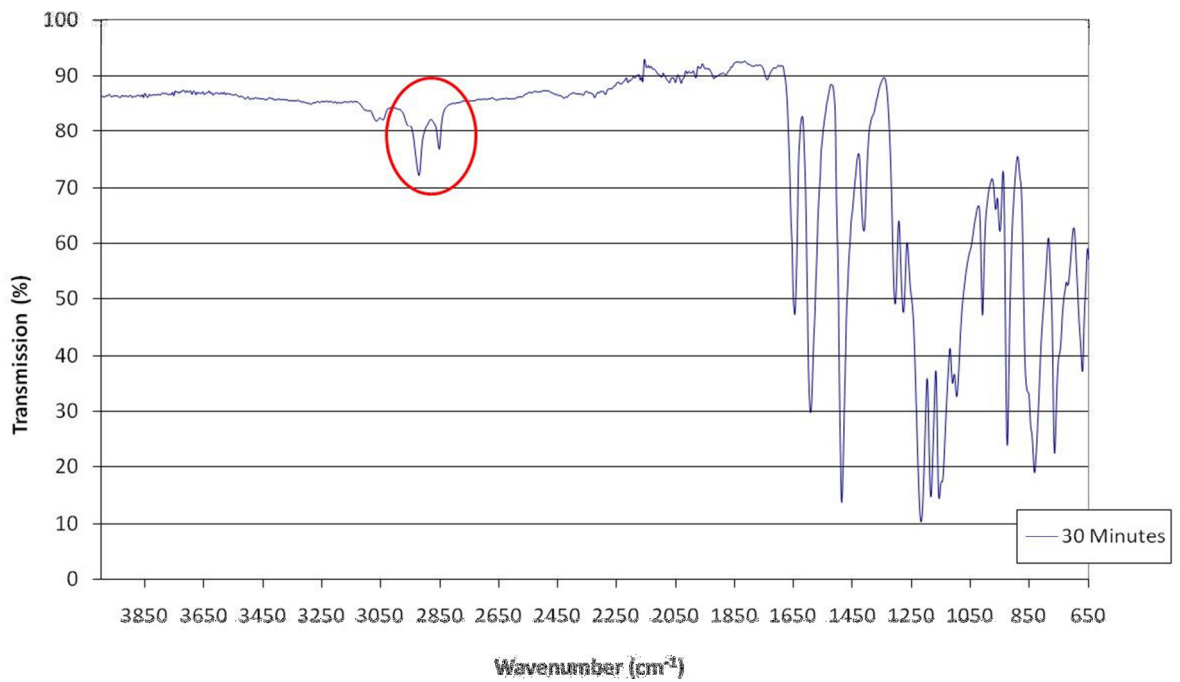


FIGURE 130. DATR-FTIR OF NATURAL PEEK FILM AGED AT 400°C FOR 30 MINUTES

The ATR-FTIR spectra of PEEK film aged at 400°C for 30 minutes is shown in Figure 130. The presence of two peaks at 2920 cm⁻¹ and 2850 cm⁻¹ is evident – both attributed to CH₂ stretching [100].

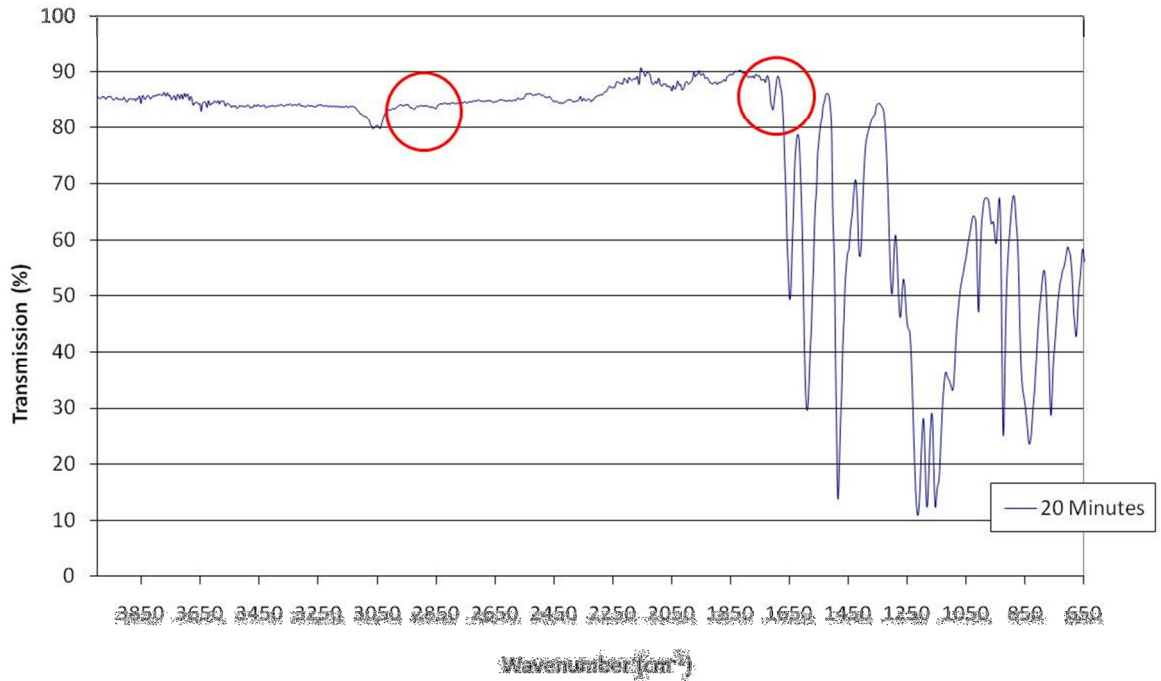


FIGURE 131. DATR-FTIR OF NATURAL PEEK FILM AGED AT 500°C FOR 20 MINUTES

The ATR-FTIR spectra of PEEK film aged at 500°C for 20 minutes is shown in Figure 131. The presence of a peak at 1700 cm^{-1} is evident, attributed to an aldehyde C=O [100]. This indicates that an aldehyde species may be an early product of PEEK decomposition. From literature [52], 1-phenoxy-4-(4-phenoxy aldehyde) has been determined at low abundance. Remnants of the CH_2 stretch are also evident.

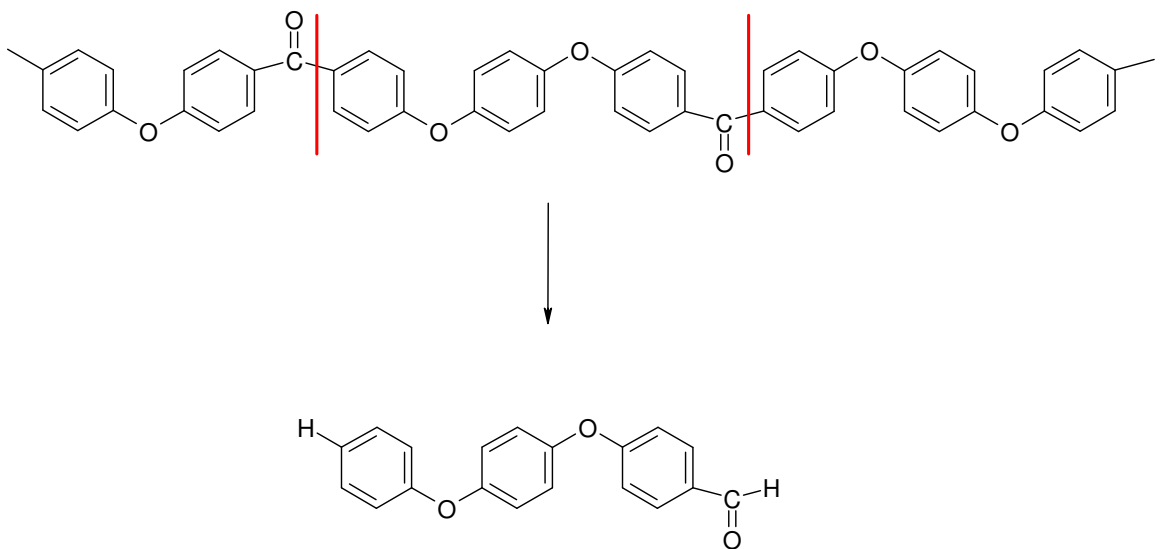


FIGURE 132. CARBONYL SCISSION FOR 1-PHENOXY-4(4-PHENOXYL ALDEHYDE)

Scission at the carbonyl bonds in the main chain would give this product, as shown in Figure 132.

5.2 Scanning Electron Microscope/Energy Dispersive X-Ray (SEM/EDAX)

The char residue remaining from cone calorimeter analysis of PEEK 450GL30 at 50 kW m⁻² was examined using the SEM coupled with EDAX. An image from the SEM is shown in Figure 133 showing the presence of fibres on the surface of the char. The fibres may be acting as a reinforcing barrier which is protecting the underlying polymer from the cone calorimeter's heat flux.

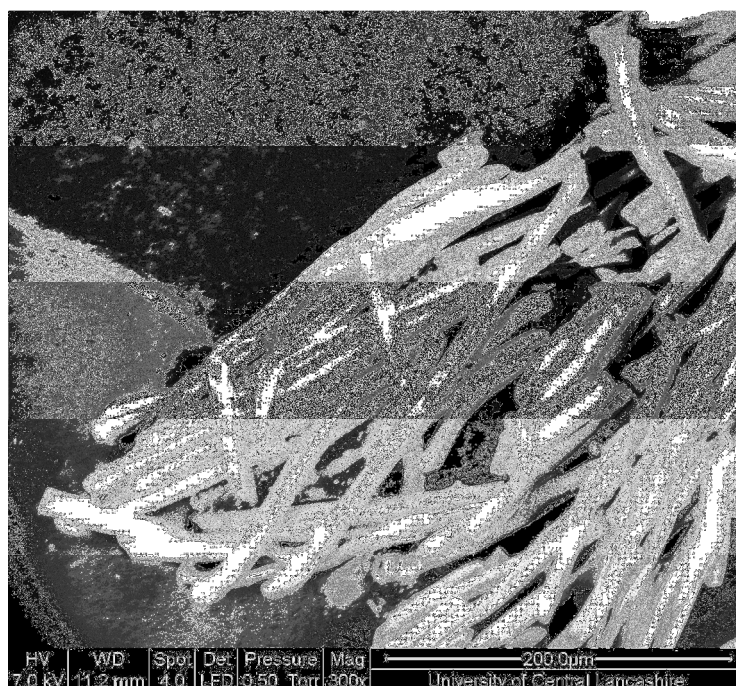


FIGURE 133. SEM IMAGE OF 450GL30 RESIDUE

In order to determine if what is present in the char was in fact glass fibre, elemental analysis was completed on the sample using EDAX. The results can be seen in Figure 134. A large percentage of the surface contains oxygen, with the second highest abundance being attributed to both silicon and calcium, thus confirming the presence of glass.

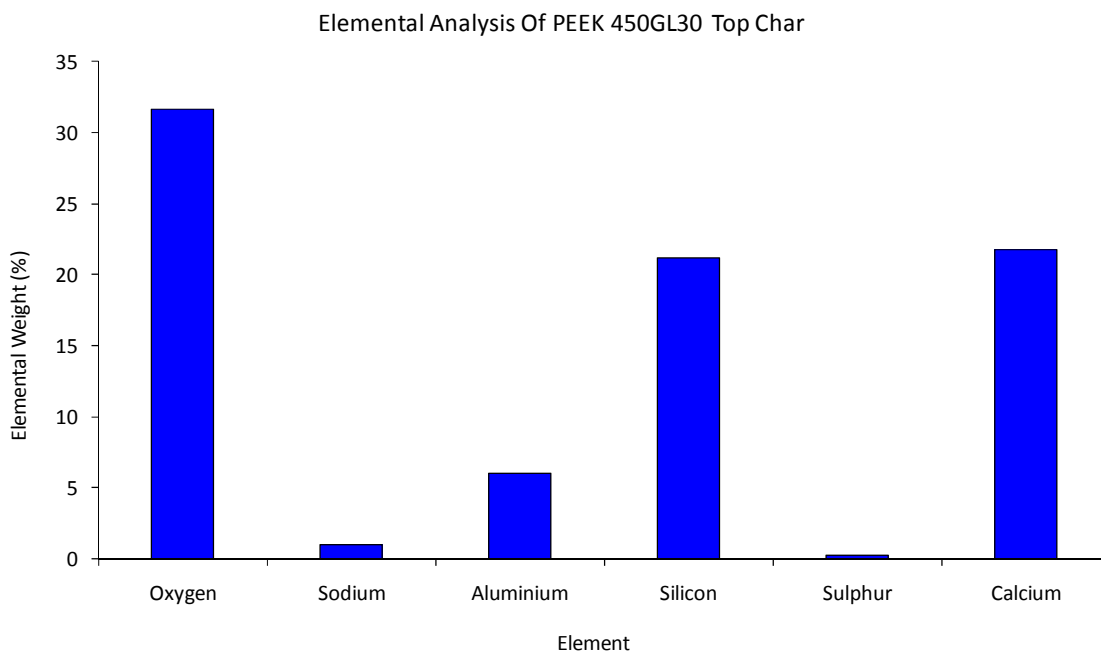
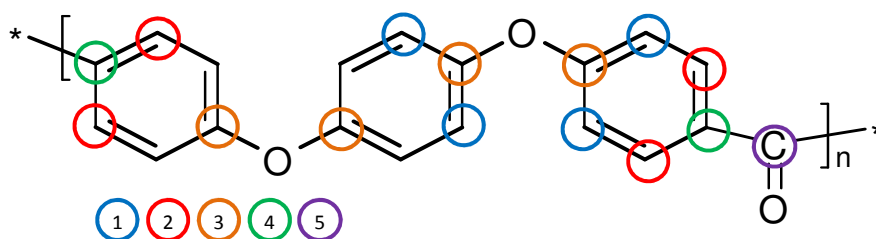


FIGURE 134. ELEMENTAL ANALYSIS OF 450GL30 CONE CALORIMETER CHAR

5.3 ^{13}C Nuclear Magnetic Resonance

MAS/NMR spectroscopy was used to obtain the ^{13}C NMR spectrum of PEEK polymer and the assignments of the atoms in Figure 135 were as follows:

FIGURE 135. PEEK REPEAT UNIT WITH ASSIGNED ^{13}C NMR PEAKS

These peaks showed insignificant changes on heating and are the same as presented in Figure 136. The assignments were: peak (1) 121 and 123 ppm, (2) 135 ppm, (3) 154 ppm, (4) 163 ppm and (5) 196 from left to right. The other peaks seen in Figure 136 are due to spinning side bands and change position with altering spin rate.

Samples of PEEK that had been aged in an oven at 400°C or 450°C, were tested using dATR-FTIR and ^{13}C NMR MAS/NMR spectroscopies. The dATR-FTIR, in particular, showed the appearance of an aliphatic C-H stretch at 2920 cm^{-1} and 2850 cm^{-1} , which appeared to increase in intensity as the samples were aged, but disappeared with prolonged aging. A sample of PEEK aged for 30 minutes at 400°C is shown in Figure 136. The chemical shifts corresponding to carbons along the PEEK chain have been assigned in Figure 135.

A rolled film sample of PEEK showed a small alkyl CH peak at about δ 35 ppm apparently confirming the IR data. However, when samples of PEEK heated at various temperatures from 400 to 500°C were powdered down to allow for higher frequency spinning in the NMR; very little trace of the proposed alkyl peak could be observed. Thus, if an alkyl CH is being produced, then it must only be forming at the surface of the polymer and not in the bulk.

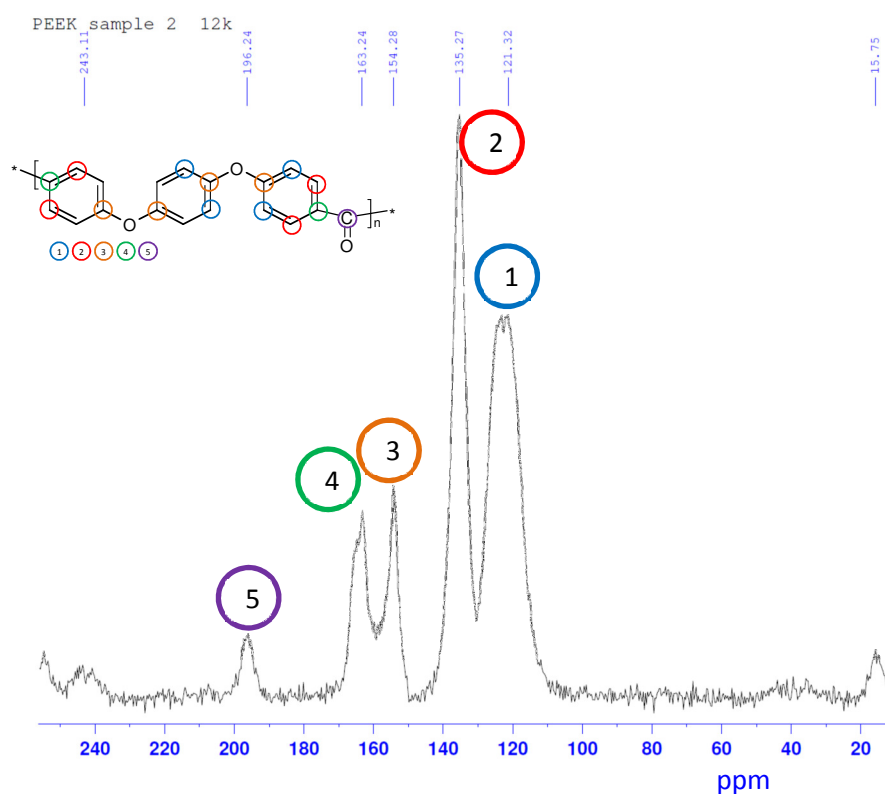


FIGURE 136. ^{13}C NMR 400°C FOR 30 MINUTES 12K

Samples of PEEK were also heated to higher temperatures, 600°C and 650°C in an oven for 10 minutes. The thermogravimetric decomposition of PEEK in air shows that PEEK is in its second stage of decomposition in this temperature range with around 40% mass remaining.

Investigating heated samples in this region may be able to determine what processes are occurring whereby PEEK ceases losing mass at a rapid rate and begins charring. A sample aged for 10 minutes at 600°C is shown in Figure 137. It can be seen that there is a reduction in the relative intensity of peaks (2) and (3) indicating that these atoms are still present but in smaller amounts than they were originally. Peaks (4) and (5), relating to the carbonyl carbon and its attachment to the ring are absent indicating that these bonds have been broken. Peak 1, corresponding to carbons ortho to the ethers, remain relatively unchanged however the peak has shifted from 121 ppm to 128 ppm suggesting that extensive graphitic formation has occurred [101]. The peak at 128 ppm is found to correspond to the peak for graphite found in other polymers at this temperature. However, the ether attachment carbon, peak (3) is still present showing some evidence for a diphenylether structure being present even at such high temperatures. Thus, Figure 137 presents evidence for the carbonyl bond being the first to be broken during the decomposition of PEEK.

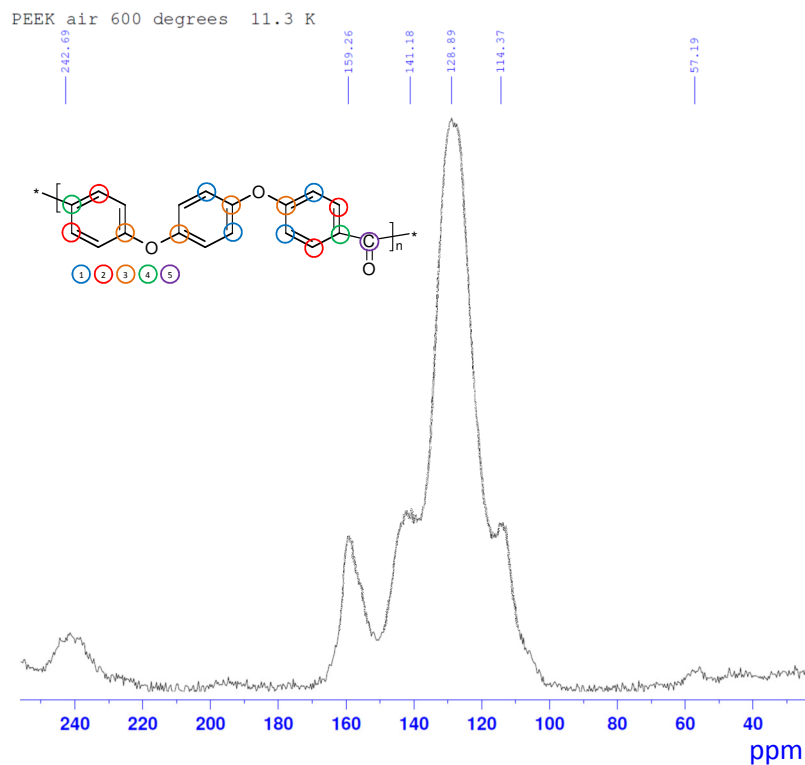


FIGURE 137. ^{13}C NMR 600°C FOR 10 MINUTES 11.3K

Samples were also conditioned at 650°C for 10 minutes, the results of the ^{13}C NMR spectrum for these samples is shown in Figure 138. The trace at 650°C is similar to that obtained from

the 600C samples; the only obvious difference is the relative intensity of the peaks to the left and right of the main peak at 128 ppm. At 600°C, these peaks appear to have a similar relative intensity whilst at 650°C, the relative intensity of the peak on the right hand side (at lower chemical shift) is less suggesting that the ether oxygen bonds are disappearing at that temperature.

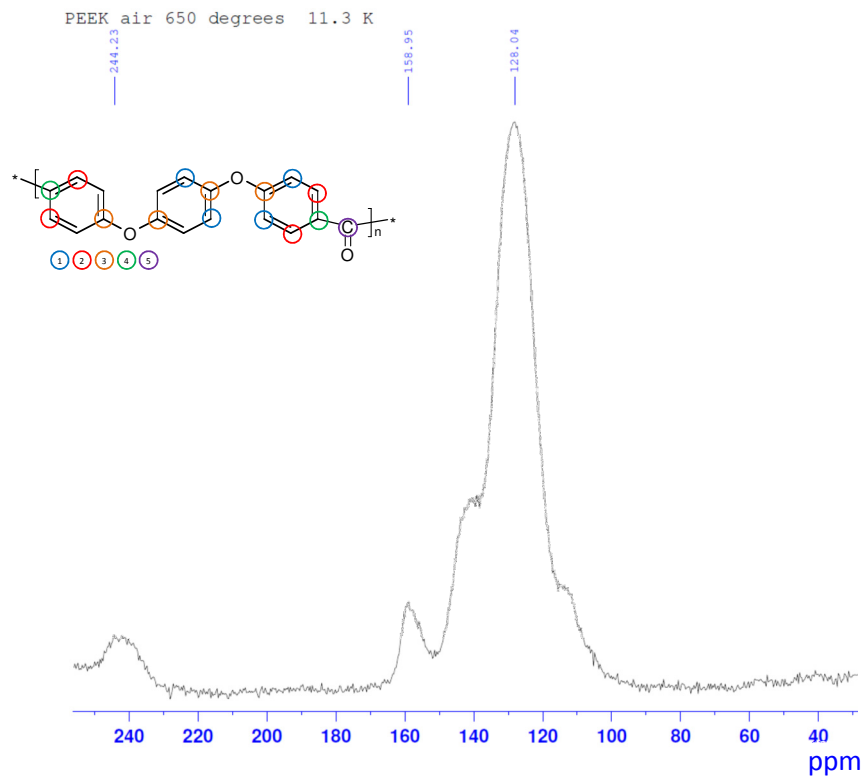


FIGURE 138. ^{13}C NMR 650°C FOR 10 MINUTES 11.3K

5.4 Summary

Peaks found in the dATR-FTIR of PEEK decomposed in air at a temperature of 400°C were attributed to the presence of a CH_2 stretch. These peaks were present when PEEK was heated for periods of time below the material's normal onset of decomposition temperature. There was no evidence for these peaks in the transmission FTIR and chemical shifts corresponding to these peaks were not found in the ^{13}C NMR, indicating that the processes occurring were doing so on the surface and not throughout the bulk of the material. For the purpose of this analysis the samples heated were small pieces of thin (100 μm) film. An

aldehyde C=O alludes to the formation of 1-phenoxy-4-(4-phenoxy aldehyde), probably an initial product of random chain scission in the condensed phase. SEM/EDAX of the glass fibre-filled chars from cone calorimeter experiments confirmed that the glass fibres in the matrix were responsible for the strengthened char structure that was allowing for a greater reduction in peak heat release rate in the cone calorimeter, compared to the carbon fibre-filled material. ^{13}C NMR showed that the carbonyl bond is the first bond to be broken, which is also maintained by the presence of an aldehyde C=O in the dATR-FTIR at 400°C. A diphenylether structure was observed at 650°C, indicating that some oxygen would be present in the initial char. As the temperature increased, the chemical shifts corresponding to the carbon atoms on the benzene rings moved closer to that which corresponds to graphite indicating that the oxygen atoms in the chain were being lost.

CHAPTER 6. THERMAL PROPERTY CALCULATIONS

In order to aid the interpretation of experimental data, a number of models of thermal decomposition and burning behaviour were investigated. These include the approach developed by Van Krevelen, separating polymers into ‘molar groups’, the somewhat simplistic model distinguishing between thermally thin and thermally thick burning behaviour and the one-dimensional pyrolysis model ThermaKin.

Separating molecules into their distinct molar groups has been used in the past as a means to calculate various flammability parameters and predict burning behaviour [102]. These calculations aim to relate the chemical structures of materials to their properties. Performing calculations for large structures, such as polymers can prove difficult. However, using their characteristic structural elements (such as -CH_3 or $\text{-C}_6\text{H}_5$) to determine the contribution made to a specific property and then adding them according to their mole fraction in the polymer repeat unit provides a simpler approach [103]. This method has been utilised to relate the thermal, mechanical, optical and flammability properties to the chemical structure of polymers, with excellent results [104]. Here these contributions will be used to determine whether or not these calculations apply to PEEK based on comparisons to data collected in previous chapters.

6.1 Molar Group Contributions

6.1.1 Thermal Analysis

The temperature of half decomposition ($T_{d,1/2}$) is the temperature at which the mass of the polymer, during pyrolysis (with temperature increasing at a constant rate), reaches 50% of its value [102]. Correlations have been noticed between this parameter and others relating to decomposition. However, since many polymers lose most (>50%) of their mass in the first stage of decomposition, this approach may be less successful with PEEK, which loses ~50% in the first stage.

$T_{d,0}$ is the temperature of initial decomposition, the temperature at which the loss of mass during heating is just measurable. This can be related to $T_{d,1/2}$ as follows:

$$T_{d,0} \approx 0.9T_{d,1/2}$$

$T_{d,max}$ is the temperature of the maximum rate of decomposition (with a temperature increase at a constant rate) and is related to $T_{d,1/2}$ in the following way:

$$T_{d,max} \approx T_{d,1/2}$$

$E_{act,d}$ is the average activation energy and can be established from the temperature dependence on the rate of mass lost. Although deemed inaccurate, due to the variation of this value during pyrolysis, this can be related to $T_{d,1/2}$ as follows:

$$E_{act,d} \approx T_{d,1/2} - 423$$

$T_{d,1/2}$ can be predicted using structural group contributions. The PEEK structure is shown below in (Figure 139) with structural group contributions assigned.

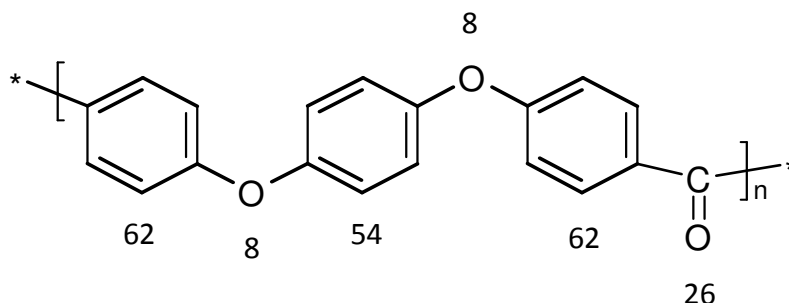


FIGURE 139. PEEK ASSIGNED WITH STRUCTURAL GROUP CONTRIBUTIONS FOR DECOMPOSITION

Due to the conjugation of the π -electrons, different values are given for such groups where conjugation with the neighbouring group is either one-sided, two-sided or, in some cases absent. These are shown in Table 47.

Chemical Group	$Y_{d,1/2i}$	N_i	$N_i \times Y_{d,1/2i}$ ($Y_{d,1/2}$)
	62	2	124
	54	1	54
	8	2	16
	20	1	26
Total			220

TABLE 47. SUMMARY OF STRUCTURAL GROUP CONTRIBUTIONS FOR DETERMINATION OF $T_{d,1/2}$

The following relationship can be used to determine $T_{d,1/2}$:

$$M \times T_{d,1/2} = Y_{d,1/2} = \sum_i N_i \times Y_{d,1/2i} \quad (2)$$

Using the values from Table 47 and that M for PEEK is 288.3 g mol^{-1} or $0.2883 \text{ kg mol}^{-1}$ (given that the units of $Y_{d,1/2}$ are K kg mol^{-1}) the following is established:

$$T_{d,1/2} = \frac{220}{0.2883} = 763.1 \text{ K}$$

Therefore, the calculated value of the temperature of half decomposition for PEEK is 763 K or 406°C.

Based on this value, and using the correlations stated previously, the following can also be calculated: $T_{d,0}$, $T_{d,max}$ and $E_{act,d}$.

The temperature of the initial decomposition of PEEK is almost equal to:

$$T_{d,0} \approx 0.9T_{d,1/2} \approx 687.6K$$

The temperature of the maximum rate of decomposition is almost equal to:

$$T_{d,max} \approx T_{d,1/2}$$

$$T_{d,max} \approx 763.1K$$

The average activation energy is almost equal to:

$$E_{act,d} \approx T_{d,1/2} - 423$$

$$E_{act,d} \approx 763.1 - 423$$

$$E_{act,d} \approx 340.1kJ$$

These results have been summarised in Table 48.

Parameter	Value
Temperature at half decomposition ($T_{d,1/2}$)	406°C
Temperature at initial decomposition ($T_{d,0}$)	364°C
Temperature at maximum rate of decomposition ($T_{d,max}$)	406°C
Average activation energy ($E_{act,d}$)	340 kJ

TABLE 48. SUMMARY OF DECOMPOSITION MOLAR GROUP CONTRIBUTION CALCULATIONS

The values shown are much lower than those collected experimentally for PEEK 450G. The temperature at half decomposition corresponds to 640°C in air and 760°C in nitrogen, from Figure 34 and Figure 45, respectively. Due to the fact that PEEK only loses ~50% mass during decomposition, using $T_{d,1/4}$ may be more consistent as this value represents 50% of the total mass lost in an inert atmosphere. The value for $T_{d,1/4}$ is 570°C in air and 589°C in nitrogen, both of which correspond better with the calculated values.

6.1.2 Flammability

The heat release capacity (η_c) is defined as the maximum heat release rate divided by the constant heating rate in an experiment [105] and is a combination of thermal stability and combustion properties such as the temperature of the peak mass loss rate and heat of complete combustion of the pyrolysis gases [32].

$$\eta_c = \frac{\psi}{M} = \frac{\sum_i n_i \psi_i}{\sum_i n_i M_i} = \frac{\sum_i N_i \psi_i}{\sum_i N_i M_i}$$

(3)

Where

η_c = heat release capacity ($\text{J g}^{-1} \text{K}^{-1}$)

ψ = molar heat release capacity ($\text{J mol}^{-1} \text{K}^{-1}$)

M_i = molar mass (g mol^{-1})

A physical means of measuring the heat release capacity has been developed [106] to evaluate the combustibility of milligram quantity samples. This method is the Pyrolysis Combustion Flow Calorimeter (PCFC) and can be used to directly measure the heat release capacity (η_c). This parameter can also be determined by means of calculation using the molar contributions of structural elements and adding these according to their mole fraction in the monomer unit. A correlation (based on the results of 80 polymers) of calculated and measured heat release capacities gives an average relative error of $\pm 15\%$ [32].

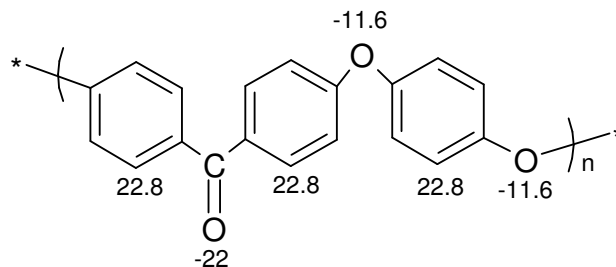


FIGURE 140. PEEK ASSIGNED WITH MOLAR GROUP CONTRIBUTIONS

Figure 140 shows the different values assigned to the structural elements which make up the monomer unit based on the structure of PEEK. These are summarised in Table 49.

Chemical Group	N	M_i (g mol ⁻¹)	ψ (kJ mol ⁻¹ K ⁻¹)	Ni M_i (g mol ⁻¹)	Ni ψ (kJ mol ⁻¹ K ⁻¹)
	3	76	28.8	228	86.4
	2	16	-11.6	32	-23.2
	1	28	-22	28	-22
Total:				288	41.2

TABLE 49. SUMMARY OF MOLAR GROUP CONTRIBUTIONS AND THEIR MOLE FRACTIONS

The final two columns in the table relate to the molar mass (M) and the molar heat release capacity (ψ) as described in (3). These values are substituted to give:

$$\eta_c = 143.1 \text{ J g}^{-1} \text{ K}^{-1}$$

The heat release capacity (η_c) is calculated as 143.1 J g⁻¹ K⁻¹. The value established through empirical methods using the PCFC was found to be 155 J g⁻¹ K⁻¹ [32] giving an 8% error. The heat release capacity (η_c) also correlates closely with the heat release rate – an important parameter with regards to predicting fire hazard [29] as is evident in Figure 141.

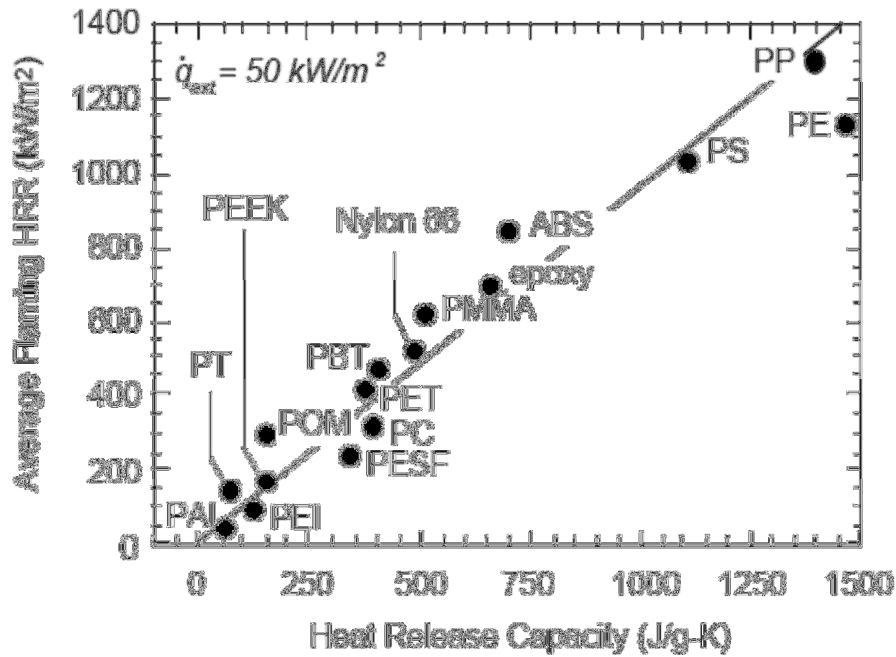


FIGURE 141. AVERAGE FLAMING HEAT RELEASE RATE (HRR) VS HEAT RELEASE CAPACITY (H_c) FOR NAMED POLYMERS [32]

Heat release capacity (η_c) as a parameter is also found to closely relate to flammability tests such as the UL-94 test. A high heat release capacity means a sharp fall in the TGA (in terms of fuel production). It is believed that for polymers with $\eta_c \leq 300 \text{ J g}^{-1} \text{ K}^{-1}$, self extinguishing behaviour is expected – a UL-94 V0 rating [32]. In LOI experiments, values greater than 21% occur when $\eta_c < 550 \pm 100 \text{ J g}^{-1} \text{ K}^{-1}$ at ambient conditions (298 K, 21% O_2) [32]. The creators of this method proposed that initial molecular-level design of fire resistant polymers can be achieved without the expense of synthesis and testing [32].

6.1.3 Char Formation

Another method has been developed to calculate the char-forming tendency (C_{FT}) of polymers through structural group contributions. Van Krevelen has deduced that the char-forming tendency of a polymer is an additive quantity and based on this, the following relationship has been created:

$$CR \approx \frac{\sum (C_{FT})_i}{M} \times 1200$$

(4)

Where

CR = Char Residue (%)

C_{FT} = Char-Forming Tendency (no units)

M = Molecular Weight

Similar to the method above, each structural group is assigned a value, although this parameter cannot be calculated for polymers which contain halogenated species as their soot-forming tendencies would significantly affect the char formation [102]. Aliphatic groups, unless connected to aromatic nuclei, are assigned a value of zero.

Figure 142 shows the values assigned to the structural groups which make up the monomer unit in PEEK:

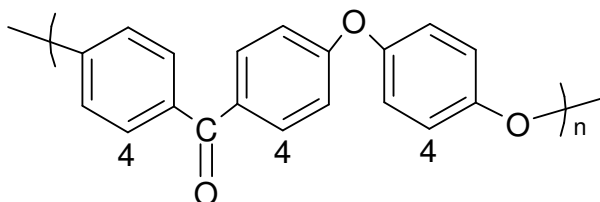


FIGURE 142. PEEK ASSIGNED WITH STRUCTURAL GROUP CONTRIBUTIONS FOR CHAR

These values are summarised in Table 50.

Chemical Group	Value	N	C_{FT}
	4	3	12
	0	2	0
	0	1	0
Total			12

TABLE 50. SUMMARY OF STRUCTURAL GROUP CONTRIBUTIONS AND THEIR CHAR-FORMING TENDENCIES

The C_{FT} of PEEK has been determined as 12 and therefore the char residue will amount to 144 g per structural unit of PEEK. The molecular weight of the PEEK monomer unit is 288.3 g mol^{-1} . These values have been substituted to give:

$$CR \approx \frac{12}{288} \times 1200 = 50\%$$

The calculated char residue (CR) is 50%. This is slightly greater than char yields determined by experimental methods which give values ranging from 41% [10] – 47% [59] [107].

The value for the calculated char residue (CR) can also be correlated with another parameter of flammability – the oxygen index (OI). This can be achieved using the following:

$$OI = \frac{17.5 + 0.4CR}{100} \quad (5)$$

Using the value previously calculated for char residue (50%), the following can be inferred:

$$OI = 37.5\%$$

The values determined through molar group contributions have been summarised in Table 51.

Parameter	Value
Heat Release Capacity (η_c)	$143.1 \text{ J g}^{-1} \text{ K}^{-1}$
UL-94	V-0
Char Forming Tendency (C_{FT})	50%
Limiting Oxygen Index (LOI)	37.5%

TABLE 51. SUMMARY OF FLAMMABILITY MOLAR GROUP CONTRIBUTION CALCULATIONS

All values which have been calculated above have been determined experimentally to establish the validity of the method with regards to PEEK. Unfilled PEEK obtains a V-0 rating in the UL-94 test. The polymer also shows around 50% char residue in the TGA in N_2 and in the cone calorimeter. The LOI of PEEK was determined to be 37.3% for the unfilled 450G and 150G samples and the heat release capacity, determined from the PCFC was $151 \text{ J g}^{-1} \text{ K}^{-1}$. In terms of flammability, molar group contributions relate well to the experimental data for PEEK. These

calculations may be useful for a polymer which exhibits so much scatter in flammability tests as determining 'average' data from experiments is not representative. However, it may also be that PEEK was used as one of the polymers from which the molar group data was first generated.

6.2 Cone Calorimeter Time to Ignition

The time to ignition parameter in the cone calorimeter showed much scatter for all PEEK samples, with filled samples which subsequently changed the colour of the polymer to black deemed as having the greatest effect on increasing this scatter. Piloted ignition occurs when the heat released from the combustion of volatilised fuel is sufficient to vaporise its replacement from the condensed phase. For the horizontal sample configuration of the cone calorimeter, only a small portion of the radiant heat will be transmitted back to the condensed phase fuel and therefore, only a portion of this heat will result in fuel volatilisation. For thermally thick solids (typically thicknesses above 15 mm [25]) the thermal inertia, $k\rho c$, the product of thermal conductivity (k), density (ρ), and specific heat (c), governs the material's ignition and flame spread properties. This determines the rate of rise in surface temperature, and consequently the time to ignition [22]. The time to ignition (t_{ig}) of a thermally thick solid exposed to a constant heat flux (\dot{Q}_R^2) has been expressed in the following equation:

$$t_{ig} = \frac{\pi}{4} k\rho c \frac{(T_{ig} - T_0)^2}{\dot{Q}_R^2} \quad (6)$$

Where T_{ig} and T_0 are the ignition and ambient temperatures, respectively. The material properties $k\rho c$ are known, at least in ambient conditions; an estimate for the temperature at ignition is obtained as the peak heat release temperature from PCFC data. Therefore, the ignition delay time can be predicted. For samples tested in the cone calorimeter of 2.5 mm thickness, the thermally thin scenario may apply. The time to ignition of a thermally thin solid exposed to a constant heat flux has been expressed through the following:

$$t_{ig} = \rho c \tau \frac{(T_{ig} - T_0)}{\dot{Q}_R} \quad (7)$$

Where τ is the thickness of the material expressed in metres. The input values used in these calculations and the data obtained are shown in Table 5. The experimental data for this table was obtained from the ‘scatter in the cone calorimeter’ experiments. It is important to note here that the relationship between these parameters and the time to ignition ignores heat losses and assumes a constant heat flux and that the material properties remain constant up to the point of ignition. The thermally thin time to ignition correlates more closely to the experimental value for 450G. The calculated time to ignition for the fibre-filled composites is lower (due to a lower value for specific heat) and suggests thermally thick burning behaviour.

	<i>Input Data</i>				<i>Predicted Thermally Thin</i> t_{ig}	<i>Predicted Thermally Thick</i> t_{ig}	<i>Actual Cone</i> t_{ig}
	k	ρ	c	T_{ig}			
	$\text{W m}^{-1} \text{K}^{-1}$	Kg m^{-3}	$\text{J Kg}^{-1} \text{K}^{-1}$	K			
450G	0.25	1300	2160	884	82	76	154 ± 13
450CA30	0.92	1410	1850	886	76	261	287 ± 78
450GL30	0.43	1510	1710	888	76	121	186 ± 48

TABLE 52. TIME TO IGNITION PARAMETERS, PREDICTION AND COMPARISON WITH ACTUAL DATA AT 50 KW M⁻²

The thermally thin scenario assumes uniform heating through the bulk of the polymer. From the shapes of the heat release rate curves produced (see Figure 93), it is evident that this is not the case and although the samples are 2.5 mm, the burning layer penetrates through the bulk of the material rather than the whole sample burning simultaneously (as expected for thermally thin polymers). The thermally thick calculations show the same time to ignition hierarchy as experimental data with 450G igniting first (at 76 seconds), followed by 450GL30 (at 121 seconds) and 450CA30 (at 261 seconds). In reality, 450GL30 ignites earlier than the carbon fibre-filled composite and so, the thermally thick model of ignition better illustrates the differences between the fibre-filled composites, indicating that PEEK 450G at 2.5 mm and 50 kW m⁻² is exhibiting behaviour that is intermediate between thermally thin and thermally thick, or thermally thin with charring behaviour. Both of these factors may be attributed to the

large difference in thermal conductivity between the filled composites. 450CA30 has a thermal conductivity of $0.920 \text{ W m}^{-1} \text{ K}^{-1}$: the thermal conductivity of 450GL30 is less than half that of 450CA30 at $0.430 \text{ W m}^{-1} \text{ K}^{-1}$. This is as expected, as the presence of carbon increases thermal conductivity of a material. In the cone calorimeter, a material with a lower thermal conductivity will ignite earlier – due to the lesser ability of the sample to conduct heat through its entire volume – causing a build up of heat at the surface. Interestingly, the thermal conductivity of 450G is under half that of 450GL30 although here, there is only an average ignition delay of around 30 seconds between 450G and 450GL30 indicating that other material properties such as absorption, reflectivity changing thermal conductivity and heat capacity may be having an effect.

Using the equation for the thermally thick scenario (6), the time to ignition for samples exposed to different heat fluxes in the cone calorimeter have been determined and compared to the actual values determined from the varied heat flux experiments (Section 4.4.5). The results are summarised in Table 53. The experimental t_{ig} values are higher than the calculated t_{ig} values in all instances.

External Heat Flux (kW m^{-2})	Calculated t_{ig} (s)	Experimental t_{ig} (s)
45	93	208 (± 38)
50	76	130 (± 4)
55	63	92 (± 4)
60	53	91 (± 3)
65	45	72 (± 3)
70	39	64 (± 4)

TABLE 53. t_{ig} CALCULATED AND EXPERIMENTAL FOR VARIED HEAT FLUXES

As this equation does not take into account the thickness of the sample, as the thermally thick equation predicts an ignition time of 76 seconds, independent of thickness, the thermally thin equation will be utilised to determine whether the time to ignition can be estimated for samples of varying thickness. The results are summarised in Table 54. The closest correlation between calculated and experimental time to ignition occurs with the thickest samples, 10 mm. The experimental error includes the calculated t_{ig} value. The other values do not correlate so well.

Thickness (mm)	Calculated t_{ig} (s)	Experimental t_{ig} (s)
2.5	82	130 (± 4)
3.2	105	186 (± 29)
3.5	115	245 (± 85)
6	197	262 (± 6)
10	329	300 (± 36)

TABLE 54. t_{ig} CALCULATED AND EXPERIMENTAL FOR VARIED THICKNESSES

6.3 ThermaKin

Numerous studies [108] [109] [110] have effectively demonstrated that a numerical pyrolysis model can be used to determine the relationships between the fundamental physical and chemical properties of polymeric materials and their gasification behaviour. Typically, the model is used to calculate the mass loss rate of a one-dimensional sample exposed to a perpendicular heat source. To date, ThermaKin has been effectively utilised for the prediction and/or extrapolation of the results of fire calorimetry experiments [111] [112] [113] [114]. The model, which combines the transport of thermal energy with Arrhenius kinetics for the decomposition of the polymer, predicts the overall behaviour of a pyrolysing object through mass and energy conservation equations. These equations are formulated in terms of rectangular finite elements, each element being characterised by component mass and temperature. Additionally, the model describes the transport of gaseous products through the condensed phase and follows changes in the volume of the bulk material. Examples of material properties utilised by the model are: density, heat capacity, emissivity, thermal conductivity, and absorption coefficient. The processes modelled by ThermaKin are detailed in Figure 143. Radiant heat produced by the cone calorimeter, from above, is absorbed, emitted and reflected, and the condensed phase heat transfer process is modelled through the solid. The temperature increases which in result drive the endothermic decomposition processes which lead to the gasification of volatile fuel components. When a critical mass flux for ignition is reached, ignition will occur, and the incident heat flux is added to by the radiation produced by the flame. Therefore, quasi-steady state conditions pertain, until the sample is so thin that it has no more capacity to absorb heat, and the rate of pyrolysis increases.

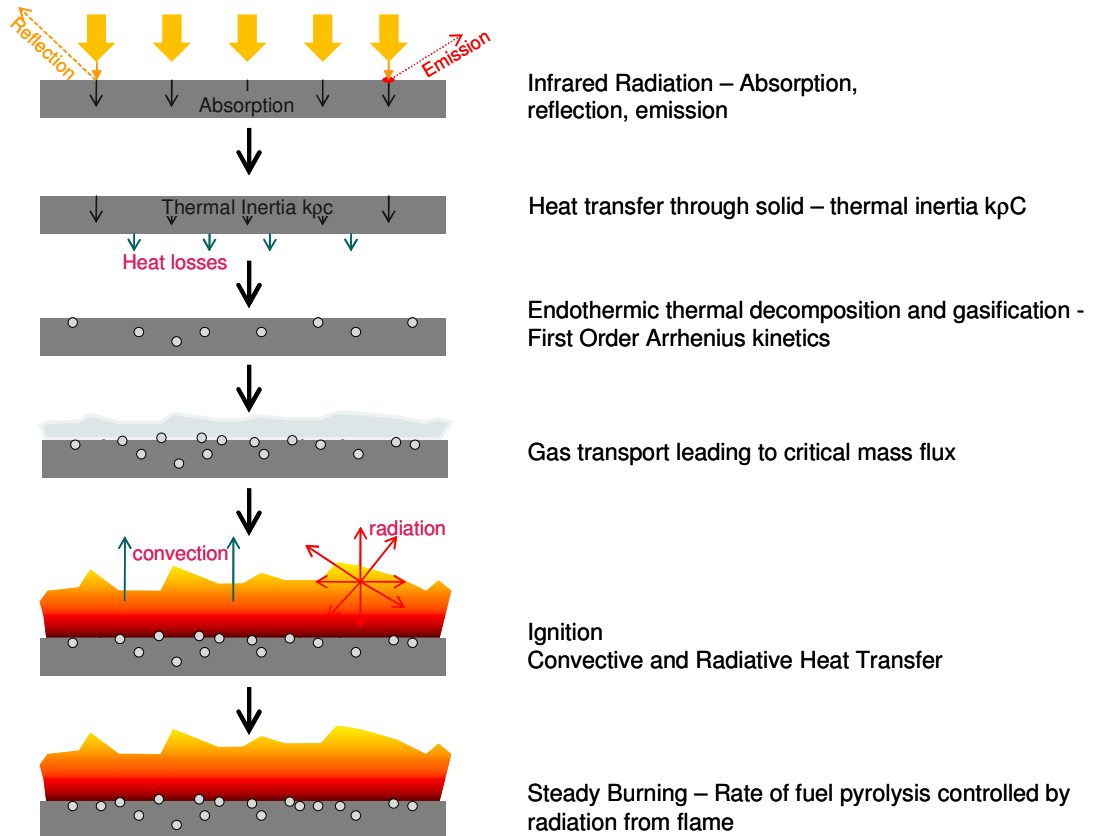


FIGURE 143. SCHEMATIC OF THE PROCESSES OCCURRING IN THE CONE CALORIMETER, AS MODELLED BY THERMAKIN

The outputs of the ThermaKin model allow for numerical differentiation of the material's mass versus time to obtain a mass loss rate. This, multiplied by the heat of combustion of the polymer being studied can produce a heat release rate for the material. When utilising the ThermaKin model, it became apparent that parameters such as the activation energy and Arrhenius factor (which when calculated in this thesis by different methods are represented by significantly different values) had a pronounced effect on the heat release rate curves created. The concept of determining the 'correct' value of the activation energy and Arrhenius factor are outside the scope of this thesis and so instead of using ThermaKin to determine heat release data for PEEK, the model was utilised as a means of explaining the effect different physical and chemical properties have on the resulting heat release curves of polymers in general. Those who are interested are referred to 'Influence of Physical Properties on Polymer Flammability in the Cone Calorimeter'.

CHAPTER 7. CONCLUSIONS AND FURTHER WORK

The aim of the project was to acquire an understanding of the decomposition and flammability behaviour of polyetheretherketone (PEEK), in order to develop fire safe PEEK-based materials, and open up new markets.

In conclusion, the main thrust of this work has been to understand the behaviour of PEEK in a variety of industry standard tests in terms of the mechanism of its thermal decomposition. Further research directions are also outlined as a means of providing the next steps towards developing PEEK materials with enhanced fire safety.

7.1 Burning Behaviour

From the thermal decomposition studies it is evident that PEEK is a polymer with extraordinary thermal stability. Although the polymer melts at 343°C, and subtle changes are evident at around 450°C, there is no significant mass loss (and hence fuel production, as observed in the TGA and PCFC) until the surface of the polymer reaches 580°C. This is 200-400°C above most common polymers. The decomposition is a two step process in air with the initial loss of phenol, benzene, carbon monoxide and carbon dioxide, leaving sufficient active sites on the remaining aromatic rings to promote cross-linking, and subsequently char formation. This work has shown that the ketone group is lost before either ether group, and some of the ether groups are still present in the cross-linked char at 650°C. In an inert environment, thermal decomposition occurs via a three-step process, the final step being attributed to a slow decomposition of the char. In both the TGA and cone calorimeter studies, the mass of the char is a fairly constant 50% of the original mass of PEEK, a ratio which remained largely unchanged in the presence of inert fillers. The char of the unfilled material has a fine needle-like structure and occupies a volume around 10 to 20 times that of the original polymer forming a pyramid-like structure in the cone calorimeter. After this first fuel production step, the char slowly oxidises at temperatures above 700°C, seen clearly at the end of all cone calorimeter experiments as a low, constant heat release rate of around 50-60 kW m⁻². The mass loss in the cone calorimeter after the end of the main peak of heat release corresponds to the char yield at 640°C in the TGA under a nitrogen atmosphere suggesting this

is the onset temperature of char oxidation (provided the char is homogenous and sitting under a flame). However, towards the end of flaming it is likely that some oxidative decomposition of the char has also occurred. In a large fire scenario, the presence of the char may protect the underlying polymer from further decomposition and volatilisation.

7.2 Effect of Thickness

The sample thickness exerts a significant influence on the burning behaviour, although this varies with test scenario and geometry. As the thickness of samples increase, the type of burning behaviour observed is altered from thermally thin to thermally thick. Samples which are thermally thin burn as one entity whereas samples which are thermally thick burn progressively from top to bottom, often with a peak of heat release towards the end of burning, as heat is no longer conducted into the sample, more is available for pyrolysis. This thermally thick behaviour was observed in samples which were 6 mm and 10 mm at 50 kW m⁻². Calculations were used to predict the time to ignition of samples of varying thickness. The equation predicting time to ignition of thermally thin samples was utilised as the equation corresponding to thermally thick ignition assumes the sample is infinitely thick. Even with the scatter in the experimental data (discussed in 7.5), the predicted times to ignition were much shorter than the experimentally determined values. Even the 10 mm sample (a thickness which should have been considered thermally thick) gave a time to ignition of 76 seconds. The longer actual time to ignition suggests that the early thermal decomposition process may result in some degree of protection (graphite-like layer on the surface of PEEK) not predicted by the simple equation.

In contrast, for thinner films tested in the small-flame ignitability test (ISO 11925) tests, as the thickness of the sample increased from 25 µm to 250 µm, so did the rate of upward flame spread. This is as expected, due to the greater amount of material that is present in thicker samples. In an earlier study [115] in the LOI, the effect of thickness from 25 µm to 625 µm is also apparent but this time for downward flame spread, where thicker samples showed a higher LOI rating.

7.3 Effect of PEEK Viscosity

As might be expected, changing the viscosity (or molecular weight) of PEEK shows only small differences in the TGA in both an inert and oxidative atmosphere since the decomposing polymer is contained within the pan and the first stage of polymer decomposition predominantly follows random chain scission. In the flammability tests, the lower viscosity, shorter chain length material can result in burning drips in the UL-94. The same behaviour however, permits for a higher LOI rating as the sample drips away from the flame. This is not seen with the higher (450G) viscosity samples. Dripping can have a profound and somewhat unpredictable effect on fire development in real fires. In some cases, such as electrical fires, an overheating component can melt an adjacent polymer which may shrink away and therefore prevent ignition. In other geometries, polymers can drip towards the heat source resulting in ignition. Once ignited, flaming drips can transfer flames downwards (normally flame spread is only upward or horizontal). Standard fire tests treat dripping inconsistently. In the LOI dripping is advantageous (as observed with lower viscosity PEEK samples), removing fuel from the flame. In the UL-94 flaming drips result in a fail (V-2 classification). The cone calorimeter attempts to disregard dripping behaviour by containing the fuel in a tray of aluminium foil. As differences were observed as the viscosity of sample increases this shows viscosity also influences other aspects of burning behaviour. In the cone calorimeter, the higher viscosity 450G material shows the highest peak heat release rate implying that the sample takes longer to heat and for fuel production to occur, before the criteria for ignition are met. 450G, as a result, releases more heat when it finally ignites. In the TGA in nitrogen, and in the PCFC, 90G begins to lose mass (TGA) or release heat (PCFC) at a lower temperature than 150G and 450G, presumably due to the shorter chain lengths, suggesting the influence of ends on the decomposition process. Even prior to ignition most decomposition occurs in the bulk (forming bubbles of fuel anaerobically) 90G ignites earlier (140 seconds for 90G rather than 180 seconds for 450G), thus the lower peak for 90G occurs because during burning more of the energy is used to heat the polymer than for the already preheated 450G.

7.4 Effect of Fillers

The presence of fillers has several effects complicating interpretation of the decomposition process. From thermal decomposition studies, it was determined that the presence of filler materials within the PEEK matrix did not have an effect on the first stage of

PEEK decomposition (other than to reduce the mass lost by 30% for the presence of 30% filler). This stage resulted in the loss of around 35% mass (within a 30°C window) in air and in nitrogen. The effect of fillers on decomposition was observed during the second stage whereby the temperature corresponding to 40% residue (T_{40}) (e.g. 10% of PEEK residue) increased with the presence of filler. Although all fillers were present at 30%, T_{40} varied by different amounts for different fillers. The presence of filler materials increases the thermal stability of PEEK in various flammability tests and in the TGA, however, these fillers do not affect the gas-phase products as observed in the TGA-FTIR and pyGC/MS and so, presumably, the decomposition mechanism of PEEK remains unchanged. The presence of fillers in the cone calorimeter and PCFC experiments show differences in terms of the hierarchy of these materials. In the cone calorimeter, the presence of 30% carbon fibre and 30% glass fibre reduced the peak of heat release by 65% and 73%, respectively. In the PCFC, these reductions were 35% and 23% although 30% may have been expected from the filler loading. This suggests that the carbon fibre is promoting char formation in the PCFC whereas the glass fibre appears to be promoting gasification. The presence of filler increases the viscosity of the melt and as a result, prevents dripping. Fillers also improve the structure of the char, leaving a protective residue, as observed in the cone calorimeter, but barely evident in the 5 mg samples used in the PCFC. In summary, on a microscopic level, glass fibre increases the rate of gasification while carbon fibre promotes char formation, whereas on a macroscopic level, glass fibre is not oxidised and reinforces the char structure, where carbon fibre may promote char formation but it itself subject to oxidation.

7.5 Quantifying PEEK Flammability

The behaviour of PEEK in most flammability tests is inconsistent in two ways: within any test there is a high degree of scatter in the data, although this is not an intrinsic property of the polymer as seen in the very reproducible TGA curves; between different tests, the rank order of different materials shows no consistent behaviour. This is indicative of its very high thermal stability of PEEK and the unsuitability of most flammability tests, designed for polymers of much lower thermal stability, to quantify its burning behaviour. This has been most apparent in the UL-94 and cone calorimeter. In order to address the issue of scatter, samples were tested at higher external heat fluxes, with the presence of additives and using different methods of conditioning. In the cone calorimeter, at higher heat fluxes, the scatter in the time to ignition was reduced, due to the external heat flux being further from the critical

heat flux for ignition (36 kW m^{-2}). However, no further reduction in scatter was seen at the highest heat flux selected (70 kW m^{-2}). A hotter flame in the UL-94 also reduced the total flaming time of samples by 23% from 91 seconds to 70 seconds. Samples containing additives, in particular, additives which caused a subsequent colour change in the composite polymer increased the scatter in the data. This is presumably due to changes in absorption (reflection/emissivity) of infrared radiation. As well as providing more consistent data, PEEK exposed to higher heat fluxes shows lower flammability, both in the cone calorimeter and UL-94. As the mechanism of fire protection for PEEK is char formation which occurs above 640°C , this requires hotter temperatures than, for example, a gas phase mechanism which would take effect when the polymer initially decomposes (in the case of Polypropylene around 350°C , for PEEK above 550°C). Most tests are designed to discriminate between polymers of a similar, high flammability and appear inadequate for high temperature polymers, such as PEEK. As an example, the UL-94 test at 50 W and the cone calorimeter at 50 kW m^{-2} are so close to the limits of ignitability for PEEK that excessive scatter is observed in the data.

7.5.1 Effect of Moisture

When samples absorbed small amounts of moisture, the scatter in the peak of heat release rate decreased significantly, giving more reproducible data, but also earlier times to ignition. Longer burn times (an increase of $\sim 50\%$) are experienced in the UL-94 as a result of testing PEEK which has been allowed to absorb moisture.

PEEK absorbs 0.5% moisture by mass at saturation. When moisture is present in PEEK, the reaction to fire behaviour changes, as seen in both the cone calorimeter and UL-94 with an earlier time to ignition and longer burn times, respectively. The presence of this moisture results in small bubbles, believed to be water vapour, forming when the PEEK melts at 343°C , penetrating on the surface of samples during testing in the cone calorimeter. These are not seen where samples have had their moisture removed by drying for 7 days (168 hours) at 100°C . This foamed PEEK has a lower thermal inertia ($k\rho c$) so the surface heats more quickly, resulting in ignition, while the underlying polymer remains cooler.

7.6 Further Work

Problems which have arisen must be solved in order to gain a better understanding of PEEK's flammability. This includes scatter in the burning behaviour data, the effect of moisture, investigating the use of higher heat fluxes in industry standard tests and the mechanism of char formation. This leads to the question of how well these industry standard tests reflect the actual burning behaviour of the material in real fires. These problems suggest some research directions which could be pursued practically in order to achieve a greater understanding of the decomposition and flammability of PEEK and its compounds.

Further investigation is needed to determine the actual mechanism behind the higher flammability of PEEK containing moisture. Three notions are proposed in this thesis, increased surface area, thin surface layer formation and foam-like behaviour. If the presence of moisture is determined to be a major cause of scatter in the results of all the flammability tests, this is not just significant in terms of further work but would also pinpoint the reasons behind scatter in the data for industries which utilise PEEK.

It is evident that fire retardants activated in the temperature range 200 – 400°C are unlikely to work with PEEK, and it seems likely that a new approach to high temperature fire retardancy and particularly char promotion must be developed. One approach may be the use of various types of nanoparticulate carbon. For example, incorporating carbon nanotubes into PEEK could be used to establish whether or not these composites show reduced flammability. In this thesis it has been suggested that the presence of carbon as a filler, due to either its presence in the matrix as an oxidisable char former, or the subsequent colour change caused, increases scatter in the cone calorimeter data. This scatter can be reduced by testing at higher heat fluxes.

It would also be beneficial to investigate the influence of higher heat fluxes in other flammability tests. It has been suggested that the inconsistent behaviour of PEEK in the OSU Calorimeter may be due to the low external heat flux employed by this test (35 kW m⁻²). The critical heat flux for ignition of 450G has been determined at 36 kW m⁻² and therefore, testing at such low heat fluxes will result in highly scattered data. Testing at a minimum of 45 kW m⁻² in this test may provide more consistent results and subsequently, allow PEEK to pass this test due to the greater amount of energy that is provided for the char-forming mechanism to take effect.

This thesis presents data on some of the initial products of thermal decomposition demonstrating that the carbonyl bond is the first to be broken. Further understanding of the products formed during the initial stages and the decomposition mechanisms arising would allow identification of the intermediate species which may be formed. Knowledge of intermediate products and mechanisms may provide information as to the types of fire retardants which would be most effective.

REFERENCES

- 1 Rose, J. B., and Staniland, P.A., Thermoplastic Aromatic Polyketones. European Patent 0001879B2, August 22 (1978).
- 2 Hergenrother, P. M., Thompson, C. M., Smith Jr, J. G., Connell, J. W., Hinkley, J. A., Lyon, R. E., and Moulton, R., (2005), *Flame Retardant Aircraft Epoxy Resins Containing Phosphorus*. *Polymer*. Volume 46, Issue 14. Pages 5012-5024.
- 3 Morgan, A. B., Gagliardi, N. A., Price, W.A., and Galaska, M. L., (2009), *Cone Calorimeter Testing of S2 Glass Reinforced Polymer Composites*. *Fire and Materials*. Volume 33, Issue 7. Pages 323-344.
- 4 Matsui, J., (1995), *Polymer Matrix Composites (PMC) In Aerospace*. *Advanced Composite Materials*. Volume 4, Issue 3. Pages 197-208.
- 5 Cole, K. C., and Casella, I. G., (1992), *Fourier Transform Infrared Spectroscopic Study of Thermal Degradation in Films of Poly(Ether Ether Ketone)*, *Thermochimica Acta*. Volume 211. Pages 209-228.
- 6 Cole, K. C., and Casella, I. G., (1993), *Fourier Transform Infrared Spectroscopic Study of Thermal Degradation in Poly(Ether Ether Ketone) – Carbon Composites*, *Polymer*. Volume 34, Issue 4. Pages 740-745.
- 7 Huo, R., Luo, Y., Liang, L., Jin, X., and Karasz, F. E., (1990), *Kinetic Studies on Thermal Degradation of Poly(Aryl Ether Ether Ketone) and Sulphonated Poly(Aryl Ether Ether Ketone) by Thermogravimetry*. *Journal Of Functional Polymers*. Volume 4. Pages 426-433
- 8 Nam, J. D., and Seferis, J. C., (1992), *Generalised Composite Degradation Kinetics for Polymeric Systems under Isothermal and Nonisothermal Conditions*. *Journal of Polymer Science*. Volume 30, Issue 5. Pages 455-463.
- 9 He, J., Duan, X., and Wang, Z.-X., (1997), *Study on the Kinetics and Mechanism of Thermal Degradation of PEEK by Temperature Programmed Decomposition*. *Acta Chimica Sinica*. Volume 55, Issue 12. Pages 1152-1157.
- 10 Zhang, H., (2004), *Fire-Safe Polymers and Polymer Composites*. US Department Of Transport. Report Number: DOT/FAA/AR-04/11. Federal Aviation Administration.
- 11 Patel, P., Hull, T. R., McCabe, R. W., Flath, D., Grasmeyer, J., and Percy, M., (2010), *Mechanism of Thermal Decomposition of Poly(Ether Ether Ketone) (PEEK) From a Review of Decomposition Studies*. *Polymer Degradation and Stability*. Volume 95, Issue 5. Pages 709-718.
- 12 Hirschler, M. M., (2000), *Chemical Aspects of Thermal Decomposition of Polymeric Materials*. Chapter 2. In Grand, A. F., and Wilkie, C. A., *Fire Retardancy of Polymeric Materials*. CRC Press, New York, USA.
- 13 Harper, C., A., (2006), *A Handbook of Plastic Technologies*. Chapter 1. McGraw-Hill Professional Publishing, Ohio, USA.
- 14 Nicholson, J. W., (2006), *The Chemistry of Polymers*. 3rd Edition. RSC Publishing.
- 15 Seymour, R. B., and Charrager, C. E., (1992), *Polymer Chemistry: An Introduction*. 3rd Edition. Marcel Dekker, New York, USA.

-
- 16 Ziff, R. M., and McGrady, E. D., (1986), *Kinetics of Polymer Degradation*. Macromolecules. Volume 19, Issue 10. Pages 2513-2519.
- 17 Hilado, C., J., (1998), *Flammability Handbook for Plastics*. Fifth Edition. Chapter 2. Technomic Publishing Company Inc, Pennsylvania, USA.
- 18 Hull, T. R., and Stec, A. A., (2009), *Polymers and Fire*. Chapter 1. In Hull, T. R., and Kandola, B., K., *Fire Retardancy of Polymers: New Strategies and Mechanisms*. Royal Society of Chemistry, UK.
- 19 Crompton, T. R., (1989), *Analysis of Polymers: An Introduction*. Pergamon Press. Oxford, UK.
- 20 ASTM E698-05: 2004. Standard Test Method for Arrhenius Kinetic Constants for Thermally Unstable Materials. ASTM International, West Conshohocken, PA, USA.
- 21 ASTM E1641-0: 2004. Standard Test Method for Decomposition Kinetics by Thermogravimetry. ASTM International, West Conshohocken, PA, USA.
- 22 Drysdale, D., (1998), *An Introduction to Fire Dynamics*. Second Edition. Chapter 6. John Wiley & Sons, Colchester, UK.
- 23 Karlsson, B., and Quintiere, J. G., (2000), *Enclosure Fire Dynamics*. CRC Press, New York, USA.
- 24 Nelson M. I., and Brindley, J., (1999), *Polymer Combustion: Effects of Flame Emissivity*. Philosophical Transactions: Mathematical, Physical and Engineering Sciences. Volume 357. Number 1764. Pages 3655-3673. The Royal Society.
- 25 Quintiere, J. G., (1997), *Principles of Fire Behaviour*. Delmar Publishers, New York, USA.
- 26 Carpenter, K., and Janssens, M., (2005), *Using Heat Release Rate to Assess Combustibility of Building Products in the Cone Calorimeter*. Fire Technology. Volume 41, Number 2. Pages 79-92.
- 27 Friedman, R., Friedman, J., and Linville, L., (2003) *Principles of Fire Protection Chemistry and Physics: Part II – Fire Protection Chemistry and Physics*. Chapter 10 – Fire Characteristics: Solid Combustibles. 3rd Edition. Jones and Bartlett Publishers, London, UK.
- 28 Lyon, R. E., and Walters, R., (2002), *A Microscale Combustion Calorimeter*. US Department of Transport. Report Number: DOT/FAA/AR-01/117.
- 29 Babrauskas, V., and Peacock, R. D., (1992), *Heat Release Rate: The Single Most Important Variable in Fire Hazard*. Fire Safety Journal. Volume 18, Issue 3. Pages 255-272.
- 30 Babrauskas, V., (2000), *Fire Test Methods for Evaluation of Fire-Retardant Efficacy in Polymeric Materials*. Chapter 3. In Grand, A. F., and Wilkie, C. A., *Fire Retardancy of Polymeric Materials*. CRC Press, New York, USA.
- 31 BS EN 4589-2: 1999. Plastics – Determination of Burning Behaviour by Oxygen Index – Part 2: Ambient-Temperature Test.

-
- 32 Walters, R., and Lyon, R. E., (2001), *Calculating Polymer Flammability from Molar Group Calculations*. US Department of Transport. Report Number: DOT/FAA/AR-01/31.
- 33 Fenimore, C. P., and Martin, F. J., (1966), *Candle-Type Test for Flammability of Polymers*. Modern Plastics. Volume 43, Page 141.
- 34 Van Krevelen, D. W., (1990), *Properties of Polymers*. Chapter 26 – Product Properties (II) Environmental Behaviour and Failure. 3rd Edition. Elsevier Science Publishers, Amsterdam.
- 35 BS EN 60695-11-10: 1999. Fire Hazard Testing – Part 11-10: Test Flames – 50 W Horizontal and Vertical Flame Test Methods.
- 36 ISO 5660-1: 1993. Fire Tests on Building Materials and Structures. Part 15-Method for Measuring the Rate of Heat Release of Products.
- 37 Babrauskas, V., (1995), *The Cone Calorimeter*. Chapter 3: Section 3. In SFPE Handbook of Fire Protection Engineering. 2nd Edition. SFPE/NFPA.
- 38 Scharfel, B., and Hull, T. R., (2007), *Application of Cone Calorimetry to the Development of Materials with Improved Fire Performance*. Fire and Materials. Volume 31. Pages 327-354.
- 39 ASTM D7309: 2007. Standard Test Method for Determining Flammability of Plastics and Other Solid Materials Using Microscale Combustion Calorimetry. ASTM International, West Conshohocken, PA, USA.
- 40 ASTM E 906: 2006. Standard Test Method for Heat and Visible Smoke Release Rates for Materials and Products. ASTM International, West Conshohocken, PA, USA.
- 41 FAR 25.853 A-1, (2000), *Heat Release Test for Cabin Materials*. Aircraft Materials. DOT/FAA/AR-00/12
- 42 ISO 5658-2:2006. Reaction to Fire Tests – Spread of Flame. Part 2-Lateral Spread on Building and Transport Products in Vertical Configuration.
- 43 Price, D., Cunliffe, L. K., Bullet, K. J., Hull, T. R., Milnes, G. J., Ebdon, J. R., Hunt, B. J., and Joseph, P., (2007), *Thermal Behaviour of Covalently Bonded Phosphate and Phosphonate Flame Retardant Polystyrene Systems*. Polymer Degradation and Stability. Volume 92. Pages 1101-1114.
- 44 Kuo, M. C., Tsai, C. M., Huang, J. C., and Chen, M., (2005), *PEEK Composites Reinforced By Nano-Sized SiO₂ and Al₂O₃ Particulates*. Materials Chemistry and Physics. Volume 90. Pages 185-195.
- 45 Murari, A., and Barzon, A., (2003), *Comparison of New PEEK Seals with Traditional Helicoflex for Ultra High Vacuum Applications*. Vacuum. Volume 72, Issue 3. Pages 327-334.
- 46 Yesodha, S. K., Pillai, C. K. S., and Tsutsuni, N., (2004), *Stable Polymeric Materials for Non-Linear Optics: A Review Based on Azobenzene Systems*. Progress in Polymer Science. Volume 29, Issue 1. Pages 45-74.

-
- 47 Stevens, M. P., (1999), *Polymer Chemistry: An Introduction*. Third Edition. Oxford University Press, New York, USA.
- 48 Kashiwagi, T., (1994), *Polymer Combustion and Flammability – Role of the Condensed Phase*. Twenty-Fifth Symposium (International) on Combustion /The Combustion Institute. Pages 1423-1437.
- 49 Kuo, M. C., Tsai, C. M., Huang, J. C., and Chen, M., (2005), *PEEK Composites Reinforced by Nano-Sized SiO₂ and Al₂O₃ Particulates*. Materials Chemistry and Physics. Volume 90. Pages 185-195.
- 50 Perng, L. H., Tsai, C. J., and Ling, Y. C., (1999), *Mechanism and Kinetic Modelling of PEEK Pyrolysis by TG/MS*. Polymer. Volume 40. Pages 731-7329.
- 51 Hay, J. N., and Kemmish, D. J., (1987), *Thermal Decomposition of Poly(Aryl Ether Ketones)*. Polymer. Volume 28. Pages 2047-2051.
- 52 Tsai, C. J., Perng, L. H., and Ling, Y. C., (1997), *A Study of Thermal Degradation of Poly(Aryl-Ether-Ether-Ketone) using Stepwise Pyrolysis/Gas Chromatography/Mass Spectrometry*. Rapid Communications in Mass Spectrometry. Volume 11. Pages 1987-1995.
- 53 Galloway, J., Hoffman, R., and Bhatt, S., (2007), *Effect of Multiple Shear Histories on Rheological Behaviour and Devolatilisation of Poly (Ether Ether Ketone)*. ANTEC 3077.
- 54 Nandan, B., Kandpal, L. D., and Mathur, G. N., (2003), *Poly(Ether Ether Ketone)/Poly(Aryl Ether Sulphone) Blends: Thermal Degradation Behaviour*. European Polymer Journal. Volume 39. Pages 193-198.
- 55 Day, M., Cooney, J. D., and Wiles D. M., (1990), *The Thermal Degradation of Poly (Aryl Ether Ether Ketone) (PEEK) as Monitored by Pyrolysis-GC/MS and TG/MS*. Journal of Analytical and Applied Pyrolysis. Volume 18. Pages 163-173.
- 56 Day, M., Sally, D., and Wiles, D. M., (1990), *Thermal Degradation of Poly(Aryl-Ether-Ether-Ketone):Experimental Evaluation of Crosslinking Reactions*. Journal of Applied Polymer Science. Volume 40. Pages 1615-1620.
- 57 Koo, J. H., (2006), *Polymer Nanocomposites: Processing, Characterisation and Applications*. McGraw-Hill, New York, USA.
- 58 Baker, A.-M. M., and Mead, J., (2000), *Thermoplastics*. Chapter 1. In Harper, C. A., Modern Plastics Handbook. McGraw-Hill Professional Publishing. Ohio, USA.
- 59 Lyon, R. E., and Janssens, M. L., (2005), *Polymer Flammability*. US Department of Transport. Report Number: DOT/FAA/AR-05/14.
- 60 Beyler, C. L., and Hirschler, M. M., (2002), *Thermal Decomposition of Polymers*. Chapter 1-7. 3rd Edition. The SFPE Handbook of Fire Protection Engineering.

-
- 61 Naffakh, M., Ellis, G., Gómez, M. A., and Marco, C., (1999), *Thermal Decomposition of Technological Polymer Blends 1. Poly (Aryl Ether Ether Ketone) With a Thermotropic Liquid Crystalline Polymer*. Polymer Degradation and Stability. Volume 66. Pages 405-413.
- 62 Goyal, R. K., Negi, Y. S., and Tiwari, A. N., (2005), *Preparation of High Performance Composites Based on Aluminium Nitride/Poly (Ether-Ether-Ketone) and their Properties*. European Polymer Journal. Issue 41. Pages 2034-2044.
- 63 Zhou, B., Ji, X., Sheng, Ye., Wang, L., and Jiang, Z., (2005), *Mechanical and Thermal Properties of Poly Ether Ether Ketone Reinforced with CaCO₃*. European Polymer Journal. Issue 40. Pages 2357-2363.
- 64 Abu Bakar, M. S., Cheang, P., and Khor, K. A., (1999), *Thermal Processing of Hydroxyapatite Reinforced Polyetheretherketone Composites*. Journal of Materials Processing Technology. Issue 89-90. Pages 462-466.
- 65 Gao, X., Wang, R., and Zhang, A., (2007), *Synthesis of Poly(Ether Ether Ketone)s Containing Tertiary Amine*. Materials Letters. Issue 61. Pages 3647-3651.
- 66 Luo, Y., Huo, R., Jin, X., and Karasz, F. E., (1995), *Thermal Degradation of Sulphonated Poly (Aryl Ether Ether Ketone)*. Journal of Analytical and Applied Physics. Volume 34. Pages 229-242.
- 67 Nakamura, H., Nakamura, N., Noguchi, T., Imagawa, K., (2006), *Photodegradation of PEEK Sheets Under Tensile Strengths*. Polymer Degradation and Stability. Pages 740-746.
- 68 Lai, Y. H., Kuo, M. C., Huang, J. C., and Chen, M., (2007), *On the PEEK Composites Reinforced by Surface- Modified Nano-Silica*. Materials Science and Engineering A. Issue 458. Pages 158-169.
- 69 Kashiwagi, T., Grulke, E., Hilding, J., Harris, R., Awad, W., and Douglas, J., (2002), *Thermal Degradation and Flammability Properties of Poly(Propylene)/Carbon Nanotube Composites*. Macromolecular Rapid Communications. Issue 23. Pages 761-765.
- 70 Costache, M. C., Heidecker, M. J., Manais, E., Camino, G., Frache, A., Beyer, G., Gupta, R. K., and Wilkie, C. A., (2007), *The Influence of Carbon Nanotubes, Organically Modified Montmorillonites And Layered Double Hydroxides on the Thermal Degradation and Fire Retardancy of Polyethylene, Ethylene-Vinyl Acetate Copolymer and Polystyrene*. Polymer. Volume 48, Issue, 22. Pages 6532-6545.
- 71 Shen, J., Huang, W., Wu, L., Hu, Y., and Ye, M., (2007), *Thermo-Physical Properties of Epoxy Nanocomposites Reinforced with Amino-Functionalised Multi-Walled Carbon Nanotubes*. Composites Part A: Applied Science and Manufacturing. Volume 38, Issue 5. Pages 1331-1336.
- 72 Xiong, J., Zheng, Z., Qin, X., Li, M., Li, H., and Wang, X., (2006), *The Thermal and Mechanical Properties of a Polyurethane/Multi-Walled Carbon Nanotube Composite*. Carbon. Volume 44, Issue 13. Pages 2701-2707.

-
- 73 Hou, X., Shan, C. X., and Choy, K., (2007) *Microstructures and Tribological Properties Of PEEK-Based Nanocomposite Coatings Incorporating Inorganic Fullerene-Like Nanoparticles*. Surface & Coatings Technology. Volume 202, Issue 11. Pages 2287-2291.
- 74 Díez-Pascual A. M., Naffakh, M., Gómez, M. A, Marco, C., Ellis, G., Martínez, M. T., Ansón, A., González-Domínguez, J. A., Martínez-Rubi, Y., and Simard, B., (2009), *Development and Characterisation of PEEK/Carbon Nanotube Composites*. Carbon, 47(13), 3079-3090.
- 75 Wang, K.-L., Liou, W.-T., Liaw, D.-J., and Huang, S.-T., (2008), *High Glass Transition and Thermal Stability of New Pyridine-Containing Polyimides: Effect of Protonation on Fluorescence*. Polymer. Volume 49. Pages 1538-1546.
- 76 Li, W., Zhang, S., Chen, G., and Zhang, Q., (2007), *A New Class of High Tg and Organosoluble Polynaphthalimides*. Polymer. Volume 48. Pages 3082-3089.
- 77 Shenderova, O., Tyler, T., Cunningham, H., Ray, M., Walsh, J., Casulli, M., Hens, S., McGuire, G., Kuznetsov, V., and Lipa, S., (2007), *Nanodiamond and Onion-Like Carbon Polymer Nanocomposites*. Diamond and Related Materials. Volume 16. Pages 1213-1217.
- 78 Dolmatov, V. Y., (2001), *Detonation Synthesis Ultra-dispersed Diamonds: Properties and Applications*. Russian Chemical Reviews. Volume 70. Pages 607-626
- 79 Chou, W.-J., Wang, C.-C., and Chen, C.-Y., (2008), *Thermal Behaviours of Polyimide with Plasma-Modified Carbon Nanotubes*. Polymer Degradation and Stability. Volume 93. Pages 745-752.
- 80 Köytepe, S., Vural, S., and Seçkin, T., (2009), *Molecular Design of Nanometric Zinc Borate-Containing Polyimide as a Route to Flame Retardant Materials*. Materials Research Bulletin. Volume 44. Pages 369-376.
- 81 Kumar, S., Rath, T., Mahaling, R. N., Reddy, C. S., Das, C. K., Pandey, K. N., Srivastava, R. B., and Yadaw, S. B., (2007), *Study on Mechanical, Morphological and Electrical Properties of Carbon Nanofibre/Polyetherimide Composites*. Materials Science and Engineering B. Volume 141, Issues 1-2. Pages 61-60.
- 82 Liu, T., Tong, Y., and Zhang, W-D., (2007), *Preparation and Characterisation of Carbon Nanotube/Polyetherimide Nanocomposite Films*. Composites Science and Technology. Volume 67. Pages 406-412.
- 83 Kaba, M., Romero, R., Essamri, A., and Mas, A., (2005), *Synthesis and Characterisation of Fluorinated Copolyetherimides with -CH₂-C₆F₁₃ Side Chains Based on the ULTEM™ Structure*. Journal of Fluorine Chemistry. Volume 126. Pages 1476-1486.
- 84 Rezac, M. E., and Schöberl, B., (1999), *Transport and Thermal Properties of Poly(Ether Imide)/Acetylene-Terminated Monomer Blends*. Journal of Membrane Science. Volume 156. Pages 211-222.
- 85 Yao, F., Zheng, J., Qi, M., Wang, W., and Qi, Z., (1991), *The Thermal Decomposition Kinetics of Poly(Ether-Ether-Ketone) (PEEK) and its Carbon Fibre Composite*. Thermochemica Acta. Volume 183. Pages 91-97.

-
- 86 Babrauskas, V., (2000), *Fire Test Methods for Evaluation of Fire-Retardant Efficacy in Polymeric Materials*. Chapter 3. In Grand, A. F., and Wilkie, C. A., *Fire Retardancy of Polymeric Materials*. CRC Press, New York, USA.
- 87 IEC 60695-11-4: 2004. Fire Hazard Testing – Part 11-4: Test Flames – 50 W Flames – Apparatus and Conformational Test Method.
- 88 ISO 11925-2: 2002. Reaction to Fire Tests – Ignitability of Building Products Subjected to Direct Impingement of Flame. Part 2 – Single-Flame Source Test.
- 89 Babrauskas, V., (1992), *Cone Calorimeter Annotated Bibliography 1982-1991*. National Institute of Standards and Technology TN 1296.
- 90 Bundy, M., and Ohlemiller, T., (2003), *Bench-Scale Flammability Measures for Electronic Equipment*. National Institute of Standards and Technology. NISTIR 7031.
- 91 Harris, D. C., (2007), *Quantitative Chemical Analysis*. Seventh Edition. W. H. Freeman and Company, New York, USA.
- 92 Elaskesh, E. O., Hull, T. R., Price, D., and Carty, P., (2005), *Effect of Stabilisers and Lubricant on the Thermal Decomposition of Chlorinated Poly(vinyl chloride) (CPCV)*. *Polymer Degradation and Stability*. Volume 88, Issue 1. Pages 41-45.
- 93 Unknown., (1935), *Thermal Decomposition Of Talc*. *Journal of the Franklin Institute*. Volume 220, Issue 4. Page 505.
- 94 Wang, Y., Zhang, F., Chen, X., Jin, Y., and Zhang, J., (2009), *Burning and Dripping Behaviours of Polymers under the UL-94 Vertical Burn Test Conditions*. *Fire and Materials*. Volume 34. Pages 203-215.
- 95 Morgan, A.B., and Bundy, M., (2007), *Cone Calorimeter Analysis of UL-94 V-Rated Plastics*. *Fire and Materials*. Volume 31. Pages 257-283.
- 96 Lyon, R. E., and Quintiere, J. G., (2007), *Criteria for Piloted Ignition of Combustible Solids*. *Combustion and Flame*. Volume 151. Pages 551-559.
- 97 ASTM D570-98: 2005. Standard Method for Water Absorption of Plastics. ASTM International, West Conshohocken, PA, USA.
- 98 Filipczak, R., and Lyon R. E., (2002), *Heat Flux Measurements in the OSU Rate of Heat Release Apparatus*. *Fire Safety Journal*. Volume 37, Issue 6. Pages 591-604.
- 99 Pouchert, C. J., (1981), *The Aldrich Library of Infrared Spectra*. 3rd Edition. Aldrich Chemical Co. Milwaukee, USA.
- 100 Williams, D. H., and Fleming, I., (1989), *Spectroscopic Methods in Organic Chemistry*. 4th Edition – Revised. McGraw-Hill, London, UK.
- 101 Freitas, J C. C., Bonagamba, T. J., and Emmerich, F. G., (2001), *Investigation of Biomass- and Polymer-Based Carbon Materials using ¹³C High-Resolution Solid-State NMR*. *Carbon*. Volume 39. Pages 535-545.

-
- 102 Van Krevelen, D. W., (1990), *Properties of Polymers*. Chapter 22 – Thermal Decomposition. 3rd Edition. Elsevier Science Publishers, Amsterdam.
- 103 Walters, R. N., (2001), *Molar Group Contributions to the Heat of Combustion*. US Department of Transport. Report Number: DOT/FAA/AR-TN01/75.
- 104 Bicerano, J., (1996), *Prediction of Polymer Properties*. 2nd Edition. Marcel Dekker Inc, New York, USA.
- 105 Schartel, B., Pawlowski, K., and Lyon, R., (2007), *Pyrolysis Combustion Flow Calorimeter: A Tool to Assess Flame Retarded PC/ABS Materials?* *Thermochimica Acta*. Volume 462. Pages 1-14.
- 106 Lyon, R. E., and Walters, R. N., (2004), *Pyrolysis Combustion Flow Calorimeter*. *Journal of Analytical and Applied Pyrolysis*. Volume 71. Pages 27-46.
- 107 Patel, P., Hull, T. R., Lyon, R. E., Stoliarov, S. I., Walters, R. N., Crowley, S., and Safronava, N., (2011), *Investigation of the Thermal Decomposition and Flammability of PEEK and its Carbon and Glass-Fibre Composites*. *Polymer Degradation and Stability*. In Press
- 108 Staggs, J. E. J., (1998), *A Theory for Quasi-Steady Single-Step Thermal Degradation of Polymers*. *Fire and Materials*. Volume 22, Issue 3. Pages 109-118.
- 109 Zhang, J., Delichatsios, M. A., and Bourbigot, S., (2009), *Experimental and Numerical Study of the Effects of Nanoparticles on Pyrolysis of Polyamide 6 (PA6) Nanocomposite in the Cone Calorimeter*. *Combustion and Flame*. Volume 156, Issue 11. Pages 2056-2062.
- 110 Jia, F., Galea, E. R., and Patel, M. K., (1999), *The Numerical Simulation of the Non-Charring Pyrolysis Process and Fire Development Within a Compartment*. *Applied Mathematical Modelling*. Volume 23, Issue 1. Pages 587-607.
- 111 Stoliarov, S. I., and Lyon, R. E., (2008), *Thermo-Kinetic Model of Burning*. Federal Aviation Administration Technical Note DOT/FAA/AR-TN-08/17.
- 112 Stoliarov, S. I., Crowley, S., Lyon, R. E., and Linteris, G. T., (2009), *Prediction of the Burning Rates of Non-Charring Polymers*. *Combustion and Flame*. Volume 156, Issue 11. Pages 1068-1083.
- 113 Stoliarov, S. I., Safronava, N., and Lyon, R. E., (2009), *The Effect of Variation in Polymer Properties on the Rate of Burning*. *Fire and Materials*. Volume 33, Issue 6. Pages 257-271.
- 114 Rahatekar, S. S., Zammarano, M., Matko, S., Koziol, K. K., Windle, M. H., Kashiwagi, T., and Gilman, J. W., (2010), *Effect of Carbon Nanotubes and Montmorillonite on the Flammability of Epoxy Nanocomposites*. *Polymer Degradation and Stability*. Volume 95, Issue 5. Pages 870-879.
- 115 Percy, M., (2010), Private Communication of Study undertaken at the University of Bolton, 2006.